INDUCIBLE VIRAL RESERVOIR ASSESSMENT

- at the Intersection of -

INNOVATIVE STRATEGIES TOWARDS HIV CURE

Cynthia Lungu

Inducible Viral Reservoir Assessment; at the Intersection of Innovative Strategies Towards HIV Cure

Beoordeling van het induceerbare virale reservoir; op het kruispunt van innovatieve strategieën richting HIV genezing

Cynthia Lungu

Financial support for the printing of this thesis was provided by Erasmus University Rotterdam.

ISBN:	978-94-6483-979-1
Cover design:	Cynthia Lungu
Lay-out:	Ridderprint | www.ridderprint.nl
Print:	Ridderprint | www.ridderprint.nl

Inducible Viral Reservoir Assessment; at the Intersection of Innovative Strategies Towards HIV Cure

Beoordeling van het induceerbare virale reservoir;
op het kruispunt van innovatieve strategieën richting HIV genezing

Thesis

to obtain the degree of Doctor from the
Erasmus University Rotterdam
by command of the
rector magnificus

Prof. dr. A.L. Bredenoord

and in accordance with the decision of the Doctorate Board.
The public defense shall be held on

Wednesday 1 May 2024 at 10:30 hrs

by

Cynthia Lungu
born in Lusaka, Zambia.

Erasmus University Rotterdam

DOCTORAL COMMITTEE:

Promotors:

Prof. dr. T. Mahmoudi
Prof. dr. C.A.B. Boucher (1958-2021)

Other members:

Dr. ir. W.M. Baarends
Prof. dr. L. Ndhlovu
Prof. dr. L. Vandekerckhove

Co-promoter:

Dr. R.A. Gruters

In loving memory of Prof. dr. Charles A. B. Boucher.

The research described in this thesis was jointly conducted at the Department of Viroscience and Department of Biochemistry at Erasmus University Medical Center, Rotterdam, the Netherlands within the framework of the Erasmus MC Graduate School.

TABLE OF CONTENTS

CHAPTER 1

General introduction

Partially based on:

C. Lungu, F.A. Procopio. TILDA: *Tat/Rev Induced Limiting Dilution Assay.* **Methods Mol Biol. (2022)**;2407:365-372

C. Lungu, F.A. Procopio, R.J. Overmars, R.J.J. Beerkens, J.J.C. Voermans, S. Rao, H.A.B. Prins, C . Rokx, G. Pantaleo, D.A.M.C.V. Vijver, T. Mahmoudi, C.A.B. Boucher, R.A. Gruters, J.J.A.V. Kampen. *Inter-laboratory reproducibility of inducible HIV-1 reservoir quantification by TILDA*. **Viruses. (2020)** Sep 2;12(9):973.

C. Lungu, R. Banga, R.A Gruters, and F.A. Procopio. *Inducible HIV-1 reservoir quantification: clinical relevance, applications and advancements of TILDA*. **Front Microbiol. (2021)** Jun 15;12:686690.

ABSTRACT

Approximately 40 million people live with human immunodeficiency virus-1 (HIV-1) globally (UNAIDS 2023). HIV-1 is a lentivirus, a subgroup of Retroviridae, and the principal causative agent of acquired immune deficiency syndrome (AIDS), which was formally recognized in the early 1980s. Upon infection, the virus targets key cells of the immune system, primarily CD4+ T lymphocytes, as well as Myeloid cells (macrophages and dendritic cells). An obligate step in HIV-1 replication, mediated by viral integrase, is the stable integration of the viral genome into the host cell genome. The integrated HIV-1 genome, or provirus, utilizes host transcriptional machinery for viral gene expression and hence productive replication, which is greatly influenced by the metabolic and activation states of the host cell. HIV-1 preferentially replicates in activated CD4+ T cells leading to their depletion. The subsequent loss of immune competence and increased susceptibility to infection is the major hallmark of AIDS, which eventually leads to death in absence of antiretroviral therapy (ART). Although ART regimens effectively suppress HIV-1 replication to below detection limits, they are not curative and thus taken lifelong. Interruption of ART results in viral rebound in the majority of participants regardless of how early they initiated ART or despite having received several years of suppressive ART. This is due to a reservoir of latent, inducible, replication-competent HIV-1 that stably persists in blood and tissue compartments despite suppressive ART and presents a major hurdle to cure. Innovative strategies towards clearance or ART-free control of HIV-1 reservoirs shape global scientific efforts towards a cure for HIV-1.

CLINICAL COURSE OF HIV-1 INFECTION

Following transmission, during the eclipse phase, HIV-1 replicates in mucosal tissues. The virus becomes first detectable in blood approximately one to two weeks after infection, marking the end of the eclipse phase (Fig. 1) [1]. The virus disseminates via the blood stream to secondary lymphoid tissue, preferentially the gut-associated lymphoid tissue (GALT) where the highest concentration of effector memory CD4+ T cells in the body reside. The large quantity of viruses replicating in the mucosa and circulating in peripheral blood (viremia) causes extensive depletion of CD4+ T cells. Up to 80% of the CD4+ T cell population in the GALT can be depleted within the first three weeks of infection [2,3].

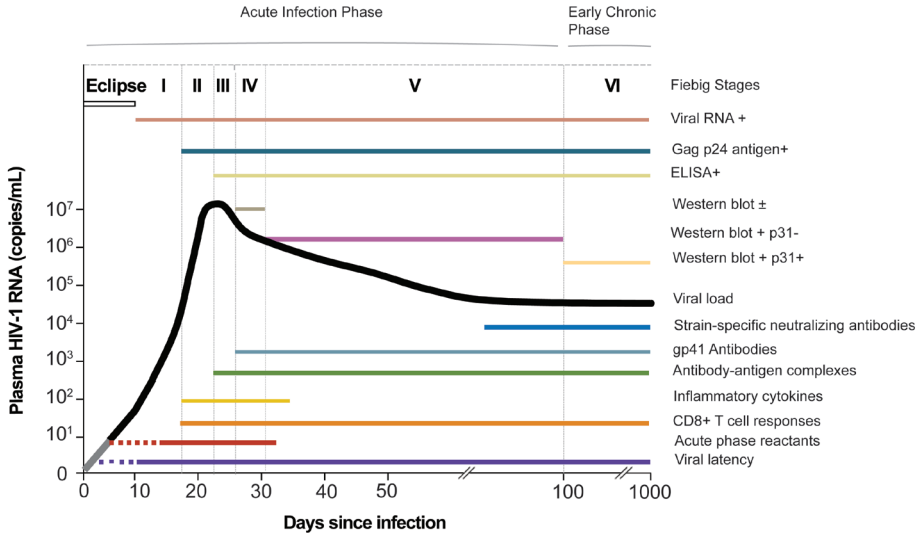

Fig. 1. Natural history and immunopathogenesis of HIV-1 infection. The six discrete stages of HIV-1 infection, defined according to the results of standard clinical laboratory tests. The stages are based on the sequential appearance of plasma HIV-1 viral RNA; Gag p24 protein antigens, HIV-1 specific antibodies by ELISA and by Western Immunoblot. Positive test results are indicated by a plus sign. The line lines below the viral-load curve show the timing of key events and immune responses that cannot be measured with standard clinical laboratory assays, beginning with the establishment of viral latency. Adapted from[1] and [2].

The clinical stages of acute infection, referred to as Fiebig stages, are based on the development of detectable concentrations of HIV-1 markers. HIV-specific antibodies in plasma become detectable in approximately three to four weeks after infection (seroconversion), which typically occurs during Fiebig stage III when plasma HIV-1 RNA levels peak [1,2]. At time of peak viremia, up to 80% of patients may present with influenza-like symptoms.

Productively infected CD4+ T cells die through apoptosis after one to two days of viral replication. The majority (95%) of CD4+ T cells that die during HIV-1 infection, likely through pyroptosis, are non-activated "bystander" CD4+ T cells, mainly present in lymphoid tissues [4,5]. CD4+ T cell depletion and enteropathy lead to microbial translocation, which contributes to immune activation. The virus itself may also trigger immune activation, which leads to the generation of more target cells thus perpetuating viral replication and gut mucosal damage [6]. During the acute phase, activated cytotoxic CD8+ T cells (CTLs) kill infected cells and control virus production but do not clear the HIV-1 viral reservoir. Subsequently, peak plasma viremia declines to a stable viral set point and CD4+ T cell counts increase to subnormal levels. The acute viremic phase is followed by a chronic, asymptomatic phase of infection that lasts for about 10 years on average [7]. During this phase, the virus continues to replicate and both the number and function of CD4+ T cells gradually decline, which eventually leads to a symptomatic phase that, in the absence of treatment, will develop into advanced disease (AIDS, marked by CD4+ T cell counts <200 cells/μL) (Fig. 2). Disease severity can be assessed based on the number of CD4+ T cells and the presence of opportunistic illnesses such as recurrent bacterial pneumonia, candidiasis, cytomegalovirus disease, chronic herpes simplex ulcers, Kaposi sarcoma, B-cell lymphoma, Mycobacterium infections, HIV-related encephalopathy and HIV-related wasting syndrome [8].

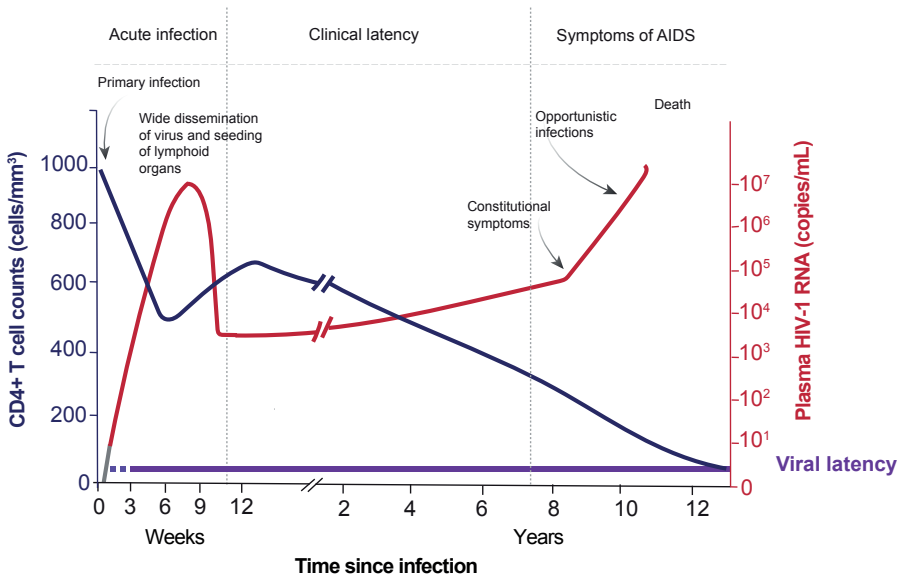

Fig. 2. Time course of untreated HIV-1 infection. The kinetics of plasma HIV-1 RNA copies and CD4+ T cell counts over the course of a typical untreated HIV-1 infection. Patterns of viremia and CD4+ T cell decline vary between individuals. Figure adapted from[9].

IMMUNE RESPONSES TO HIV-1

The initial interaction between HIV-1 and the host's immune system is critical for the subsequent clinical outcome [9-11]. HIV-1 proviruses generate a diverse set of transcripts, which provide multiple targets for detection by nucleic acid innate immune sensors that in turn initiate signaling events leading to the activation of interferon (IFN) responses and inflammatory cytokine production [12,13]. IFNs and other proinflammatory cytokines help recruit additional target cells to the sites of viral replication and facilitate viral spread. Primary HIV-1 infection thus results in a burst of viremia and induces a potent immune response that, although substantial, does not completely curtail viral replication [9,13]. To minimize the protective effects of innate responses, HIV-1 resists control by natural killer cells and may impair macrophage and dendritic cell function, including antigen presentation, thereby impacting CD4+ and CD8+ T cell responses [11]. Overall, these innate immune responses to diverse HIV-1 RNA transcripts in HIV-1 infection have the potential to contribute to CD8+ T cell dysfunction and systemic inflammation that over time leads to profound immunosuppression [6]. Indeed, longitudinal analysis of polyfunctional HIV-1 specific CD8+ T cells *in vivo* has demonstrated that persistent antigen stimulation leads to a reduction in the breadth of cytokines produced and this correlates with increased expression of PD-1, TIGIT, and LAG-3, which are molecules associated with cell exhaustion. Although HIV-1 specific CD8+ T cell numbers remain elevated in chronically-infected individuals, they produce less IFNγ, express relatively high levels of check-point inhibitor receptors like PD-1, and have altered metabolic properties, which overall render them ineffective in clearing HIV-1-infected cells [12].

ANTIRETROVIRAL THERAPY

Since the introduction of antiretroviral therapy (ART), HIV-related morbidity and mortality rates have significantly reduced. Antiretroviral drugs are broadly classified based on their mode of action, which inhibit pivotal steps in the viral replication cycle (Fig. 3). Due to the highly mutagenic nature of the virus, HIV-1 can escape from single antiretroviral drug regimen within a period of days. Therefore, ART is administered as a drug cocktail comprising of three drugs that target different steps of viral replication. Typically, standard ART includes a combination of two Nucleoside reverse transcriptase inhibitors (NRTIs) with a third drug, either a Protease inhibitor (PI), non-Nucleoside reverse transcriptase inhibitor (NNRTI) or an Integrase strand transfer inhibitor (INSTI).

Antiretroviral therapy inhibits active viral replication causing an initial rapid decline in plasma HIV-1 RNA. This decline, however, slows into a second phase of exponential decay with a longer half-life of one to four weeks, which is likely due

to persistent HIV-1 in longer lived cells. During the second phase of decay, plasma HIV-1 RNA drops below the threshold of detection of clinical assays, 20 or 50 copies/mL, which is considered adequate to control the spread of HIV-1 infection (Fig. 4).

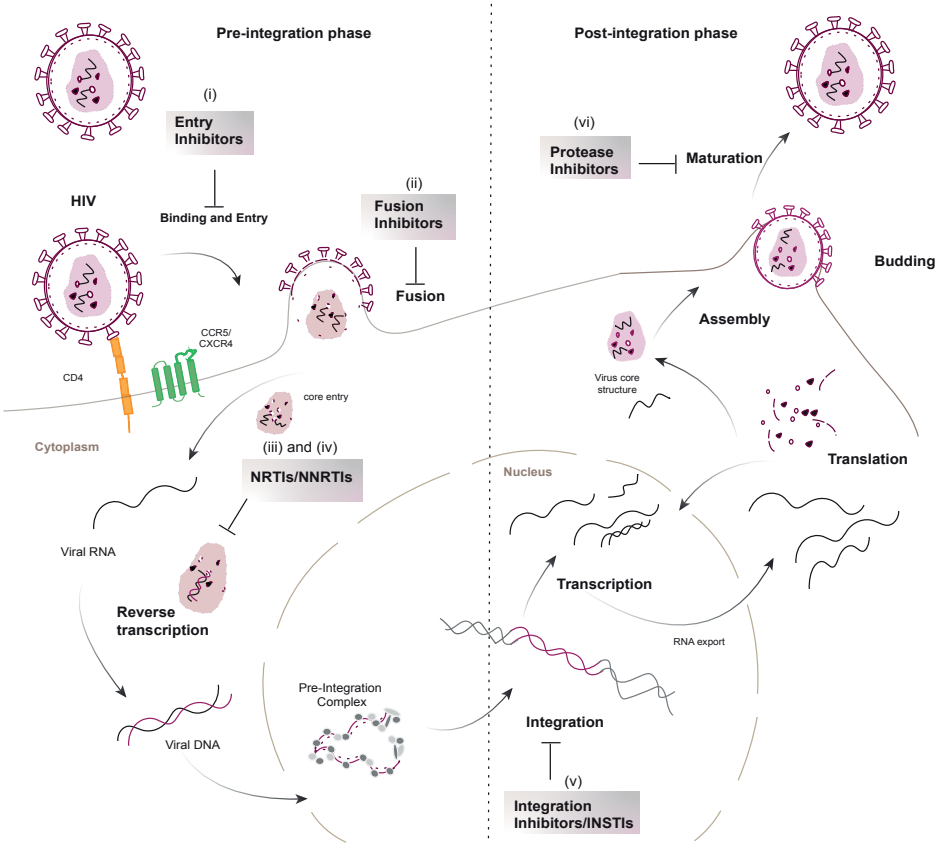

Fig. 3. Antiretroviral drug targets

i. Entry inhibitors prevent initial virus infection by blocking the interaction between the virus particle and cell surface receptors (e.g., CCR5 antagonists and attachment inhibitors that bind to envelope gp120).
ii. Fusion inhibitors bind envelope gp41 and block the fusion of viral and cellular membranes, which prevents viral capsid entry into the cell cytoplasm.
iii. Nucleoside reverse transcriptase inhibitors (NRTI) are analogues of deoxynucleotide triphosphates (dNTPs) but lack the 3′-hydroxyl (-OH) group that is essential for DNA strand elongation. Incorporation of NRTIs into the HIV-1 strand being reverse transcribed halts its synthesis leading to incomplete cDNA.
iv. Non-nucleoside reverse transcriptase inhibitors (NNRTI) bind directly to the reverse transcriptase (RT), inducing allosteric inhibition thereby altering its active site.
v. Integrase strand transfer inhibitors (INSTI) or integrase inhibitors prevent the integration of HIV cDNA into the host genome.
vi. Protease inhibitors (PI) interact with protease in immature virions. By blocking proteolytic cleavage of gag and gag-pol precursor proteins, PIs prevent the maturation of new infectious virions.

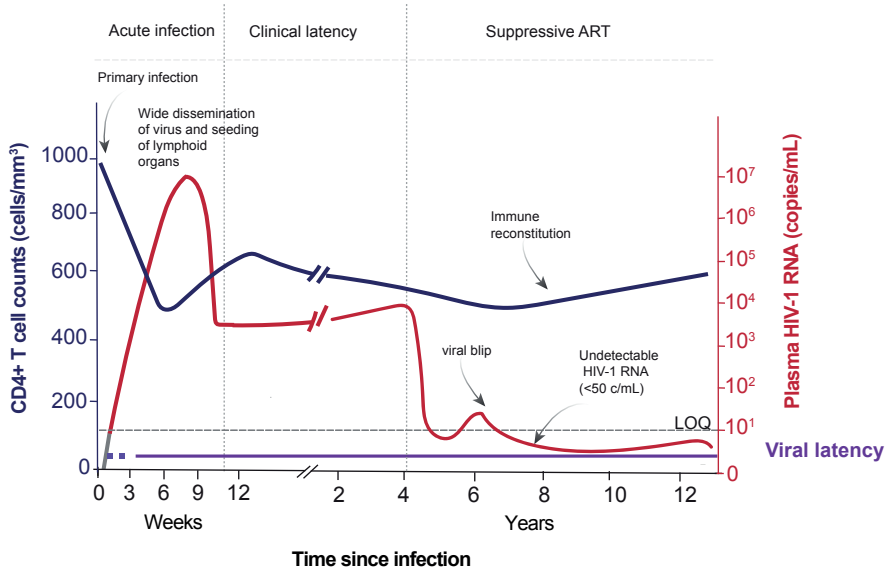

Fig. 4. Time course of treated HIV-1 infection. The kinetics of plasma HIV-1 RNA copies and CD4+ T cell counts over the course of a treated HIV-1 infection. Viremia is suppressed to undetectable levels in response to antiretroviral therapy (LOQ=Limit of Quantification). Patterns of viremia and CD4+ T cell decline vary between individuals. Figure adapted from[9].

Residual plasma HIV-1 RNA below the 20 copies/mL threshold can often be detected by ultrasensitive single copy assays. However, it is an ongoing debate whether residual plasma viremia is a result of ongoing viral replication or merely a reflection of HIV-1 RNA release from HIV-1 reservoirs.

BEYOND VIRAL SUPPRESSION

ART is highly effective at suppressing HIV-1 replication but demands daily adherence as periodic or complete cessation of therapy leads to a resurgence of viremia, resulting in the infection of new cells [14,15]. Uncontrolled viremia gives rise to drug resistant HIV-1 strains that lead to treatment failure and disease progression. Drug resistance may be pre-existing due to the rapid viral turnover and error prone RT, which may cause single or multidrug-class resistant HIV-1 strains before the initiation of therapy. Drug resistant mutants can also emerge during therapy either due to suboptimal adherence, insufficient antiviral potency, inadequate drug levels or incomplete drug penetrance. Moreover, incomplete viral suppression with notable viremia "blips" or low-level viremia has been reported in many people living with HIV-1 (PLWH) on ART – hence the need for implementation of HIV-1 monitoring programmes [16-19]. Although viral blips or low-level viremia in

ART-adherent individuals may not readily predict virologic breakthrough, they still have implications for long term clinical, immunological, and virological outcomes [20-23]. Moreover, life-long ART is associated with cumulative ART toxicity and chronic HIV-1 infection is associated with persistent immune dysfunction and inflammation [24,25], which has been implicated in various comorbidities. Individuals with HIV-1 on suppressive ART have increased risk of coronary heart disease, various cancers, leaky gut syndrome, HIV-1-associated neurological disorders and other end-organ diseases, which are consistent with inflammaging [26]. The increased risk of HIV-1 comorbidities and associated diseases pose a considerable public health and economic burden especially in LMIC settings with inadequate healthcare infrastructure.

HIV-1 PERSISTENCE

Upon infection, HIV-1 disseminates throughout the body within one to two weeks[1]. Although ART can effectively suppress viremia, a reservoir of immune cells harboring replication-competent HIV-1, established early during infection, stably persists in blood and tissues [27-29]. Within a few weeks of interrupting ART, viremia rebounds in most PLWH necessitating life-long adherence to maintain viral suppression, block viral transmission, and delay disease progression. The nature of HIV-1 persistence is multidimensional comprising: (1) anatomical and microanatomical locations (tissue reservoirs); (2) cell type (for example, CD4+ T cell or macrophage; (3) cell functional profile (i.e., activated/resting and inherent resistance to clearance/killing); (4) pool of proviruses with a particular functional profile or (5) response to specific stimuli and integration site features of the rebounding virus [30,31]. These intricacies of HIV-1 persistence challenge efforts to standardize the definition of the HIV-1 reservoir. Generally, persistent HIV-1 can be classified on the basis of proviral genome integrity (intactness), inducibility; the ability to express viral genes (transcription and/or translation, and replication-competence (the ability to produce infectious viral progeny) [32,33].

Defective HIV-1 reservoir

The majority of infected cells in PLWH on suppressive therapy harbor replication-defective proviruses, which mostly contain large internal deletions, hypermutations, or harbor defects that inactivate the packaging signal or the major splice donor site [34,35]. Defective genomes rapidly accumulate early during acute HIV-1 infection as a result of intrinsic host cell restriction factors and error-prone viral replicative processes [34]. The reservoir of defective proviral genomes is remarkably stable over decades of suppressive ART [36,37]. HIV-1 latency has traditionally been defined as

'transcriptionally silent', but there has been a shift in this paradigm as emerging studies have also demonstrated viral RNA and protein expression from defective proviruses [38-40], which, although unable to contribute to new infections, could drive innate sensing mechanisms and damaging inflammatory responses leading to various comorbidities and pathogenesis in PLWH on suppressive ART (reviewed in [41]) .

Intact HIV-1 reservoir

A rare fraction of infected cells harbors intact HIV-1 provirus [42,43], which makes up 2-5% of the pool of reservoir cells in PBMCs. Longitudinal assessment of intact HIV-1 genome sequences, from probable replication-competent proviruses, in PLWH before and after ART initiation suggest that most of the intact viral reservoir has been seeded at the time of ART initiation and there is no additional infection post suppressive ART [44,45]. Thus, ART initiation has been suggested to shape the proviral reservoir landscape and the virus circulating at the time of ART initiation is likely overrepresented in the HIV-1 reservoir [45]. Recent work has demonstrated that intact genomes decline more rapidly than defective genomes [37,46]. In addition, the rate of decline within the first seven years following initial suppression is substantially variable between individuals [37]. Another study in fourteen individuals with HIV-1 on two decades of suppressive ART revealed three patterns of intact proviral DNA decay; 1) a biphasic decline with a markedly slower second phase decline; 2) an initial decline that transitions to a zero-slope plateau; and 3) initial decline followed by later increases in intact proviral DNA [46]. The slowing of the second phase decay of intact proviral DNA or, in some individuals, increase in the intact proviral DNA may be attributed to the inability of host immune responses to clear cells and the clonal expansion of cells with intact proviruses [47-50]. Notably, while HIV-1 intactness may be a likely indicator for replication-competence, not all intact HIV-1 proviruses are inducible, which warrants further research into the mechanisms driving the persistence of these proviruses and the implications for HIV-1 curative interventions.

INVESTIGATING MECHANISMS OF HIV-1 PERSISTENCE

To develop successful cure interventions, it is essential to know the basic mechanisms underlying HIV-1 latency establishment, maintenance and reversal. Recent work has demonstrated that most of the latent, replication-competent HIV-1 reservoir cannot be induced *in vitro* (reviewed in [51]). The mechanisms influencing control of provirus inducibility in different immune cells, from different bodily compartments, as well as the impact of biological sex and age, requires further

investigation. Indeed, mechanistic studies are challenging to carry out in samples from PLWH due to the limited availability of sample, the scarcity of latent HIV-1 reservoir cells *in vivo* and the absence of known phenotypic markers that can distinguish them from uninfected cells. Cell lines harboring integrated HIV-1 genomes and primary cell models of HIV-1 latency thus serve as important tools in investigating the biology of HIV-1 latency. Multiple HIV-1 latency cell line-model systems have been extensively used in biased and unbiased screens to discover and evaluate latency-reversing agents (LRAs) and to perform mechanistic studies involved in the establishment and maintenance of latency [52]. While latently infected T cell lines are genetically and experimentally tractable, they are limited by their cycling nature and by their proviral integration site clonality [52-54]. Moreover, the transformed cell lines lack the ability to differentiate and naturally switch between phases of quiescence and active proliferation in response to biological stimuli. Bulk cell HIV-1 transcription profiling studies revealed dramatic differences between cell lines and primary cells from ART-suppressed individuals where latent cell lines show lower levels of HIV-1 transcriptional initiation and higher levels of polyadenylation and splicing [52]. Different forms of transcriptional interference were shown to occur in ACH-2 and J-Lat cells while U1 cells showed a block to transcript elongation [52]. The differences in mechanisms of HIV-1 latency among these cell lines translate to notable variations in response to latency reversal stimuli [54,55]. Most cell line models demonstrate sensitivity to latency reversal that is skewed towards a specific drug class and poorly translate to *ex vivo* responses in latently infected primary cells from ART-suppressed individuals [54]. The innate immune response and type 1 IFN defenses are critical for early control of HIV infection within CD4+ T cells and have recently been proposed to play an important role in driving elimination of HIV-1-infected cells. While latently infected T cell lines have functional RNA sensing and IFN signaling pathways, they fail to induce specific interferon-stimulated genes (ISGs) in response to innate immune activation or type 1 IFN treatment [56]. Jurkat cells latently infected with a fluorescent reporter HIV-1 similarly demonstrate attenuated responses to type 1 IFN, which renders these models less suitable for assessing innate immune-mediated elimination of HIV-1-infected cells [56]. These notable limitations have led to the development of more physiologically relevant primary T cell models of HIV-1 latency, which use replication-competent HIV-1 cultured in the presence of antiviral drugs and select cytokines, to more closely reflect HIV-1 latency *in vivo* [55,57]. Indeed, gene ontology analysis of highly represented genes from patient samples found little overlap with HIV-containing genes from latently infected cell lines [58]. Primary T cell models of HIV-1 latency share several similarities with latently infected cells isolated from PLWH including similar integration patterns, the presence of clonally expanded

integration sites, comparable provirus inducibility profiles and similar blocks in HIV-1 splicing, which allow investigators to study proposed mechanisms governing latency and to evaluate small compound molecules for induction of proviral reactivation and/or selective depletion of reactivated HIV-1 reservoir cells [53-55,57,59-66].

INNOVATIVE STRATEGIES TOWARDS HIV-1 CURE

Despite the intricate nature of HIV-1 persistence, the reservoir of cells infected with inducible, replication-competent HIV-1, which can lead to viral rebound in absence of ART, are considered a major hinderance to developing a cure. Therefore, strategies aiming to control or eliminate these HIV-1-infected cells are currently being explored.

Early ART

Very early ART can substantially reduce the size of the HIV-1 reservoir. Studies have shown that treatment-initiated within two weeks of infection (at Fiebig stages I to III) results in nearly undetectable HIV-1 reservoir size in blood and tissues compared to ART initiated at later stages (Fiebig stages IV/V and chronic infection) [67-69]. Thus, the HIV-1 reservoir established during early stages of infection is unstable in nature while that present after peak viremia display greater ability to persist [68]. However, a diminished viral reservoir size, as a result of early treatment, has limited potential in preventing viral recrudescence. Indeed, no significant delay in time to viral rebound after ART interruption is observed for early-treated participants [14,70]. Additional interventions are therefore required to eliminate the latent, replication-competent HIV-1 reservoir. However, early treatment during Acute HIV infection, although practically challenging in high HIV-1 burdened, low-resource settings, may be the critical first step in restricting HIV-1 reservoirs [69].

Shock and kill

One of the most pursued HIV-1 elimination strategies is the “Shock and kill” approach, which assumes that potent reactivation of the latent HIV-1 reservoir by diverse pharmacological or biologic agents targeting distinct mechanisms of viral persistence, will trigger intrinsic or extrinsic destruction and clearance of reactivated reservoir cells. The molecular mechanisms regulating HIV-1 proviral latency and reactivation are complex and multifactorial (reviewed in [71]). Key elements involved in HIV-1 transcriptional reactivation include: 1) the site of viral integration; 2) Transcription factor NF-κB, which is induced by pro-inflammatory cytokines; 3) the specific Long Terminal Repeat (LTR) activation-induced remodeling

of a single nucleosome (nuc-1, located immediately downstream of the HIV-1 transcription start site under latency conditions); 4) post-translational acetylation of histones and non-histone proteins (by histone deacetylase inhibitors, which induce viral transcription and nuc-1 remodeling); and 5) the viral trans-activator of transcription (Tat) protein [72], which promotes transcription through mediating the recruitment of histone modifying enzymes and ATP-dependent chromatin remodeling complexes. These are required to disrupt nucleosome repression of the LTR and to enhance transcription elongation [71,73,74]. These distinct elements of proviral latency and reactivation are targeted in experimental approaches toward HIV-1 cure [75]. The pre-clinical discovery phase of latency reversal agents (LRAs), used in the widely studied "shock and kill" approach, starts with screening of drug libraries using latent HIV-1-infected cell lines. Positive hits are evaluated using *ex vivo* primary cell-based HIV-1 latency models, which better recapitulate the nature of latent viral reservoirs *in vivo* [55,57,62,64]. Putative LRAs are further selected based on efficacy and toxicity profile and then validated in primary cells derived from individuals with HIV-1 on suppressive ART. Toxicology studies in animal models (humanized mice and non-human primates) may be performed in case of novel molecules [76].

To rapidly advance to clinical trials, it is highly beneficial to screen molecules that are already approved drugs, which can be repurposed as putative LRAs. The most extensively investigated LRAs are histone deacetylase (HDAC) inhibitors [71,77], which include valproic acid (VPA), vorinostat (SAHA), romidepsin, and panobinostat, which have been investigated in a number of clinical trials (reviewed in [78]). VPA is clinically used to treat epilepsy and bipolar disorders, while vorinostat and romidepsin are used to treat cutaneous T-cell lymphoma. Panobinostat is used in patients with multiple myeloma. LRAs are administered as adjunct therapy to ART, which suppresses de novo infection, thereby restricting viral reservoir expansion. The focus on HDACi is due to their ability to unwind the compact chromatin structure at the latent proviral promoter. Inhibition of HDACs leads to an increase of histone acetylation level by histone acetyltransferases (HATs) [71]. HDACs 1, 2, and 3 considerably contribute to HIV-1 repression, and are thus interesting targets. Unfortunately, trials with HDACis alone have not yielded sufficient or sustained reactivation of proviral RNA levels (reviewed in [78]). Moreover, since HDACs are involved in general regulation of gene expression, they have pleiotropic effects causing toxicities, which requires strict and controlled monitoring to ensure maximal safety [79,80]. In addition, certain HDACis (e.g., vorinostat and romidepsin) are metabolized or transported by polymorphic enzymes or drug transporters. Therefore genotype-directed dosing could improve pharmacotherapy by limiting off-target risk toxicities, preventing suboptimal treatment and, in extreme cases, sudden death (reviewed in [81]).

A combination of LRAs, with distinct mechanisms of action, will likely be more effective in reactivating the latent provirus. However, very few LRA combination trials have been performed to date with poor efficacy outcomes [77]. Therefore, more specific, potent and less toxic LRAs are still needed. Recent work has demonstrated the integral role that the BAF-complex (SWI/SNF-A), an ATP-dependent chromatin remodeler, plays in establishment and maintenance of HIV-1 latency [73]. A library screen of compounds that mimic BRG-1 knock out identified 20 compounds that transcriptionally mimicked BAF-complex disruption. Several of these molecules were able to decrease the frequency of latency establishment and induced reactivation of HIV-1 in cell lines and primary cell models of latency. Moreover, BAF complex inhibitors were shown to synergize with other LRAs, specifically SAHA and prostratin [82]. Clinical studies are ongoing to identify suitable candidate drugs to combine with a BAF complex inhibitor compound pyrimethamine, which has demonstrated efficacy in reactivating HIV-1 *in vivo* [83]. Some other examples of LRAs being investigated include toll-like receptor agonists, activators of NF-κB, disulfiram, immune checkpoint inhibitors, and agents that affect the STAT5 signaling pathway and mTOR signaling (reviewed in [77]).

Innovative immune-based approaches towards ART-free viral control

While latent reservoir reactivation *in vivo* is attainable, the impact on the size of the viral reservoir has been negligible, which suggests several inadequacies in the immune system to eliminate reactivated reservoirs (reviewed in [84]). Strikingly, recent work demonstrated that LRAs reactivated merely 5% of cells harboring a latent provirus. Sequencing analysis of reactivatable and non-reactivatable reservoirs revealed distinct chromatin functional states correlating with proviral reactivation [85]. Overall, these findings, along with the unproven effectiveness *in vivo*, challenge the feasibility of the "shock and kill" approach. The diverse mechanisms of latency establishment and maintenance *in vivo* likely influence the spectrum of agonists that induce proviral reactivation. Priming cells for proviral reactivation and/or enhancing the immune system to recognize and target reactivated cells expressing HIV-1 RNA or protein could potentially lead to the sustained reduction and control of the replication-competent viral reservoir that is crucially sought for [84,86]. Interestingly, one study showed that the magnitude, breadth and cytokine secretion profile of HIV-1-specific CD8+ T cells did not correlate with the changes in HIV-1 DNA levels in CD4+ T cells during treatment with the HDACi panobinostat. In contrast, the proportions of total Natural Killer (NK) and cytotoxic NK cells inversely correlated with HIV-1 DNA levels throughout the study [87]. Declines in HIV-1 DNA during latency reversing treatment with panobinostat were also closely linked to the proportions of plasmacytoid dendritic cells and distinct expression

profiles of interferon-stimulated genes, suggesting an important role of the innate immune response in reducing the latent HIV-1 reservoir. Similarly, Palermo *et al.*, demonstrated a significant increase in HIV-1 proviral reactivation and specific apoptosis of HIV-infected primary T cells and CD4 memory T cell population in patient samples *in vitro* following the combined treatment of the FDA-approved epigenetic modulator, resminostat (an HDACi), and the STING agonist cGAMP (cyclic GMP-AMP), which activated antiviral innate immune response and selective killing [88]. Rao *et al.*, reported selective depletion of the inducible reservoir following *ex vivo* treatment with DDX3 inhibitors, which induced proviral transcription and in turn triggered intrinsic cell apoptosis mediated by type 1 IFN pathway signaling [66].

ELITE CONTROL OF HIV-1 INFECTION

A rare number of individuals exceptionally control HIV-1 viral replication without the use of ART and do not experience immune dysfunction. There is no disease progression and these individuals have extraordinarily low burdens of HIV-1, which can only be detected with specialized laboratory assays [95,96]. There may be a waning of HIV-specific antibodies over time and weakened HIV-specific immune responses implying a reduction in HIV-1 antigens. Such individuals, referred to as exceptional elite controllers, may be a good model for an HIV-1 cure. Investigating means of modulating or enhancing the immune system to its maximum potential could thus hold the key to inducing ART-free control of HIV-1.

PROOF-OF-CONCEPT HIV-1 CURE

Although an HIV-1 cure that's easy to administer, affordable and, most importantly, widely available is still far from sight, researchers have rare opportunities to learn from the handful of individuals that have reportedly been cured from HIV-1 or from those who exceptionally control HIV-1 in the absence of ART (post-treatment controllers).

Stem cell transplantation

Five cases of HIV-1 cure to date have resulted from stem cell transplantations using cells from donors with a C-C chemokine receptor type 5 (CCR5) Δ32 genetic mutation, which renders cells almost impervious to HIV-1 infection. Timothy Ray Brown, referred to as the Berlin patient, received chemotherapy, total body irradiation, and two stem cell transplants to treat an underlying acute myeloid leukemia. He was reportedly cured in 2009 and he remained free of any signs of HIV-1 infection for more than a decade until his death following a relapse of his

leukemia [89]. The second case of HIV-1 cure, Adam Castillejo (referred to as the London patient), was reported in 2019 following a CCR5 Δ32 stem cell transplant to treat his Hodgkin lymphoma [90]. He received a reduced intensity preparatory chemotherapy but no irradiation prior to his transplant. He has remained HIV-1 free since he interrupted ART in 2017. Additional cases of HIV-1 cure are the New York patient [91], the City of Hope patient (first reported in July 2022), and the Dusseldorf patient (now known to be Marc Franke), confirmed in February 2023 [92]. The City of Hope and Dusseldorf cases received CCR5 Δ32 stem cell transplants to treat their myeloid leukemia and have not shown signs of viral rebound since interrupting ART for more than two years. The New York patient, the first woman reported cured of HIV-1, received CCR5 Δ32 stem cells from cord blood combined with adult stem cells from a relative, which was the first such haplo-cord blood transplant leading to a potential HIV-1 cure [91]. She has shown no signs of HIV-1 infection since interrupting ART for more than 18 months (reported in March 2023).

Quite interestingly, a new case reported in July 2023 (International AIDS Society Conference 2023), referred to as the Geneva patient, received wild-type donor cells, which are not resistant to HIV-1 infection as the donor cells with CCR5 Δ32 genetic mutation used in the other cure cases. Although the virus remains undetectable 20 months after interrupting ART, it is yet to be confirmed whether the Geneva patient has in fact been cured or is actually a case of post-treatment control. Two landmark studies to date (CHAMP and VISCONTI) identified several individuals that maintain control of HIV-1 after stopping ART either at low levels or undetectable (≤ 400 copies/mL) at two-thirds of time points or more for ≥24 weeks [93,94]. The mechanisms that may mediate ART-free post-treatment control are not fully understood and warrant further research.

Cell and Gene therapy

Indeed, the CCR5 receptor, which enables HIV-1 entry and infection of cells, has been central to the stem cell transplantation-based HIV-1 cures reported to date. CCR5 thus remains a prime target in alternative cellular immune therapy approaches (e.g., CCR5 blockade using monoclonal antibodies and/or antagonists e.g., Maraviroc). Moreover, monoclonal antibodies targeting CCR5 can also induce antibody-dependent cellular cytotoxicity (ADCC), leading to the killing of HIV-1-infected cells by immune effector cells such as NK cells and macrophages.

Gene therapy-based interventions using gene editing tools such as CRISPR/Cas9, can be used to disrupt the CCR5 gene in CD4+ T cells or hematopoietic stem cells, rendering them resistant to HIV-1 infection. This approach mimics the natural

resistance observed in individuals with the CCR5 Δ32 mutation. Clinical trials have explored the *ex vivo* modification of patient-derived CD4+ T cells using CRISPR/Cas9 to disrupt the CCR5 gene and confer resistance to HIV-1 infection. These genetically modified cells are then infused back into the patient as a potential HIV-1 therapy [97-99].

Overall, these innovative approaches targeting CCR5 offer promising strategies for controlling HIV-1 infection and reducing latent HIV-1 viral reservoirs in PLWH. Immunotherapeutic interventions, which might include the (combinatorial) use of CCR5 blockade and other therapies such as broadly neutralizing monoclonal antibodies (bNAbs), Bispecific T cell Engagers (BiTEs) and Dual-Affinity Re-targeting Molecules (DARTS), immune checkpoint antibodies, immunomodulatory compounds or therapeutic vaccination, may have an important role in the development of a viable cure for HIV-1 infection (reviewed in [84,86]). However, continued research is needed to optimize these therapies and assess their long-term safety and efficacy in diverse patient populations.

ASSESSING HIV-1 RESERVOIRS IN EXPLORATIVE HIV-1 CURE STRATEGIES

Eliminating the vast majority of, if not all, latent, replication-competent HIV-1 proviruses, which fuel viral rebound, is likely crucial to achieve a cure for HIV-1 infection. However, robust and accurate biomarkers of the latent, replication-competent HIV-1 reservoir and responses to intervention are lacking, which complicates the evaluation of combination interventions [100]. Analytical ART interruption (ATI) and intensive plasma HIV-1 RNA monitoring (time to viral rebound and evaluating the magnitude of viral setpoint), while raising debatable ethical concerns, is thus the most definitive approach to assess the efficacy of therapeutic strategies designed to control HIV-1 in absence of ART [101,102].

HIV-1 reservoir technologies

The success of putative HIV-1 cure intervention trials demands the ability to evaluate the magnitude and dynamics of the latent, replication-competent HIV-1 reservoir before and after such interventions to guide ART interruption. Numerous techniques, which assess different aspects of the provirus and its functionality, have been developed and used to quantitate and qualitatively characterize HIV-1 reservoirs in samples from PLWH on suppressive ART [32,103-106]. However, these assays often produce divergent results leading to inconclusive interpretation of research findings. Discordant findings can be attributed to several factors. While majority of

persistent proviruses in ART-treated PLWH are defective and unable to replicate, not all intact genomes are inducible to produce infectious virions [43,51]. Moreover, the frequency of latently infected cells is very low, requiring large blood sample volumes to increase the likelihood of precise and accurate detection of viral reservoirs. Most importantly, the vast majority of HIV reservoirs are in tissues that cannot be accurately sampled with current specimen collection approaches. However, there are some recommendations on which viral reservoir measurements to prioritize in HIV-1 cure intervention trials (Reviewed in[107]). The need to simultaneously assess the HIV-1 reservoir at different molecular levels (i.e., at proviral DNA, RNA, and protein, virus) necessitates large blood draws (>100 mL) and leukapheresis sampling when culture-based assays such as the viral out growth assay, RNA and protein induction assays, and integration site analyses are intended [107].

HIV-1 DNA assays

Single amplicon PCR-based assays have for a long time been used to determine the fraction of cells harboring total or integrated HIV-1 DNA. Although practical, these assays considerably overestimate the size of the latent, viral reservoir. Recently, digital PCR-based technologies have been exploited to quantitate intact copies of viral DNA (Intact proviral DNA Assay, IPDA) and (intact) viral RNA transcripts through multiplexing assays that detect more than one region of the HIV-1 genome [108-110], which increases target specificity and overall assay accuracy. Furthermore, single genome/proviral sequencing assays (e.g., FLIP-seq [111] and MIP-seq[112]) enable a comprehensive characterization of HIV-1 populations resulting from different selective pressures related to cell type, tissue type, compartment or therapy [113].

HIV-1 RNA assays

Since proviral DNA sequence intactness alone is not a direct measure of inducibility (let alone replication-competence), which greatly depends on viral integration sites and therein the potential for viral expression, it is necessary to couple IPDA measurements with viral inducibility measurements such as quantitation of cell-associated HIV-1 RNA species (for instance, unspliced HIV-1 RNA, multiply spliced RNA, and mature transcripts with poly-A tails) (Fig. 5), which can be detected using quantitative PCR (qPCR) or digital PCR-based technologies [110,114]. Quantification of cell-associated HIV RNA is one of the most important and commonly used methods to evaluate efficacy of latency reversal agents (LRAs), which are explored in shock and kill approaches [115]. Copies of unspliced HIV-1 RNA, measured by RT-qPCR, are often normalized to internal reference genes or to cell number [116]. Fold-changes in unspliced HIV-1 RNA transcripts pre and post LRA intervention are used to evaluate LRA efficacy.

Single molecule assays

Cell-free plasma HIV-1 RNA using single copy assays may also be used to measure HIV-1 latency reversal. In addition, ultrasensitive single molecule assays could be used to measure the induced expression of HIV-1 Gag p24 protein (e.g., p24 SIMOA) [113,117].

Single cell assays

Recent technological advancements have enabled simultaneous measurements of cell associated HIV-1 RNA (unspliced, multiply spliced), protein (e.g., Gag p24 protein) in different cell populations by fluorescent *in situ* hybridization coupled to flow cytometry [118-120]. These single cell approaches are a powerful tool to assess the effect of LRAs, immune modulatory compounds or apoptosis inducing agents in distinct CD4+ T cell subpopulations and allow for simultaneous phenotypic characterization of viral reservoir cells [66,121]. However, major caveats of these assays include their limited scalability, low throughput, and requirement for vast input number of target cells.

Detection of multiply spliced HIV-1 RNA

Majority of genomes harbor large internal deletions of hypermutations in the 3' end of the proviral genome and multiply spliced HIV-1 RNA is more likely to be expressed from intact rather than defective genomes [43] (Fig 5). Thus, detection of multiply spliced HIV-1 RNA has been incorporated into several techniques to enable quantification of latent, inducible viral reservoirs, as a surrogate marker for the latent, replication-competent viral reservoir. One such assay, *tat/rev*-induced limiting dilution assay (TILDA, [Fig. 6]) [123,124] has been widely applied in various studies using cells from blood and tissue specimen collected from PLWH and non-human primates. The assay detects *tat* and *rev* transcripts that are produced by the splicing of the HIV-1 RNA genome (the two *tat* and *rev* exons are located on opposite sides of *env*-gp120 gene). HIV-1 Tat protein is a potent activator of viral transcription [72,125], whereas HIV-1 Rev protein regulates the export of unspliced HIV-1 RNA from the nucleus [126,127]. A large number of defective HIV-1 genomes have deletions and mutations in the *tat/rev* regions [43] thus *tat/rev*-based assays greatly reduce the likelihood of detecting defective proviruses and minimize quantification bias.

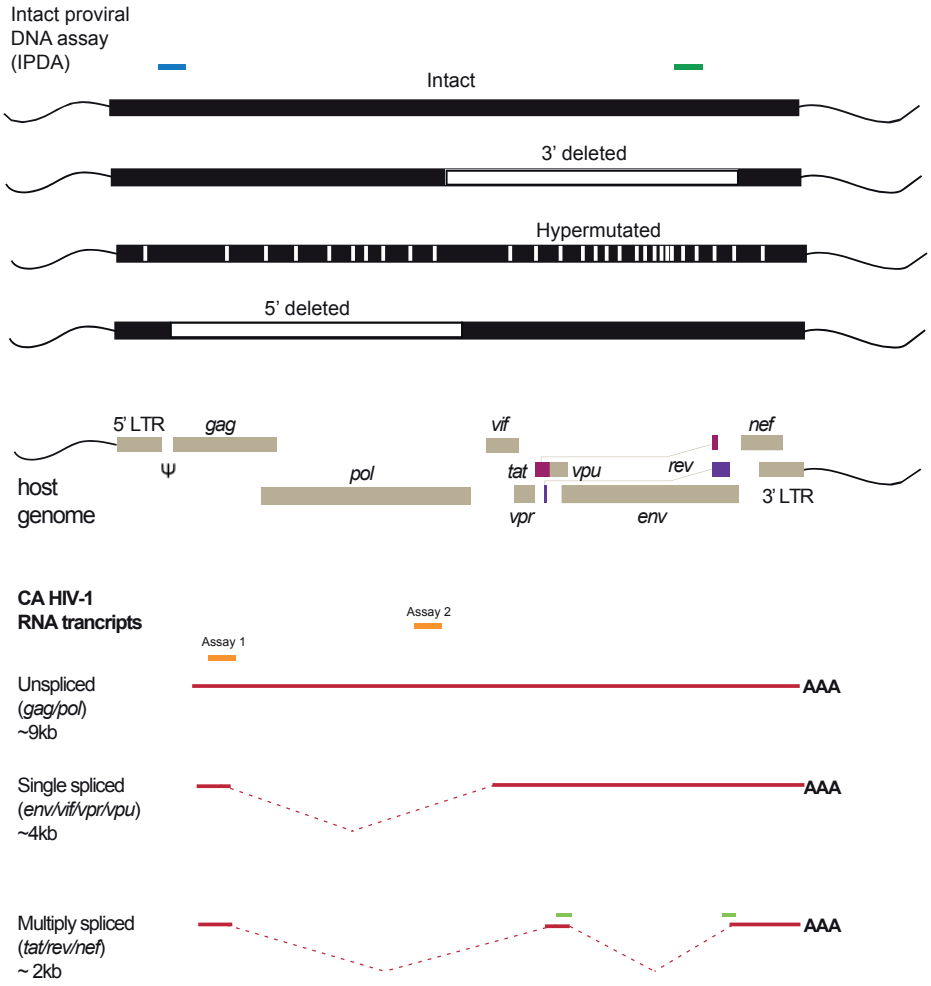

Fig. 5. Genomic organization of HIV-1 and schematic overview of viral reservoir assay targets. The dual probe intact proviral DNA assay (IPDA) targets the conserved packaging signal sequence (φ) and the *rev* response element (RRE) within the *env* gene. Cell associated HIV-1 RNA assays for unspliced HIV-1 RNA target conserved regions in *gag* or *pol* gene. Single Gag/pol probes assays will inclusively detect defective viral RNA genomes. Multiply spliced RNA probe assays at the splice junction of *tat* and *rev* genes will exclusively detect multiply spliced RNA, excluding genomic RNA and genomic DNA. Figure adapted from [108] and [122]

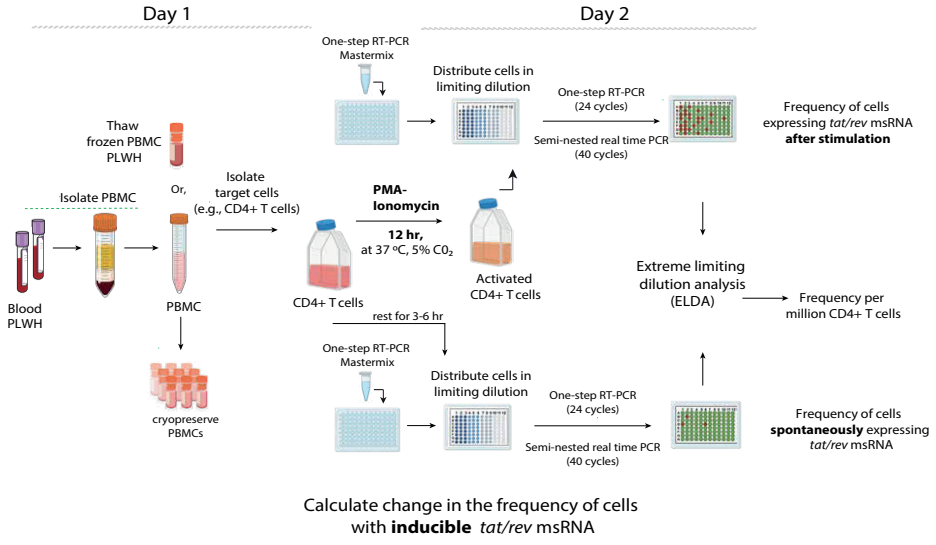

Fig. 6. Tat/rev Induced Limiting Dilution Assay – TILDA workflow. Figure adapted from [124]: **Lungu C.** and Procopio F.A. Methods Mol Biol. (2022);2407:365-372

TILDA typically requires a very low input number of cells (<2 million CD4+ T cells) and has a faster turnaround time, completed in two days, in comparison to quantitative viral outgrowth assays that require up to three weeks. Moreover, for a PCR-culture based assay, TILDA has shown good inter-assay and inter-laboratory reproducibility (Fig. 7) [128].

Initial evaluations demonstrating negligible inter-laboratory variability of TILDA, despite limited protocol modifications to improve technical operation, supports the application of TILDA for reservoir quantification and cross-comparison of results [128]. However, further research is warranted to investigate TILDA's suitability for measuring HIV-1 reservoir dynamics in HIV cure-focused interventions. The clinical relevance, applications, advancements of TILDA, and how the assay has thus far contributed to our understanding of HIV-1 persistence is reviewed in Chapter 1.1 [129].

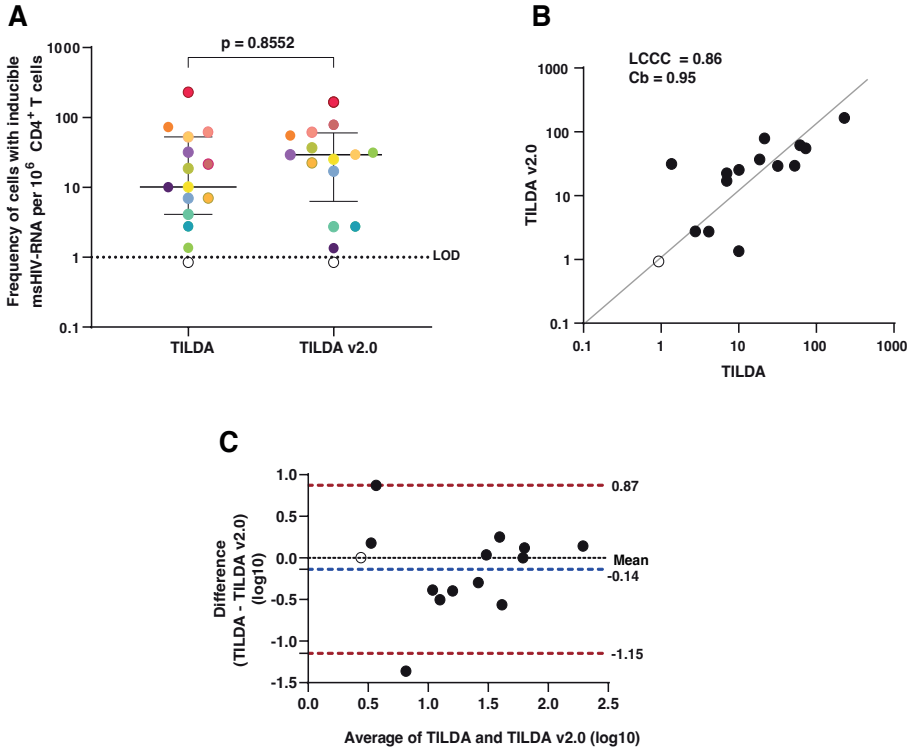

Fig. 7. TILDA inter-laboratory reproducibility. (**A**) The frequency of CD4+ T cells expressing *tat/rev* msRNA after in vitro stimulation with PMA/Ionomycin in a subset of individuals (*N* = 15), quantified by TILDA and TILDA v2.0. Each individual is represented by a different colored dot. The open circles are below the LOD. Wilcoxon's matched-pairs test was used to compare the medians. Statistical significance is determined by $p < 0.05$. (**B**) Lin's Concordance Correlation Coefficient (LCCC) plot. The black dots represent inducible reservoir size quantified by TILDA and TILDA v2.0. The open circle is below the LOD. The grey diagonal line represents the best-fit line. Coefficient of bias (Cb) is a measure of accuracy. (**C**) Bland–Altman plot using log-transformed inducible reservoir size measurements by the two assays. The open circle is below the LOD. The blue dotted line represents the mean bias, and the red dotted lines represent the 95% limits of agreement. Figure sourced from[128]: **Lungu C.** et al., Viruses. (2020) Sep 2;12(9):973.

CHAPTER 1.1

Inducible HIV-1 reservoir quantification: clinical relevance, applications and advancements of TILDA

C. Lungu, R. Banga , R. A. Gruters and F. A. Procopio

Lungu C., Banga R., et. al., Front Microbiol. 2021 Jun 15;12:686690. Doi: 10.3389/fmicb.2021.686690

ABSTRACT

The presence of a stable HIV-1 reservoir persisting over time despite effective antiretroviral suppression therapy precludes a cure for HIV-1. Characterizing and quantifying this residual reservoir is considered an essential prerequisite to develop and validate curative strategies. However, a sensitive, reproducible, cost-effective, and easily executable test is still needed. The quantitative viral outgrowth assay (QVOA) is considered the gold standard approach to quantify the reservoir in HIV-1-infected patients on suppressive ART, but it has several limitations. An alternative method to quantify the viral reservoir following the reactivation of latent HIV-1 provirus detects multiply-spliced tat/rev RNA (msRNA) molecules by real-time PCR (tat/rev induced limiting dilution assay [TILDA]). This article provides a perspective overview of the clinical relevance, various applications, recent advancements of TILDA, and how the assay has contributed to our understanding of the HIV-1 reservoir.

INTRODUCTION

Over the past decade, multiple interventions to reduce or eliminate the latent HIV-1 reservoir have been proposed. A prominent strategy is to pharmacologically reactivate latently infected cells through so called latency reversal agents (LRAs) in conjunction with immune-modulating interventions to enhance extrinsic immune-based clearance or induce intrinsic apoptosis of reactivated cells[130]. Other eradication strategies include genome editing of target molecules such as the HIV co-receptor *CCR5* [131] or on the HIV-1 genome itself using CRISPR/Cas9 [132] (reviewed in [133]) or Zinc finger nucleases [134]. "Block and lock" strategies using pharmacological compounds [135,136] or via therapeutic vaccination using broadly neutralizing monoclonal anti-HIV-1 antibodies (bNAbs) [137] to permanently silence the provirus have also been proposed. The advent of these strategies has prompted the development of several methods to quantify the HIV-1 reservoir and validate the effectiveness of potential cure interventions. However, existing cure strategies require further optimization and new assays with higher sensitivity, accuracy, precision, and reproducibility [106] are urgently needed.

A panel of latent HIV-1 reservoir assays have been recommended for use in HIV-1 cure intervention trials (reviewed in[107]). The quantitative viral outgrowth assay (QVOA), currently considered the reference assay for quantifying the replication-competent HIV-1 reservoir[138], quantifies the number of resting $CD4^+$ T cells releasing infectious virus after *in vitro* stimulation and subsequent co-culture with feeder cells[139,140]. However, the widespread use of QVOA in clinical trial settings is precluded by several factors related to the complexity of the assay (large blood draws, high variability [recently evaluated in the RAVEN studies [141,142]], labor intensity, and execution time [14-21 days]). Moreover, QVOA underestimates the size of the reservoir and has a low dynamic range [43]. Several efforts to improve QVOA (sensitivity and dynamic range, assay turn-around time, and overall costs) have been implemented [105,117,143,144]. A general concern, however, is that QVOA protocol modifications further complicate assay standardization [142].

Alternatively, real-time or digital PCR-based methods, which are better suited for large clinical trials, have widely been used to detect HIV-1 DNA in infected cells from peripheral blood and lymphoid tissue cells [145-148]. Although these methods are relatively easy to perform, fast, and cost-effective, they overestimate the reservoir size because most integrated HIV-1 genomes are not replication-competent [43]. Advanced HIV-1 DNA quantification methods such as the intact proviral DNA assay (IPDA) [108] and Q4PCR [149], distinguish intact proviruses from defective ones thereby providing a better resolution for studying the dynamics of defective and intact HIV-1 proviral DNA [36,37,150]. However, proviral intactness does not guarantee virion

production[43,51], and the fraction of intact proviruses that can be induced to produce virions cannot be determined by these assays, which is a critical limitation given that many intact proviruses exhibit low inducibility [43,51]. In long-term ART-suppressed people living with HIV (PLWH), intact HIV-1 proviruses are preferentially integrated in an opposite orientation to host genes, in relative proximity or increased distance from active transcriptional start sites and accessible chromatin regions [112].

The transcription-competent (inducible) HIV-1 reservoir can be quantified by several methods [105,151-153] including an approach developed by Procopio *et al*. [123], which detects multiply-spliced *tat/rev* RNA (msRNA) molecules by real-time PCR (*tat/rev* induced limiting dilution assay [TILDA]), and reduces the likelihood of quantifying defective genomes [39,40,123]. The percentage of intact proviruses capable of producing *tat/rev* msRNA transcripts is uncertain but a recent study showed no association between inducible HIV-1 measures (TILDA, p24 SIMOA) and IPDA-intact proviruses but with IPDA-total measures[154]. TILDA correlates poorly with QVOA[123,142], which may be explained by several factors including: technical (inherent assay variation, poor sensitivity); differences in provirus inducibility[43,51]; the biological targets measured as readouts (*tat/rev* msRNA [TILDA] and HIV-1 p24 *gag* RNA or Gag protein [QVOA]) [105]; *tat/rev* msRNA is measured after 12-18 hours of activation, whereas QVOA measurements are taken after 7-14 days of culture and virus production. TILDA probes total $CD4^+$ T cells, whereas QVOA uses sorted resting CD4+ T cells. Furthermore, due to post-transcription blocks in RNA processing [114], not all cells producing *tat/rev* msRNA transcripts will yield infectious virus[155], and therefore quantifying these cells overestimates the replication-competent HIV-1 reservoir size. Despite these discrepancies and limitations, TILDA is a well-established approach to quantify the inducible HIV-1 reservoir as a proxy for replication competence, and a technically feasible alternative to QVOA for routine execution in large scale HIV-1 cure intervention trials (requires less blood, shorter assay turn-around time [2 days], medium throughput). In this article we provide a perspective overview of the clinical relevance, various applications, and recent advancements of TILDA, and how the assay has contributed to our understanding of the HIV-1 reservoir.

PRINCIPLE OF THE *TAT/REV* INDUCED LIMITING DILUTION ASSAY (TILDA)

The fundamental steps in performing TILDA as published by Procopio *et al*. [123] include: (i) isolation of CD4+ T cells from 10 mL blood collected from HIV-1-infected individuals; (ii) *in vitro* stimulation for 12 hours with 100 ng/mL phorbol 12-myristate 13-acetate (PMA) and 1 µg/mL ionomycin to induce production of *tat/rev* msRNA;

(iii) distribution of cells in a limiting dilution scheme (24 replicates of 1.8 x10^4 to 1.0 x10^3 cells per well) in a 96-well plate containing a one-step reverse transcription PCR (RT-PCR) master mix, which bypasses RNA extraction, allowing simultaneous RT and pre-amplification of *tat/rev* msRNA; (iv) quantification of *tat/rev* msRNA using a diluted fraction of the pre-amplification product; v) estimation of the frequency of *tat/rev* msRNA+ cells using maximum likelihood method[156]. TILDA has a limit of detection of ~1 cell expressing *tat/rev* msRNA per million CD4+ T cells, a coefficient of variation of ~20%[123,128], and correlates with various assays to measure latency, reactivation and reservoir (total and integrated HIV DNA, p24 SIMOA, HIV FISH-Flow) [123,157]. In-depth comparisons of these assays have been reviewed elsewhere[103,106,107,138].

CLINICAL RELEVANCE OF INDUCIBLE HIV-1 RESERVOIR QUANTIFICATION BY TILDA

In ART-suppressed PLWH, the median frequency of latently infected CD4+ T cells estimated by TILDA is ~24 per million CD4+ T cells[123,128,157], 48 times larger than the frequency measured with QVOA. Nevertheless, the median frequency of intact, non-induced proviruses is reported to be 60-fold higher than the frequency of induced proviruses detected in QVOA[43]. The chromosomal integration site is a critical factor determining provirus inducibility and there is recent evidence that long-term ART-suppressed PLWH harbor intact proviruses with features of deeper viral latency[85,112]. TILDA readouts therefore serve as intermediate, surrogate measures for the frequency of latently infected cells harboring replication-competent HIV-1. Procopio *et al*. demonstrated that the size of the inducible HIV-1 reservoir was smaller in subjects who initiated ART during acute HIV infection (AHI) when compared to those who began therapy at a later stage of the disease (median frequencies of 11 and 29 cells per million CD4+ T cells in acute and chronic infection respectively) [123]. This trend has also been shown in other studies using QVOA and HIV-1 DNA (total and integrated) [35,158]. Notably, the frequency of cells with inducible msRNA in most samples obtained from individuals who initiated ART during Fiebig stages I to III is even lower [68], nearing or below the TILDA limit of detection[14,68,70]. Comparing TILDA estimates before and after stimulation of CD4+ T cells obtained from ART-naïve individuals, most infected cells (81.4%) were latently infected and produced msRNA only after stimulation. In contrast, merely 18.6% of the infected cells spontaneously produced msRNA[123]. Therefore, similarly to ART-suppressed PLWH, ART-naïve individuals harbor a large pool of latently infected CD4+ T cells. Moreover, the frequency of latently infected CD4+ T cells in ART-naïve individuals positively correlated with the duration of HIV-1 infection, which suggests that the size of the latent and inducible reservoir increases over time in ART-naïve

individuals as a result of continuous seeding of the HIV-1 reservoir[123]. A recent study reported a correlation between the inducible HIV-1 reservoir measured by TILDA and the CD4/CD8 ratio[159], an important clinical parameter reflecting the immune system's functionality and linked to reservoir size [160,161].

APPLICATION OF TILDA IN HIV-1 CURE INTERVENTIONS

Evaluating latent HIV-1 reservoir reactivation and elimination using TILDA

Transcriptional activation of HIV-1 provirus from latently infected cells using LRAs and subsequent immune-mediated clearance is viewed as one of the most promising approaches towards HIV-1 eradication. During the last years, multiple LRAs have been tested *in vitro* and *ex vivo*, and in combination with other interventions in clinical trials [reviewed in [162,163]]. In two clinical trials evaluating depsipeptide romidepsin's latency reversal potential *in vivo*, no substantial changes in HIV-1 reservoir size could be observed by total HIV-1-DNA quantification, QVOA, or TILDA[164], despite detectible HIV-1 viral reactivation measured using standard plasma HIV-1 RNA assays. In another *in vivo* clinical study, the histone deacetylase inhibitor vorinostat induced a sustained increase of CA unspliced HIV-1 RNA from CD4+ T cells from the blood. Still, there was no significant change in plasma HIV-1 RNA or HIV-1 reservoir size measured by TILDA and HIV-1 DNA (total and integrated) [165]. These and other studies highlight that while it is possible to disrupt HIV-1 latency in patients on suppressive ART, the LRA interventions so far have not significantly impacted the latent HIV-1 reservoir size or time to viral rebound (reviewed in [163]).

All considered, TILDA could be valuable in LRA studies; the initial step of viral reactivation is the early expression of *tat* and *rev* RNAs, the assay's primary targets. Therefore, TILDA would be an ideal screening tool to validate promising compounds. For instance, TILDA contributed to defining a new class of novel pure phorbol ester-class compounds, isolated from an African medicinal plant (Mukungulu) [166], with the capacity to promote HIV-1 latency reversal *ex-vivo* in J-Lat cells containing an HIV-1-GFP provirus[167]. TILDA results could also be used to differentiate T cell populations with large and small inducible HIV-1 reservoirs. In multiple studies, TILDA revealed that CD4+ T effector memory cells harbor the largest inducible HIV-1 reservoir in peripheral blood when compared to CD4+ T central memory cells and CD4+ T transcriptional memory cells[168,169]. This finding suggests the possibility to induce the differentiation toward effector memory cells as a strategy to increase the HIV-1 reservoir susceptibility to LRAs[111,170-172], and TILDA may be useful for measuring the effects of such novel approaches. Furthermore, innovative

strategies to enhance killing mechanisms in different T cell populations are gaining more attention [reviewed in[84]]. Several recent studies have demonstrated the use of pharmacological compounds that selectively induce cell apoptosis in HIV-1-infected cells as a strategy to eliminate these cells[173-175]. In a study by Rao *et al.* [66], CD4+ T cells obtained from ART-suppressed HIV-1-infected individuals were cultured for five days in the absence or presence of DDX3 inhibitors. The addition of DDX3 inhibitors resulted in a reduction (~50%) of the inducible HIV-1 reservoir, determined by quantifying CA HIV-1 RNA, the frequency of cells expressing *tat/rev* msRNA (TILDA), and the frequency of cells positive for *gag* RNA using FISH-flow[66].

Characterizing latently infected cells using TILDA

The elimination or reduction of HIV-1-infected cells is a priority towards an HIV cure. Unfortunately, there is not a specific biomarker for the identification of infected cells. It is well known that CD4+ memory T cells[176] and CD4+ T cells with stem cell-like properties[158] in peripheral blood, and follicular helper T (Tfh) cells (PD-1^{high}/CXCR5^{high}) and memory CD4+ T cells[177] in lymph nodes are enriched in cells harboring replication-competent HIV-1. These cell populations share multiple co-inhibitory molecules (immune checkpoints, ICs), which down-modulate the immune response and prevent hyper-immune activation. ICs are typically upregulated after T-cell activation, and their overexpression is associated with T-cell exhaustion in cancer and chronic viral infections, including HIV-1[178-180]. A recent study identified PD-1, TIGIT, and LAG-3 as ICs, which are positively associated with the frequency of CD4+ T cells harboring integrated HIV-1 DNA[168]. Notably, the same populations were three-fold more positive for *tat/rev* msRNA when compared to the PD-1^{neg}, TIGIT^{neg}, and LAG-3^{neg} CD4+ T cell populations, suggesting that resting or exhausted cell status favors HIV-1 persistence. integrated HIV-1 DNA, TILDA, and plasma HIV-1 RNA measurements were also used to characterize the HIV-1 reservoir in another study that aimed to identify molecular signatures that may support the role of Tfh cells as a significant compartment for HIV-1 persistence[181]. Notably, BCL6 gene expression, which is the master regulator of Tfh cell differentiation and modulator of a series of other transcription factors and their downstream targets, positively correlated with integrated HIV-1 DNA as well as TILDA and plasma viral load[181]. Multiple studies demonstrate that α4β7-expressing cells represent early targets for HIV-1 and that pre-infection frequencies of α4β7 on circulating CD4+ T cells may predict the risk of HIV-1 acquisition and disease progression[182-185]. In a phase I clinical trial to study the impact of anti-α4β7 monoclonal infusion on HIV-1 reservoir size TILDA was used to determine change in inducible reservoir size after treatment. A reduction in msRNA post-treatment was observed in two out of four donors, but the low sample size impaired the test's statistical significance[186].

TILDA ADVANCEMENTS

Broadening the detection of *tat/rev* msRNA beyond HIV-1 Clade B

High sequence diversity in the *tat/rev* region demands the modification of primers and probes to increase TILDA's specificity for different HIV-1 clades. In its original design, TILDA optimally quantifies the HIV-1 reservoir in individuals infected with clade B[123], the dominant clade in North America and Europe. This primer and probe restriction is a limitation considering that 46.6% of HIV-1 infections worldwide are clade C, the most dominant HIV-1 clade in Africa[187]. Given this, C-TILDA was recently developed with primers and probes modified specifically for clade C viruses[159], which extends the possibility of screening other HIV-1-infected populations and implementing the assay in eradication strategies in regions where clade C is more abundant. In two other studies, primers and probes were designed to efficiently amplify *tat/rev* msRNA for clade A/E, A1, and A/G viruses as well[14,188]. We aligned the published TILDA primer and probe sequences to a consensus sequence generated from 2695 global HIV-1 sequences downloaded from the Los Alamos HIV-1 sequence database (Fig. 1). The highest degree of variability is evident in the Tat 2.0 forward primer in which 9/34 positions have <80% (39.2–63%) identity to consensus. Further studies should validate a generalized approach using combinations of primer and probe sets for these and other circulating HIV-1 subtypes, broadening the detection and increasing the assay's applicability.

Indeed, non-human primate (NHP) models are critical to test novel therapeutic strategies and better understand the HIV-1 reservoir[76,189]. Considering the limited number of cells available, performing QVOA is impractical in NHP studies, therefore Frank *et al*. developed a simian version of TILDA (termed SIV/SHIV-1 TILDA) to detect msRNA of SIVmac251/mac239 and SHIV-1_{AD80E} viruses, which are widely employed in NHP studies[190]. The SIV/SHIV-1 TILDA could detect msRNA also in the setting of very low/undetectable viremia. Interestingly, in animals that started ART early after infection, the results from reservoir estimation by TILDA correlated with the viral rebound post ART interruption[190].

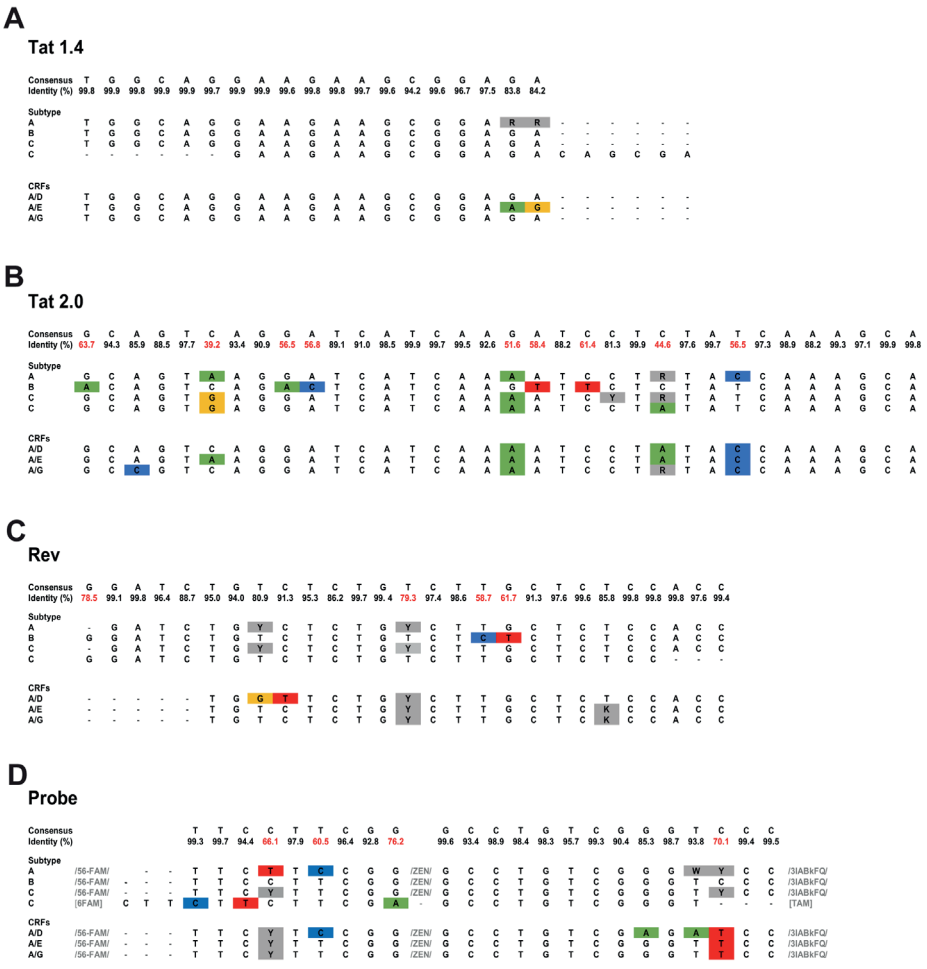

Fig.1. **Sequence analysis of TILDA primers and probes specific for different HIV-1 subtypes.** TILDA primer and probe sequences were retrieved from literature [HIV-1 subtype: A [188], B [123], C [159,188], A/E [14], A/D and A/G [188]] and aligned to a consensus sequence generated from an alignment of 2695 HIV-1 sequences downloaded from the Los Alamos HIV-1 sequence database. Nucleotide substitutions are colored blue, green, yellow, and red. Nucleotide positions with degenerate bases are colored grey. The least conserved nucleotide positions (<80% identity) are marked in red.

Improving TILDA Sensitivity

A major advantage of TILDA is the direct amplification of *tat/rev* msRNA from whole cell lysate. However, the cell lysate complexity itself can reduce the signal to noise ratio impacting overall *tat/rev* msRNA amplification efficiency. To improve msRNA detection, a new TILDA protocol that includes an RNA extraction step was developed, the results of which strongly correlated with those of the original

protocol[191]. In a recent study, activating cells with phytohemagglutinin for an extended period (18 hours instead of 12 hours) enhanced the expression of *tat/rev* msRNA in CD4+ T cells isolated from infants living with HIV-1[188]. Several studies have shown that the frequency of cells that could be induced to express HIV-1 msRNA is small in most individuals treated during AHI (Fiebig stages 1-III) [14,68]. Furthermore, some long-term suppressed patients or elite HIV-1 controllers have significantly lower latent viral reservoirs[159,192-194]. In these cases, reservoir estimation using TILDA is technically challenging. A higher cell input is required to increase the assay's sensitivity, which can be achieved by increasing the number of replicates through processing multiple assay plates[123]. However, processing multiple TILDA plates per sample reduces assay throughput and increases the overall cost. To circumvent these limitations, maximizing the number of cells that can be probed per reaction is essential. In the recently developed C-TILDA[159], the authors increased cell input (up to 5.4 $x10^4$ cells per reaction instead of 1.8 $x10^4$) to maximize detection of *tat/rev* msRNA.

In another study, which assessed assay robustness and amenability for routine use in clinical studies of the latent reservoir, TILDA was performed using alternative RT-qPCR reagents according to a modified (TILDA v2.0) protocol[128]. Particularly, *tat/rev* msRNA pre-amplification reactions were carried out in larger volumes (10 µl instead of 1µl) to minimize pipetting imprecisions. Furthermore, the pre-amplification products were directly added to the real-time PCR mix to detect msRNA, which improves assay throughput by reducing the number of pipetting steps and minimizes the risk of cross-contamination associated with diluting PCR products[128]. In our preliminary assessment of TILDA v2.0 performance using a higher input number of ACH-2 or HIV-1-infected CD4+ T cells per reaction (7.2 $x10^4$ cells to1.4 $x10^5$ cells), resulting in six to eight-fold more cells per assay, improved target detection and precision (narrower 95% Confidence Intervals) when quantifying small reservoirs (Fig. 2). Further studies are necessary to assess TILDA or TILDA v2.0 reproducibility with these higher cell inputs, which require an increased total blood volume of 30-50 mL, and the capacity thereof to quantify inducible reservoirs below the current detection limits. Indeed, such validation studies would reveal more insight into TILDA's suitability for evaluating HIV-1 reservoir-reduction clinical interventions.

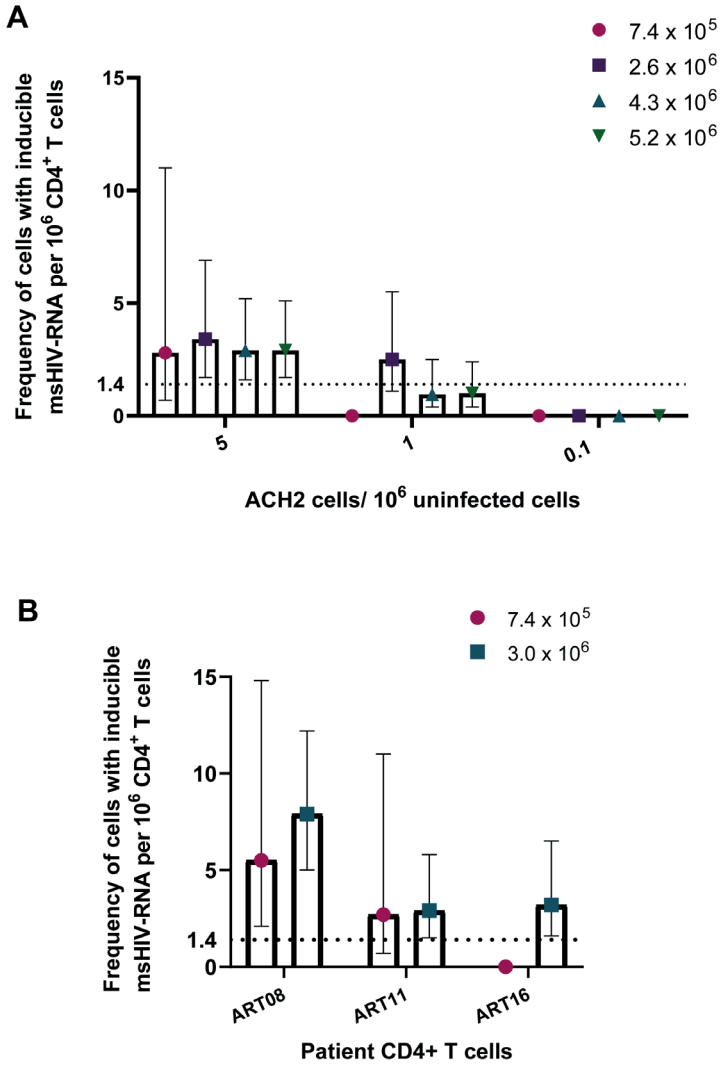

Fig. 2. Detection of tat/rev msRNA in low reservoir samples. (**A**) Target detection in three low concentrations of ACH-2 cells mixed with one million uninfected $CD4^+$ T cells. The total number of cells tested per plate ranged from 7.4 $x10^5$ cells - 5.2 $x10^6$ cells (**B**) CD4+ T cells obtained from three ART-suppressed individuals (plasma HIV RNA <20 c/mL) were stimulated with PMA/ionomycin for 12-14 hours. The frequency of cells expressing tat/rev msRNA was determined using TILDA v2.0 [128] with standard (7.4$x10^5$ cells) or higher cell inputs (colored symbols). The mean estimates of inducible cells/10^6 $CD4^+$ T cells are plotted in both graphs. The error bars represent the 95% confidence interval upper and lower limits. The horizontal line represents the assay limit of detection (LOD) based on the standard cell input (7.4 $x10^5$ cells).

CONCLUSION

As we advance towards large, scalable clinical interventions to significantly deplete or permanently restrict inducible HIV-1 reservoirs in well-suppressed PLWH, TILDA stands out as a suitable option for implementation in the aforementioned HIV cure clinical trials. Within two days, inducible HIV-1 reservoir measurements can be generated using less than 1 x10^6 viable target cells per condition with the possibility to increase cell input (six to eight-fold [TILDA v2.0]) without significantly impacting overall assay costs. The assay is also very robust, as demonstrated in multiple studies to test intra- and inter-laboratory reproducibility, which is important for the cross-validation of results in multi-center, multi-laboratory clinical trials.

AUTHOR CONTRIBUTIONS

CL and FP conceptualized the perspective article. CL and FP researched the literature. CL performed the experiments and analyzed the data. CL and FP wrote the first draft of the manuscript. All authors read and approved the final manuscript**.**

FUNDING

This work is supported by EHVA, funded by the European Union's Horizon 2020 Research and Innovation Program (grant number 681032) and the Swiss Government (grant number 15 0337).

ACKNOWLEDGMENTS

In loving memory of Prof. Charles A.B. Boucher, who strongly supported HIV cure-related research endeavors and the implementation of innovative tools to evaluate HIV persistence in clinical settings. We also thank Dr Tokameh Mahmoudi and Dr Shringar Rao for helpful discussions.

SCOPE OF THE THESIS

As novel HIV-1 therapeutic trials continue advancing, there is a critical need for standardized, clinically validated HIV-1 reservoir assays to evaluate intervention efficacy. Established and emerging HIV-1 reservoir assays require rigorous evaluation of performance characteristics (sensitivity, specificity, reproducibility, scalability) and their relationship to the outcomes of pre-clinical and clinical HIV-1 cure studies. These studies are imperative to address key questions, which are critical to the evaluation of therapeutic interventions toward HIV-1 cure. Given the multifaceted nature of HIV-1 persistence, what molecular compartments of the latent HIV-1 reservoir should be prioritized (DNA, RNA, protein, virus?) and what tools should be used to monitor changes in these molecular compartments? (Fig. 8).

Furthermore, in context of a putative HIV-1 cure intervention, when should we sample to monitor changes in the latent HIV-1 reservoir and how frequent should we monitor? What is the short and long-term impact of an intervention on different molecular compartments of the HIV-1 reservoir and which of these measures of persistence are clinically significant? Thus, the research described in this thesis aims to address these critical questions surrounding the evaluation of novel putative strategies towards HIV-1 cure or ART-free viral control.

Multiply spliced RNA detection by the *tat/rev* induced limiting dilution assay (TILDA) is one of few established techniques that has been widely applied to determine the fraction of latently infected cells capable of expressing *tat/rev* msRNA, which is a promising surrogate indicator of HIV-1 replication-competence (reviewed in Chapter 1.1 [129]).

In Chapter 2, we advanced findings from promising *ex vivo* pre-clinical studies to evaluate the *in vivo* efficacy of a novel latency reversal agent (LRA) targeting the BAF complex, a chromatin remodeler, which was previously demonstrated to play a key role in HIV-1 latency establishment and maintenance. We conducted one of the first randomized controlled clinical trials to evaluate a combinatorial latency reversal strategy in 28 participants with HIV-1 on suppressive ART. Cell-associated HIV-1 RNA measurements were used to monitor changes in HIV-1 proviral transcription in response to two intervention drugs tested alone or in combination – pyrimethamine and valproic acid, which have been clinically approved for the treatment of other conditions. The *tat/rev* induced limiting dilution assay (TILDA) was applied to assess potential impact of the LRA intervention on the size of the latent, inducible HIV-1 reservoir. We prove the conceptual approach to induce HIV-1 latency reversal, via BAF complex inhibition, in ART-suppressed individuals.

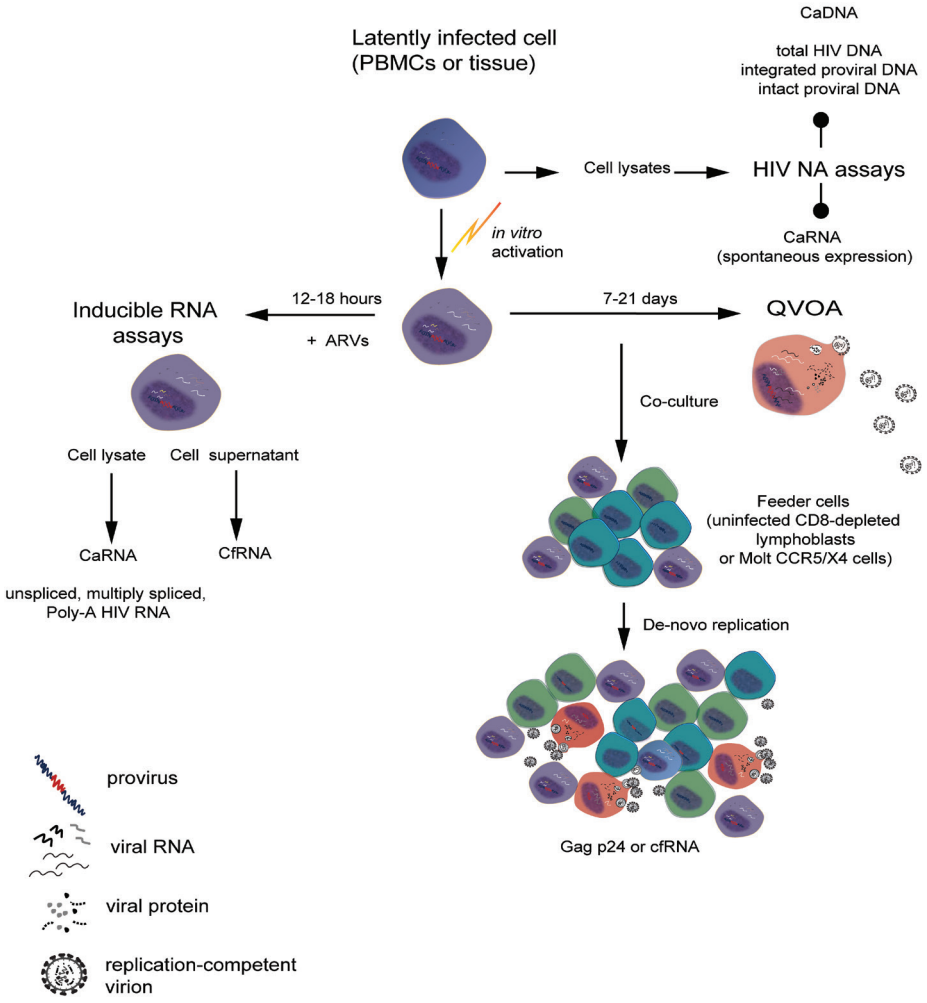

Fig. 8. Molecular levels and measures of HIV-1 persistence. Cell-associated HIV DNA (CaDNA) assays amplify single or multiple regions of the HIV-1 genome to measure total HIV-1 DNA or to distinguish intact from defective proviral genomes. Cell-associated RNA assays (CaRNA) on unstimulated cell lysates enable measures of spontaneous expression of viral transcripts (e.g., unspliced, multiply spliced RNA). RNA induction assays incorporate in vitro activation of target cells using various stimuli e.g., PMA/ionomycin, CD3/CD28 antibodies, and latency reversal agents (LRAs), in the presence of antiretrovirals (ARVs), to induce or enhance HIV-1 gene expression, which is measured by levels of unspliced, multiply spliced, mature poly-A HIV-1 RNA transcripts in cell lysates. Long-term co-culture of activated latently infected cells together with permissive feeder cells (uninfected CD8-depleted lymphoblasts or Molt CCR5/X4-expressing cell line) in absence of ARVs enables de novo rounds of replication and spread of infection to assess viral replication competence and infectivity (QVOA). Readouts in QVOA include viral RNA or viral protein quantitation.

In Chapter 3, we explored an alternative pharmacological approach to enhance the clearance of the inducible HIV-1 reservoir upon latency reversal. We evaluated the role of DDX3 inhibition in inducing selective cell apoptosis *ex vivo*. Proviral inducibility was determined by expression of unspliced and multiply spliced viral RNA using parallel HIV-1 reservoir techniques; single cell fluorescent *in situ* hybridization (Fish-flow) and TILDA, respectively. We demonstrate a novel role for DDX3 in HIV-1 latency reversal and a potential mechanism underlying the selective depletion of the inducible HIV-1 reservoir mediated by innate immune responses.

In Chapter 4, we mapped HIV-1 reservoir dynamics in different molecular compartments in peripheral blood CD4+ T cells from individuals who interrupted ART during an autologous dendritic cell vaccination trial that aimed to induce ART-free viral control. We enrolled study participants in a follow-up study more than a decade post ART interruption, viral rebound and subsequent ART-mediated viral re-suppression. Proviral intactness was assessed using the intact proviral DNA assay (IPDA) and proviral inducibility was assessed using RNA and/or protein induction assays (FISH-flow, one-step TILDA and SQuHIVLa). We observe discordant outcomes in the different molecular compartments of the latent HIV-1 reservoir with potential implications for monitoring HIV-1 reservoir dynamics in future immune based, combination ATI trials.

Chapter 5 summarizes the findings of the research described under the thematic areas; i) assessing HIV-1 proviral inducibility; ii) HIV-1 latency reversal *in vivo* ; iii) inducing apoptosis of HIV-1 reservoir cells *ex vivo* ; and iv) impact of immune-based approaches towards ART-free control.

Chapter 6 describes the implications of the findings from the research described in this thesis, which relate to HIV-1 subtype B infection and viral persistence in peripheral blood CD4+ T cells. Moreover, the translational studies described herein were conducted in male, predominantly Caucasian, participants. Therefore, the findings from this work cannot be generalized to all people living with HIV-1. There are tremendous gaps in our understanding of HIV-1 persistence in diverse populations, particularly in high HIV-1 burdened, resource-constrained settings in Sub-Saharan Africa. I highlight emerging insights and key factors to consider in applying latent HIV-1 reservoir technologies in resource-constrained laboratory settings in the Global South.

CHAPTER 2

The BAF complex inhibitor pyrimethamine reverses HIV-1 latency in people with HIV-1 on antiretroviral therapy

H. A. B. Prins†, R. Crespo†, **C. Lungu**†, S. Rao, L. Li, R. J. Overmars, G. Papageorgiou, Y. M. Mueller, M. Stoszko, T. Hossain, T. W. Kan, B. J. A. Rijnders, H. I. Bax, E. C. M. van Gorp, J. L. Nouwen, T. E. M. S. de Vries-Sluijs, C. A. M. Schurink, M. de Mendonça Melo, E. van Nood, A. Colbers, D. Burger, R.J. Palstra, J. J. A. van Kampen, D. A. M. C. van de Vijver, T. Mesplède, P. D. Katsikis, R. A. Gruters, B. C. P. Koch, A. Verbon, T. Mahmoudi†, C. Rokx†

†These authors contributed equally to this work.

Prins H.A.B., Crespo R., Lungu C., et al Sci Adv. 2023 Mar 17;9(11):eade6675. doi: 10.1126/sciadv.ade6675

ABSTRACT

Reactivation of the latent HIV-1 reservoir is a first step toward triggering reservoir decay. Here, we investigated the impact of the BAF complex inhibitor pyrimethamine on the reservoir of people living with HIV-1 (PLWH). Twenty-eight PLWH on suppressive antiretroviral therapy were randomized (1:1:1:1 ratio) to receive pyrimethamine, valproic acid, both, or no intervention for 14 days. The primary end point was change in cell-associated unspliced (CA US) HIV-1 RNA at days 0 and 14. We observed a rapid, modest, and significant increase in (CA US) HIV-1 RNA in response to pyrimethamine exposure, which persisted throughout treatment and follow-up. Valproic acid treatment alone did not increase (CA US) HIV-1 RNA or augment the effect of pyrimethamine. Pyrimethamine treatment did not result in a reduction in the size of the inducible reservoir. These data demonstrate that the licensed drug pyrimethamine can be repurposed as a BAF complex inhibitor to reverse HIV-1 latency *in vivo* in PLWH, substantiating its potential advancement in clinical studies.

INTRODUCTION

Despite markedly improved treatment prospects brought about by combination antiretroviral therapy (cART), an infection with HIV-1 remains a chronic condition that, with few exceptions, necessitates lifelong cART. A pool of long-lived CD4+ T cells harbors latent, replication-competent provirus integrated in the genome. This latent HIV-1 reservoir is established in the first weeks after HIV-1 infection and persists stably even after prolonged periods of cART [1]. Treatment cessation results in rapid plasma viral rebound causing disease progression in people living with HIV-1 (PLWH) [2, 3]. Therefore, interventions beyond cART are needed toward an HIV-1 cure.

One of the key approaches currently proposed to eradicate the latent HIV-1 reservoir in PLWH is to pharmacologically reverse latency via latency reversing agents (LRAs). Elimination of the reactivated reservoir cells could then be triggered by intrinsic proapoptotic pathways or via extracellular immune cell–mediated mechanisms [4–6]. The ultimate aim is to accomplish a prolonged state of sustainable viral remission without cART in PLWH. The multitude of LRAs that have been identified through mechanism-based approaches or large-scale screening of compound libraries can be categorized based on distinct molecular and pharmacological targets [7, 8], all leading to reactivation of HIV-1 transcription. The LRA classes that influence this process can be classified as derepressors antagonizing the repressive latent HIV-1 promotor locus, or as activators that directly stimulate viral transcription initiation or elongation. The importance of blocks at post-transcriptional level has also come to light recently and may be targetable by LRAs [9–12]. In contrast to the numbers identified *in vitro*, only a few LRAs have regulatory approval and can currently be used in clinical settings.

The deacetylation of histones has been identified and extensively studied as a major mechanism to promote HIV-1 latency [13–15], and histone deacetylase inhibitors (HDACis) have become the main evaluated LRA class in HIV-1 cure clinical trials [16]. The first case series used the HDACi valproic acid (VPA) and showed an impact on the reservoir of PLWH who also received intensified cART [17]. However, subsequent larger clinical studies using VPA as HDACi without intensified cART did not demonstrate a reduction in the size of the reservoir [18–22]. Other studies were conducted with clinically approved HDACis that were repurposed as LRAs including vorinostat [23 - 33], Panobinostat [34] and romidepsin [35–39] and showed that, in general, HDACis can safely induce HIV-1 transcription at tolerable concentrations in PLWH. However, no HDACi led to a significant reduction of the proviral reservoir when used alone.

Studies on the limited number of other LRA classes explored in PLWH have resulted in similar conclusions [40–43]. Cumulative evidence therefore indicates the need for identification of previously unidentified LRA classes that potently reactivate HIV-1 and induce reservoir eradication and/or to use combinatorial LRA approaches to reach the potency required to obtain a significant impact on the size of the replication-competent reservoir.

Our preclinical studies identified BRG-Brahma associated factor (BAF) complex inhibitors (BAFi) as a novel LRA class, which we demonstrated enhanced the activity of other LRA classes [44-46]. The BAF (mammalian SWI/SNF) chromatin remodeling complex is a key repressor of HIV-1 latency that uses adenosine triphosphate (ATP) hydrolysis to position repressive nucleosome nuc-1 at the HIV-1 long-terminal repeat, causing transcriptional silencing of HIV-1 gene expression, thereby maintaining HIV-1 latency [47,48]. The pharmacological inhibition of the BAF complex leads to derepression of HIV-1 transcription, resulting in latency reversal [44, 45]. The clinically licensed drug pyrimethamine was subsequently identified as a potent BAFi to reverse HIV-1 latency in primary cell models of latency and in cells obtained from PLWH on cART at tolerable concentrations for humans [44]. Pyrimethamine also enhanced the activity of other LRAs, including HDACis, in cell lines and primary cell models of HIV-1 latency [44]. Pyrimethamine is an orally administered, inexpensive anti-protozoan drug widely used in humans, including in people with AIDS, rendering pyrimethamine an attractive candidate for LRA studies [49–57].

To study the efficacy of BAF complex inhibition by pyrimethamine to reactivate the HIV-1 reservoirs in PLWH, we conducted a proof-of-concept, randomized controlled clinical trial [LRAs United as a Novel Anti-HIV strategy (LUNA), clinicaltrials.gov identifier: NCT03525730]. Apart from a monotherapy arm, we designed a parallel arm where pyrimethamine was combined with an HDACi as partner drug to study an all-oral, affordable, generic combination of LRAs. In contrast to previous studies, we chose the HDACi VPA at maximized dose, in an acid-resistant enteric formulation for better gastrointestinal drug absorption [18–22]. While the previous clinical studies using VPA alone did not show a reduction in the reservoir size in PLWH, VPA had thus far never been used at optimized dosing or in combination with other LRAs [18–22]. Our previous study showed that VPA was able to synergize in reactivating latent HIV-1 with (not yet clinically advanced) drugs from the BAF inhibitor class [45], in line with other data indicating activity of VPA as LRA [23, 58, 59]. We reasoned that this optimized dosing of VPA may enhance the effect of pyrimethamine additively or synergistically *in vivo*. We therefore designed the study to examine whether the activity of the individual LRAs can be potentiated *in vivo*. We enrolled participants on suppressive cART and randomized them to 14 days of pyrimethamine (200 mg once daily at day 1, then 100 mg once daily), VPA (30 mg/kg per day in two equal

doses), pyrimethamine and VPA, or control with a 4-week follow-up after treatment to study clinical safety and efficacy. Our findings demonstrate that pyrimethamine reactivated HIV-1 *in vivo* in PLWH on suppressive cART, supporting its further development into clinical strategies to target the latent reservoir for reactivation. Despite reversal of latency, pyrimethamine treatment did not lead to a reduction in the size of the inducible reservoir.

RESULTS

Combination therapy led to treatment adjustments but no serious adverse events

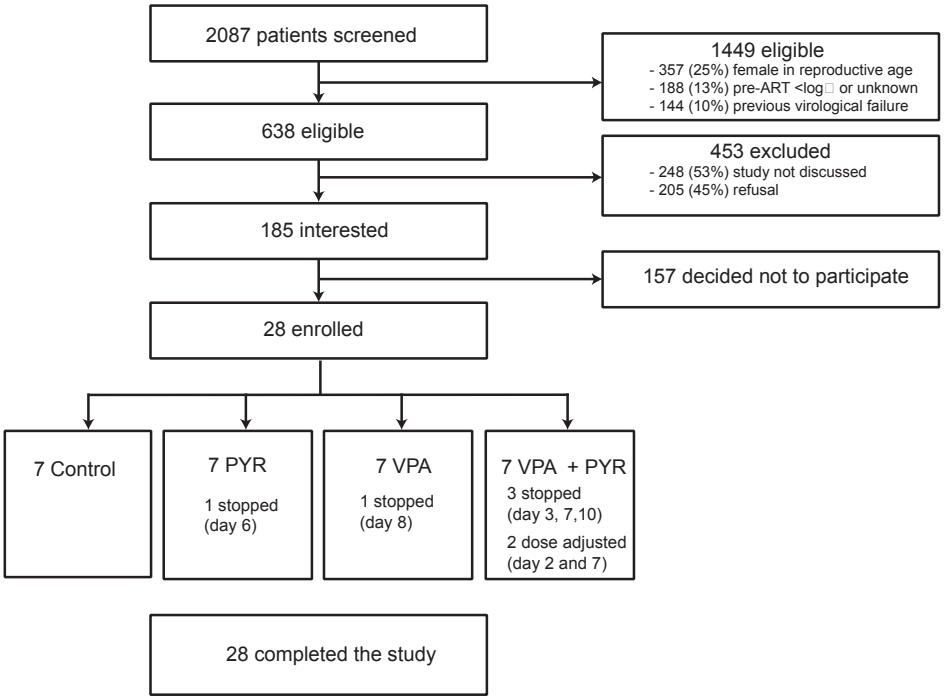

Fig. 1. Study flow diagram showing the information about the method of recruitment and the number of participants that completed the LUNA study. Miscellaneous category for ineligibility covers not fitting the other study inclusion and exclusion criteria, clinical judgment of treating physician, and study not discussed. ART, antiretroviral therapy; PYR, pyrimethamine.

Twenty-eight individuals living with HIV-1 on suppressive cART were enrolled and randomized into four arms of seven participants including three interventional arms and one control arm (Fig. 1). All participants continued daily cART throughout the study. Participants were men, predominantly white European, and on cART for

a median of 7.5 years [interquartile range (IQR), 5.6 to 11.7] with a median CD4+ T cell count of 665 cells/µl (IQR, 530 to 820) at inclusion (Table 1). Integrase inhibitor–based cART regimens were used by 43% of participants; the remainder used non-nucleoside reverse transcriptase inhibitor–based cART. Baseline characteristics were comparable between the study arms including the median duration of therapy.

Table 1. Baseline characteristics of the participants at inclusion

Baseline Characteristics	Overall n =28	PYR N=7	VPA N=7	PYR+VPA N=7	Control N=7
Male	28 (100)	7 (100)	7 (100)	7 (100)	7 (100)
Ethnic origin					
-White European	24 (86)	4 (43)	7 (100)	6 (86)	7 (100)
-Latin American or Hispanic	3 (11)	3 (57)	0	0	0
-Black Caribbean	1 (4)	0	0	1 (14)	0
Age (years)	54 (47-61)	53 (48-55)	51 (54-67)	51 (45-58)	55 (51-64)
HIV subtype B[a]	24 (85.7)	7 (100)	6 (86)	6 (86)	5 (71)
History of AIDS	8 (29)	2 (29)	1 (14)	3 (43)	2 (29)
Years from HIV diagnosis until inclusion	8.5 (7.5-15.4)	7.7 (7.5-14.5)	7.8 (7.6-12.8)	7.6 (5.2-9.4)	15.6 (10.5-20.2)
Years on cART	7.5 (5.6-11.7)	7.3 (6.4-12.0)	7.6 (6.1-10.8)	5.6 (4.7-7.4)	9.8 (8.0-13.0)
Years with HIV-RNA <50 copies per mL	6.8 (4.9-11.1)	6.7 (5.1-11.5)	7.2 (5.4-9.5)	5.1 (4.5-7.1)	7.2 (5.2-12.5)
Initiated cART during acute HIV infection	3 (11)	2 (29)	1 (14)	0	0
Pre-cART plasma viral load zenith $\log_{10}$ copies per mL	4.9 (4.7-5.3)	5.3 (4.9-5.6)	4.8 (4.6-5.0)	4.9 (4.8-5.0)	4.9 (4.7-5.4)
Pre-cART nadir CD4+ T-cell count per µL	235 (160-315)	290 (135-310)	250 (225-295)	240 (175-420)	210 (170-225)
CD4+ T-cell count per µL at inclusion	665 (530-820)	610 (490-770)	750 (560-810)	630 (475-1005)	680 (590-740)
cART					
-NNRTI based[b]	16 (57)	5 (71)	4 (57)	4 (57)	3 (43)
-INSTI based[c]	12 (43)	2 (29)	3 (43)	3 (43)	4 (57)

Data are number with percentage or median with interquartile ranges.
[a]Other HIV-1 subtypes include CRF01-AE (n=2), CRF01-AG (n=1), C (n=1).
[b]NNRTI were rilpivirine (n=6), nevirapine (n=6), efavirenz (n=4). 15 NRTI backbones consisted of emtricitabine (FTC) and either tenofovir disoproxil fumarate (TDF) or tenofovir alafenamide (TAF) and 1 NRTI backbone consisted of abacavir with lamivudine.
[c]INSTI were dolutegravir (n=10) and elvitegravir/cobicistat (n=2). 7 NRTI backbones consisted of FTC and either TDF or TAF, 3 NRTI backbones consisted of lamivudine (3TC) and abacavir (ABC); and 2 had dolutegravir with 3TC as NRTI backbone.
Abbreviations: cART: combination antiretroviral therapy; INSTI: integrase strand transfer inhibitor; NNRTI: non-nucleoside reverse transcriptase inhibitor.

During the 6-week study duration after inclusion, a total of 103 adverse events (AEs) were reported by the trial participants (tables S1 and S2). Except for three grade 3 AE (two with pyrimethamine alone and one in the combination arm), all were of grade 2 or lower severity (table S3). Most AEs (84 of 103) were experienced on pyrimethamine at a comparable rate between the monotherapy and the combination arms. Neurological and gastrointestinal symptoms were the most common AE categories across all interventional arms, with nausea, vomiting, and headache being the most frequently reported.

No serious AEs (SAEs) were observed during the trial, and all AEs were resolved after the intervention. No AIDS-defining illnesses occurred during or after the study. The blood CD4+ T cell counts remained stable during the study without CD4+ T cell counts below the predefined safety limit of 200/μl. However, reported grade 1 and 2 AEs in seven of the participants necessitated the trial physicians to adjust the allocated treatment regimens. The PLWH with and without dose adjustments had a largely comparable clinical profile (table S4). Three participants in the combination arm stopped treatment at day 3 (LUNA-23), day 7 (LUNA-06), and day 10 (LUNA-21); one participant in the pyrimethamine arm stopped treatment at day 6 (LUNA-10) for a grade 1 AE; and one participant in the VPA arm stopped treatment at day 8 (LUNA-09). In one participant of the combination arm, we halved pyrimethamine dosage at day 7 (LUNA-12), while in another participant in the combination treatment arm we halved the VPA dose at day 2 and pyrimethamine dose at day 7 (LUNA- 25) due to drug-related AE.

These events stayed below the upper limit of our predefined safety criteria where we would stop the trial if more than two PLWH in a treatment arm had to discontinue treatment when 50% inclusion was reached, or if at any moment in the trial more than five PLWH had to discontinue their treatment for drug-related AE. We concluded that there was sufficient clinical-scientific and medical ethical basis to complete the study and had 100% follow-up of all 28 participants.

Pyrimethamine induces HIV-1 transcription *in vivo*

To assess the potential of HIV-1 latency reversal in PLWH induced by pyrimethamine and VPA alone and in combination, we measured cell-associated unspliced (CA US) HIV-1 RNA by reverse transcription quantitative polymerase chain reaction (RT-qPCR) in CD4+ T cells isolated from peripheral blood at baseline (day 0, t = 0 hours), 6 hours after initiating the intervention regimen (day 0, t = 6 hours), at the end of the 2-week intervention phase (day 14), and 4 weeks thereafter (day 42) (fig. S1). Because of low cell numbers in the baseline sample, LUNA-06 (combination arm, participant stopped at day 7) was excluded from this primary end point analysis.

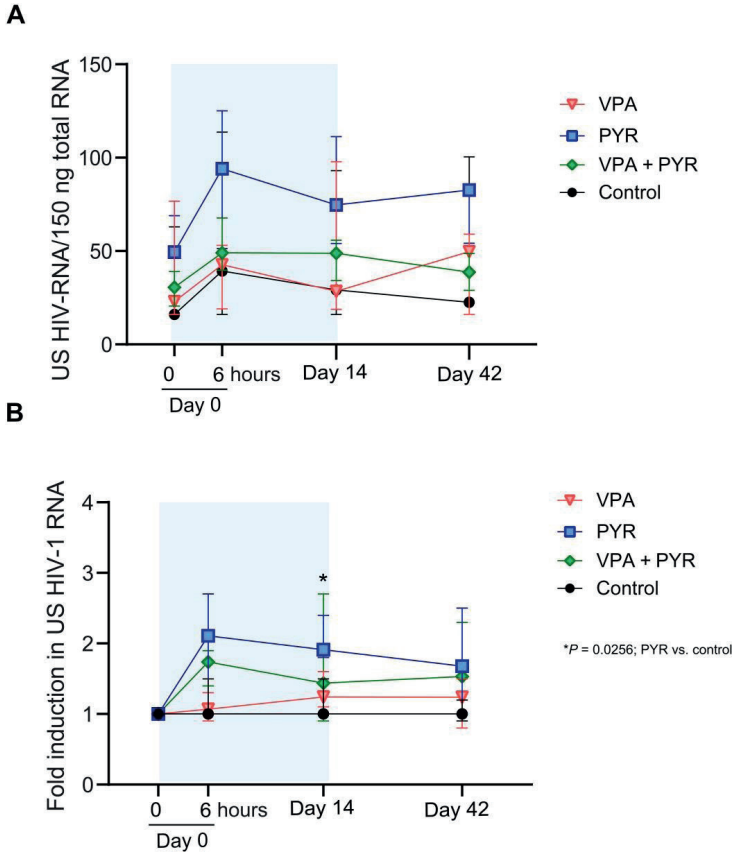

Fig. 2. Changes in CA HIV-1 US RNA per arm at four time points during the LUNA study. (**A**) Median (IQR) total CA US HIV-1 RNA per 150 ng of total RNA in all four study arms at treatment initiation (day 0, t = 0 hours) and 6 hours after first dosing (day 0 t = 6 hours), at the end of the treatment period (day 14), and 28 days after the end of treatment (day 42). (**B**) Median (IQR) fold change in CA US HIV-1 RNA in all four study arms relative to baseline (day 0, t = 0 hours). * indicates the effect comparisons at the time points of the treatment arms compared to controls with P < 0.05.

Addressing the primary end point of the study, we found that, overall, the absolute change in CA US HIV-1 RNA from baseline during the 6-week study period between the treatment groups was different ($P < 0.001$) (Fig. 2A). This overall analysis cannot be used to conclude which groups or time points determined the effect, but the graphical data suggested a relevant contribution of the groups exposed to pyrimethamine. We performed additional analyses to substantiate this possibility. Overall, the fold change in CA US HIV-1 RNA is significantly induced in the pyrimethamine arm at day 14 both compared to day 0 pre-treatment and compared to the control arm (Fig. 2B, Table 2, and table S5).

Table 2. The median fold change in CA US HIV-1 RNA per time point and per treatment arm compared to the control arm

Treatment arm	Time point	Median fold change (normalized to day 0, 0 hours)	Interquartile range	*P* value compared to control arm[1]	*P* value within arm compared to day 0, 0 hours[2]
Control	0 t=0 hours	1	1.0-1.0	-	-
	0 t=6 hours	1	1.0-1.5	-	*P*=0.14
	14	1	1.0-1.5	-	*P*=0.27
	42	1	0.9-1.2	-	*P*=0.47
Pyrimethamine	0 t=0 hours	1	1.0-1.0	-	
	0 t=6 hours	2.1073	1.5-2.7	*P*=0.140	*P*=0.028
	14	1.9129	1.8-2.4	*P*=0.026	*P*=0.018
	42	1.6775	1.2-2.5	*P*=0.109	*P*=0.043
Valproic acid	0 t=0 hours	1	1.0-1.0	-	
	0 t=6 hours	1.0667	0.9-1.3	*P*=0.698	*P*=0.046
	14	1.2401	1.1-1.6	*P*=0.518	*P*=0.12
	42	1.2377	0.8-1.5	*P*=0.698	*P*=0.25
Pyrimethamine + Valproic acid	0 t=0 hours	1	1.0-1.0	-	
	0 t=6 hours	1.7396	1.4-1.9	*P*=0.315	*P*=0.046
	14	1.4372	0.9-2.7	*P*=0.473	*P*=0.12
	42	1.5312	1.0-2.3	*P*=0.340	*P*=0.27

[1]*Mann-Whitney U tests*
[2]*Wilcoxon signed-rank sum test*

As a consequence of the treatment adjustments, the 6-hour time point after the first dosing is the only sampling time point where all participants were similarly exposed to their allocated therapies and at the same doses. We therefore focused on the effects observed here as the most unbiased measurement time point consequent to drug treatment. From baseline to 6 hours, CA US HIV-1 RNA increased median 2.1-fold (IQR, 1.5 to 2.7; $P = 0.028$) in response to pyrimethamine alone (Fig. 3, A and E) and median 1.7-fold (IQR, 1.4 to 1.9; $P = 0.046$) in response to the combination therapy (Fig. 3, B and F). In contrast, the CA US HIV-1 RNA at this time point from baseline did not change significantly for PLWH allocated to the VPA arm (median fold change, 1.1; IQR, 0.9 to 1.3; $P = 0.46$) (Fig. 3, C and G) or the control arm (median fold change, 1.0; IQR, 1.0 to 1.5; $P = 0.14$; Fig. 3, D and H). Overall, PLWH in the two arms exposed to pyrimethamine had a greater fold change CA US HIV-1 RNA after 6 hours (median, 1.8; IQR, 1.4 to 2.4) compared to those in the two arms without pyrimethamine exposure (median, 1.0; IQR, 1.0 to 1.4; $P = 0.029$).

On pyrimethamine monotherapy, six of seven PLWH responded after the first dose at the 6-hour time point (Fig. 3, A and E). Of these six, five retained an increased CA US HIV-1 RNA during pyrimethamine treatment including LUNA-24 who had CA US HIV-1 RNA below the level of quantitation at baseline. The median fold

change from baseline at day 14 was 1.9 (IQR, 1.5 to 2.4; *P* = 0.018), which was in line with the median fold change at 6 hours after dosing (*P* = 0.612) and remained comparable (*P* = 0.50) from days 14 to 42 when a median 1.7-fold change (IQR,1.2 to 2.5) was still observed. Excluding the single participant (LUNA-10) who stopped pyrimethamine from these analyses did not relevantly alter these median fold change estimates from baseline at day 14 (1.8; IQR, 1.4 to 2.6) or day 42 (1.6; IQR, 1.1 to 3.1). Controls did not exhibit relevant median fold change increases in CA US HIV-1 RNA from baseline at day 14 (1.0; IQR, 1.0 to 1.5; *P* = 0.27) or day 42 (1.0; IQR, 0.9 to 1.2; *P* = 0.47). Two PLWH in the control arm showed some reactivation without a clear clinical explanation, which skewed the estimated effect ranges upward. On VPA, PLWH did not have significantly increased median CA US HIV-1 RNA at any time point compared to pre-treatment levels (Fig. 3, C and G) and these responses were also similar to the responses measured in untreated controls (*P* > 0.5 for all comparisons; Table 2). Together, these observations strongly indicate that pyrimethamine induces HIV-1 transcription as early as 6 hours after intake.

We did not observe plasma viremia despite the observed increases in CA US HIV-1 RNA. We found no evidence that pyrimethamine induced plasma viremia at the day 1 time point when all PLWH were on their allocated treatments; five PLWH exposed to pyrimethamine and four PLWH not exposed to pyrimethamine had plasma HIV-1 RNA detected below the assay quantitation limit. These included six PLWH, equally divided by pyrimethamine exposure or not, who had no viral genome detected before drug administration. When evaluating the entire 6-week trial period, plasma HIV-1 RNA remained below the lower limit of quantification (LOQ) in the majority of participants (table S6) except for two participants on VPA, one participant on pyrimethamine, and one participant on combination treatment (all <50 copies/mL). These findings indicate that the intracellular effect of pyrimethamine did not result in measurable cell-free HIV-1 RNA in the plasma of participants.

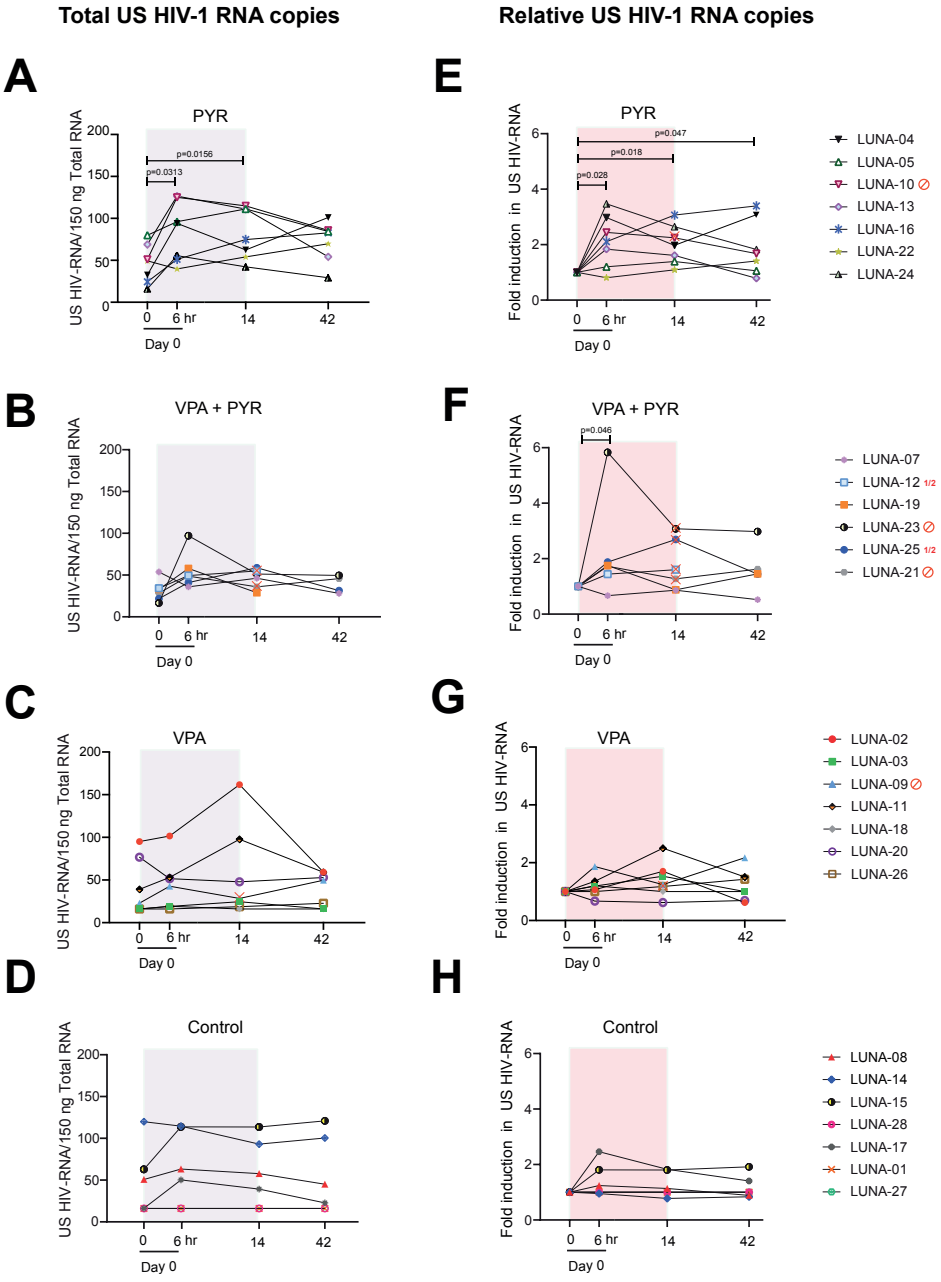

Fig. 3. Changes in CA HIV-1 US RNA per participant per arm at four time points during the LUNA study. (**A** to **D**) Graphs represent absolute CA US HIV-1 RNA copies in all participants from the pyrimethamine (A), pyrimethamine with VPA (B), VPA (C), and control (D) arms at treatment initiation (day 0, t = 0 hours) after 6 hours after the first dosing (day 0, t = 6 hours), at the end of treatment period (day 14), and 28 days after the end of treatment (day 42). (**E** to **H**) Graphs represent fold induction of CA US HIV- 1 RNA at different study time points compared to baseline (day 0, t = 0) in all participants from the pyrimethamine (E), pyrimethamine with VPA (F), VPA (G), and control (H)

arms at the same time points. A total of 1.5 million CD4+ T cells were isolated from peripheral blood mononuclear cells, lysed in triplicate, followed by total RNA isolation and reverse transcription. Total copies of CA US HIV-1 RNA were quantified by nested qPCR. The gray/red boxes represent treatment duration. Participants that stopped study medication or had dose adjustments are indicated with either a red stop sign or red ½ symbol and a red cross on the individual points in the graph. In both the VPA arm and the pyrimethamine arm, one participant stopped their study medication on day 8 (LUNA-09) and day 6 (LUNA-10), respectively. In the combination treatment arm, three participants stopped both compounds (LUNA-23 on day 3, LUNA-06 on day 7, and LUNA-21 on day 10), and two participants had their dosage adjusted (LUNA-25 had VPA dose halved from day 2 on, pyrimethamine dose halved from day 7 on, and LUNA-12 had pyrimethamine dose halved from day 7 on). P values are indicated. Statistical significance was calculated using Wilcoxon signed rank tests.

Pyrimethamine and VPA do not synergize to induce HIV-1 transcription *in vivo*

Because of the treatment adjustments that occurred in the combination treatment arm, we used the measurements at 6 hours after the first dose to test the hypothesis that synergy occurred between pyrimethamine and VPA in the context of their combined latency reversal activity on HIV-1. In PLWH exposed to the combinatorial treatment, five of six PLWH had increased CA US HIV-1 RNA 6 hours after the first dose (Fig. 3, B and F). There was one individual (LUNA-23) with a particularly large 5.83-fold increase, while the other five PLWH had fold changes ranging from 0.67 to 1.88. Apart from an HIV-1 CRF02-AG subtype infection, the clinical characteristics of this participant were fitting the characteristics of the overall study population. At this 6-hour time point, the median fold change response in the combination treatment arm did not differ significantly from the median response observed with pyrimethamine alone (P = 0.475). As per protocol defined, the data also formally excluded synergy since the mean fold change and its full 95% confidence interval (2.2, 0.3 to 4.1) did not exceed the expected mean fold change of 2.25, which was based on the mean fold change effects estimated in the pyrimethamine (2.11) and VPA (1.14) arms separately. Hence, synergy could not be demonstrated and neither do these data indicate additive effects.

In the four PLWH (LUNA-07, LUNA-12, LUNA-19, and LUNA-25) in the combination arm who continued uninterrupted pyrimethamine exposure throughout the study, the median fold change in CA US HIV-1 RNA was 1.2 (IQR, 0.9 to 2.1) at day 14. This effect was comparable to the changes observed when evaluating all PLWH including those who stopped combinatorial treatment (median, 1.4; IQR, 0.9 to 2.7). Unfortunately, the CD4+ T cells yield from the samples were insufficient for LUNA-12 and LUNA-19 to measure CA US HIV-1 RNA at the day 42 end point. Given the treatment adjustment in LUNA-25, at this time point, only LUNA-07 had completed the full allocated treatment and had end point results available. This participant did not exhibit CA US HIV- 1 RNA increases at any time point. Apart from a longer duration of plasma viral suppression in the upper quartile of the cohort (nearly

12 years), the other baseline characteristics in this participant were consistent with the general cohort. When evaluating the four PLWH who had exposure to pyrimethamine in this combination treatment arm, and with samples at day 42 available (LUNA-07, LUNA-21, LUNA-23, and LUNA-25), the median fold change was 1.5 (IQR, 1.0 to 2.3), comparable to pyrimethamine alone and not significantly different from controls (Table 2). Overall, these data support the conclusion that VPA did not augment the activity of pyrimethamine in reactivating HIV-1.

Low pyrimethamine plasma levels occur with concomitant VPA exposure

For this trial, we established an in-house assay to measure total pyrimethamine plasma levels (Fig. 4). At the 6-hour timepoint, the median plasma total pyrimethamine concentration in the seven participants that received solely pyrimethamine was 1.63 mg/L (IQR, 1.40 to 1.83), and in the combination arm, this was 1.16 mg/L (IQR, 1.0 to 1.31) (Fig. 4A). This difference was more accentuated at day 14 when the six PLWH in the monotherapy arm and the four PLWH in the combination therapy arm with uninterrupted pyrimethamine exposure had median C_{trough} of 3.48 mg/L (IQR, 3.21 to 3.83) and 1.99 mg/L (1.63 to 2.63) (Fig. 4B). Although these concentrations fall within the expected range from previous human studies [49–52, 60], and despite taking out those who stopped pyrimethamine before day 14 from the analysis, the data suggest lower pyrimethamine concentrations when combined with VPA (Fig. 4). This might be the result of protein binding displacement or an unexpected drug-drug interaction. We did not find such an effect when comparing the median plasma total VPA concentration at the 6-hour time point between monotherapy (median, 47.3 mg/L; IQR, 47.2 to 60.1) and combination treatment (47.4 mg/L IQR, 26.0 to 57.3) (fig. S2). The median C_{trough} observed at the day 14 timepoint in the six PLWH with uninterrupted exposure to VPA monotherapy and the four PLWH with uninterrupted exposure to VPA in the combination treatment was 84.8 mg/L (36.4 to 99.6) and 113.2 mg/L (IQR, 83.1 to 137.5) respectively, both above VPA's therapeutic range lower border for epilepsy (50 mg/L).

We found no correlations between pyrimethamine plasma exposure and the fold change in CA US HIV-1 RNA from baseline at 6 hours (r = 0.26, P = 0.39) or day 14 (r = 0.041, P = 0.91) in those exposed to pyrimethamine or in the participants from the two pyrimethamine arms separately (fig. S3). We explored median pyrimethamine C_{trough} by integrase inhibitor exposure but found no relevant differences at 6 hours (1.3 mg/L versus 1.4 mg/L) or day 14 (2.8 mg/L versus 3.2 mg/L) in those with uninterrupted pyrimethamine. Conversely, median unbound dolutegravir concentrations were comparable between those with and without

pyrimethamine exposure at 6 hours (11.7 µg/L versus 10.1 µg/L) but decreased during the treatment course. This effect has been attributed to VPA by protein displacement as we described previously [61]. PLWH with exposure to efavirenz- or nevirapine-containing cART (both CYP3A inducers) did not have lower median plasma concentration of pyrimethamine (a CYP3A substrate). No pyrimethamine or VPA was detectable in the plasma at day 42. The combined data do not support relevant drug-drug interactions between pyrimethamine and dolutegravir but do support relevant drug-drug interactions of VPA on dolutegravir and pyrimethamine.

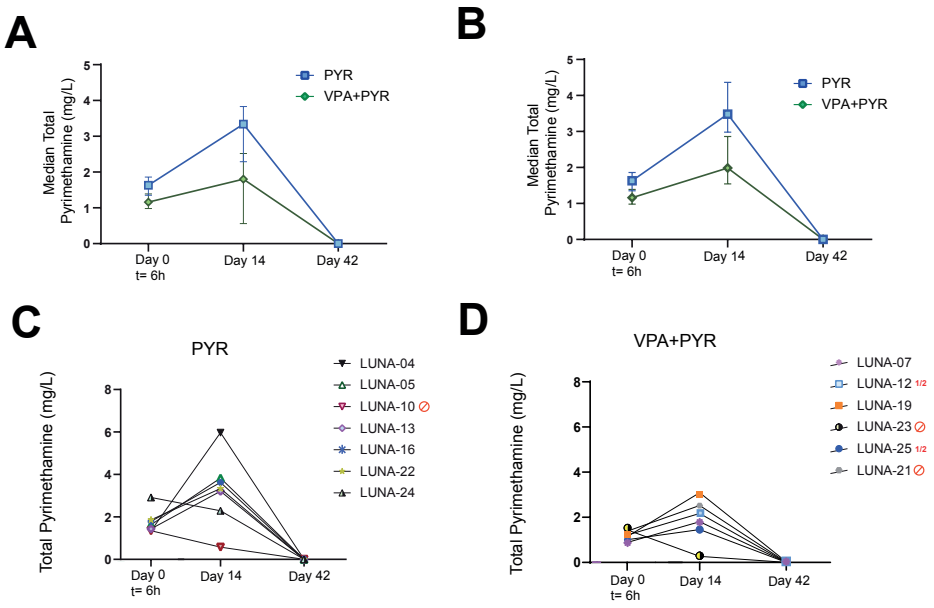

Fig. 4. Pharmacokinetics of the drug pyrimethamine in study participants. (**A** and **B**) Pharmacokinetic analysis of the drug pyrimethamine in study participants from pyrimethamine (blue) and the combination treatment arm with pyrimethamine and VPA (green) as measured by median total pyrimethamine (mg/liter) levels in plasma with IQRs at 6 hours after first dosing (day 0, t = 6 hours), at the end of treatment period (day 14), and 28 days after the end of treatment (day 42) overall (A) and in those with uninterrupted pyrimethamine exposure (B) and represented as plasma pyrimethamine levels at the time points per individual on pyrimethamine (**C**) or the combination treatment with pyrimethamine and VPA (**D**).

We found no clear outliers in the data on pyrimethamine and VPA plasma exposure for the seven PLWH who had treatment adjustments for toxic effects (table S6). Of those seven, the ones in the pyrimethamine-containing arms had pyrimethamine plasma levels at 6 hours after the first dose that were at or below the median plasma exposure found in the pyrimethamine monotherapy arm at that time

point. All participants where pyrimethamine was stopped had clearly lower plasma levels at day 14 with the notable exception of LUNA-21 (2.52 mg/L) who stopped treatment at day 10, later than the others who interrupted pyrimethamine (table S6). In the same line, three of the five PLWH, who had their therapy adjusted for toxicity while receiving VPA, had plasma levels at day 7 exceeding the therapeutic window defined for epilepsy (up to 100 mg/L) compared to three of nine who continued VPA (table S6). This provides some evidence that VPA plasma exposure related to clinical toxicity, comparable to the use of therapeutic drug monitoring for VPA for other conditions [62]. For pyrimethamine, the therapeutic window and relationship between plasma exposure and toxicity are far less well defined but no exceptional high plasma exposures were found.

Pyrimethamine induces expression of biomarkers associated with BAF inhibition

Pharmacological inhibition of the BAF complex by pyrimethamine leads to functional changes in the expression levels of several genes [44, 63–66]. To assess the pharmacodynamics, activity, and specificity of pyrimethamine in this clinical trial, we analyzed the gene expression profile of three target genes of the BAF complex (*IL- 10*, *SOCS3*, and *CBX7*) and a control gene (*B-ACT*) on day 0 before treatment and day 0 at 6 hours after the first dose. We reasoned that the effect on the expression of these gene targets at later time points (days 14 and 42) would be less useful as specific biomarker of BAF complex inhibition due to treatment interruptions and potential induction via other pathways. We observed a significant fold increase in the median gene expression levels of *IL-10*, *SOCS3*, and *CBX7* (2.55-, 2.53-, and 1.68-fold, respectively; table S7) in the pyrimethamine treatment arm (Fig. 5A).

As expected, we observed no increase in the mRNA levels of these genes in either the control arm or the VPA intervention arm (Fig. 5, B and C), indicating that these molecular targets are specific for pyrimethamine. No significant increase in gene expression levels of BAF target genes was observed in the combined intervention arm (Fig. 5D). These findings are consistent with, and might be the consequence of, the generally lower plasma pyrimethamine C_{trough} in participants that received the combined intervention regimen compared to those that received solely pyrimethamine.

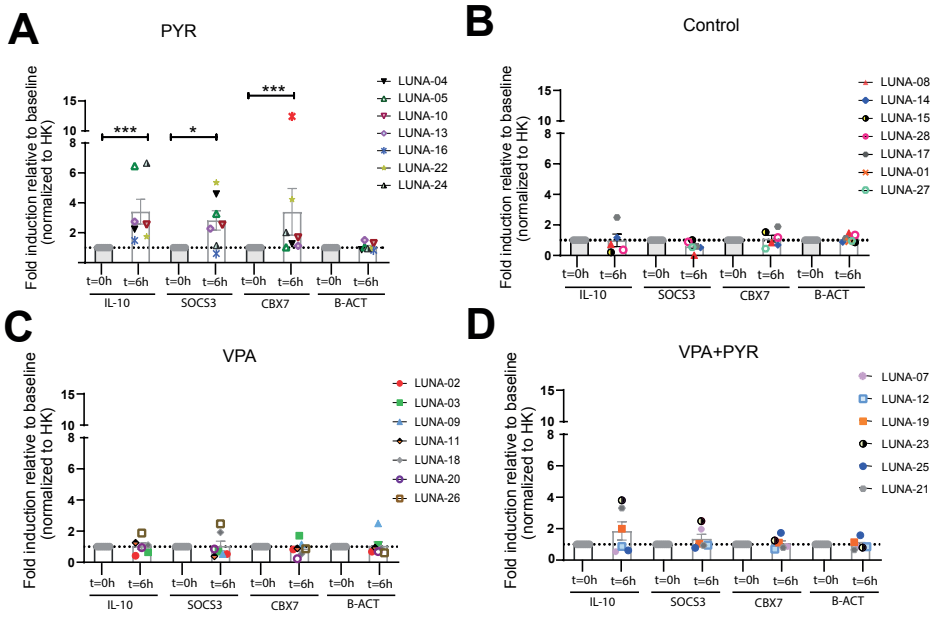

Fig. 5. Pharmacodynamics of the drug pyrimethamine in study participants. (**A** to **D**) Gene expression profile of BAF complex molecular targets IL-10, SOCS3, and CBX7 in all participants from pyrimethamine (A), control (B), VPA (C), and the combination treatment arm with pyrimethamine and VPA (D) at 6 hours after first dosing (day 0, t = 6 hours). Graphs represent mean (SEM) fold induction relative to pretreatment level (day 0, t = 0 hours). Cyclophilin A was used as a housekeeping (HK) gene for normalization, and β-actin (B-ACT) was used as a control. P values were calculated using Mann-Whitney U test with * representing $P < 0.05$ and *** representing $P < 0.01$.

Pyrimethamine exposure does not lead to a reduction of the inducible HIV-1 reservoir

To assess whether *in vivo* HIV-1 transcription induced by pyrimethamine or VPA alone or in combination affected the inducible reservoir, we used a *tat/rev*-induced limiting dilution assay (TILDA) to quantify the frequency of cells expressing multiply spliced (Ms) HIV-1 RNA upon *ex vivo* cellular activation with phorbol 12-myristate 13-acetate (PMA)/ionomycin at baseline (day 0, t= 0 hours) and day 42 (Fig. 6 and fig, S4, A to C) [67, 68]. Since low cell yields at day 42 occurred in several individuals during the trial, which would impede accurate reservoir assessments, we decided during the trial, before data collection and analysis, to invite all participants back when all were more than 1 year after day 42. A total of 27 of 28 PLWH responded and were sampled at a 1- to 2.2-year range after their last visit (table S8). Ultimately, TILDA could be performed for 20 to 28 study participants with available samples (71%) including all participants on pyrimethamine monotherapy. For eight participants

without TILDA data, sample material was insufficient in four (three on combination treatment and one control) and four had non-B HIV-1 subtypes (including one participant in the combination arm). For the remaining 10 participants with pyrimethamine exposure that could be evaluated, two on pyrimethamine alone (LUNA-05 and LUNA- 22) had insufficient cells available at day 42. Here, the measurement from the cells obtained >1 year after the last visit was used.

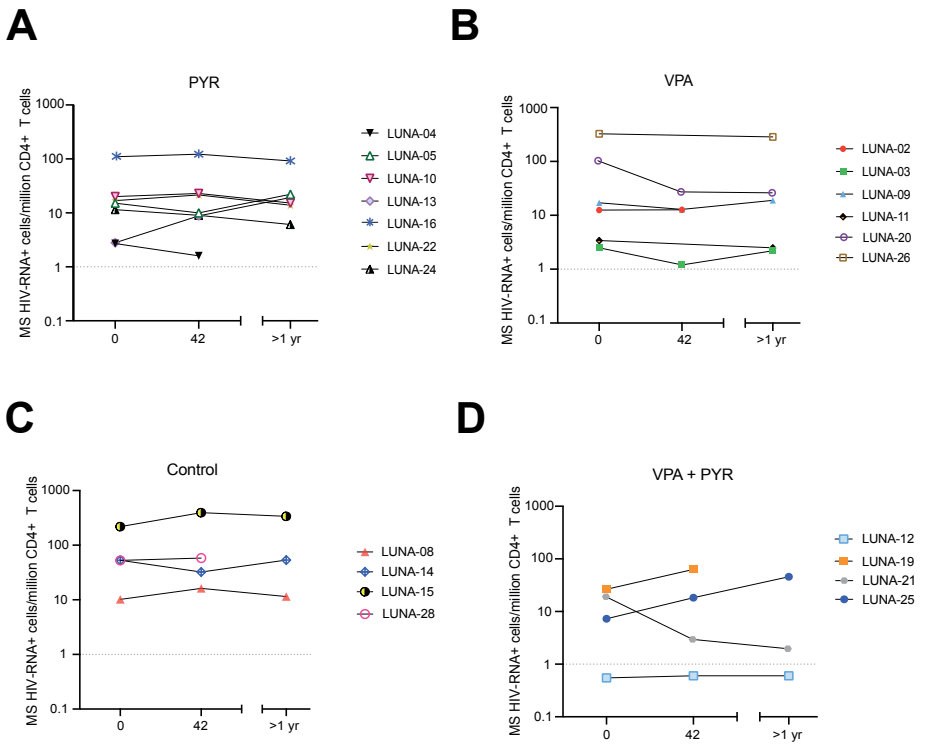

Fig. 6. Effect of the intervention regimen on the HIV-1 inducible reservoir size. (**A** to **D**) Graphs represent measurements of inducible reservoir size in samples obtained from participants from pyrimethamine (A), VPA (B), control (C), and the combination treatment arm with pyrimethamine and VPA (D) at treatment initiation (day 0, t = 0 hours), 28 days after the end of treatment (day 42), and >1 year after the end of treatment. Isolated CD4⁺ T cells were activated ex vivo with PMA/ionomycin for 12 hours, and the frequency of CD4⁺ T cells expressing MS HIV-1 RNA was determined using a TILDA. The dotted horizontal line represents the assay limit of detection.

The overall results do not indicate a significant change in the reservoir size with pyrimethamine exposure (Fig. 6A). The reservoir was estimated at median 15.1 (range, 2.7 to 109.8) cells per million CD4+ T cells before treatment with pyrimethamine alone and at 10.0 (range, 1.6 to 122.8) cells per million CD4⁺ T cells

after treatment. This variation was well within the assay coefficient of variation (25.1%). The reservoir remained stable on VPA: median 14.8 cells per million CD4+ T cells at day 0 and median 19.4 CD4+ T cells per million at day 42 (Fig, 6B). The number of participants with reservoir results available in the other two arms (n=3 in each) was considerably lower and precluded statistical inferences, but the data points that are available do not challenge the main conclusion that overall no decrease in the reservoir can be observed (Fig. 6 C and D). In one of these participants (LUNA-12, combination arm), TILDA was below the limit of detection (LOD) at all sampling points (Fig. 6D). Individual level changes in reservoir size were observed in a post-hoc analysis of an at least twofold increase or decrease in four (LUNA-13, LUNA-15, LUNA-19, and LUNA-25) and three participants (LUNA-03, LUNA-20, and LUNA-21), respectively, between days 0 and 42 (Fig. 6) without signs of clustering to a specific treatment arm or an associated clinical predictor variable.

DISCUSSION

The BAF complex is an important molecular regulator of HIV-1 latency and offers a new yet clinically unstudied pharmacological target for latency reversal. In this randomized controlled trial, we demonstrated that BAF complex inhibition by pyrimethamine induces cellular HIV-1 transcription and reversal of latency in cART-suppressed PLWH. A comparable effect on the reservoir by pyrimethamine was also observed when VPA was added as partner LRA. Thus, the combination treatment failed to show synergistic or additive effects. Furthermore, interventional treatment adjustments occurred most frequently in PLWH randomized to the combinatorial arm, although the number and grade of the reported AE were in line with the ones observed in the individual monotherapy arms. We cannot exclude the possibility of physician- or participant-directed biases in the combinatorial arm where both the treating physician and the participant were aware of the higher drug burden. However, we believe that this trial, as the first randomized controlled clinical study on combinations of LRA, underlines that testing combinatorial LRA approaches is feasible. It also highlights the need to monitor for drug tolerability and provides a safety benchmark for future studies combining LRAs in the clinical HIV-1 cure trial field.

The most important finding is the identification of pyrimethamine as an effective drug to reverse HIV-1 latency in PLWH. It acts through a novel mechanism of action that we unraveled first in *in vitro* and *ex vivo* studies and now successfully moved into clinical practice [44,48]. We found an approximately two-fold induction of cellular HIV-1 transcription from pre-treatment levels that persisted during treatment. The effect on the proviral reservoir was only observed in the presence of measurable

pyrimethamine plasma concentrations, accompanied by selective induction of other BAF complex target genes and not observed in individuals that were not exposed to pyrimethamine. These observations support that the inhibition of the BAF complex at the HIV-1 promotor region is responsible for this effect *in vivo*, comparable to its established working mechanism *in vitro*. In addition, although BAF complex inhibition by pyrimethamine was able to induce HIV-1 transcription *in vivo*, it did not lead to a reduction in the inducible reservoir. This might be due to an insufficient antigen production and further recognition by cytotoxic immune cells. Of note, a total of four participants had an apparent increase in the size of the inducible reservoir in a post hoc analysis. We did not find a defining clinical characteristic or common factor underlying these observations. Because some fluctuation was also observed in the control arm, clustering to any arm was absent, it is currently unclear whether these observations on an individual level are reflective of, for example, the antiretroviral or LRA treatment course in specific participants or are rather due to limitations of viral reservoir quantification tools or natural variability. Future studies should take these possibilities into consideration.

With regard to VPA, we optimized the dosing and used an acid-resistant formulation for a more direct gastrointestinal absorption unlike the previous studies where underdosing or underexposure might have been the cause of the observed discrepant effects of VPA as LRA [17–22]. In our trial, participants receiving VPA had higher plasma levels than those reported in prior studies [17–22]. Although higher systemic VPA peak concentrations could more likely induce HIV-1 reactivation, we did not observe an increase in CA US HIV-1 RNA or viral plasma load in PLWH treated with VPA alone. Strategies that use combinatorial approaches of LRAs could result in higher efficacy in reactivating HIV-1 latency [5]. We have shown in previous studies that the effect of pyrimethamine on HIV-1 latency *ex vivo* could be potentiated when combined with other LRAs including HDACi [44, 46]. We therefore designed the study to include a combinatorial arm to test whether the effect of the individual LRAs could be potentiated *in vivo*. Our results showed, however, no synergistic or additive effects on the HIV-1 reservoir in PLWH in the combinatorial arm. Future HIV-1 cure studies using pyrimethamine would benefit from combinations with other LRAs that could induce higher levels of HIV-1 transcription and compounds that enhance immune-mediated killing.

To put our clinical study and the role of pyrimethamine as an LRA in the context of HIV-1 cure clinical studies, we compared the effect of pyrimethamine on HIV-1 latency with other LRAs tested in PLWH. First, the effect of pyrimethamine on HIV-1 transcription did not appear to augment with multiple dosing. This is in contrast to observations made in studies with other LRAs from the HDACi class and disulfiram,

where the mean effect on cellular HIV- 1 transcription increased with sequential dosing during treatment [26, 34, 39, 40]. Our observation fits a more dichotomous (on/off) effect dependent on whether sufficient intracellular concentrations are reached rather than a gradual effect seen with HDACi, where multiple doses are apparently necessary to reach a maximum effect. Our prior *in vitro* observations showing that the BAF complex at the nucleosome 1 region of the HIV-1 promotor locus was comparable at different dosages support this assumption [44]. A certain maximized potential to reactivate HIV-1 is also suggested since further increase in pyrimethamine plasma levels did not result in an additional CA US HIV-1 RNA increase during the trial. Second, pyrimethamine's effect waned several weeks after the last drug exposure. This is in line with most other trials on effective LRAs that act through derepressing HIV-1 transcription [34, 35 ,39] with the exception of one trial on vorinostat [26]. Third, the combinatorial approach used in this trial with pyrimethamine and a derepressor HDACi as a partner LRA may be less likely to work synergistically compared to combining a derepressing and an activating LRA. Our data support this hypothesis although we certainly acknowledge that different results may have been obtained with a more potent partnering HDACi. Last, regarding the observed safety profile, pyrimethamine as monotherapy had a favorable clinical safety profile, comparable to studied effective HDACi in HIV-1, with only mild AE observed. Pyrimethamine's additional advantages of being a globally available, orally administered, inexpensive drug, together with considerable experience to treat AIDS patients with it, further support its use in follow-up cure studies. These future studies should nonetheless focus on optimizing the necessary pyrimethamine dose to reactivate HIV-1 latency while minimizing drug exposure and toxicity, identifying the relevance of the used loading dose and treatment duration, and, given our trial findings, determine the optimal partner drug for pyrimethamine in terms of efficacy and safety.

In our study, pyrimethamine alone led to a twofold increase in levels of CA US HIV-1 RNA at the time point where all participants had received their allocated dose. While this effect is rather modest, it is comparable to recent reports using other classes of LRAs. The HDACi VPA did not result in an increase in CA US HIV-1 RNA in this trial, as opposed to what has been observed with other HDACi such as vorinostat, romidepsin, and panobinostat [26, 28, 33–39]. In a study designed more comparably to our study, CA US HIV-1 RNA increased a mean 2.6-fold at time points during vorinostat treatment [26]. No reactivation was, however, observed when vorinostat was combined with a T cell-inducing HIV-1 vaccine in PLWH who initiated cART during acute HIV-1 [28], and a 1.5-fold change in CA US HIV-1 RNA was observed with vorinostat treatment in a recent study in postmenopausal women [33]. For the HDACi romidepsin, initial studies reported an approximately threefold increase

in CA US HIV-1 RNA [35, 36]. Additional studies on romidepsin's pharmacodynamics profile unexpectedly found no significant effect on HIV-1 transcription [38]. In trials that combined romidepsin with 3BNC117 or a therapeutic HIV-1 vaccine, cellular HIV-1 transcript levels generally changed overall less than threefold [37, 39]. This was also true for the reactivation effects observed with disulfiram, bryostatin, a Toll-like receptor 9 (TLR9) agonist, or pembrolizumab [40–43]. Another HDACi, panobinostat, reactivated cellular HIV-1 transcription more potently compared to all other HDACis in the only clinical trial with this compound [34]. Overall, when comparing pyrimethamine to other LRAs, its effect to reactivate HIV-1 transcription can be classified as at least comparable.

The assay we developed and validated to measure pyrimethamine plasma levels turned out to be critical since, unexpectedly, the combination arm had lower pyrimethamine plasma levels with a concomitant lower induction of various BAF target genes. Given that both pyrimethamine and VPA are highly protein-bound, a plausible explanation for this effect could be attributed to plasma protein-protein competition dynamics, although further research needs to be conducted to support this statement. We identified a similar mechanism previously where VPA affected dolutegravir levels [61]. This signals that routine pharmacokinetic profiling of the interventional drugs and cART should be included in the design of future cure trials, even if no interaction is expected. This is particularly important when testing combinations of LRAs.

This proof-of-concept study has strengths and limitations. The study's main strength is the inclusion of a control arm and a combination arm that allowed us to assess the specific effect of pyrimethamine alone and in combination with an HDACi. Regarding limitations, although not exceeding predefined safety criteria, the combinatorial arm faced a disproportionate amount of treatment adjustments before the end of the intervention period. This influenced our ability to draw solid conclusions on potential late LRA effects combination therapy might have. However, the absence of an effect with VPA alone together with the absent synergism or additive effects in PLWH on the combination of drugs makes potential late effects less likely.

Our sampling strategy for this pilot favored having many timepoints for the primary endpoint over blood quantity for in depth analyses. Leukapheresis was practically not possible. This turned out to be a challenging strategy in some cases, especially in individuals with less blood CD4+ T cells. We prioritized using CD4+ T cells for the main end points, although this meant that in-depth analysis of resting memory CD4+ T cells or other cell types was therefore not possible. Another challenge was to measure the size of the reservoir by TILDA post-treatment at day 42 as a main secondary end point. This was not possible in four PLWH due to limited

sample availability and four PLWH had non–B subtypes that resulted in critical primer-probe mismatches. However, all PLWH in the most relevant arm with pyrimethamine had a sufficient number of cells for reservoir analysis. We amended the protocol and invited all participants for an additional sampling at least 1 year after the last study visit with the purpose to more confidently support the reservoir findings. We did not observe marked changes in the size of the latent reservoir over this time course. As a pilot study, the exploratory analyses and relatively small sample size could have resulted in type 1 and 2 errors, respectively. Future LRA trials should take into account these limitations for initial design with regard to diversity in participant inclusion, assays, sampling time points, and materials required.

In summary, inhibition of the BAF complex by pyrimethamine resulted in modest but significant reversal of HIV-1 latency in PLWH immediately after the first dose and persisted during treatment course. Our data are supportive of the BAF inhibitor pyrimethamine as a novel drug option in the LRA arsenal, which has widespread use in the clinic, excellent safety profile, and favorable pharmacological features, including its excellent brain penetration that offers potential for penetration in HIV-1 reservoir sanctuary sites [50, 53, 54, 56, 60]. Thus, pyrimethamine is an attractive candidate for inclusion in future pharmacological approaches toward an HIV-1 cure.

MATERIALS AND METHODS

Eligibility

The LUNA trial (clinicaltrials.gov identifier: NCT03525730) is a proof-of-concept, four-arm, open-label randomized controlled interventional clinical trial to assess the effect of the BAF inhibitor pyrimethamine on the HIV-1 reservoir when given alone or as a combination of LRAs with the HDACi VPA. Individuals aged ≥18 years visiting the outpatient department of infectious diseases at the Erasmus University Medical Center (Rotterdam, the Netherlands) were eligible if they had a confirmed HIV-1 infection and a CD4+ T cell count of at least 200 cells/μL, receiving cART with a pre-cART HIV-1 RNA zenith of ≥10,000 copies/mL and plasma HIV-1 RNA levels of <20 copies/mL in the year before the intervention (with a minimum of two measurements taken). Exclusion criteria were female with a reproductive potential due to VPA's teratogenic potential, previous virological failure with resistance-associated mutations acquired on cART, active hepatitis B or C infection, prior exposure to LRAs, immunomodulating medication, or medication known to interact with VPA or pyrimethamine. The inclusion period of the study was between April 2018 and September 2020 following approval by the Medical Research Ethics Committee (MEC-2017-476) in accordance with the principles of

the Helsinki Declaration. The protocol was amended once in February 2020 before the analysis of end points. The reason for this amendment was to allow additional blood sampling to overcome potential low cell yields for a main end point analysis on the reservoir size. All participants provided written informed consent. The full protocol is available as appendix, and a synopsis is available in the Supplementary Materials. Study reporting follows the CONSORT reporting guidelines.

Intervention

Eligible and consenting trial participants were screened within 6 weeks before the start of the intervention phase and subsequently randomized to one of four arms to receive oral doses of either: pyrimethamine once a day for 14 days (200 mg on the first day followed by 100 mg onward), VPA (30 mg/kg per day) (divided into two equal doses) for 14 days, a combination of pyrimethamine and VPA dosed likewise, or no intervention. For the randomization process, an independent statistician delivered sealed opaque envelopes that included the study identifier with the allocated treatment based on random allocation performed in R. VPA and pyrimethamine were administered in dosages used in the chronic treatment of epilepsy [62], and previous clinical studies on the treatment of cerebral toxoplasmosis in AIDS patients or as prophylaxis or malarial treatment in pregnant women [49, 53–57]. The dose and duration of VPA and pyrimethamine treatment, and the timing of viral reservoir analysis on day 0 after 6 hours, was based on T_{max} of both compounds, available literature, expert opinion, and our previous work [69–71]. Blood samples were collected 6 hours after the participants received the intervention regimen assuming T_{max} to be reached by pyrimethamine and VPA after approximately 4 hours, and an additional 2 to 3 hours for HIV-1 transcription and HIV-1 RNA accumulation [24]. To achieve a constant and the earliest T_{max} possible, participants received their first dose of the intervention regimen on day 0 in a fasted state. On day 0, cART and study medication intake were taken under direct supervision of the study staff. The 2-week intervention phase was followed by a 4-week post-intervention phase. Overall, participation involved 11 study visits. To obtain an additional post-intervention phase measurement for the inducible HIV-1 reservoir size, the study was amended and participants were asked to give written consent to an extra blood draw after the 4-week post-intervention phase ended. Plasma HIV-1 RNA levels (COBAS TaqMan; Roche, Basel, Switzerland; LOQ, 20 copies/mL) were monitored at all 11 visits. CD4+ T cell counts were determined at screening, at the start and end of the intervention phase (days 0 and 14), at day 42, and at the post-intervention phase (≥day 42).

Safety

Hematological parameters and kidney and liver function were monitored before treatment and on days 7, 14, and 42. At each study visit, participants were clinically assessed by the study physician and safety assessments were performed. All participant-reported AE and SAE were evaluated in relation to VPA and pyrimethamine. Severity was graded according to the Common Terminology Criteria for Adverse Events (CTCAE) version 4.0. In the study protocol, a number of stopping rules were defined including a prespecified interim analysis after the inclusion of 14 participants focusing on the number of participants discontinuing study medication during the intervention phase, CD4+ T cell count <200 cells/μL, possibly drug-related SAE/AE ≥ grade 4, or AIDS-related illness (Centers for Disease Control category C events).

Study endpoints

The prespecified primary end point was the change in HIV-1 reactivation at treatment initiation and at the end of treatment in the study arms, measured as the change in CA US HIV-1 RNA between treatment initiation (day 0 at 0 hours) and at the end of the study (day 42). Secondary end points reported here included the change in inducible HIV-1 reservoir size as quantified by TILDA, the synergistic effects of pyrimethamine with VPA on the induction of CA US HIV-1 RNA, the change in CA US HIV-1 RNA between time points within and between study arms, plasma HIV-1 RNA changes, the pharmacokinetic and pharmacodynamic profiles of the intervention regimens, and the clinical safety and tolerability of the intervention regimen.

CA US HIV-1 RNA

For quantification of CA US HIV-1 RNA, CD4+ T cells were isolated from peripheral blood mononuclear cells (PBMCs) by negative selection using EasySep Human CD4+ T Cell Enrichment Cocktail (STEMCELL Technologies). Isolation of CD4+ T cells was per- formed on ice or at 4°C (unless indicated otherwise by the manufacturer). Approximately 1.5×10^6 CD4+ T cells were lysed in triplicate with TRI reagent. Total RNA was isolated by the phenol/chloroform isolation method following the manufacturer's instructions. A minimum of 150 ng of total RNA was deoxyribonuclease (DNase)–treated following the manufacturer's instructions (DNase I, Amplification Grade, Invitrogen), and complementary DNA (cDNA) synthesis was performed in duplicate with Super-Script II (Invitrogen) following the manufacturer's instructions. Absolute quantification of CA US HIV-1 RNA was

performed following a modified version of Pasternak *et al.* methodology [72]. Briefly, the first round of nested amplification was performed in a final volume of 25 µL using 10 µL of cDNA, 2.5 µL of 10× PCR buffer (Life Technologies), 1 µL of 50 mM $MgCl_2$ (Life Technologies), 1 µL of 10 mM deoxynucleotide triphosphate (dNTP) (Life Technologies), 0.075 µL of 100 µM US forward primer, 0.075 µL of 100 µM US reverse 1 primer, and 0.2 µL of Platinum Taq polymerase (Life Technologies) at 95°C for 5 min, followed by 15 cycles at 95°C for 30 s, 55°C for 30 s, and 72°C for 15 min. The second round of amplification was performed in a final volume of 25 µL using 2 µL of preamplified cDNA, 2.5 µL of 1× PCR buffer (Life Technologies), 1 µL of 50 mM $MgCl_2$ (Life Technologies), 1 µL of 100 µM US reverse 2 primer, 0.0375 µL of US probe, and 0.2 µL of Platinum Taq polymerase (Life Technologies) at 95°C for 5 min, followed by 45 cycles at 95°C for 30 s and 60°C for 1 min. The list of primers and probe is available in table S9. The absolute number of US copies in the PCR was calculated using a standard curve ranging from 2 to 512 copies of a plasmid containing the full-length HIV-1 genome (pNL4.3.Luc.R-E-). On the basis of standard curve analysis, we assigned a LOQ of 16 copies with an intra-assay coefficient of variation of <5% (fig. S4D). The quantity of CA US HIV-1 RNA was expressed as the number of copies per 150 ng of input RNA in reverse transcription.

BAF complex target gene expression

RT-qPCR reactions were conducted using GoTaq qPCR Master Mix (Promega) following the manufacturer's protocol. The following thermal cycling protocol was used for amplification: 3 min at 95°C, followed by 40 cycles of 95°C for 10 s and 60°C for 30s. Expression data were calculated using the $2^{-\Delta\Delta Ct}$ methodology [73]. Cyclophilin A was used as a housekeeping gene for the analysis. The list of primers is available in table S9.

Pharmacokinetic analysis

Self-reported adherence was assessed at each study visit, and empty pill strips were collected after the 2-week intervention phase. EDTA plasma samples were collected at the start of the intervention phase on day 0 (at 0 hours and at 6 hours after the first dose), day 7 (VPA only), day 14, and day 42. Plasma concentrations of VPA were analyzed by using a routinely implemented and validated assay (Multigent Valproic Acid Assays) at the Erasmus University Medical Center Pharmacy. For pyrimethamine measurements, we developed an assay (validated according to U.S. Food and Administration/European Medicines Agency guidelines) using the Waters Acquity UPLC-MS/MS. Samples (50 µL) were prepared and pumped into the column [Waters Acquity BEH C18 (1.7 µm, 2.1 × 100 mm), at 50°C]. A gradient (0.3

mL/min) with two eluents was used (A: 2 mM ammonium acetate + 0.1% formic acid in water; B: 2 mM ammonium acetate + 0.1% formic acid in methanol). The total run time was 4.2 min. Mass transitions used were mass/charge ratio (*m/z*) 249.09 to 176.97 (pyrimethamine) and *m/z* 325.05 to 307.05 (quinine), cone voltages were 22 V (pyrimethamine) and 58 V (quinine), and collision energies were 20 eV (pyrimethamine) and 14 eV (quinine). Capillary voltage was 3 kV, source temperature was 150°C, desolvation temperature was 400°C, and desolvation gas flow was 900 liters per hour. For measurement validation, we per- formed linearity, correctness, LOD and lower LOQ, repeatability, reproducibility, measurement uncertainty, robustness, and carry-over. The detection range was validated between 0.3 and 22 mg/L. Unbound dolutegravir plasma concentrations were quantified with a validated UPLC-MS/MS bioquantification method as previously described [61].

Inducible HIV-1 reservoir

The frequency of CD4+ T cells expressing MS HIV-1 RNA was determined using TILDA with some modifications to the protocol described previously by our group [68]. Briefly, total CD4+ T cells were isolated from PBMCs by negative magnetic selection using EasySep CD4+ Human CD4+ T Cell Enrichment kit (STEMCELL Technologies). Following isolation, 1.5×10^6 CD4+ T cells/ml were rested in complete RPMI 1640 for 5 to 8 hours before 12 hours of stimulation with PMA (100 ng/mL) and ionomycin (1 µg/mL) (both from Sigma- Aldrich). After stimulation, CD4+ T cells were washed and resuspended in serum-free RPMI 1640. Cells were counted and serially diluted accordingly: 1.8×10^6 cells/mL, 9×10^5 cells/mL, 3×10^5 cells/ mL, and 1×10^5 cells/ mL. For certain samples with smaller reservoirs, TILDA was performed using a higher input of CD4+ T cells (two- to fourfold). In the preamplification reaction, 10 µL of the cell suspension from each dilution was dispensed into 24 to 48 wells of a 96-well plate containing 2 µL of one-step RT-PCR enzyme (Qiagen), 10 µL of 5× one-step RT-PCR buffer (Qiagen), 10 µL of Triton X- 100 (0.3%), 0.25 µL of RNAsin (40 U/µL), 2 µl of dNTPs (10 mM each), 1 µL of tat1.4 forward primer (20 µM) and rev reverse primer (20 µM) (as published), and nuclease-free water to a final reaction volume of 50 µL. The one-step RT-PCR was run using the following thermocycling conditions: 50°C for 30 min, 95°C for 15 min, followed by 25 cycles of 95°C for 1 min, 55°C for 1 min, and 72°C for 2 min, and a final extension at 72°C for 5 min. After preamplification, 2 µL of the products was used as input for the real-time PCR to detect *tat/rev* MS HIV-1 RNA in a final reaction volume of 20 µL, which consisted of 5 µL of 4× TaqMan Fast Advanced Master mix (Thermo Fisher Scientific), 0.4 µL of tat2.0 forward primer, rev reverse primer (each at 20 µM), and MS *tat/ rev* probe (5 µM). The real-time PCR was performed using the following program: 50°C for 5 min, 95°C for 20 s, followed by 45 cycles of 95°C for 3 s and 60°C for 30 s. Positive

wells at each dilution were recorded and used to determine the frequency of cells expressing *tat/rev* MS HIV-1 RNA by the maximum likelihood method. The inter-operator reproducibility of the assay was evaluated using samples obtained from participants in the pyrimethamine arm (fig. S5, B to D). Primers used for qPCR to generate the endpoints by TILDA and the other PCR-based assays are listed in table S9.

Statistical analysis

The sample size was based on the null hypothesis that the change in CA US HIV-1 RNA between the study arms is equal and the alternative hypothesis that the change in CA US HIV-1 RNA is not equal. Assuming a mean change of 31 copies of CA US HIV-1 RNA (SD estimated at 20) by the intervention based on previous trials [35], we could detect a twofold increase between any of the four groups with six participants per group at 80% power and alpha 0.05. A twofold change has also been observed in other clinical trials and in our preclinical experiments with pyrimethamine ex vivo [24, 34, 44]. This therefore was considered a realistic target to substantiate the power calculation on. We included seven participants per study arm to account for dropout. The measurements related to the end points CA US HIV-1 RNA, MS HIV-1 RNA, plasma HIV-1 RNA, and drug plasma levels were described as median with IQR or full range. When the CA US HIV- 1 RNA measurement was below the limit of quantitation set at 16 copies per 150 ng of total RNA, we imputed 16 copies at these data points for further calculations. The fold change difference per study arm from pretreatment CA US HIV-1 RNA levels to the time points 6 hours, day 14, and day 42 after first dosing was calculated by adding up the fold change per individual divided by the total number of measurements available per time point. We analyzed the primary end point by a generalized estimating equation model to evaluate whether any difference in the CA US HIV-1 RNA existed at any time point during the trial in any of the three interventional arms compared to the control arm. An interaction term of time and treatment was included. We used the Bliss independence method to conclude on synergism between pyrimethamine and VPA using the following equation $\mu_{(1+2)exp.} = [1 - (1 - \mu_1) \times (1 - \mu_2)]$. The difference between the observed and expected amount of CA US HIV-1 RNA was calculated, and combination therapy was considered synergistic if the difference and its 95% confidence interval were >0. Because of the number of participants in this pilot, all secondary end points were exploratory. We therefore limited the use of inferential statistics to assessing the median fold changes between the time points in CA US HIV-1 RNA and BAF target genes within and between treatment arms by Wilcoxon signed-rank tests or Mann Whitney *U* tests, and we used Pearson's test to explore correlations between clinical variables and plasma pyrimethamine levels with the primary end point CA US HIV-1 RNA. We did not adjust for multiple testing post

hoc because we powered this pilot study to analyze the primary end point and did not predefine the number of exploratory analyses.

ACKNOWLEDGEMENTS

We want to express our gratitude to all participants in the study. Furthermore, we want to thank all internist–infectious diseases specialists at Erasmus MC for help in recruitment and the scientists from the Erasmus MC HIV Eradication Group (EHEG). P. Bollen is acknowledged for help with analyzing the dolutegravir–valproic acid interaction. The logistics and sample processing of the work were greatly supported by the research nurses (R. van Engen, A. Karisli, and M. Wagemaker), laboratory technicians, and the MSc students who contributed (K. Hensley and D. Teijema). Last, this study would not have been possible without the scientific vision of C. A. B. Boucher, a professor in virology and our dear colleague, who unfortunately passed away too early in February 2021.

FUNDING

C.R. received funding from ErasmusMC MRace (project no. 108172) and Aidsfonds (grant no. P-53601). S.R. received funding from Aidsfonds (grant no P-53102). R.A.G. received funding from Horizon Europe (grant no. 681032) and Health Holland (grant no. LSHM19100-SGF), and T.Ma. received funding from Health Holland (grant nos. LSHM19100-SGF and EMCLSH19023) and ZonMW (grant no. 40-44600-98-333).

AUTHOR CONTRIBUTIONS

Conceptualization: H.A.B.P., R.A.G., A.V., T.Ma., and C.R. Methodology: H.A.B.P., R.C., C.L., S.R., L.L., R.J.O., G.P., T.H., T.W.K., J.J.A.v.K., A.C., D.B., D.A.M.C.v.d.V., R.-J.P., B.C.P.K., R.A.G., Y.M.M., M.S., P.D.K., A.V., T.Ma., and C.R. Investigation: H.A.B.P., R.C., C.L., S.R., L.L., G.P., T.H., B.J.A.R., E.C.M.v.G., J.L.N., C.A.M.S., E.v.N., M.d.M.M., H.I.B., T.E.M.S.d.V.-S., J.J.A.v.K., A.C., D.B., D.A.M.C.v.d.V., T.Me., R.-J.P., B.C.P.K., R.A.G., Y.M.M., P.D.K., A.V.,T.Ma., and C.R. Visualization: H.A.B.P., R.C., C.L., T.Ma., and C.R. Funding acquisition: S.R., R.A.G. A.V., T.Ma., and C.R. Project administration: H.A.B.P., R.C., C.L., T.Ma., and C.R. Supervision: S.R., D.B., R.-J.P., B.C.P.K., R.A.G., P.D.K., A.V., T.Ma., and C.R. Writing – original draft: H.A.B.P., R.C., C.L.,T.Ma., and C.R. Writing – review and editing: H.A.B.P., R.C., C.L., S.R., L.L., R.J.O., G.P., T.H., B.J.A.R.,E.C.M.v.G., J.L.N., C.A.M.S., E.v.N., M.d.M.M., H.I.B., T.E.M.S.d.V.-S., J.J.A.v.K., A.C., D.B.,, T.Me., R.-J.P., B.C.P.K., R.A.G., Y.M.M., P.D.K., A.V., T.Ma., and C.R.

INTERESTS

J.J.A.v.K. reports research grants from NIH and ZonMW, an advisory board membership for Gilead Sciences, and consultancy for HaDEA. D.B. reports research grants from ViiV Healthcare, Gilead Sciences, and Merck and acted as an advisor to ViiV Healthcare, Gilead Sciences, Merck, and Pfizer. R.A.G. reports research grants from NIH, Health~Holland, EU, and Aidsfonds. P.D.K. reports funding from Aidsfonds. C.R. reports research grants from ViiV Healthcare, Gilead Sciences, Janssen-Cilag, Health~Holland, Erasmus MC, Aidsfonds, ZonMW, and Dutch Federation Medical Specialist and advisory board membership and travel reimbursement from ViiV Healthcare and Gilead Sciences. The other authors declare that they have no competing interests.

DATA AND MATERIALS AVAILABILITY

All data needed to evaluate the conclusions in the paper are present in the paper and/or the Supplementary Materials.

SUPPLEMENTARY DATA

Prins H.A.B., Crespo R., Lungu C., et al Sci Adv. 2023 Mar 17;9(11):eade6675. doi: 10.1126/sciadv.ade6675

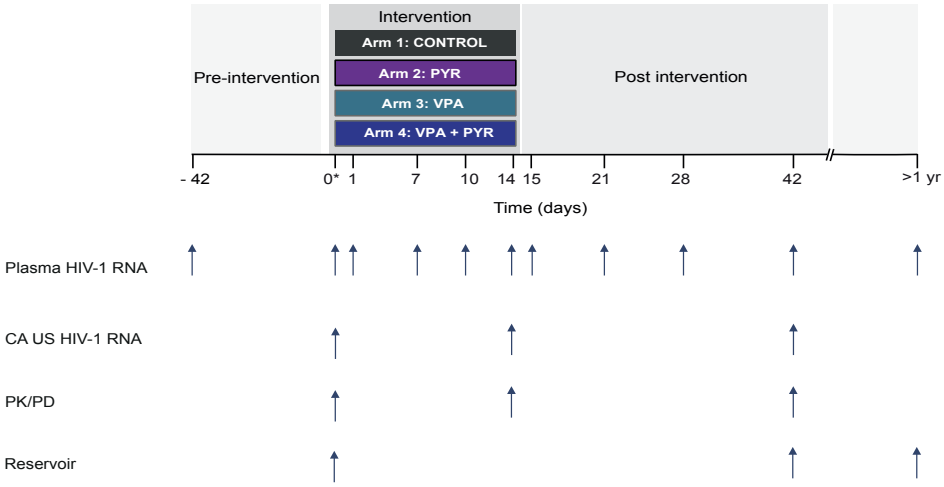

Fig. S1. Study design overview. The screening time point is shown at day -42. The three treatment arms and a fourth control arm are shown in blue (VPA arm), purple (PYR arm), dark blue (VPA+PYR), and black (control). Sampling time points for primary and secondary endpoint analysis are indicated by small solid arrows below the timeline. All participants provided 1 extra blood sample at least 1 year after the day 42 visit. * On day 0, CA HIV-1 RNA was measured in samples taken at t=0 hours and after 6 hours. VPA: valproic acid; PYR: pyrimethamine; CA HIV-1 RNA: cell associated HIV-1 RNA; PK: pharmacokinetics; PD: pharmacodynamics.

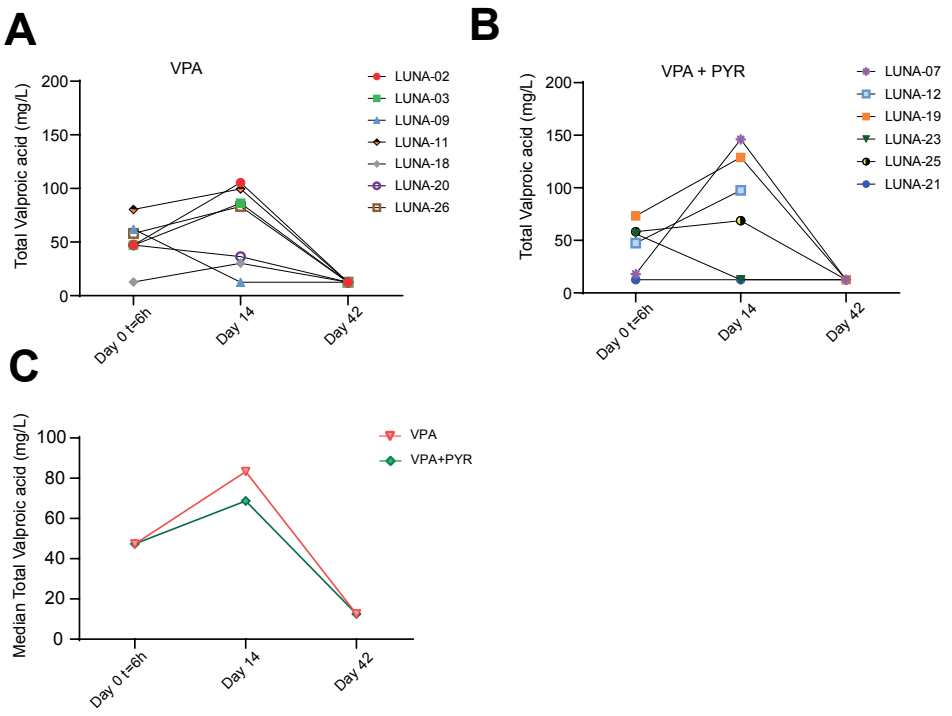

Fig. S2. Pharmacokinetics of the drug valproic acid in study participants. (**A-B**) Pharmacokinetics analysis of the drug valproic acid in study participants represented as plasma valproic acid levels per individual on valproic acid (**A**) or the combination treatment with pyrimethamine and valproic acid (**B**) and the median total valproic acid (mg/L) level in plasma (**C**) including all participants of the valproic acid arm (red) and the combination treatment arm with pyrimethamine and valproic acid (green) at 6 hours after first dosing (day 0, t=6 hr), at day 7, at the end of treatment period (day 14) and 28 days after end of treatment (day 42). Valproic acid concentration measurement was unsuccessful at day 42 for LUNA-12. Participants that stopped study medication or had dose adjustments are indicated with either a red stop sign or red ½ symbol and a red cross on the individual points in the graph. In the valproic acid arm one participant stopped his study medication on day 8 (LUNA-09). In the combination treatment arm, three participants stopped both compounds (LUNA-23 on day 3, LUNA-06 on day 7 and LUNA-21 on day 10), and two participants had their dosage adjusted (LUNA-25 had VPA dose halved from day 2 on, PYR dose halved from day 7 on, and LUNA-12 had PYR dose halved from day 7 on).

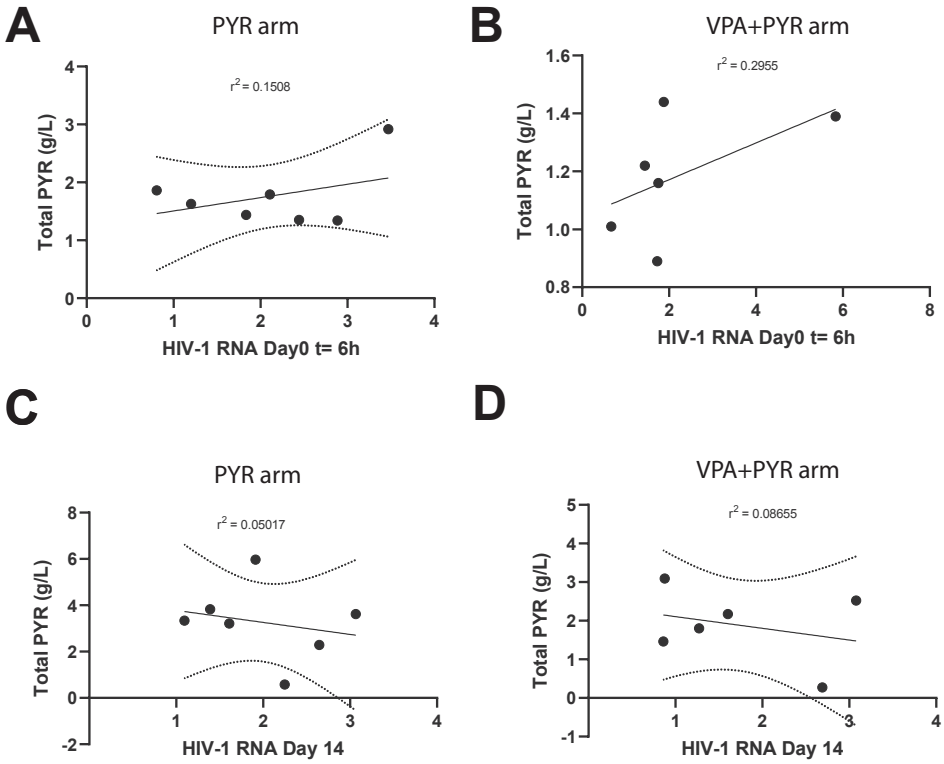

Fig. S3. Correlation plots of pyrimethamine plasma levels with the primary endpoint cell associated HIV-1 RNA. Mean and 95% confidence interval correlations with coefficient values (r) between total pyrimethamine (mg/L) and CA US HIV-1 RNA fold change at 6 hours after the first dosing participants on pyrimethamine (**A**), combination treatment with pyrimethamine and valproic acid (**B**) and at day 14 for these 2 groups (**C-D**) in 13 of 14 participants exposed to pyrimethamine with sufficient cells available for CA US HIV-1 RNA measurements. Coefficients were calculated by Pearson correlations.

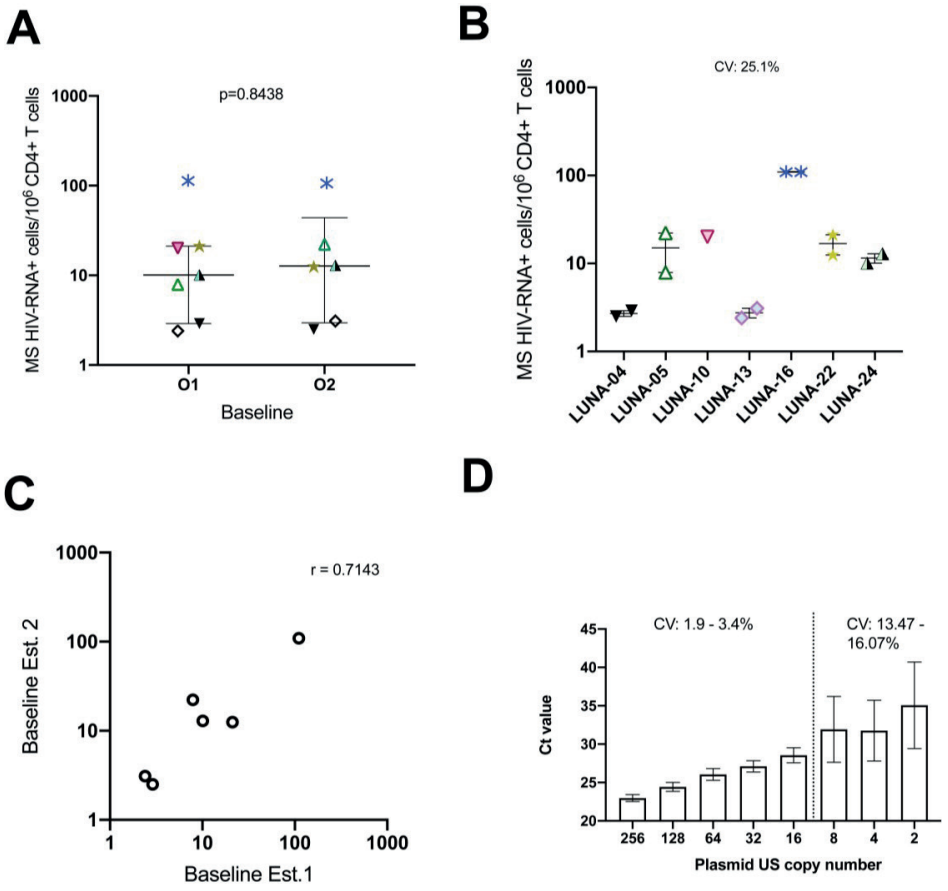

Fig. S4. Assay reproducibility and standard curve analysis. (**A**) and (**B**) Inter-operator reproducibility of TILDA. Measurements of inducible reservoir size in baseline samples obtained from participants in the pyrimethamine arm. TILDA was performed by different operators [O1 and O2] in independent experiments. The error bars represent the interquartile range. A Wilcoxon matched-pairs signed rank test was used to compare the medians of the TILDA data generated by O1 and O2. CV indicates coefficient of variation. (**C**) Spearman correlation of the TILDA data between operators. (**D**) Standard curve interpolation of absolute number of US copies ranging from 2 to 256 copies of a plasmid containing the full-length HIV-1 genome (pNL4.3.Luc.R-E-) and cycle threshold value (Ct value) in the PCR. CV indicates coefficient of variation. Based on standard curve analysis we assigned a limit of quantification (LOQ) of 16 copies with an intra assay coefficient of variation of <5%.

Table S1. Total number of self-reported adverse events and their severity during trial participation

	Grade 1	Grade 2	Grade3	Any Grade
Control arm	4	0	0	4
Pyrimethamine arm	33	3	2	38
Valproic acid arm	13	2	0	15
Valproic acid + pyrimethamine arm	32	13	1	46
Total adverse events	82	18	3	103
Presumed related	72	16	3	91
Presumed not related	10	2	0	12

Table S2. Total number of self-reported adverse events (AE) per treatment arm during trial participation

AE considered related	PYR	VPA	PYR+VPA	Control
Gastrointestinal	9	5	17	0
Nausea	4	2	6	
Vomiting	3	3	6	
Diarrhea	1		1	
Dysgeusia	1			
Dyspepsia			2	
Early satiety			1	
Bloating			1	
Neurological	12	7	21	1
Vertigo		1	5	
Headache	2	2	2	
Somnolence		1	4	
Involuntary muscle movement		1		
Lethargy		1	2	
Dizziness	1	1		
Insomnia	3		1	
Presyncope	1			1
Syncope	2		1	
Light-headedness	1		2	
Tremor	1			
Dysarthria	1			
Tinnitus			2	
Agitation			1	
Hypersomnia			1	
Other organ systems	12	1	6	0
Sweats	1			
Rash	2			
Nosebleed	1			
Pruritus	1		1	
Cold extremities	1		1	
Malaise	2		1	
Urine frequency			1	
Edema limbs		1		
Backache			1	
Anemia	1			
Neutropenia	1		1	
Thrombocytopenia	2			
Any related	**33**	**13**	**44**	**1**
AE considered not related				
Sore throat	1			
Nausea	1			
Vomiting	1			1
Diarrhea				1
Flu-like symptoms				1
Backache	1			
Ache right upper arm	1			
Headache		1		
Disturbed sleep		1		
Hyperglycemia			1	
Pharyngitis			1	
Any non-related	**5**	**2**	**2**	**3**

Table S3. Total number of self-reported adverse events (AE) and their severity during trial participation

AE considered related	Grade 1 N(%)	Grade 2 N(%)	Grade3 N(%)	Any Grade N(%)	No. of patients N(%)
Malaise	2	1	0	3	3
Nausea	8	4	0	12	12
Dyspepsia	2	0	0	2	2
Early satiety	1	0	0	1	1
Bloating	1	0	0	1	1
Vomiting	11	1	0	12	9
Diarrhea	2	0	0	2	2
Headache	5	1	0	6	6
Somnolence	5	0	0	5	4
Hypersomnia	1	0	0	1	1
Insomnia	4	0	0	4	4
Involuntary muscle movement	1	0	0	1	1
Vertigo	3	3	0	6	5
Tinnitus	1	1	0	2	2
Lethargy	2	1	0	3	3
Agitation	0	1	0	1	1
Dizziness	2	0	0	2	2
Light headedness	3	0	0	3	3
Presyncope	2	0	0	2	2
Syncope	0	0	3	3	3
Edema limbs	1	0	0	1	1
Cold extremities	2	0	0	2	2
Sweats	1	0	0	1	1
Rash	2	0	0	2	1
Pruritus	2	0	0	2	2
Dysarthria	1	0	0	1	1
Dysgeusia	1	0	0	1	1
Tremor	1	0	0	1	1
Urinary frequency	1	0	0	1	1
Back pain	1	0	0	1	1
Nosebleed	1	0	0	1	1
Anemia	1	0	0	1	1
Platelet count decreased	1	1	0	2	1
Neutrophil count decreased	0	2	0	2	2
Any related AE	72	16	3	91	84
AE considered not related					
Nausea	1	0	0	1	1
Vomiting	2	0	0	2	2
Diarrhea	1	0	0	1	1
Headache	1	0	0	1	1
Disturbed sleep	1	0	0	1	1
Ache right upper arm	0	1	0	1	1
Upper back ache	1	0	0	1	1
Sore throat	1	0	0	1	1
Hyperglycemia	0	1	0	1	1
Pharyngitis	1	0	0	1	1
Flu like symptoms	1	0	0	1	1
Any not related	10	2	0	12	12
Total AE	**82**	**18**	**3**	**103**	**96**

Table S4. Baseline characteristics of participants with and without adjusted interventions

Baseline Characteristics	With treatment adjustment n =28	Without treatment adjustment N=7
Male	7 (100)	21 (100)
Ethnic origin		
-White European	5 (71.4)	19 (90.5)
-Latin American or Hispanic	1 (14.3)	2 (9.5)
-Black Caribbean	1 (14.3)	0
Age (years)	51 (42-58)	54 (50-61)
HIV subtype B[a]	6 (85.7)	18 (85.7)
History of AIDS	2 (28.6)	6 (28.6)
Years from HIV diagnosis until inclusion	7.6 (6.2-8.0)	10.7 (7.6-18.5)
Years on cART	7.2 (4.7-7.3)	8.5 (5.6-12.3)
Years with HIV-RNA <50 copies per mL	5.1 (4.5-7.1)	7.2 (5.1-11.8)
Initiated cART during acute HIV infection	0	3 (14.3)
Pre-cART plasma viral load zenith $\log_{10}$ copies per mL	4.81 (4.58-5.04)	4.90 (4.77-5.35)
Pre-cART nadir CD4+ T-cell count per µL	300 (205-420)	220 (140-290)
CD4+ T-cell count per µL at inclusion	750 (580-930)	650 (530-790)
cART		
-NNRTI based[b]	3 (42.9)	13 (61.9)
-INSTI based[c]	4 (57.1)	8 (38.1)

Data are number with percentage or median with interquartile ranges.
[a]Other HIV-1 subtypes include CRF01-AE (n=2), CRF01-AG (n=1), C (n=1).
[b]NNRTI were rilpivirine (n=6), nevirapine (n=6), efavirenz (n=4). 15 NRTI backbones consisted of emtricitabine (FTC) and either tenofovir disoproxil fumarate (TDF) or tenofovir alafenamide (TAF) and 1 NRTI backbone consisted of abacavir with lamivudine.
[c]INSTI were dolutegravir (n=10) and elvitegravir/cobicistat (n=2). 7 NRTI backbones consisted of FTC and either TDF or TAF, 3 NRTI backbones consisted of lamivudine (3TC) and abacavir (ABC); and 2 had dolutegravir with 3TC as NRTI backbone.
Abbreviations: cART: combination antiretroviral therapy; INSTI: integrase strand transfer inhibitor; NNRTI: non-nucleoside reverse transcriptase inhibitor.

Table S5. Individual clinical characteristics and cell associated unspliced HIV-1 RNA during LUNA

	Age	Recent CD4 T-cell count per µL	Years on cART	cART	CA US HIVRNA copies/150ng Total RNA Day 0, pretreatment	CA US HIVRNA copies/150ng Total RNA Day 0, 6 hours	CA US HIVRNA copies/150ng Total RNA Day 14	CA US HIVRNA copies/150ng Total RNA Day 42
PYR								
LUNA-04	50	580	7,3	FTC, TAF, EVG/c	32,60	94,04	62,36	101,16
LUNA-05	53	390	5,5	FTC, TDF, EFV	79,98	96,01	111,26	84,39
LUNA-10	35	810	7,2	FTC, TAF, NVP	51,15	125,01	114,91	85,80
LUNA-13	46	850	5,6	FTC, TDF, EFV	68,92	126,50	111,02	54,17
LUNA-16	59	400	16,3	FTC, TDF, NVP	24,35	51,31	74,67	82,71
LUNA-22	53	610	7,7	FTC, TAF, DTG	49,43	39,82	54,10	69,81
LUNA-24	57	730	23,1	FTC, TAF, NVP	16,00	55,52	42,33	29,28
PYR+VPA								
LUNA-06[1]	44	630	7,2	FTC, TAF, RPV				
LUNA-07	46	960	12,2	FTC, TDF, RPV	53,68	35,85	46,27	28,10
LUNA-12	55	1050	3,5	3TC, ABC, DTG	34,27	49,48	54,91	
LUNA-19	65	240	5,6	FTC, TAF, RPV	32,97	57,84	28,92	
LUNA-21	61	420	4,8	FTC, TDF, RPV	28,25	48,73	35,93	45,78
LUNA-23	51	530	7,5	3TC, ABC, DTG	16,64	97,05	51,25	49,58
LUNA-25	40	1180	4,5	3TC, DTG	21,83	41,01	58,74	31,47
VPA								
LUNA-02	50	790	4,8	FTC, TAF, RPV	95,16	101,51	161,79	59,33
LUNA-03	52	590	7,6	FTC, TAF, DTG	12,93	10,16	18,41	16,00
LUNA-09	65	750	7,4	FTC, TAF, DTG	22,90	42,74	28,40	49,74
LUNA-11	54	1250	21,1	FTC, TDF, NVP	39,10	53,04	97,80	59,03
LUNA-18	70	530	12,3	FTC, TDF, NVP	16,00	19,23	16,00	16,00
LUNA-20	28	830	4,3	FTC, TDF, EFV	76,70	51,59	47,89	52,98
LUNA-26	68	330	9,3	FTC, TAF, DTG	16,00	16,00	18,82	22,83
CONTROL								
LUNA-01	47	780	3,9	FTC, TDF, RPV	16,00	16,00	16,00	16,00
LUNA-08	66	700	14,7	FTC, TDF, EFV	50,82	63,21	57,75	45,16

	Age	Recent CD4 T-cell count per µL	Years on cART	cART	CA US HIVRNA copies/150ng Total RNA Day 0, pretreatment	CA US HIVRNA copies/150ng Total RNA Day 0, 6 hours	CA US HIVRNA copies/150ng Total RNA Day 14	CA US HIVRNA copies/150ng Total RNA Day 42
LUNA-14	54	650	7,4	3TC, DTG	120,00	114,52	93,02	100,41
LUNA-15	61	680	21,7	FTC, TAF, EVG/c	62,96	113,72	113,54	120,88
LUNA-17	70	530	8,5	3TC, ABC, NVP	16,00	39,37	29,24	22,56
LUNA-27	55	980	9,8	FTC, TDF, DTG	16,00	16,00	16,00	16,00
LUNA-28	46	470	11,2	3TC, ABC, DTG	16,00	16,00	16,00	16,00

[1] LUNA-06 had insufficient PBMC at day 0 at 6 hours post dosing to measure the primary endpoint. Due to the missing baseline measurement, no CA US HIV-1 RNA was measured at the other time points. Abbreviations: cART: combination antiretroviral therapy; PYR: pyrimethamine; VPA: valproic acid; FTC: emtricitabine; 3TC: lamivudine; ABC: abacavir; TDF: tenofovir disoproxil fumarate; TAF: tenofovir alafenamide; EFV: efavirenz; NVP: nevirapine; RPV: rilpivirine; DTG: dolutegravir; EVG/c: elvitegravir/cobicistat; .

Table S6. Plasma HIV-1 RNA evolution during LUNA per participant

	Day 0, 0hr	Day 0, 6hr	Day 1	Day 7	Day 10	Day 14	Day 15	Day 21	Day 28	Day 42
PYR										
LUNA-04	<20/P	*	<20/N	<20/N	<20/N	<20/P	<20/N	<20/P	<20/N	<20/P
LUNA-05	<20/N	*	<20/P	<20/N	<20/N	<20/N	<20/N	<20/N	<20/P	<20/N
LUNA-10	<20/N	*	<20/N	<20/N	<20/N	<20/P	<20/N	<20/P	<20/P	<20/N
LUNA-13	<20/P	<20/N	<20/N	<20/N	<20/P	<20/N	<20/N	<20/N	<20/N	<20/P
LUNA-16	<20/N	<20/N	<20/N	<20/P	<20/N	<20/N	<20/N	<20/N	20	<20/N
LUNA-22	<20/N	<20/P	<20/N	<20/N	<20/N	<20/N	<20/P	<20/N	<20/N	<20/N
LUNA-24	<20/P	<20/P	<20/P	<20/N	<20/N	<20/N	<20/N	<20/N	<20/N	<20/N
PYR+VPA										
LUNA-06	<20/N	*	<20/N	<20/N	<20/N	<20/N	<20/N	<20/N	<20/N	<20/N
LUNA-07	<20/N	*	<20/N	<20/P	<20/N	<20/N	<20/N	<20/P	<20/P	<20/N
LUNA-12	<20/N	*	<20/P	<20/N	<20/N	<20/N	<20/N	<20/N	<20/N	<20/N
LUNA-19	<20/N	<20/N	<20/N	<20/N	<20/N	<20/N	<20/N	<20/N	<20/N	<20/P
LUNA-21	<20/N	<20/N	<20/N	<20/N	<20/N	<20/N	<20/N	<20/N	<20/N	<20/N
LUNA-23	<20/P	<20/N	<20/P	22	<20/P	<20/N	<20/P	<20/P	<20/N	<20/P
LUNA-25	<20/N	<20/N	<20/P	<20/N	<20/P	<20/N	<20/P	<20/N	<20/N	<20/P
VPA										
LUNA-02	<20/N	*	<20/N	<20/N	<20/N	<20/N	<20/P	<20/N	<20/N	<20/N
LUNA-03	<20/N	*	<20/N	<20/N	<20/N	<20/N	<20/N	<20/N	<20/N	<20/N
LUNA-09	<20/N	*	<20/P	<20/N	<20/N	<20/N	<20/N	<20/N	<20/N	<20/P
LUNA-11	<20/N	*	<20/N	<20/N	<20/N	<20/P	<20/N	<20/P	<20/N	<20/N
LUNA-18	<20/N	<20/N	<20/N	<20/N	<20/N	<20/N	<20/N	<20/N	<20/N	<20/P
LUNA-20	<20/P	<20/N	41	<20/P	<20/N	<20/P	<20/P	<20/P	<20/N	<20/P
LUNA-26	<20/N	<20/P	<20/N	<20/N	<20/N	<20/N	<20/P	21	<20/N	<20/P
CONTROL										
LUNA-01	<20/N	*	<20/N	<20/N	<20/P	<20/N	<20/N	<20/N	<20/N	<20/N
LUNA-08	<20/N	*	<20/N	<20/N	<20/P	<20/P	<20/N	<20/P	<20/P	<20/N
LUNA-14	<20/N	<20/N	<20/N	<20/P	<20/N	<20/P	<20/N	<20/P	<20/P	<20/N
LUNA-15	<20/N	<20/N	<20/P	<20/N	<20/N	<20/N	<20/N	<20/N	<20/N	<20/N
LUNA-17	<20/N	<20/N	<20/N	<20/N	<20/N	<20/P	<20/N	<20/N	<20/N	<20/P
LUNA-27	<20/N	<20/N	<20/N	<20/N	<20/N	<20/N	<20/N	<20/N	<20/N	<20/P
LUNA-28	<20/N	<20/N	<20/P	<20/N	<20/P	<20/P	<20/N	<20/P	<20/N	<20/N

*Protocol violation where day 0, 6 hour time point was not collected for participants LUNA-01 till LUNA-12.
/N denotes target viral genome not detected below level of quantitation.
/P denotes target viral genome detected below level of quantitation.
Those with and without pyrimethamine exposure were comparable with regard to the proportions of samples with plasma HIV-1 RNA above the assay detection limit both during routine care prior to study inclusion since cART initiation (20.7% versus 17.8%) and during the study at the fixed measurements (22.2% versus 23.6%). Abbreviations: PYR: pyrimethamine; VPA: valproic acid.

Table S7. Fold-induction gene expression values for BAF target genes

	Fold-induction in IL-10 gene expression at Day 0, 6 hours relative to Day 0, pretreatment	Fold-induction in SOCS3 gene expression at Day 0, 6 hours relative to Day 0, pretreatment	Fold-induction in CBX7 gene expression at Day 0, 6 hours relative to Day 0, pretreatment	Fold-induction in B-ACTIN gene expression at Day 0, 6 hours relative to Day 0, pretreatment
PYR				
LUNA-04	2.24	4.59	1.25	0.86
LUNA-05	6.4	3.27	1.03	1.04
LUNA-10	2.54	2.52	1.68	1.29
LUNA-13	2.74	2.27	1.12	1.51
LUNA-16	1.48	0.60	12.42	0.82
LUNA-22	1.74	5.35	4.23	0.94
LUNA-24	6.66	1.14	2.02	0.94
PYR+VPA				
LUNA-07	0.53	1.96	0.87	0.87
LUNA-12	0.86	0.94	0.70	0.85
LUNA-19	1.99	1.03	1.11	1.14
LUNA-21	3.31	0.93	0.79	0.65
LUNA-23	3.81	2.48	1.25	0.8
LUNA-25	0.61	0.78	1.73	1.58
VPA				
LUNA-02	0.42	0.53	0.82	0.68
LUNA-03	0.64	0.67	1.71	1.12
LUNA-09	NA	0.52	1.16	2.5
LUNA-11	1.25	0.38	0.9	0.94
LUNA-18	1.10	1.92	0.54	0.9
LUNA-20	0.94	0.85	0.23	0.69
LUNA-26	1.87	2.47	0.87	0.61
CONTROL				
LUNA-01	NA	NA	NA	0.92
LUNA-08	0.72	0.02	0.83	NA
LUNA-14	1.16	0.52	0.69	NA
LUNA-15	0.20	1.00	1.53	NA
LUNA-17	2.49	0.59	1.89	NA
LUNA-27	NA	0.54	0.44	0.94
LUNA-28	0.36	0.88	1.18	1.34

NA denotes not available due to insufficient sample. Abbreviations: PYR: pyrimethamine; VPA: valproic acid.

Table S8. TILDA reservoir as number of cells with multiply spliced HIV-RNA detectable per million CD4+ T-cells per participant

	Day 0, 0 hour	Day 42	>1year
PYR			
LUNA-04	2.7	1.6	NA
LUNA-05	15.1	10	22.2
LUNA-10	20.1	22.9	15.2
LUNA-13	2.8	8.8	19.3
LUNA-16	109.8	122.8	91.8
LUNA-22	16.9	22.8	13.9
LUNA-24	11.5	9.0	6.1
PYR+VPA			
LUNA-06	NA (low PBMC)		
LUNA-07	NA (low PBMC)		
LUNA-12	<LOD	<LOD	0.6
LUNA-19	26.5	63.0	NA
LUNA-21	19.0	3.0	2.0
LUNA-23	NA (subtype AG)	NA	NA
LUNA-25	7.3	18.3	45.7
VPA			
LUNA-02	12.5	12.7	NA
LUNA-03	2.5	1.2	2.2
LUNA-09	17.1	12.9	19.0
LUNA-11	3.4	NA	2.5
LUNA-18	NA (subtype C)		
LUNA-20	100.7	26.0	25.5
LUNA-26	326.5	NA	286.2
CONTROL			
LUNA-01	NA (subtype AE)		
LUNA-08	10.2	16.2	11.5
LUNA-14	53.0	32.3	53.5
LUNA-15	131.4	394.6	338.1
LUNA-17	NA (low PBMC)		
LUNA-27	NA (subtype AE)		
LUNA-28	52.7	57.8	NA

No TILDA were performed in participants with missing day 0 measurements due to primer mismatches or low CD4+T-cell yields.
NA denotes not available due to primer mismatches or low CD4+T-cell yields.
Abbreviations: PYR: pyrimethamine; VPA: valproic acid.

Table S9. List of primers used for PCR for CA US HIV-1 RNA, TILDA and BAF complex target genes

Primer name	Sequence 5'-3'
US Forward	TCAGCCCAGAAGTAATACCCATGT
US Reverse 1	TGCTATGTCAGTTCCCCTTGGTTCTCT
US Reverse 2	CACTGTGTTTAGCATGGTGTTT
US Probe	[6FAM]ATTATCAGAAGGAGCCACCCCACAAGA[BHQ1]
IL-10 Forward	GAGTCCTTGCTGGAGGACTTT
IL-10 Reverse	CACGGCCTTGCTCTTGTTTT
CBX7 Forward	GAGAAGGAGGAGAGAGACCGA
CBX7 Reverse	CCCTTGTCCACCAGCTCAG
SOCS3 Forward	CCAAGGACGGAGACTTCGAT
SOCS3 Reverse	GGTACTCGCTCTTGGAGCTG
B-ACTIN Forward	CACAGGGGAGGTGATAGCAT
B-ACTIN Reverse	TCAAGTTGGGGGACAAAAAG
Cyclophilin A Forward	TCATCTGCACTGCCAAGACTG
Cyclophilin A Reverse	CATGCCTTCTTTCACTTTGCC
Tat 1.4	TGG CAG GAA GAA GCG GAG A
Tat 2.0	ACAGTCAGACTCATCAAGTTTCTCTATCAAAGCA
Rev	GGATCTGTCTCTGTCTCTCTCTCCACC
TILDA Probe	5'-/56-FAM/TTCCTTCGG/ZEN/GCCTGTCGGGTCCC/3IABkFQ/-3

STUDY PROTOCOL SYNOPSIS

Protocol version 3.0
27 January, 2020

Rationale

The retrovirus HIV integrates as proviral DNA in the genome of our CD4+ T cells. A subset forms a reservoir of latently infected long-lived memory T-cells with nearly absent HIV-DNA transcription. This persistent latent HIV reservoir is the major obstacle for a cure. HIV latency is sustained by multiple host factors that restrict the viral promotor and expression of the viral genome. Latency reversing agents (LRA) can remove these restrictive components and mediate HIV latency reversal. LRA monotherapy with histone deacetylase inhibitors (HDACi), including valproic acid, vorinostat, romidepsin, panobinostat, reactivates HIV but seems insufficient to eliminate the reservoir *in vivo*. Our research group has identified the BAF complex as a repressive factor that maintains HIV latency. We investigated the activity of a panel of recently identified small molecule inhibitors of BAF (BAFi) as a new LRA group and showed that BAFi, including the clinically approved drug pyrimethamine at tolerable concentrations, are capable of reversing HIV latency and act synergistic with HDACi *in vitro* and in CD4+ T cells obtained from people with HIV on suppressive antiretroviral therapy. This offers new opportunities for cure research. We want to conduct the first study with BAFi and assess the potential synergism of 2 LRA with different modes of action on the reservoir in people with HIV.

Design and primary objective

The LUNA study is a 6-week prospective, open label, randomized controlled clinical trial. The primary objective is the longitudinal assessment of the BAFi pyrimethamine and of the HDACi valproic acid on the HIV reservoir in people with HIV on antiretroviral therapy.

The main hypothesis tested is:

H0: the change in CA-US HIVRNA between the groups during treatment are equal.
H1: the change in CA-US HIVRNA between the groups during treatment are not equal.

Study population

Inclusion criteria

1. HIV-1 infected patients ≥18 years.
2. WHO performance status 0 or 1.
3. Confirmed HIV-1 infection by 4th generation ELISA, Western Blot or PCR.
4. Wild type HIV infection or polymorphisms associated with at highest low-level resistance to any class of ART according to Stanford HIV drug resistance database. Transmitted mutations and acquired mutations due to virological failure associated with resistance of at highest low-level resistance are allowed.
5. On cART.
6. Current plasma HIV-RNA <50 copies/mL for at least 365 days and measured on at least 2 occasions of which at least 1 must be obtained within 365 and 90 days prior to study entry.
7. Current CD4 count at study entry of ≥200 cells/mm^3.
8. Pre-cART HIV-RNA ≥10.000 copies/mL.

Exclusion criteria

A potential subject who meets any of the following criteria will be excluded from participation in this study.

1. Previous virological failure, defined as either acquired resistance mutations (>low level resistance) on cART or HIV-RNA >1000 copies/mL on two consecutive measurements during cART.
2. Uncontrolled hepatitis B or C co-infection.
3. Prior exposure to any HDACi, BAFi or other known LRA.
4. Prior exposure to cytotoxic myeloablative chemotherapy for hematological malignancies during cART.
5. Concurrent exposure to strong interacting medication on glucuronidation.
6. Exposure within 90 days prior to study entry to immunomodulators, cytokines, systemic antifungals, dexamethasone, vitamin K antagonists, anti-epileptics, antipsychotica, carbapenems, mefloquine, colestyramine. Any documented opportunistic infection related to HIV in the last 90 days.
7. Inadequate blood counts, renal and hepatic function tests.
    a. Haemoglobin <6.5 mmol/L (males) or <6.0 mmol/L (females), leucocytes <2.5 x10^9/L, absolute neutrophil count <1000 cells/mm^3, thrombocytes <100 x10^9/L, international standardized ratio >1.6, activated partial thromboplastin time >40 seconds.
    b. Estimated glomerular filtration rate <50 mL/min (CKD-EPI).
    c. ALAT or total bilirubin >2.5 x upper limit of normal.

d. All laboratory values must be obtained within 42 days prior to the baseline visit.

8. Megaloblastic anemia due to folate deficiency.
9. Pancreatitis in last 6 months, or chronic pancreatitis.
10. Active malignancy during the past year with the exception of basal carcinoma of the skin, stage 0 cervical carcinoma, Kaposi Sarcoma treated with cART alone, or other indolent malignancies.
11. Females in the reproductive age cannot participate. Males cannot participate if they refuse to abstain from sex or condom use in sero-discordant sexual contact during the study, except if their sexual partner(s) use PREP.
12. Patients with active substance abuse or registered allergies to the investigational medical products.
13. Last, any other condition (familial, psychological, sociological, geographical) which in
14. the investigator's opinion poses an unacceptable risk or would hamper compliance with the study protocol and follow up schedule, will prohibit participation.

For hepatitis B: patients should be vaccinated, or on pre-exposure prophylaxis through the use of lamivudine/emtricitabine or tenofovir in their cART. Otherwise, standard serological testing should be available within the last 365 days for men with HIV who have sex with men. For other persons with HIV, there should be at least one negative hepatitis B test (either by serology or PCR). For men with HIV who have sex with men, a negative hepatitis C IgG, HCV antigen, blot or HCV-RNA PCR should be available within the previous 365 days. For other persons with HIV, there should be at least one negative hepatitis C test (either IgG, blot or PCR) available.

Primary endpoint

The change in HIV reactivation in the reservoir *in vivo* at treatment initiation and at the end of treatment, measured as the change in cell associated HIV-RNA. The change in reactivation is compared between the treatment arms. The primary outcome measure is the change in cell associated HIV-RNA between treatment initiation (week 0) and at the end of study (week 6).

Safety definitions

The study was terminated in case of excessive serious adverse events based on predefined safety criteria. Patients were monitored for adverse events. Study drugs were stopped if a drug-related SAE or AE of grade 4 or higher occurred, in case of AIDS-related illnesses CDC C, or if the blood CD4+ T cell count dropped below 200.

This was an open label study using approved drugs with a known safety profile for a shorter duration (pyrimethamine and valproic acid) than in usual care. The lab results (blood CD4+T-cells, plasma HIV RNA) and clinical condition that define the safety of this trial were readily available of all patients for the investigators. To protect the safety of the patients, the following study stopping rules were used:

1. A pre-specified interim analysis will be done after 14 patients (50%) are randomized. This will focus on the number of patients that had to discontinue treatment on investigators discretion due to blood CD4+T-cell count <200 during the IMP use, CDC-C events, possibly drug related SAE/AE ≥grade4, or AIDS related illness CDC C. If this exceeds 2 (10% of 21 patients that undergo an intervention) patients, the study will be stopped.
2. If ≥2 patients (of the 21 patients that undergo an intervention) have discontinued treatment due to possibly drug related AE before the planned interim analysis is done, the study will be stopped.
3. If at any time in the study the number of discontinuations due to blood CD4+T-cell count <200 during IMP use, or CDC-C events or possibly drug related SAE/AE ≥grade4, AIDS related illness CDC C exceeds 25% of 21 patients undergoing an intervention (>5 patients), the study will be stopped.
4. If ≥2 patients (10%) experience HIV treatment failure with acquisition of resistance associated mutations in HIV, the study will be stopped.

CHAPTER 3

Selective cell death in HIV-1-infected cells by DDX3 inhibitors leads to depletion of the inducible reservoir

S. Rao, **C. Lungu**, R. Crespo, T. H. Steijaert, A. Gorska, R.J. Palstra, H.A. B. Prins, W. van Ijcken, Y. M. Mueller, J. J. A. van Kampen, A. Verbon, P. D. Katsikis, C. A. B. Boucher, C. Rokx, R. A. Gruters & T. Mahmoudi

Rao S., Lungu C., et al., Nat Commun. 2021 Apr 30;12(1):2475.
doi: 10.1038/s41467-021-22608-z

ABSTRACT

An innovative approach to eliminate HIV-1-infected cells emerging out of latency, the major hurdle to HIV-1 cure, is to pharmacologically reactivate viral expression and concomitantly trigger intracellular pro-apoptotic pathways in order to selectively induce cell death (ICD) of infected cells, without reliance on the extracellular immune system. In this work, we demonstrate the effect of DDX3 inhibitors on selectively inducing cell death in latent HIV-1- infected cell lines, primary CD4+ T cells and in CD4+ T cells from cART-suppressed people living with HIV-1 (PLWHIV). We used single-cell FISH-Flow technology to characterise the contribution of viral RNA to inducing cell death. The pharmacological targeting of DDX3 induced HIV-1 RNA expression, resulting in phosphorylation of IRF3 and upregulation of IFNβ. DDX3 inhibition also resulted in the downregulation of BIRC5, critical to cell survival during HIV-1 infection, and selectively induced apoptosis in viral RNA-expressing CD4+ T cells but not bystander cells. DDX3 inhibitor treatment of CD4+ T cells from PLWHIV resulted in an approximately 50% reduction of the inducible latent HIV-1 reservoir by quantitation of HIV-1 RNA, by FISH-Flow, RT-qPCR and TILDA. This study provides proof of concept for pharmacological reversal of latency coupled to induction of apoptosis towards the elimination of the inducible reservoir.

INTRODUCTION

The main obstacle towards a human immunodeficiency virus type-1 (HIV-1) cure is the presence of a latent viral reservoir that does not actively produce viral particles, but retains the ability to do so and is not eliminated by combination antiretroviral therapy (cART) [1,2]. One strategy to eliminate the latent HIV-1 reservoir is the shock and kill approach that involves the use of latency-reversing agents (LRAs) to reactivate viral gene expression (Shock), followed by the elimination of cells harbouring reactivated provirus (Kill) [3]. The 'Kill' aspect of this approach has largely depended on an effective host adaptive immune response. Although clinical studies with LRAs demonstrated induced reactivation *in vivo*, limited to no reduction in the size of the viral reservoir or time to viral rebound post-cessation of cART was observed, indicating that elimination of reactivating cells warrants more attention [4-6]. So far, broadly neutralizing antibodies, therapeutic vaccines, chimeric antigen receptors, checkpoint inhibitors and engineered bispecific antibodies have been investigated to eliminate reactivated HIV-1-infected cells (reviewed in [7]). However, dependency on cell-mediated and humoral responses, which are already compromised in HIV-infected individuals because of impaired CD4+ T cell help and exhausted immune compartments, pose a considerable obstacle to these strategies. Indeed, early results from combinatorial clinical trials, which combine LRAs and immune enhancing clearance strategies, demonstrated that although HIV-1 specific immune responses were induced, no decrease in the size of the viral reservoir or viral control in the absence of cART were observed (refs. [8-10], reviewed in ref [11]).

A parallel approach to eliminate the viral reservoir independently of the extracellular immune system is to pharmacologically trigger pathways that intrinsically induce cell death (ICD) in reactivated HIV-1-infected reservoir cells. For example, using compounds to activate innate intracellular signalling pathways could trigger apoptosis. Several HIV-1 proteins have been demonstrated to have both anti-apoptotic activities in the early stages of the viral replication cycle and pro-apoptotic activity in the later replication stages [12]. By inhibiting viral anti-apoptotic activity or by promoting pro-apoptotic functions, HIV-1-infected cells can be selectively eliminated, leading to a reduction in the size of the viral reservoir. Multiple pro-apoptotic compounds that have been developed in the context of cancer research could potentially be repurposed for viral reservoir elimination and some have been investigated for their ability to ICD of HIV-infected cells (reviewed in refs. [13,14]). Interestingly, an important characteristic of the latent viral reservoir that has recently come to light is that while it is transcriptionally competent, it does not necessarily produce viral proteins due to post-transcriptional blocks [15,16]. Induced viral RNA does however retain the ability to trigger innate antiviral signalling

pathways [17,18] and possibly ICD of reactivated cells. The potential contribution of inducing viral transcription as a strategy to induce death of infected cells has been thus far under-investigated[19].

Advanced single-cell fluorescence in situ hybridisation flow cytometry (FISH-Flow)[15,16,20,21] provides a powerful tool to examine the specific contribution of HIV-1 unspliced RNA (herein referred to as vRNA) in inducing cell death. Unlike previous single-cell HIV-1 flow cytometry-based studies that could only detect viral protein production and the translationally competent reservoir, FISH-Flow allows for the delineation of the contribution of the under characterised transcriptionally competent cells that produce vRNA, can trigger innate immune responses and may or may not express viral proteins [19,22]. The single-cell analysis thus provides an additional layer of insight when studying the contribution of vRNA to apoptosis.

Dead-box polypeptide 3, X-linked, herein referred to as DDX3, is a host protein belonging to the DEAD-box (Asp-Glu-Ala-Asp) family of ATP-dependent RNA helicases. It is involved in all aspects of RNA metabolism including processing, transport and translation, as well as in cell cycle progression, stress response, innate immune sensing and apoptosis [23-25]. DDX3 has been implicated in several cancers due to its oncogenic function but also plays a dual role in cancer progression because of its tumour suppressive activity [26-30]. Moreover, DDX3 plays distinct roles in HIV-1 infection by enhancing viral RNA gene expression, but also in activating components of the innate antiviral signalling pathway [31]. During HIV-1 replication, DDX3 has an integral function in the nucleocytoplasmic export of vRNA [32,33] as well as in vRNA translation in the cytoplasm [34-36]. In dendritic cells, DDX3 senses abortive HIV-1 RNA transcripts to induce type I interferon immune response via mitochondrial antiviral signalling protein (MAVS) [37]. Because of its widely described roles in viral replication as well as in tumorigenesis, DDX3 has thus emerged as an attractive target for both anti-cancer and antiviral drugs [27,38].

Due to DDX3's roles in both HIV-1 RNA metabolism as well as in the regulation of apoptosis, we hypothesised that treatment of HIV-1-infected cells with small molecule inhibitors of DDX3 would inhibit vRNA export and translation; while the residual vRNA would activate innate antiviral immune signalling pathways and trigger apoptosis of vRNA-expressing cells, thereby resulting in the depletion of the viral reservoir. Here we evaluated the effects of DDX3 inhibition on the latent HIV-1 reservoir using two clinically advanced inhibitors of DDX3, RK-33 and FH1321, which target the ATPase and RNA-binding domains of DDX3 respectively. Pharmacological inhibition of DDX3 reversed HIV-1 latency in the latent HIV-1-infected J-Lat 11.1 cell line, *ex vivo* latently infected CD4+ T cells, and CD4+ T cells obtained from cART-suppressed HIV-1-infected donors, likely via NF-κB activation.

DDX3 inhibitor-mediated HIV-1 latency reversal was observed predominantly at the RNA level, which is consistent with the role of DDX3 as an inhibitor of vRNA export and translation. Chemical inhibition of DDX3 resulted in induction of IRF3 phosphorylation, upregulation of IFN-β expression and apoptosis in vRNA-expressing cells. In accordance with its pharmacological inhibition, depletion of DDX3 via shRNA-mediated knockdown in J-Lat cells also reversed HIV-1 latency and induced IFNβ expression. RNA sequencing analysis of primary CD4+ T cells obtained from uninfected independent donors revealed significant down regulation of the inhibitor of apoptosis protein BIRC5 and Heat Shock protein 70 (HSP70) upon DDX3 inhibition. Importantly, treatment of latent HIV-1-infected cells with DDX3 inhibitors resulted in selective induction of apoptosis in vRNA-expressing cells but not in the uninfected/bystander cells. We quantitated the impact of treatment with DDX3 inhibitors on the inducible latent HIV-1 reservoir in CD4+ T cells obtained from cART-suppressed people living with HIV-1 (PLWHIV) in an *in vitro* culture model using three different methods of reservoir quantitation. Strikingly, treatment with DDX3 inhibitors over 5 days resulted in an ~50% reduction of the inducible reservoir as determined by quantitation of cell-associated vRNA, by *tat/rev*-induced limiting dilution assay, as well as at the single-cell level using FISH-Flow technology. These results demonstrate that pharmacological inhibition of DDX3 induces latency reversal and selective apoptosis of latent HIV-1-infected cells and serve as a proof-of-concept that ICD inducers can decreases the inducible HIV-1 reservoir in infected patient cells *ex vivo*.

RESULTS

DDX3 inhibition induces viral reactivation in J-Lat 11. cells

Our initial screening studies focus on examining whether pharmacological inhibition of DDX3 can affect proviral reactivation in a cell line model of HIV-1 latency, J-Lat 11.1. This model is a Jurkat-derived cell line that contains a latent integrated copy of the HIV-1 provirus defective in *env* with a GFP reporter in place of *nef* open reading frame [39]. J-Lat-11.1 cells harboured a basal frequency of GFP+ cells at <7.5% that was reactivated by treatment with PKC agonist phorbol myristate acetate (PMA) to >80% (Supplementary Fig.1a). J-Lat 11.1 cells were treated with increasing concentrations (0.5 – 2 μM) of the DDX3 inhibitor RK-33 that has been developed for cancer treatment. RK-33 binds to the ATPase domain of DDX3 and is reported to improve radiation sensitisation of tumours in models of lung cancer, colorectal cancer, prostate cancer and Ewing's carcinoma [27,28,40-44]. Interestingly, treatment with RK-33 alone induced viral reactivation in a dose-dependent manner, with ~18% of cells producing GFP when treated with 2 μM RK-33 (Fig. 1a), thus unravelling a role for DDX3 inhibitors as LRAs. A larger latency reversal activity for

RK-33 was observed at the RNA-levels with a 70-fold and 25-fold increase in the relative expression of the HIV-1 promoter-controlled GFP and vRNA transcripts, respectively, as quantified by RT-qPCR (Fig. 1b, c).

Since DDX3 has been reported to play important roles in the nucleocytoplasmic export and translation of HIV-1 vRNA [32,34-36], we hypothesised that RK-33 could also influence HIV-1 gene expression at a post-transcriptional level by impairing either vRNA export or translation. To investigate this, we conducted FISH-Flow after treatment of J-Lat 11.1 cells with 2 μM RK-33 for 18 h. Using probes that amplify and allow identification and quantification of vRNA expression in cells, FISH-Flow allows for the simultaneous detection of distinct populations: (1) latent cells, which express neither viral RNA nor viral protein (vRNA-/GFP+), (2) efficiently reactivated cells, which express both HIV-1 viral RNA and proteins (vRNA+/GFP+), (3) transcriptionally competent viral RNA-expressing cells with either untranslated vRNA or a block in post transcriptional vRNA processing and viral RNA expression (vRNA+/GFP-) and (4) cells only expressing GFP from multiply spliced viral RNA transcripts (vRNA-/GFP+) (Fig. 1d). Thus, FISH-Flow gives an additional layer of insight on vRNA-regulation and, given DDX3's previously characterised roles in post-transcriptional regulation of vRNA, FISH-Flow that uses RNA expression as a read out is the most appropriate tool to investigate the effects of DDX3 inhibition of HIV-1. On average, under uninduced conditions, only 3% of cells constitutively produced vRNA, whereas vRNA was produced in more than 80% of cells upon PMA stimulation (Fig. 1d, e). Treatment with 2 μM RK-33 resulted in the expression of vRNA in ~15% of J-Lat cells (Fig. 1d, e), corroborating its latency reversal activity. Interestingly, ~8% of cells were observed in the vRNA+/GFP-quadrant, corresponding to ~42% of all vRNA+ cells (Fig. 1d, e). In contrast, merely 0.02% of the vRNA-expressing PMA-treated cells did not express GFP (Fig.1 d, e). These data indicate a post-transcriptional block in vRNA metabolism upon DDX3 inhibition.

To determine if this block was at the level of nucleocytoplasmic export, we seeded the cells that underwent FISH-Flow analysis on a coverslip and observed them by confocal microscopy. In representative images, we observed that the vRNA+/GFP- cells in RK-33-treated conditions contained vRNA sequestered in the nucleus, while in the double positive cells in both PMA and RK-33-treated condition, vRNA was present in the cytoplasm of the cells (Supplementary Fig. 1b). GFP is expressed from the multiply spliced viral RNA transcript and the full-length vRNA codes for the viral protein pr55Gag [39]. Therefore, to further validate that RK-33 treatment affects post-transcriptional metabolism of the vRNA, we measured pr55Gag expression in cells treated with RK-33 by Western blot and did not observe significant upregulation of pr55Gag expression at a protein level (Supplementary Fig. 1c, d) despite vRNA expression at an RNA level (Fig 1 c-e). Therefore, DDX3 inhibition

by RK-33 hinders nucleocytoplasmic export of vRNA and viral protein expression, thereby highlighting the importance of using vRNA expression and not viral protein production as a marker for HIV-1 infection when investigating the effects of DDX3 inhibitors.

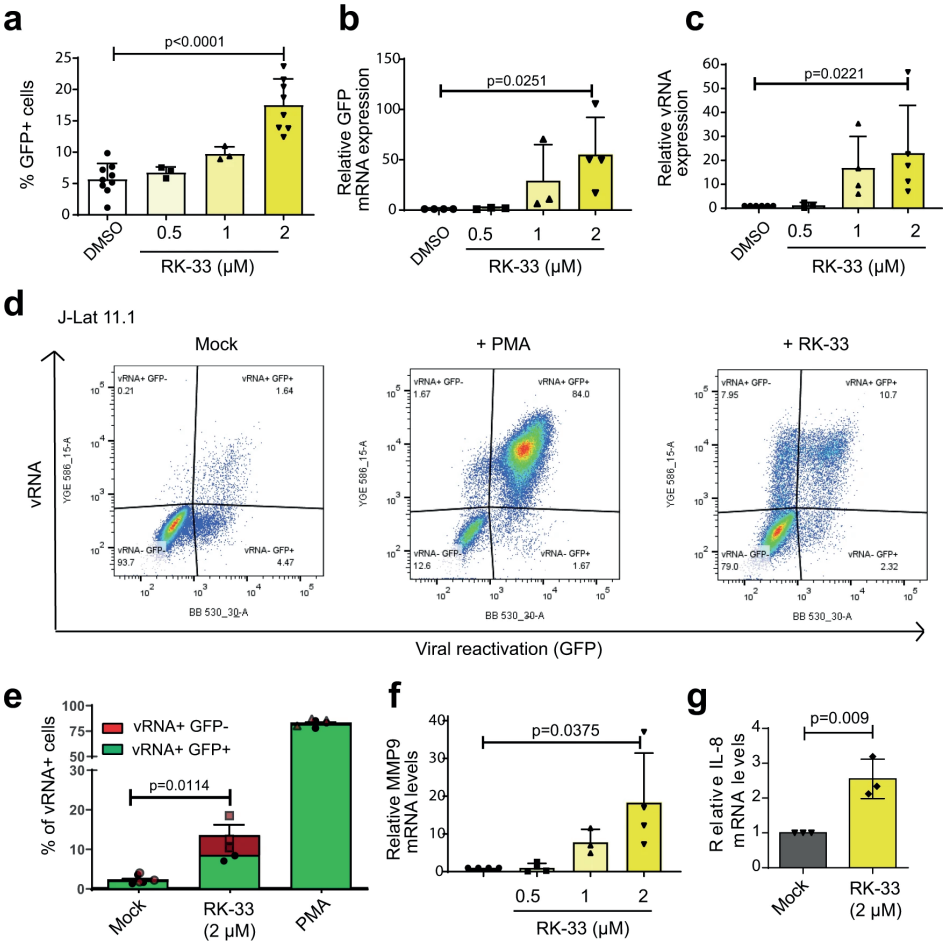

Fig. 1. DDX3 inhibition reverses HIV-1 latency in J-Lat 11.1 cells. **a** J-Lat 11.1 cells were treated with increasing concentrations of the DDX3 inhibitor RK-33. % of reactivation, monitored by GFP production, was quantified by Flow cytometry. Error bars represent mean ± SD of three to nine independent experiments with at least 10,000 cells counted per treatment (paired, two-tailed t-test). The relative expression levels of (**b**) GFP mRNA and (**c**) vRNA in the RK-33-treated J-Lat cells were quantified by RT-qPCR. Error bars represent mean ± SD of three to five independent experiments (unpaired, two-tailed t-test; p value <0.00001). **d** Representative FISH-Flow dot plots from an independent experiment of J-Lat cells treated with DMSO (Mock), PMA or 2 μM RK-33. Gating strategy as depicted in Supplementary Fig. 1a. **e** The % of vRNA-expressing cells (GFP− or GFP+) as treated in **a** were quantified. Error bars represent mean ± SD of three independent experiments with at least 10,000 cells counted per treatment (unpaired, two-tailed t-test). Relative (**f**) MMP9 and (**g**) IL-8 mRNA expression levels from cells treated as in a were quantified by RT-qPCR. Error bars represent mean ± SD of three to four independent experiments (unpaired, two-tailed t-test).

DDX3 has previously been reported to have cell-type dependent differential effects on the upregulation of the NF-κB pathways and has been implicated in binding to the p65 subunit thus inhibiting NF-κB-mediated transcription [45,46]. To determine if RK-33 is capable of activating NF-κB, Jurkat cells were nucleofected with firefly luciferase reporter plasmids either containing or lacking NF-κB consensus sites upstream of a minimal reporter, along with an internal Renilla control plasmid. Cells were then either Mock-treated or treated with 2 μM RK-33 for 18 h. Treatment with RK-33 resulted in a modest increase in relative luciferase expression in the NF-κB reporter-transfected cells as compared to the Mock-treated cells (Supplementary Fig. 1e). The NF-κB target genes MMP9, IL-8, and IL-10 were also upregulated in J-Lat 11.1 cells treated with RK-33, suggesting activation of the NF-κB pathway (Fig. 1f, g and Supplementary Fig. 1f). Our data suggest that the DDX3 inhibitor RK-33 acts as a LRA that reactivates the HIV-1 provirus, possibly via activation of NF-κB.

DDX3 inhibition results in increased cell death in vRNA-expressing cells

In order to further characterise the impact of DDX3 inhibition, and hence DDX3 function, in HIV-1 latency, we performed shRNA-depletion of DDX3 in J-Lat 11.1 cells and monitored latency reversal and NF-κB target upregulation. Lentiviral transduction of J-Lat 11.1 cells with shRNA against DDX3 (shDDX3) resulted in a 90% decrease in DDX3 mRNA expression and 80% decrease in DDX3 protein expression compared to the cells treated with scrambled shRNA (shControl) as quantified by RT-qPCR and Western blot, respectively (Fig. 2a, b and Supplementary Fig. 2a).

DDX3-depleted cells demonstrated a twofold increase in GFP expression as compared to the shControl transduced cells (Fig. 2c), thereby confirming that inhibition of DDX3 reverses HIV-1 latency. Latency reversal (vRNA and GFP mRNA) and NF-κB target upregulation (IL-10, IL-8, and MMP9) were also measured by RT-qPCR in DDX3-depleted cells and a significant increase in GFP mRNA and vRNA expression was observed compared to mock-treated cells, reaffirming latency reversal at a transcriptional level (Fig. 2d). Moreover, similar to our observations with chemical inhibition of DDX3 with RK-33, NF-κB target genes IL-10, IL-8 and MMP9 were significantly upregulated in DDX3-depleted cells as compared to the control (Fig. 2d).

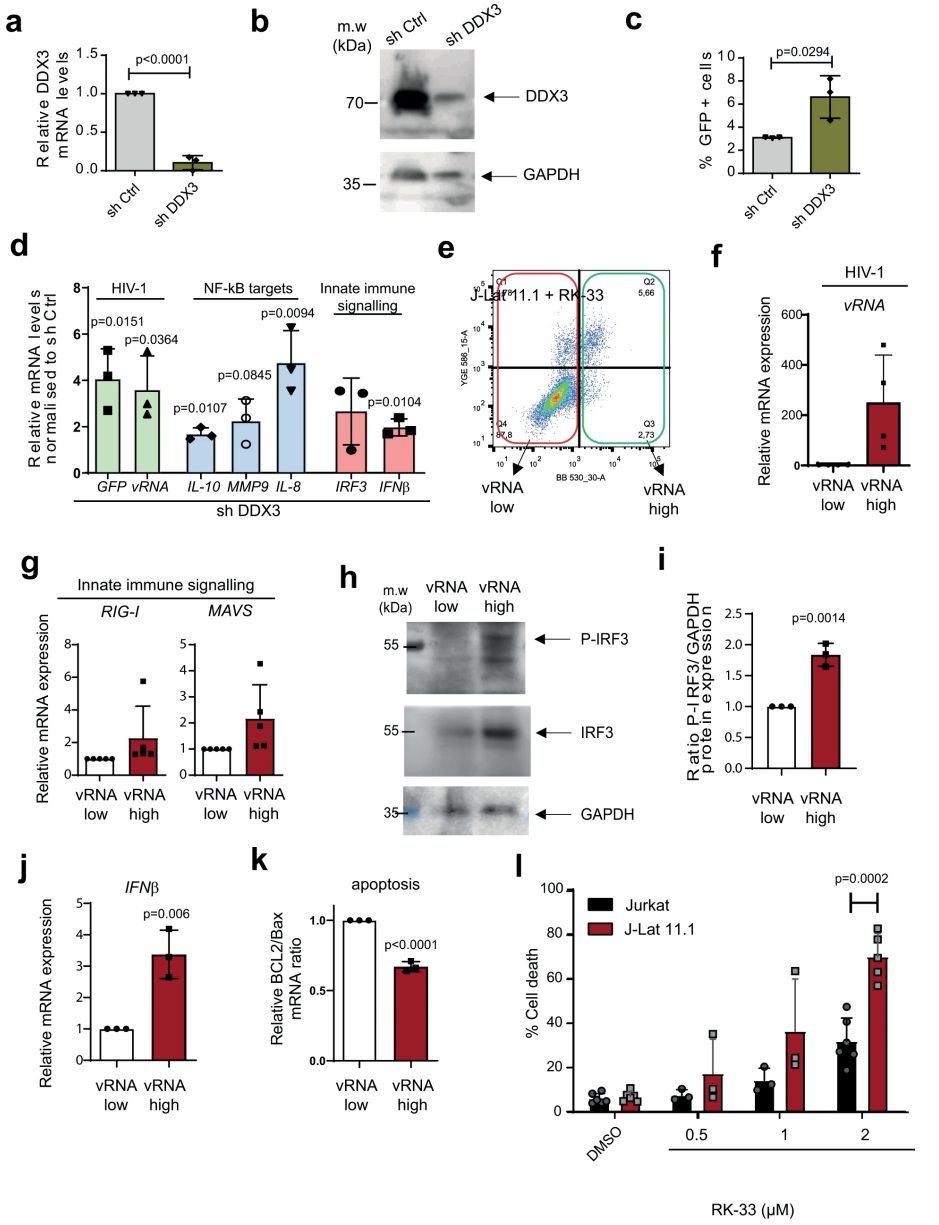

Fig. 2. DDX3 inhibition induces IRF3 phosphorylation, IFNβ expression and cell death in J-Lat 11.1 cells. a J-Lat 11.1 cells were transduced with a control lentiviral vector expressing a scrambled shRNA (shControl) or with lentivirus expressing shRNA against DDX3 (shDDX3) and relative DDX3 mRNA expression was quantified by RT-qPCR. Error bars represent the mean ± SD of three independent experiments (unpaired, two-tailed t-test; p value=0.001038). **b** Representative Western blots depicting DDX3 and GAPDH in shControl and shDDX3 conditions. **c** The % of reactivation monitored as GFP production from cells as treated in **a** were quantified by Flow cytometry. Gating strategy as depicted in Supplementary Fig. 1a. Error bars represent mean ± SD of three independent

experiments with at least 10,000 cells counted per treatment (paired, two-tailed t-test). **d** In cells treated as in **a**, relative GFP, vRNA, IL-10, IL-8, MMP9, IRF3 and IFNβ mRNA expression levels in shDDX3 treated cells were quantified by RT-qPCR and normalised to the shControl. Error bars represent mean ± SD of three independent experiments (unpaired, two-tailed t-test). **e** RK-33-treated J-Lat cells were sorted into GFP− (vRNA low) and GFP+ (vRNA high) fractions and the relative mRNA expression of vRNA using primers against (**f**) the vRNA and (**g**) RIG-I and MAVS expression were quantified by RT-qPCR. **h** Representative Western blots depicting phosphorylated IRF3, total IRF3 and GAPDH protein expression in RK-33-treated vRNA low and vRNA high populations. **i** Quantification of the densitometric analysis of P-IRF3 to GAPDH protein expression ratios from 2 h. Error bars represent mean ± SD from three independent experiments (unpaired, two-tailed t-test). The relative expression of (**j**) IFNβ mRNA and (**k**) ratios of Bcl2 and Bax mRNA expression in RK-33-treated vRNA low and vRNA high populations were quantified by RT-qPCR. Error bars represent mean ± SD from three independent experiments (unpaired, two-tailed t-test). **l** % Cell death was measured in Jurkat vs. J-Lat cells treated with increasing concentrations of RK-33 by flow cytometry. Error bars represent the mean ± SD of at least three independent experiments with at least 10,000 cells counted per treatment (paired, two-tailed t-test).

During viral infection, single stranded RNA is recognised by RIG-I that induces downstream innate antiviral responses mediated by NF-κB and IRF3 resulting in IFN-β expression [47-49]. We investigated whether these effectors are activated by HIV-1 vRNA in the absence of DDX3. shRNA-mediated depletion of the DDX3 resulted in a significant twofold increase in IFN-β mRNA expression compared to mock-treated cells (Fig. 2d). Similarly, chemical inhibition of DDX3 using 2 μM RK-33 resulted in modest upregulation of IFN-β expression in J-Lat 11.1 cells (Supplementary Fig. 2b).

To enrich for vRNA-expressing cells and examine the specific contribution of HIV-1 vRNA to the activation of innate immune pathway components during DDX3 inhibition, we sorted J-Lat 11.1 cells into vRNA low and vRNA high populations by FACS following treatment with 2 μM RK-33 as shown (Fig. 2e). Our gating strategy was based on GFP expression (Supplementary Fig. 1a), which resulted in two populations of cells; vRNA low (in which 96% of cells were vRNA negative) and vRNA high (where 68% of cells were vRNA positive). As expected, the vRNA high J-Lat 11.1 sorted cells contained ~300-fold more vRNA than the vRNA low population (Fig. 1f). The vRNA high population demonstrated induction of the innate antiviral signalling pathway components RIG-I and MAVS, consistent with previous work demonstrating HIV-1 vRNA's ability to activate these pathways (Fig. 2g) [17,18]. Interestingly, concomitant significant phosphorylation of IRF3 was also observed in the vRNA-high expressing cells, confirming the activation of innate antiviral signalling pathways in vRNA-expressing cells (fig 2h, i). The phosphorylation of IRF3 in combination with NF-κB activation results in the production of type I interferons [47-49]. In agreement, we observed a significant increase in IFN-β mRNA expression in the vRNA-high cell population (Fig. 2j).

The characterised role of IFN-β in contributing to apoptosis, also during viral infection [50-52] together with RK-33's described roles in inducing cell death [40], prompted us to examine whether the vRNA high cells are more susceptible to apoptosis. Concomitant with the observed increased vRNA expression, we also observed an ~35% decrease in the ratio of the anti-apoptotic BCL2 to the pro-apoptotic Bax mRNA expression levels in the HIV-1 vRNA high population, indicating that the vRNA-expressing cells have a higher susceptibility to undergo apoptosis (Fig. 2k). To further probe the selectivity of cell death, J-Lat 11.1 cells and parental Jurkat cells lacking integrated HIV-1 provirus and vRNA were treated with increasing concentrations of RK-33 (0.5 –2 μM). Eighteen hours post-treatment, cells were stained with Hoescht 33342 and the percentage of viable cells quantified by flow cytometry. We observed a dose-dependent increase in cell death in RK-33-treated J-Lat cells compared to parental Jurkat cells, most strikingly at 2 μM RK-33 (Fig. 2l). In this condition, cell death was observed in 70% of J-Lat 11.1 cells, but only 30% of Jurkat cells representing a significant increase in cell death of HIV-1-infected cells. Since they are a cancer-derived cell line, the viability of Jurkat cells was also affected upon treatment with RK-33, albeit not as much as the J-Lat 11.1 cells (Supplementary Fig. 2c). In comparison, RK-33 had negligible effects on the viability of primary CD4+ T cells (Supplementary Fig. 2c). Our data, therefore, indicate that DDX3 inhibition results in latency reversal, upregulation of NF-κB target genes and IRF3, leading to induction of IFN-β expression and a pro-apoptotic state, thereby rendering vRNA-expressing cells more susceptible to cell death during vRNA expression.

DDX3 inhibition downregulates genes involved in cell survival

The inhibition of DDX3 helicase function, i.e., dsRNA unwinding, can be achieved by competitive inhibition of the ATP or RNA-binding sites. RK-33 was demonstrated to inhibit RNA helicase activity in a concentration-dependent manner reducing ATP consumption in enzymatic assays [40]. A class of inhibitors competitive for the DDX3 RNA-binding site have been reported by Radi *et al*. [53] and were further developed leading to the identification of the potent and selective compound FH-1321 (compound 16d in [38]), that specifically targets the DDX3 RNA-binding site with no effect in its ATPase activity [38]. A hypothetical binding model obtained by molecular docking calculation for both RK-33 and FH-1321 depicts the predicted binding of RK-33 to the ATP-binding site of DDX3, while FH-1321 binds the RNA-binding site (Fig. 3a and Supplementary Fig. 3a, b). For both molecules, the downstream effect is inhibition of RNA helicase activity of DDX3 [40,53]. We therefore investigated the potential function and mechanism of action of RK-33 and FH-1321 in HIV-1 reactivation and reservoir dynamics in the more relevant primary CD4+ T cells.

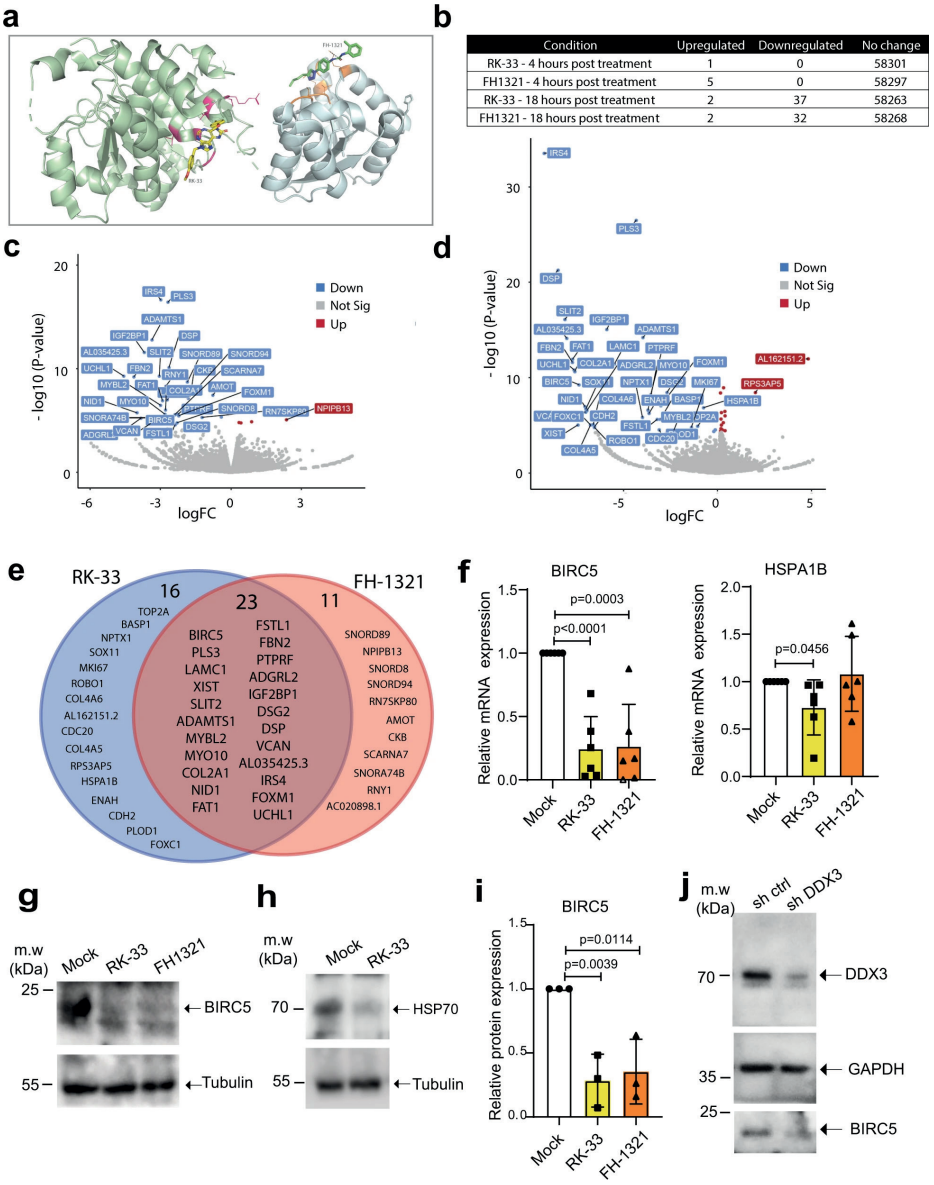

Fig. 3. Effects of DDX3 inhibition on CD4+ T cells. a Molecular docking of RK-33 and FH-1321 to pre-unwound DDX3 confirmation as predicted by AutoDock Vina. DDX3 domain 1 is shown as a pale green cartoon, domain 2 is shown as a pale blue cartoon and the surface colour code is pink for ATP-binding residues and orange for RNA-binding residues. The colour code for RK-33 is yellow for carbon, red for oxygen, dark blue for nitrogen. The colour code for FH-1321 is green for carbon, red for oxygen, dark blue for nitrogen. The predicted hydrogen bond between FH-1321 and Lysine 541 from the DDX3 RNA-binding pocket is indicated with a dashed line. **b** Table of differentially expressed genes upon treatment of CD4+ T cells with DDX3 inhibitors. Volcano plot of differentially expressed genes 18 h post-treatment with (**c**) RK-33 and (**d**) FH-1321. **e** Venn diagram of overlapping

differentially expressed genes 18 h post-treatment with DDX3 inhibitors. **f** CD4+ T cells from healthy donors were treated with DMSO (Mock), RK-33 and FH-1321 and the relative expression of BIRC5 and HSPA1B mRNAs were quantified by RT-qPCR. Error bars represent the mean ± SD of independent experiments with cells from six different donors (unpaired, two-tailed t-test; p value for BIRC5 expression in RK-33 treated cells is 0.000027). **g** Representative Western blots of CD4+ T cells treated with 2 μM RK-33 or 1 μM FH-1321 depicting BIRC5 and (**h**) HSP70 expression with loading controls as indicated. **i** Quantification of the densitometric analysis of BIRC5 protein expression from cells as treated in Fig. 2g. Error bars represent the mean ± SD from three donors (unpaired, two-tailed t-test). **j** Representative Western blots depicting DDX3, BIRC5 and GAPDH protein levels from CD4+ T cells stimulated with CD3-CD28-coated beads and infected with a control lentiviral vector (shControl) or a lentiviral vector expressing shRNA against DDX3 (shDDX3).

We observed no significant decrease in viability when primary CD4+ T cells from three healthy donors were treated with up to 10 μM of either compound (Supplementary Fig. 3c). We also cultured CD4+ T cells in the presence or absence of 2 μM RK-33 or 1 μM FH-1321, for 5 days and observed no significant differences in cell viability between the DDX3 inhibitor-treated and Mock-treated conditions (Supplementary Fig. 3d).

To gain insight into the molecular mechanism by which DDX3 inhibition may ICD in HIV-1-infected cells, we treated primary CD4+ T cells obtained from two healthy donors with RK-33 and FH-1321 and performed RNA-sequencing. Minimal changes in gene expression were observed 4 h post-treatment with 2 μM RK-33 or 1 μM FH-1321, with a one and five differentially expressed genes, respectively, with a 1.5-fold difference in expression, and a false discovery cut-off rate set to 0.05 (Supplementary Fig. 3e, f). At 18 h post-treatment: primary CD4+ T cells treated with 1 μM FH-1321 displayed only 34 genes differentially expressed, while treatment with RK-33 (2 μM) resulted in 39 genes differentially expressed in both donors (Fig. 3b –d) and Tables 1 and 2). Interestingly, the majority of the differentially expressed genes were common to both the RK-33 and FH-1321 treatments (n=23). Since these effects are common between compounds belonging to two different classes of DDX3 inhibitors, they are bound to be specific to the inhibition of DDX3 helicase activity (Fig. 3e).

Table 1. EdgeR report of differentially expressed genes 18 h post treatment with 2 µM RK-33

GeneID	Name	log2 fold change	log2 counts per million	*F* Value	*P* Value	False Discovery Rate
ENSG00000133124	IRS4	-9.220240267	1.229125796	149.1749	2.89E-34	1.69E-29
ENSG00000096696	DSP	-8.484792295	0.549901848	93.17747	4.97E-22	9.65E-18
ENSG00000145147	SLIT2	-8.122797551	0.215628794	69.49186	7.84E-17	1.14E-12
ENSG00000261409	AL035425.3	-8.022265953	0.113605342	60.57704	7.19E-15	5.99E-11
ENSG00000138829	FBN2	-7.721874417	-0.141878891	49.16692	2.38E-12	1.39E-08
ENSG00000083857	FAT1	-7.711916601	-0.142206665	50.58668	1.15E-12	7.47E-09
ENSG00000154277	UCHL1	-7.629659662	-0.220071849	45.5358	1.51E-11	7.35E-08
ENSG00000139219	COL2A1	-7.594048405	-0.247211954	44.80238	2.20E-11	9.86E-08
ENSG00000229807	XIST	-7.425086724	4.779411144	281.6285	8.79E-06	0.013432
ENSG00000089685	BIRC5	-7.372112695	-0.421255852	38.53409	5.42E-10	2.26E-06
ENSG00000116962	NID1	-7.05272162	-0.69051715	28.24878	1.07E-07	0.000297
ENSG00000038427	VCAN	-7.017959819	-0.727725687	25.70546	3.99E-07	0.000861
ENSG00000176887	SOX11	-7.004754934	-0.728056321	27.13324	1.91E-07	0.000483
ENSG00000117114	ADGRL2	-6.95027203	-0.766705238	26.38183	2.81E-07	0.000655
ENSG00000054598	FOXC1	-6.756514098	-0.931471077	19.71939	8.99E-06	0.013432
ENSG00000188153	COL4A5	-6.756514098	-0.931471077	19.71939	8.99E-06	0.013432
ENSG00000197565	COL4A6	-6.610183248	-1.02235097	19.90055	8.17E-06	0.013236
ENSG00000169855	ROBO1	-6.551036428	-1.069611081	18.62718	1.59E-05	0.021095
ENSG00000170558	CDH2	-6.544969004	-1.069721671	18.90017	1.38E-05	0.019153
ENSG00000159217	IGF2BP1	-5.889308666	0.348421941	64.80318	8.72E-16	1.02E-11
ENSG00000135862	LAMC1	-5.486512767	0.002490741	48.29217	3.71E-12	1.97E-08
ENSG00000102024	PLS3	-4.323906265	1.49827749	117.2158	3.02E-27	8.81E-23
ENSG00000171246	NPTX1	-3.992292706	-0.550303193	23.25519	1.42E-06	0.002675
ENSG00000154734	ADAMTS1	-3.971030294	0.580596315	60.82655	6.34E-15	5.99E-11
ENSG00000145555	MYO10	-3.696600515	-0.303481708	26.65852	2.44E-07	0.000592
ENSG00000154380	ENAH	-3.64365296	-0.274861002	25.06365	5.59E-07	0.001124
ENSG00000142949	PTPRF	-3.553235332	-0.021528142	33.79895	6.35E-09	1.95E-05
ENSG00000163430	FSTL1	-3.20753747	-0.332407149	22.31002	2.33E-06	0.003987
ENSG00000117399	CDC20	-3.098292124	-0.420984699	17.47004	2.92E-05	0.034778
ENSG00000176788	BASP1	-3.03195077	-0.24810378	22.38461	2.24E-06	0.003952
ENSG00000111206	FOXM1	-3.015861999	0.001271235	28.7242	8.38E-08	0.000244
ENSG00000046604	DSG2	-2.684610226	0.484772447	34.90713	3.48E-09	1.19E-05
ENSG00000101057	MYBL2	-2.316037106	0.025267442	17.38763	3.06E-05	0.035688
ENSG00000148773	MKI67	-1.384356143	1.091562301	18.66531	1.56E-05	0.021095
ENSG00000083444	PLOD1	-1.18441556	1.399169378	17.50631	2.88E-05	0.034778
ENSG00000131747	TOP2A	-1.054906153	1.866051914	19.13111	1.25E-05	0.017772
ENSG00000204388	HSPA1B	-0.741213605	3.325135537	27.77549	1.39E-07	0.000367
ENSG00000178429	RPS3AP5	2.015230135	1.279297836	36.33718	3.41E-09	1.19E-05
ENSG00000234648	AL162151.2	4.827847593	0.344327701	50.73859	1.07E-12	7.47E-09

Differential expression and P values are calculated for each gene using an exact test analogous to Fisher's exact test adapted for overdispersed data in the EdgeR package[88].

Table 2. EdgeR report of differentially expressed genes 18 h post treatment with 1 µM FH-1321

GeneID	Name	log2 fold change	log2 counts per million	*F* value	*P* Value	False Discovery Rate
ENSG00000154277	UCHL1	-4.565471687	-0.206793672	38.67266739	5.05E-10	3.31E-06
ENSG00000261409	AL035425.3	-4.424650789	0.138068277	48.33716477	3.63E-12	3.52E-08
ENSG00000138829	FBN2	-4.131894042	-0.10684436	38.38083941	5.86E-10	3.42E-06
ENSG00000116962	NID1	-3.999181717	-0.658930046	22.77369298	1.83E-06	0.0053254
ENSG00000117114	ADGRL2	-3.832053102	-0.731611642	20.4765316	6.05E-06	0.0125945
ENSG00000159217	IGF2BP1	-3.68912559	0.398606752	48.96044087	2.64E-12	3.08E-08
ENSG00000229807	XIST	-3.488985213	4.901654584	651.1533715	7.66E-143	4.47E-138
ENSG00000038427	VCAN	-3.429296401	-0.658534387	18.19677341	2.00E-05	0.0323138
ENSG00000154734	ADAMTS1	-3.363272907	0.603352768	54.52344803	1.56E-13	2.27E-09
ENSG00000212402	SNORA74B	-3.359506375	0.031288549	24.79248338	5.34E-06	0.0115336
ENSG00000145147	SLIT2	-3.051459541	0.34517457	38.64546164	5.12E-10	3.31E-06
ENSG00000101057	MYBL2	-2.996889004	-0.083099003	26.07056348	3.34E-07	0.0010805
ENSG00000133124	IRS4	-2.98565677	1.371029055	71.98000489	2.22E-17	6.48E-13
ENSG00000083857	FAT1	-2.913815462	-0.014539277	28.05815995	1.18E-07	0.0004052
ENSG00000145555	MYO10	-2.805586002	-0.261404374	22.18212809	2.49E-06	0.0066275
ENSG00000139219	COL2A1	-2.783583292	-0.107869982	24.02115361	9.55E-07	0.0029316
ENSG00000201098	RNY1	-2.770572459	0.413772602	35.10682622	4.80E-09	2.33E-05
ENSG00000135862	LAMC1	-2.712320987	0.135877854	28.32916412	1.03E-07	0.0003743
ENSG00000102024	PLS3	-2.681318527	1.605768497	71.57130553	3.77E-17	7.32E-13
ENSG00000096696	DSP	-2.636756013	0.730407853	42.41260665	7.45E-11	6.21E-07
ENSG00000089685	BIRC5	-2.490957592	-0.234929297	18.96212263	1.34E-05	0.02512
ENSG00000238741	SCARNA7	-2.387719434	0.361869871	24.20859794	2.61E-06	0.0066275
ENSG00000163430	FSTL1	-2.380561336	-0.26218126	17.71426598	2.57E-05	0.0405086
ENSG00000200785	SNORD8	-2.299517907	-0.084333496	18.58796384	1.64E-05	0.0290541
ENSG00000142949	PTPRF	-2.256619192	0.113519171	22.13114508	2.55E-06	0.0066275
ENSG00000111206	FOXM1	-2.226389714	0.092218251	21.57249486	3.41E-06	0.0082946
ENSG00000212283	SNORD89	-1.860714666	1.311190667	36.42603494	1.90E-09	1.01E-05
ENSG00000208772	SNORD94	-1.822933237	1.022233292	29.05095049	7.20E-08	0.0002797
ENSG00000166165	CKB	-1.686278111	1.500619457	33.19463106	9.30E-09	4.17E-05
ENSG00000046604	DSG2	-1.609604699	0.644434181	18.28993873	1.90E-05	0.031651
ENSG00000202058	RN7SKP80	-1.234932643	1.641387087	21.21111392	4.96E-06	0.011119
ENSG00000126016	AMOT	-0.773124251	3.662624092	30.45093151	3.53E-08	0.0001469
ENSG00000130164	LDLR	-0.411325614	5.764550633	21.07423587	4.43E-06	0.0103253
ENSG00000101745	ANKRD12	0.339396244	7.502647544	18.65815618	1.57E-05	0.0285379
ENSG00000170881	RNF139	0.423776234	5.074578288	18.46989874	1.74E-05	0.0297963
ENSG00000213757	AC020898.1	0.876931574	2.474353677	19.06819338	1.27E-05	0.0246334
ENSG00000198064	NPIPB13	2.365643737	0.043629688	19.87731825	8.31E-06	0.0167005

Differential expression and P values are calculated for each gene using an exact test analogous to Fisher's exact test adapted for overdispersed data in the EdgeR package[88].

Notably, the overall change in gene expression was limited, consistent with the minimal potential for off-target or cytotoxic effects associated with the use of these compounds. Interestingly, two of the differentially expressed genes significantly downregulated in CD4+ T cells in response to RK-33, the inhibitor of apoptosis protein BIRC5 and HSPA1B (Hsp70), have been previously implicated to play a role in HIV-1 induced cell death. BIRC5, which is also significantly downregulated in response to FH-1321 treatment, has been previously demonstrated to be upregulated in latent HIV-1-infected cells, and its inhibition resulted in increased cell death of HIV-1-infected cells [54]. Also involved in regulating apoptosis in infected cells, Hsp70 was shown to inhibit apoptosis induced by the HIV-1 protein Vpr [55]. Consistent with the observed DDX3-mediated upregulation of NF-κB target genes, Hsp70 was also shown to inhibit HIV-1 gene expression [56], possibly via suppression of NF-κB signalling through its interaction with Hsp70 binding protein 1[57]. RK-33 and FH-1321-mediated downregulation of BIRC5 and RK-33-mediated HSPA1B downregulation were confirmed at the RNA level by RT-qPCR in six additional uninfected donor CD4+ T cells (Fig. 3f) and at the protein level by Western blot analysis in CD4+ T cells from three donors (Fig. 3g-i and Supplementary Fig. 3g). We also conducted shRNA-mediated depletion of DDX3 in CD4+ T cells from three donors and observed a decrease in DDX3 protein expression upon shDDX3-containing lentiviral transduction (Fig. 3j and Supplementary Fig. 3h). This also corresponded to a decrease in expression of BIRC5 at both protein and mRNA levels, but no decrease in HSPA1B at an mRNA level (Fig.3j and Supplementary Fig. 3h, i).

To ensure that DDX3 inhibitors do not induce T cell activation, we examined CD25 expression upon treatment with RK-33 and FH-1321 (Supplementary Fig. 3j). Consistent with the minimal effects observed with the RNA-sequencing, treatment with DDX3 inhibitors did not result in the induction of T cell activation, nor did DDX3 inhibition compromise effector function of CD4+ T cells (Supplementary Fig. 3k, l) or CD8+ T cells (Supplementary Fig. 4a, b) as determined by flow cytometry measuring IL-2 and IFNγ upon PMA-induced activation. Moreover, treatment with DDX3 inhibitors did not affect the capacity for proliferation in either CD4+ T or CD8+ T cells (Supplementary Fig. 4c-f) as determined after induction/stimulation with CD3/CD28. We also confirmed that DDX3 inhibition at the concentrations used does not affect de novo host cell translation in primary CD4+ T cells (Supplementary Fig. 4g, h). Finally, we determined if treatment of CD4+ T cells with DDX3 inhibitors could induce an upregulation of NF-κB target genes by RT-qPCR. Treatment with RK-33 and FH-1321 resulted in induction of the targets IL-8 and MMP9 mRNA expression, whereas FH-1321 treatment induced expression of IL-8 and IL-10 mRNA expression (Supplementary Fig. 4i-k).

DDX3 inhibitors reactivate and selectively kill HIV-1-infected cells in a primary model of latency

Given our observations that DDX3 inhibition reverses latency, induces more cell death in the J-Lat model and does not affect primary CD4+ T cell function, we wondered if we could use the DDX3 inhibitors to reactivate the provirus and ICD in a primary CD4+ T cell model of HIV-1 latency, developed by Lassen *et al.* [58-60] (Fig. 4a). In this model of HIV-1 latency, the virus used to infect the primary CD4+ T cells contained a luciferase reporter inserted in the *nef* open reading frame, which is encoded by the multiply spliced vRNA transcript (similar to the GFP in the J-Lat cells). We treated latently infected cells with 2 μM RK-33, 1 μM FH-1321 or PMA-ionomycin (as a positive control) and monitored latency reversal 18 h post-treatment by Fish-flow [22], RT-qPCR and relative luciferase expression (Fig. 4a). To quantify ICD, we also co-stained cells with a fixable viability dye and either with a fluorophore-conjugated antibody that detects AnnexinV or cleaved Caspase-3/7, both markers for host cell apoptosis (Gating strategy in Supplementary Fig. 5a). Fish-flow has a high specificity for the target HIV-1 vRNA with a negligible background in the uninfected CD4+ T cells and a sensitivity to detect down to 10 HIV-1 vRNA+ cells per million cells [16,22] (Fig. 4b). In latent HIV-1-infected CD4+ T cells, basal levels of vRNA were produced in the uninduced (Mock) condition (~165 vRNA+ cells/million), with a frequency of >650 vRNA+ cells/million upon PMA-ionomycin stimulation, corresponding to a 4.8 (s.d.± 3.3) fold increase (Fig. 4b, c and Supplementary Fig. 5b). Treatment with the DDX3 inhibitors RK-33 and FH-1321 resulted in ~410 vRNA+ cells per million and ~364+ cells/million, respectively, corresponding to a 2.8 (s.d.± 1.1) fold and 2.5 (s.d.± 1.4) fold increase in the frequency of vRNA-expressing cells as compared to the Mock-treated condition (Fig. 4b, c and Supplementary Fig. 5b).

We also measured intracellular vRNA expression and HIV-1 multiply spliced RNA (msRNA) from cell lysates by RT-qPCR and observed a 12.4-fold increase in vRNA expression with RK-33, a15.7-fold increase with FH-1321 and a 66.8-fold increase with PMA-ionomycin as compared to the Mock-treated cells (Fig. 4d and Supplementary Fig. 5c). When treated with DDX3 inhibitors, a 1.5-fold increase in relative luciferase units as compared to the Mock-treated condition was observed in both RK-33 and FH-1321-treated conditions (Fig. 4e). DDX3 influences viral gene expression at a post-transcriptional level (Fig. 1e). In agreement, the observed fold increase in luciferase expression upon DDX3 inhibition was not as high as that of vRNA expression. Together, these data demonstrate that the DDX3 inhibitors also induce latency reversal in a primary CD4+ T cell model of HIV-1 latency.

Based on our observations of increased cell death in J-Lat 11.1 cells in comparison to the Jurkat cells minimal cell death at the working concentrations in uninfected

primary CD4+ T cells (Fig. 2I and Supplementary Fig. 3c, d), we sought to determine if increased cell apoptosis could be observed specifically in the vRNA-expressing primary CD4+ T cells in the *in vitro* model of HIV-1 latency. For this we quantified the percentage of AnnexinV positive cells in cultures treated with Mock, RK-33, FH-1321 or PMA-ionomycin. Because FISH-Flow is a single-cell technique, we could distinctly quantify the differential expression of the vRNA+ cells or the vRNA–/ bystander cells from our latency model. To validate the selectivity of cell death upon drug treatment, we also quantified the percentage of AnnexinV expression in uninfected CD4+ T cells. Basal levels of AnnexinV and Caspase 3 positivity (<1%) were observed in the uninfected cells or the vRNA– bystander cells (Fig. 4f, g). Of the vRNA+ cells, 4.8 (s.d.± 4) % were AnnexinV positive in the cultures treated with PMA-ionomycin, indicating that viral reactivation might already make the cells more susceptible to cell death (Fig. 4f). Interestingly, in the cultures treated with RK-33 and FH-1321, 11.1 (s.d.± 8.1) % and 9.6 (s.d.± 4.5) % of vRNA-expressing cells respectively, were AnnexinV positive (Fig. 4f). To further validate that the vRNA+ cells are indeed undergoing apoptosis, we repeated these studies in three additional donors and measured the expression of cleaved Caspase-3/7 by Fish-Flow. We observed that 40.5 (s.d.± 8.5) % and 38.9 (s.d.± 15.5) % of RK-33 and FHI-1321-treated cells were cleaved Caspase-3/7 positive as compared to the 13.2 (s.d.± 5.9) % positive cells in the Mock-treated condition (Fig. 4g). To determine if BIRC5 downregulation plays a role in latency reversal we treated J-Lat-11.1 cells with the BIRC5 inhibitor YN155 [61], but did not observe significant latency reversal, suggesting that BIRC5, plays a more prominent role in the death of vRNA-expressing cells rather than their latency reversal (Supplementary Fig. 5d). We were unable to observe vRNA+ mediated effects on the relative expression of the anti-apoptotic protein Bcl2 and the pro-apoptotic protein Bax by RT-qPCR (Supplementary Fig. 5e) since only a small fraction of cells (<1%) is HIV-1-infected within the total population, further highlighting the importance of FISH-Flow, which enables investigation of HIV-1-induced selective cell death at the single-cell level. Together, these data show that DDX3 inhibitors exacerbate apoptosis triggered by the vRNA and selectively ICD in vRNA-expressing cells, while uninfected cells are not affected.

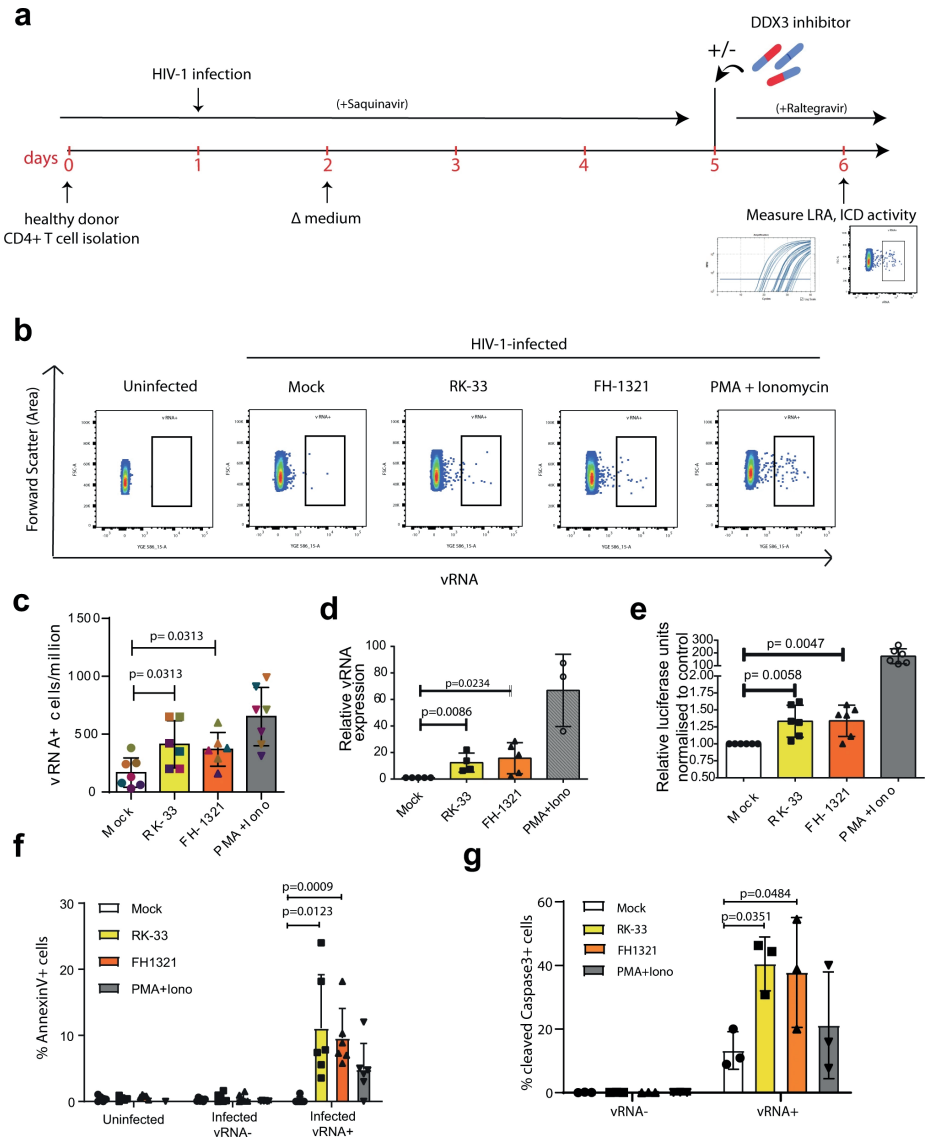

Fig. 4. DDX3 inhibition has LRA and ICD activity in a primary model of HIV-1 latency. a Schematic for latency establishment in primary human CD4+ T cells using the Lassen and Greene model. Latent HIV-1-infected cells were treated on day 5 with DMSO (unstimulated), PMA/Ionomycin, and the DDX3 inhibitors 2 μM RK-33 and 1 μM FH-1321. Uninfected cells were used as negative control. **b** Representative FISH-Flow dot plots of cells as treated in **a** representing 50,000 cells from each condition. Gating strategy depicted in Supplementary Fig. 5a. **c** The frequency of vRNA-expressing cells per million as depicted in **b** were quantified. Individual donors are represented by the same colour and symbols represent treatments (Mock = circles, RK-33= squares, FH-1321 =upward triangles and PMA = downward triangles). Error bars represent the mean ± SD of independent experiments using cells from six to seven different donors, with a minimum of 100,000 events acquired for each condition (paired, two-tailed, Wilcoxon test). **d** The relative vRNA expression levels from cells as treated in **a** were quantified by RT-qPCR. Error bars represent the mean ± SD of

independent experiments with cells from three to five different donors (unpaired, two-tailed t-test). **e** Relative luciferase activity of cells as treated in **a** was measured and normalised to the Mock-treated condition. Error bars represent the mean ± SD of independent experiments with cells from six different donors (unpaired, two-tailed t-test). **f** The percentages of AnnexinV positive cells from the uninfected, infected vRNA− fractions, or infected vRNA+ cells as quantified by FISH-Flow. Error bars represent the mean ± SD of independent experiments with cells from six different donors, with a minimum of 100,000 events acquired for each condition (paired, two-tailed t-test). **g** The percentages of cleaved Caspase-3 positive cells from the infected vRNA− fractions or infected vRNA+ cells as quantified by FISH-Flow. Error bars represent the mean ± SD of independent experiments with cells from three different donors, with a minimum of 100,000 events acquired for each condition (paired, two-tailed t-test).

DDX3 inhibitors induce latency reversal in CD4+ T cells from HIV-1-infected donors

To further investigate the clinical potential of DDX3 inhibitors we examined their ability to induce latency reversal and selective cell death in CD4+ T cells from chronic HIV-1-infected donors on suppressive cART with undetectable viral loads for at least 12 months (minimum n =6). Following isolation from cryopreserved PBMCs obtained by leukapheresis of HIV-1-infected donors, CD4+ T cells were treated according to the schematic in Fig 5a. Briefly, cells were cultured either with Mock treatment, 2 μM RK-33 or 1 μM FH-1321 overnight in the presence of an HIV-1 integrase inhibitor (Raltegravir). Cells were collected 18 h post treatment and analysed by FISH-Flow using probes against the vRNA, a viability stain and antibodies directed against AnnexinV to quantify viral reactivation and selective early apoptosis using a similar gating strategy as described in Supplementary Fig. 5a. A nested RT-qPCR was also performed to measure cell-associated vRNA with primers targeting the Gag region of the vRNA. Compared to a frequency of 9.5 (s.d.± 4.8) vRNA-expressing cells per million (Mock-treated conditions), 28.9 (s.d.± 9), 22 (s.d.± 4.5) and 52.8 (s.d.± 22.6) vRNA+ cells per million were observed in the RK-33, FH-1321 and PMA-ionomycin-treated cells, respectively; corresponding to a 3.6 (s.d.± 12.1) fold and a 2.7 (s.d.± 1) fold increase in the percentage of vRNA-producing cells in the RK-33 and FH-1321-treated conditions respectively (Fig. 5b, c and Supplementary Fig. 6a). Importantly 28.6 (s.d.± 13.5) % and 34.8 (s.d.± 10.3) % of vRNA+ cells in the RK-33 and FH-1321 conditions were AnnexinV positive, while all the vRNA- populations had <1% AnnexinV positivity (Fig. 5d). When LRA activity was measured by RT-qPCR, significantly higher copies of cell-associated vRNA per μg RNA were observed upon RK-33 and FH-1321 treatment (Fig. 5e and Supplementary Fig. 6b). We also validated that both BIRC5 and HSPA1B mRNA expression was significantly downregulated upon RK-33 treatment, while FH-1321 treatment resulted in decreased expression of BIRC5 (Supplementary Fig. 6c, d). Therefore, treatment with DDX3 inhibitors also demonstrated latency reversal activity and selective cell death in vRNA-containing CD4+ T cells from HIV-1-infected donors.

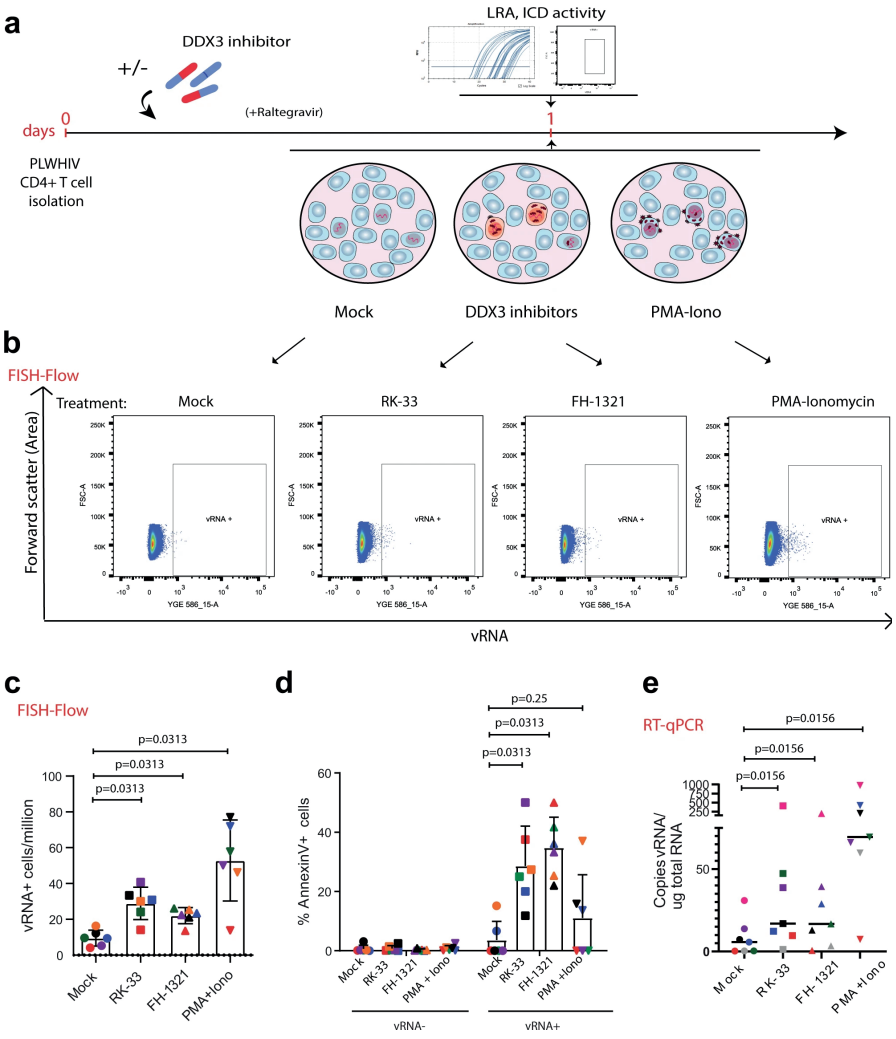

Fig. 5. DDX3 inhibition reverses latency in CD4+ T cells from HIV-1-infected donors and selectively induces cell death. a Schematic of the experiment to test the LRA and ICD activity of DDX3 inhibitors in samples from PLWHIV. CD4+ T cells isolated from HIV-1-infected donors were treated with DMSO (unstimulated), PMA/Ionomycin, and the DDX3 inhibitors RK-33 and FH-1321. For all graphs, different donors are represented by their individual colours consistently as described in Table 3 and symbols represent treatments (Mock= circles, RK-33 =squares, FH-1321= upward triangles and PMA = downward triangles). **b** Representative FISH-Flow dot plots from an HIV-1-infected donor as treated in **a** representing 100,000 cells from each condition. Gating strategy depicted in Supplementary Fig. 5a. **c** The frequency of vRNA-expressing cells per million as depicted in **b** were quantified. Error bars represent the mean ± SD of independent experiments with cells from six different donors, with a minimum of 100,000 events acquired for each condition (Wilcoxon test). **d** The percentages of AnnexinV positive cells from the vRNA− or the vRNA+ cells as quantified by FISH-Flow. Error bars represent mean ± SD from independent experiments from six different donors, with a minimum of 100,000 events acquired for each condition (Wilcoxon test). **e** Copies of vRNA/µg RNA from cells as treated in **a** were quantified by nested RT-qPCR. Error bars represent the mean ± SD of independent experiments with cells from seven different donors (Wilcoxon test).

DDX3 inhibition results in a reduction in the size of the inducible viral reservoir

The induction of the pro-apoptotic AnnexinV marker in HIV-1-expressing cells that we observed upon DDX3 inhibitor treatment was consistent with the notion that DDX3 treatment could result in the depletion of the inducible HIV reservoir. We therefore determined whether the DDX3 inhibitor-treated, reactivated and pro-apoptotic cells were actually eliminated over time, resulting in a decrease in the size of the inducible viral reservoir *in vitro*. CD4+ T cells isolated from PLWHIV were cultured in the presence of the DDX3 inhibitors for 5 days and then treated with PMA-ionomycin to reactivate them to maximal capacity (Fig. 6a). The size of the inducible viral reservoir upon PMA stimulation after culturing with DDX3 inhibitors was measured by three parallel methods of reservoir quantitation: cell-associated vRNA quantification by nested RT-qPCR, FISH-Flow and TILDA (Fig. 6a). We confirmed that culturing patient CD4+ T cells with DDX3 inhibitors for 5 days did not significantly impair viability (Supplementary Fig. 6e), consistent with the mild change in overall gene expression observed by RNA sequencing.

Strikingly, as determined by FISH-Flow, CD4+ T cells cultured in presence of the DDX3 inhibitors RK-33 and FH-1321 showed a 35 (s.d. ± 24.9) % and 47.8 (s.d. ± 20.35) % decrease in the frequency of vRNA-expressing cells respectively as compared to the Mock-treated cells (Fig. 6b, c and Supplementary Fig. 6f). Similarly, upon treatment with PMA-ionomycin, a significant decrease in cell-associated vRNA production was observed by nested RT-qPCR in the RK-33 and FH-1321-treated cells as compared to the Mock-treated cells (Fig. 6d and Supplementary Fig. 6g). For three representative donors, we also conducted TILDA, to quantify the inducible viral reservoir and observed a decrease in the size of the viral reservoir after 5 days of treatment with RK-33 (Fig. 6e-g and Supplementary Fig. 6h). To confirm that RK-33 and FH-1321 do not impair PMA-induced HIV-1 reactivation, we examined the effect of co-treatment with PMA and DDX3 inhibitors in the Lassen and Green *in vitro* CD4+ T cell model of HIV-1 latency. Co-treatment of cells with PMA together with RK-33 or FH-1321 do not impair PMA-induced reactivation, confirming that the decrease in reactivation observed is indeed due to a reduced number of latently infected cells (Supplementary Fig. 6i). Altogether, our data demonstrate that not only do DDX3 inhibitors function as LRAs in primary CD4+ T cells from HIV-1-infected donors, they also selectively ICD in the vRNA-expressing cells, resulting in their elimination and a decrease in the size of the inducible viral reservoir (Fig. 7).

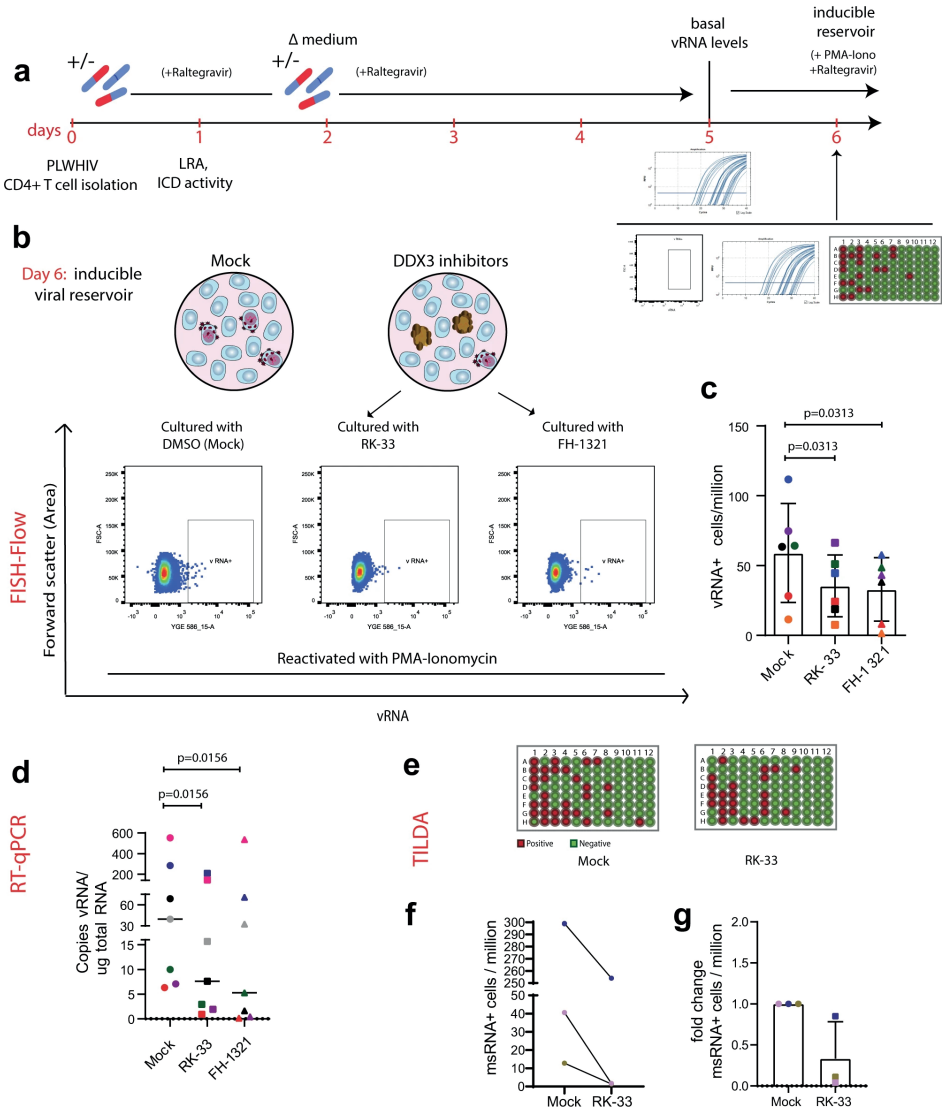

Fig. 6. Prolonged DDX3 inhibition can reduce the size of the inducible viral reservoir. a Schematic of the experiment to test the size of the inducible viral reservoir after culturing CD4+ T cells from PLWHIV with DDX3 inhibitors. CD4+ T cells isolated from HIV-1-infected donors were cultured in the presence of the DDX3 inhibitors RK-33 and FH-1321 or mock-treated for 5 days. On day 5, basal vRNA levels were measured and then cells were maximally stimulated with PMA-Ionomycin for 12–18 h. On day 6, the inducible viral reservoir was measured by FISH-Flow, vRNA RT-qPCR and TILDA. For all graphs, different donors are represented by their individual colours consistently as described in Table 3 and symbols represent treatments (Mock = circles, RK-33= squares and FH-1321 = triangles). **b** Representative FISH-Flow dot plots on day 6 of cultured cells from an HIV-1-infected donor as treated in a representing 50,000 cells from each condition. Gating strategy depicted in Supplementary Fig. 5a. c The frequency of vRNA+ cells/million on day 6 as depicted in **b** were quantified and normalised to the unstimulated condition. Error bars represent the mean ± SD of independent experiments with

cells from six different donors in duplicate, with a minimum of 100,000 events acquired for each condition (Wilcoxon test). d Copies of vRNA/µg total RNA quantified by RT-qPCR on day 6 as treated in **a** and depicted in d. Error bars represent the mean ± SD of independent experiments with cells from seven different donors (Wilcoxon test). **e** Representative TILDA results from cells treated with DDX3 inhibitors. **f** Frequency of msRNA-expressing cells as measured by TILDA and (**g**) fold change of the frequency of msRNA-expressing cells upon treatment with RK-33 normalised to the Mock-treated cells. Error bars represent the mean ± SD of independent experiments with cells from three donors.

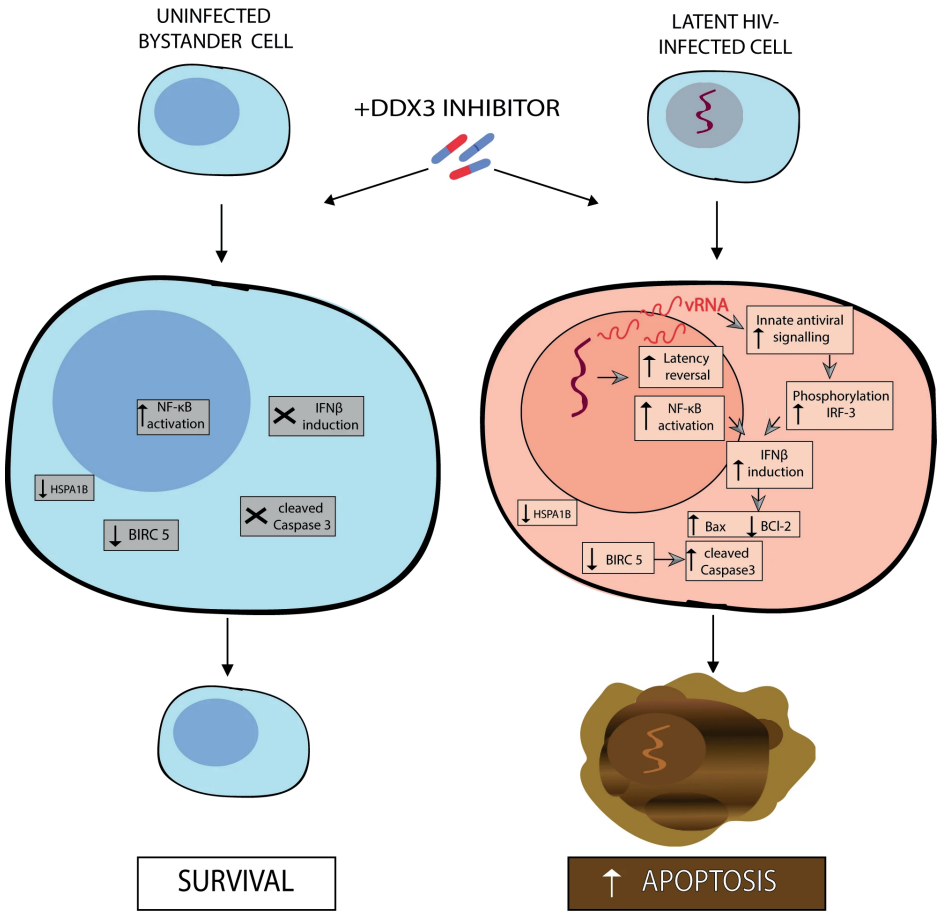

Fig. 7. Model for latency reversal and cell death induced by DDX3 inhibition. DDX3 inhibition results in HIV-1 latency reversal, possibly via NF-κB activation, and BIRC5 and HSPA1B downregulation in both uninfected bystander and latent proviral-containing cells. The HIV-1 provirus is reactivated generating vRNA that can activate innate antiviral signalling pathways, phosphorylate IRF3 and induce IFNβ expression, which when combined with BIRC5 or HSPA1B downregulation, results in upregulated Bax, downregulated BCl2, increased cleaved caspase-3 and apoptosis of the vRNA-expressing cells, but leaving the uninfected cells unharmed, thereby resulting in a reduction in the viral reservoir.

DISCUSSION

We demonstrate that the treatment of latent HIV-1-infected cells with pharmacological inhibitors of the host RNA-binding protein DDX3 modestly reverses viral latency and impairs vRNA translation. This leads to the accumulation of vRNA in infected cells, which activates the innate antiviral signalling pathways [17,18,62,63], phosphorylates IRF3 and induces the production of IFN-β that renders vRNA+ cells pro-apoptotic (Fig. 2e-k) [50-52]. In combination with the DDX3 inhibition-induced downregulation of the anti-apoptotic proteins BIRC5 and HSPA1B, this results in the selective induction of apoptosis in HIV-1 vRNA-expressing cells, with minimal toxicity to uninfected/bystander cells that do not express pro-apoptotic IFN-β (Fig. 7). Importantly, we demonstrate a reduction in the size of the inducible viral reservoir when latently infected cells were cultured in the presence of DDX3 inhibitors. Our data support the proof of concept that pharmacological induction of selective cell death in HIV-1-infected cells following latency reversal may be a viable HIV-1 curative strategy.

The ability of pro-apoptotic molecules to induce NF-κB pathways and reactivate HIV-1 latency is not without precedence. Second mitochondria-derived activator of caspase (SMAC) mimetics such as LCL-161, SBI-0637142, birinipant, Debio1143 and AZD5582 that target host anti-apoptotic factors XIAP and cIAPI/BIRC2 have been demonstrated to be potent LRAs via the activation of non-canonical NF-κB pathways [64-66]. Some LRAs have also been demonstrated to promote cell death, as seen with benzolactam derivatives that are PKC agonists and induce apoptosis in latent HIV-1-infected cells [67,68]. A recent report also demonstrated that romidepsin treatment in a clinical trial resulted in an increase in the frequency of apoptotic T cells [69]. Therefore, the link between apoptosis and latency reversal is highly promising to further exploit as a strategy to reactivate the viral reservoir and induce selective elimination. The DDX3 inhibitors described in this report are such compounds that have both LRA and ICD capability and were able to decrease the size of the inducible viral reservoir.

DDX3 inhibitors are especially interesting as a potential therapeutic class of compounds for use in curative strategies against HIV-1 because they target multiple steps of the HIV-1 life cycle. In this report, we describe the effects of DDX3 inhibition on viral reactivation, possibly mediated by the activation of NF-κB [46] and in agreement with a previous study, we found DDX3 inhibitor-mediated hindering of vRNA export [32,35]. Additionally, DDX3 inhibitors may also impair the translation of the vRNA [34,36]. Recent studies have demonstrated that the treatment of PBMCs with DDX3 inhibitors targeting the RNA-binding site results in a decrease in released infectious viral particles and that these compounds are also effective against HIV-1 strains harbouring resistant mutations to currently approved

antiretroviral drugs[38,70]. This characteristic impairment of host cell translation is an advantage when applying DDX3 inhibitors towards an HIV-1 cure strategy since the generation of infectious viral particles is impaired and therefore treatment with DDX3 inhibitors would prevent both unnecessary activation of the cell-mediated and humoral immune responses or inflammation induced by viral production.

Additionally, we demonstrate a role for DDX3 inhibitors as ICD inducers to eliminate the viral reservoir. DDX3 inhibitors demonstrated the ability to target the HIV-1-infected cells selectively, an important characteristic when developing ICD inducers. In this work, we demonstrate that the DDX3 inhibitors have negligible effects on the viability of uninfected cells as well as on non-HIV-1 vRNA-containing cells from PLWHIV at concentrations effective in reversing latency and selectively inducing apoptosis in cells harbouring HIV-1. We hypothesise that this selectivity may arise from the contribution of several factors. Firstly, DDX3 inhibition results in latency reversal possibly through the activation of NF-κB (fig. 1). The vRNA generated upon latency reversal activates innate antiviral signalling pathways resulting in the phosphorylation of IRF3 and the production of IFN-β, thereby rendering vRNA-expressing cells pro-apoptotic (Fig. 2e-k). Therefore vRNA-producing cells are more susceptible to dying than uninfected cells that do not express IFN-β (Fig.2l). DDX3 inhibition could also abrogate its function as a pathogen recognition receptor and instead could lead to increased vRNA levels for sensing by other factors, including RIG-I like receptors, thereby enhancing innate antiviral signalling. The second factor that contributes to the selectivity of cell death is that DDX3 inhibition downregulates the expression of the anti-apoptotic protein BIRC5 in both healthy and HIV-1-infected cells. Since the infected cells are already pro-apoptotic due to IFN-β production, they are selectively eliminated leaving uninfected/bystander cells unharmed. Consistent with our findings, BIRC5 inhibitors resulted in cell death of HIV-1 protein-expressing cells [54]. Our data are thus consistent with a model whereby BIRC5 is essential to protect cells from the additional stress induced by the presence of HIV-1. HSPA1B that codes for Hsp70 is another gene that we found significantly downregulated in CD4+ T cells in response to treatment with the DDX3 inhibitor RK-33. Hsp70 has been shown to protect cells from apoptosis induced by the HIV-1 protein Vpr [55]. Therefore, we can speculate that an additional mechanism of RK-33 by which it promotes selectively cell death is through downregulation of Hsp70, whose absence leads to an induction of cell death in the Vpr-expressing infected cells and not in the uninfected bystander cells. Additionally, the depletion of Hsp70 via binding to HSPBP1 has been implicated in the reactivation of HIV-1 via NF-κB activation [57], providing another possible mechanism for the observed latency reversal property of RK-33. Moreover, DDX3 inhibition interferes with vRNA metabolism and the residual vRNA that does not efficiently generate infectious

viral particles could still induce cellular stress [18], activate innate antiviral signalling pathways and induce IFN-production[17] and, in combination with the downregulation of factors important for the survival of latently infected cells, result in the selective killing of HIV-1-infected cells. This selective toxicity is also important when promoting the translation of these compounds into clinical settings. The paracrine effect of the production of type I IFNs on uninfected/bystander cells as previously observed in the context of HIV-1 infection [62,63] was negligible in our experiments, likely because of the very low percentages of vRNA-producing primary CD4+ T cells in both our *in vitro* model system and from PLWHIV donors (Figs. 4c and 5c). We validated that both RK-33 and FH-1321 have a negligible effect on cell viability and gene expression in primary cells and that they do not impair the effector function and proliferation of CD4+ T cells. Importantly, these compounds also do not affect CD8+ T cell effector function and proliferation so that the essential cell-mediated immune responses would not be affected during treatment.

Extensive toxicology, biodistribution and pharmacokinetics of RK-33[40] and FH-1321[38] have been conducted in mice and rats respectively, and both demonstrate a good toxicology profile in these pre-clinical studies, thereby advocating for their translation into clinical studies. DDX3 inhibition has however been shown to alter the cell cycle by causing G1 cell cycle arrest, a factor not evaluated in the context of this work, but to be noted for future work or clinical translation. Next-generation DDX3 inhibitors with significantly lower IC50s have also recently been developed with a high potential for clinical advancement [70].

We also present in this work a primary CD4+ T cell model that we have established as a pipeline to further investigate compounds that ICD and to test their potential to reduce the size for the inducible viral reservoir using three parallel methods of reservoir quantitation (Fig. 5 a). Since the ICD strategy does not depend on other components of the host immune system such as CD8+ T cells or NK cells, this system can be used to measure pro-apoptotic compounds that have previously been studied to selectively eliminate HIV-1 expressing cells. Some examples of compounds that can be tested include Bcl2 agonists such as venetoclax[71,72], SMAC mimetics like birinipant, GDC-0152 and embelin[73]; Benzolactam derivatives such as BL-V8-310[67]; p38/JNK pathways activator anisomycin[18], specific autophagy inducing peptides Tat-Beclin 1 and Tat-vFLIP-α2[74]; PI3K/Akt inhibiotrs[75]; or synthesised compounds such as L-HIPPO that inhibit viral trafficking and budding of Gag[76], which have all been implicated in killing of HIV-1-infected cells.

Pharmacological inhibition of BIRC5, also one of the genes downregulated by DDX3 expression, has been demonstrated to target HIV-1-infected cells and reduce the frequency of proviral-containing cells *in vitro* [54]. However, some of these treatments

have been associated with global T cell activation and toxicity, selective myeloid cell-type dependent activity or non-reproducibility. Moreover, these studies have not specifically investigated the contribution of the HIV-1 vRNA in inducing cell death, made possible here using FISH-Flow technology. Further investigation of these compounds, possibly in combination with DDX3 inhibitors, will be important to assess their ability to decrease the size of the inducible viral reservoir in CD4+ T cells obtained from PLWHIV using an *in vitro* model such as the one we describe in Fig. 6a, and also to investigate the contribution of vRNA to cell death.

These studies suggest that pharmacological induction of selective cell death in HIV-1-infected cells, alone or in combination with other approaches, including those that promote extracellular killing of HIV-1-infected cells may prove effective towards an HIV-1 cure.

One of the caveats of this study is that DDX3 inhibitors are modest LRAs that do not maximally reactivate the HIV-1 provirus as compared to the PMA-treated cells, thereby resulting in reactivation of only a fraction of the latently infected cells and hence a partial decrease of the viral reservoir but not its elimination. Moreover, since our studies have focussed on using RNA-based readouts for the viral reservoir, it is yet to be determined if treatment with DDX3 inhibitors also results in a decrease in the translation-competent reservoir. Therefore, a combinatorial strategy will be important to test in future work, combining different classes of LRAs to maximally reactivate the latent HIV-1-infected reservoir together with DDX3 inhibitors with the ultimate aim to ICD in all cells harbouring inducible replication-competent HIV-1, also measuring the amount of released viral particles, thereby accounting for the translational-competent reservoir. Attractive candidate LRAs for inclusion in this combinatorial approach are de-repressors of HIV-1 LTR chromatin (BAF and HDAC inhibitors)[60], activators of transcription (PKC agonists), as well as facilitators of HIV-1 transcription elongation such as the newly characterised Gliotoxin [77]. Using a pipeline to measure vRNA production and cell death at a single cell level may enable the identification of an optimal combination of LRA-ICDs that lead to a maximal reduction of the viral reservoir.

So far, more than 160 compounds have been identified with latency reversing activity, and our work has identified DDX3 inhibitors as another category of compounds to reverse viral latency[78]. In addition to latency reversal, DDX3 inhibitors target multiple steps of the HIV-1 replication cycle: transcription, nucleocytoplasmic export of vRNA, translation and generation of infectious viral particles. Importantly, they also promoted ICD and were selectively able to induce IFN-β production and apoptosis in vRNA-expressing cells resulting in the decrease in size of the inducible viral reservoir. Previous combinatorial studies and clinical trials with LRAs and immune enhancing

clearance strategies demonstrated minimal effects on the clearance of the viral reservoir [4-6]. Although multiple compounds have been identified to induce apoptosis of HIV-1-infected cells[13], no ICD inducer has been evaluated for the capability to reduce the viral reservoir in PLWHIV yet. Our data support DDX3 inhibitors as a promising class of ICD inducers that can be utilised in HIV-1 curative therapies.

METHODS

Cell culture and reagents

Jurkat cells and J-Lat 11.1 cells (Jurkat cells containing integrated full-length HIV-1 genome mutated in *env* gene and GFP replacing *nef*)[39] were maintained in RPMI-1640 medium (Sigma-Aldrich) supplemented with 7% FBS and 100 µg/ml penicillin-streptomycin at 37 °C in a humidified, 5% CO_2 atmosphere. J-Lat latent proviruses were reactivated by adding 10 µM of phorbol 12-myristate 13-acetate (PMA) (Sigma-Aldrich) to the culture media for 18 h. Primary CD4+ T cells were isolated from buffy coats from healthy donors by Ficoll gradient followed by separation via negative selection with RosetteSep Human CD4+ T-cell Enrichment Kit (StemCells Technologies) according to the manufacturer's instructions. After isolation, CD4+ T cells were maintained in RPMI-1640 medium (Sigma-Aldrich) supplemented with 10% FBS and 100 µg/ml penicillin-streptomycin at 37 °C in a humidified, 5% CO2 atmosphere. Cells were activated with 100 ng/ml PMA and 1 µg/ml Ionomycin (Sigma-Aldrich). HEK293T cells were cultured in DMEM medium (Sigma-Aldrich) supplemented with 10% FBS and 100 µg/ml penicillin-streptomycin at 37 °C in a humidified, 5% CO2 atmosphere. RK-33 (SelleckChem) was used at a concentration of 2 µM unless indicated otherwise. FH-1321 was provided by First Health Pharmaceuticals and used at concentrations of 1 µM. YM155 (SelleckChem) was used at concentrations of 200 nM.

Total RNA isolation and quantitative RT-PCR (RT-qPCR)

Total RNA was isolated from the cells using TRIzol reagent (Thermo Fisher Scientific) according to the manufacturer's instructions. cDNA synthesis was performed using Superscript II Reverse Transcriptase (Life Technologies) kit following the manufacturer's protocol. RT-qPCR was performed using GoTaq qPCR Master Mix (Promega) following the manufacturer's protocol. Amplification was performed on the CFX Connect Real-Time PCR Detection System thermocycler using CFX Manager version 3.0 (Bio-Rad) using the following thermal cycling programme starting with 3 min at 95 °C, followed by 40 cycles of 95 °C for 10 s and 60 °C for 30 s. The specificity of the RT-qPCR products was assessed by melting curve analysis. Primers used for real-time PCR are listed in Supplementary Table 1. Expression data were calculated

using a 2−ΔΔCt method[79]. GAPDH housekeeping gene expression was used for normalisation for J-Lat cell lines and Cyclophilin A was used for primary cells.

NF-κB reporter assay

To generate the plasmids used in this assay, custom gBlock gene fragments (Integrated DNA Technologies) containing either the minimal mouse heat shock protein (Hspa1a) promoter, or four NF-κB target sites followed by an Hspa1a promoter were designed with flanking NheI-NcoI restriction sites and then cloned upstream of the luciferase gene in the pGL3 luciferase reporter plasmid at the NheI-NcoI sites (Promega). Jurkat cells were transfected with pBluescript II SK (+) (empty vector), pRL Renilla Luciferase Control Reporter Vector (Promega) to normalise for transfection efficiency, and either the HSP-Luc or the NF-κB-HSP-Luc plasmids by nucleofection using Amaxa Nucleofector (Amaxa AG-Lonza, Cologne, Germany)[59]. Ten million cells were centrifuged at 200 x g for 10 min at room temperature, resuspended in 100 µl of solution R, and nucleofected with 2 µg plasmid DNA (1.5 µg pBluescript II SK (+), 200 ng pRL and either Hspa1a-pGL3 or NF-κB-Hsp1a-pGL3) using programme O28. Nucleofected cells were resuspended in 5 ml of pre-warmed, serum-free antibiotic-free RPMI at 37 °C for 15 min and then plated in 6 ml of pre-warmed complete media. Twenty-four hours post-nucleofection cells were either Mock-treated or treated with 2 µM RK-33. Luciferase expression was measured 24 h post-treatment in a GloMax 96 microplate luminometer using the GLOMAX software (version 1.9.2) (Promega) using the Dual-Glo Luciferase assay system (Promega) and normalised to Renilla luciferase expression. Data represent at least three independent experiments.

FISH-Flow

Cells were collected, fixed, permeabilised and subjected to the PrimeFlow RNA assay (Thermo Fisher Scientific) following the manufacturer's instructions and as described in [20,21]. In primary CD4+ T cells, cells were first stained in Fixable Viability dye 780 (Thermo Fisher Scientific) for 20 min at room temperature (1:1000 in dPBS) followed by either AnnexinV-450 (560506, BD Biosciences) or with 2 µM CellEvent™ Caspase-3/7 Green Detection Reagent (Thermo Fisher Scientific) for 30 min at room temperature (1:150 in AnnexinV binding buffer-Biolegend). For both CD4+ T cells and J-Lat 11.1 cells, mRNA was labelled with a set of 40 probe pairs against the GagPol region of the vRNA (Catalogue number GagPol HIV-1 VF10-10884, Thermo Fisher Scientific) diluted 1:5 in diluent provided in the kit and hybridised to the target mRNA for 2 h at 40 °C. Positive control probes against the housekeeping gene RPL13A (VA1-13100, Thermo Fisher Scientific) were used to determine assay

efficiency. Samples were washed to remove excess probes and stored overnight in the presence of RNAsin. Signal amplification was then performed by sequential 1.5 h, 40 °C incubations with the pre-amplification and amplification mix. Amplified mRNA was labelled with fluorescently tagged probes for 1 h at 40 °C. Samples were acquired on a BD LSR Fortessa Analyzer and gates were set using the unstimulated J-Lat 11.1 control sample or uninfected CD4+ T cells. The analysis was performed using the FlowJo V10 software (Treestar).

Confocal microscopy following FISH-Flow

J-Lat 11.1 cells that underwent the FISH-Flow assay were seeded on 18 mm diameter coverslips and air-dried. Coverslips were mounted in ProLong Gold Antifade Reagent (Life Technologies). Immunofluorescence images were acquired using a confocal microscope (Leica, SP5). All phase-contrast pictures were acquired using a Leica DMIL microscope and a DFC420C camera. Images were analysed and processed using Fiji/ ImageJ (NIH).

Production of shRNA lentiviral vectors and transduction

Lentiviral constructs containing the desired shRNA sequences (shControl—SHC002 and shDDX3) were amplified from bacterial glycerol stocks obtained in house from the Erasmus Center for Biomics and part of the MISSION® shRNA library. In total, 5.0 x 10^6 HEK293T cells were plated in a 10 cm dish and transfected with 12.5 µg of plasmids mix. In total, 4.5 µg of pCMVΔR8.9 (envelope)[80], 2 µg of pCMV-VSV-G (packaging)[80] and 6 µg of shRNA vector were mixed in 500 µl serum-free DMEM and combined with 500 µl DMEM containing 125 µl of 10mM polyethyleneimine (PEI, Sigma). The resulting 1 ml mixture was added to HEK293T cells after 15 min incubation at room temperature. The transfection medium was removed after 12 h and replaced with a fresh RPMI medium. Virus-containing medium was harvested and replaced with fresh medium at 36, 48, 60 and 72 h post-transfection. After each harvest, the collected medium was filtered through a cellulose acetate membrane (0.45 µm pore) and used directly for shRNA infections or stored at -80 °C for subsequent use. For lentiviral transduction of J-Lat 11.1 cells, 1 ml of the collected virus was seeded with 2 x 10^6 cells in a final volume of 4 ml. Transduced cells were selected with 1 µg/ml Puromycin 72 h post-infection and cells were collected 4 days post-selection. For primary CD4+ T cells, cells were stimulated for 3 days with anti-CD3-CD28-coated Dynabeads (Thermo Fisher Scientific) and 5 ng/ml IL-2 (Thermo Fisher Scientific), and then resuspended with 1 ml of virus per 6 x 10^6 cells. Transduced cells were selected with 1 µg/ml Puromycin 72 h post-infection and cells were harvested 4 days post-selection.

Western blotting

At least 500,000 J-Lat 11.1 cells or 2 x 10^6 CD4+ T cells were lysed per condition. Cells were washed with dPBS and lysed in ice-cold lysis buffer (100 mM NaCl, 10 mM Tris, pH 7.5, 1 mM EDTA, 0.5% Nonidet P-40, protease and phosphatase inhibitor cocktail [Roche]). Cell lysates were denatured in Laemmli sample buffer and incubated for 5 min at 95 °C. The proteins were separated by SDS-PAGE and transferred onto nitrocellulose membranes (Bio-Rad). Membranes were blocked with 5% non-fat milk in Tris-buffered saline pH 7.4 and 0.5% Tween 20 (TBST) and then incubated with primary antibodies. After three washes with TBST, the membranes were incubated with horseradish peroxidase-conjugated secondary antibodies (Rockland Immunochemicals; 1:10,000) and detected using Western Lightning Plus-ECL reagent (Perkin Elmer). Signal intensity and densitometry analyses were conducted using ImageJ (NIH). The following antibodies were used: anti-Puromycin (12D10 Sigma-Aldrich; 1:1000), anti-GAPDH (ab8245, Abcam; 1:5000) and anti-DDX3 (ab128206, Abcam; 1:2000), anti-Phospho-IRF3 (Ser386) (37829, Cell Signalling Tech; 1:1000), anti- HSP70 (4872, Cell Signalling Tech; 1:1000), anti-IRF3 (sc33641, Santa Cruz; 1:1000), anti BIRC5 (sc17779, Santa Cruz; 1:1000) and anti-tubulin (B7, Santa Cruz; 1:3000).

Molecular docking

Molecular docking analysis was used to determine the most likely binding mode of RK-33 and FH-1321 to pre-unwound DDX3 conformation. Crystal structure of human DDX3 in complex with dsRNA (PDB ID code 6O5F) in the pre-unwound confirmation was used as a template to define the receptor for the docking simulation by elimination or protein chain B and RNA domain C and D. RK-33 and FH-1321 ligand structure was built and energy minimised using the programme Chimera[81]. Molecular docking of RK-33 and FH-1321 to pre-unwound DDX3 confirmation was performed using Chimera's AutoDock Vina function[82]. The resulting solutions were ranked based on the highest binding affinity (or lowest binding energy). Figures were created using PyMol Molecular Graphics System, Version 1.8. 2015 (Schrödinger L).

RNA-seq

RNA was isolated using TRI Reagent (Sigma-Aldrich). RNA-seq was performed according to the manufacturer's instructions (Illumina) using the TruSeq Stranded mRNA Library Prep kit. The resulting DNA libraries were sequenced according to the Illumina TruSeq v2 protocol on an Illumina HiSeq2500 sequencer. Reads of 50 bp in length were generated. Reads were mapped against the UCSC genome

browser GRCh38 reference genome with HiSat2 (version2.1.0). Gene expression was quantified using htseq-count (version 0.11.2). For all samples, at least 14.4 million reads were generated with counts on 22.6–24.2 thousand expressed genes.

Differential expression analysis of the RNA-seq data was performed using edgeR package run under Galaxy (https://bioinf-galaxian.erasmusmc.nl/galaxy/). False discovery rate cut-off was set to 0.05 and a fold change of ±1.5 was counted as differentially expressed. Heat maps were generated using MORPHEUS (https://software.broadinstitute.org/morpheus/index.html).

Viability and activation assays

In Jurkat and J-Lat cells, 10 ng/ml Hoescht 33342 was added to the cells and 30 min later, the viability and reactivation were quantified by measuring 405 nm+ and GFP+ expression, respectively, by flow cytometry. In primary CD4+ T cells, to determine viability and cell activation following DDX3 inhibition, cells were collected and stained with Fixable Viability Dye eFluor® 780 (Thermo Fisher Scientific) and anti-CD25-PE (Becton Dickinson). Mock-treated and cells treated with PMA-Ionomycin were used as negative and positive controls, respectively. Cells were stained for 30 min at 4 °C, washed with PBS and resuspended for flow cytometric analysis.

T cell proliferation and functionality assay

To analyse the effect of the LRA on CD8+ and CD4+ T cells, proliferation and cytokine expression were analysed by flow cytometry. Primary CD8+ and CD4+ T cells were isolated from buffy coats from healthy donors by Ficoll gradient (GE Healthcare) followed by negative selection with RosetteSep Human CD8+ T-Cell Enrichment Cocktail or RosetteSep Human CD4+ T-Cell Enrichment Cocktail (StemCell Technologies), respectively. Isolated cells were left overnight for recovery. To analyse T cell proliferation capacity, one million CD8+ or CD4+ T cells were stained with 0.07 µM CellTrace Far Red Cell Proliferation dye (Thermo Fisher Scientific) following the manufacturer's instructions. Cells were then cultivated for 72 h in either unstimulated or stimulated conditions in the presence of the LRA, and analysed by flow cytometry. Stimulation of T cells was performed using Anti-CD3/CD28-coated Dynabeads (Thermo Fisher Scientific) following the manufacturer's protocol. Proliferation capacity was determined by a decrease in proliferation of dye intensity in daughter cells upon cell division. To analyse T cell functionality through cytokine expression, one million CD8+ or CD4+ T cells were left untreated or treated with the LRA for 18 h. Cells were then left unstimulated or stimulated with 50 ng/ml PMA and 1 µM Ionomycin for 7 h in the presence

of a protein transport inhibitor (BD Golgi-PlugTM, BD Biosciences). To stain for intracellular cytokines cells were washed with PBS supplemented with 3% FBS followed by fixation and permeabilisation step with FIX & PERM Kit (Invitrogen) following manufacturer's protocol and incubated with 1:25 BV510 anti-IL-2 (563265, BD Biosciences) and PE-Cy7 anti-IFNγ (27-7319-41, eBioscience) in permeabilisation buffer for 45 min at 4 °C. Stained cells were washed with PBS supplemented with 3% FBS and analysed by flow cytometry.

Measurement of de novo protein synthesis

De novo protein synthesis upon DDX3 inhibition was measured by the incorporation of puromycin into peptide chains[83]. Briefly, cells were incubated with 10 µg/ml puromycin (Sigma-Aldrich) for 10 min before cell lysis followed by Western blot according to the protocol described above using antibodies against puromycin. Puromycin incorporation was assessed by summating the immunoblot intensity of all de novo synthesised protein bands normalised to the signal intensity of the GAPDH band. CD4+ T cells were treated with 10 µg/ml Cycloheximide (Sigma-Aldrich) for 4 h to inhibit translation as a control for the technique.

Primary CD4+ T cell infection and *in vitro* HIV-1 latency model generation

Infections were performed using a pseudotyped virus expressing luciferase that was generated by co-transfecting HXB2-Env together with the HIV-1 backbone plasmid with a luciferase reporter (pNL4.3.Luc.R-E-) into HEK293T cells using PEI (Polyethylenimine) transfection reagent. In total, 48 and 72 h post-transfection, the pseudovirus-containing supernatant was collected, filtered through a 0.45 µm filter, aliquoted and concentrated by ultracentrifugation (20,000 x g for 1 h at 4 °C). The pellet was resuspended in RPMI-1640 and stored at -80 °C. The *in vitro* model of HIV-1 latency was set up using the Lassen and Greene method[58] as follows: CD4+ T cells were infected with the pNL4.3.Luc-R-E- virus by spinoculation (2 h at 1200 x g) 24 h after isolation and cultured overnight in RPMI 10% FBS and 100 µg/ml penicillin-streptomycin in presence of Saquinavir Mesylate (5 µM). Eighteen hours after spin-infection cells were washed and cultured in growth media supplemented with 5 µM Saquinavir Mesylate. Three days after infection cells were treated with DDX3 inhibitors in presence of Raltegravir (3 µM). HIV-1 molecular clone pNL4.3.Luc.R-E-, HIV-1 HXB2-Env expression vector, Saquinavir Mesylate and Raltegravir were kindly provided by the NIH AIDS Reagents. HIV-1 molecular clone pNL4.3.Luc.R-E- and HIV-1 HXB2-Env expression vector were donated by Dr. Nathaniel Landau and Drs. Kathleen Page and Dan Littman, respectively. Cells

were harvested 24 h after stimulation with DDX3 inhibitors, washed once in PBS and either lysed for RNA extraction, used for FISH-Flow analysis or lysed in passive lysis buffer to measure luciferase activity using Luciferase Assay System (Promega). Relative light units were normalised to protein content determined by Bradford assay (Bio-Rad).

Assays with HIV-1-infected donor samples

PBMCs from HIV-1-infected donors were obtained by Ficoll density gradient isolation of leukapheresis material from donors that were older than 18 years, cART-treated for at least 1 year, with viral loads below 50 copies/ml for more than 2 months. This study was conducted in accordance with and in compliance with the ethical principles of the Declaration of Helsinki. HIV-1-infected patient volunteers were informed and provided signed consent to participate in the study. The authors also affirm that research participants provided informed consent for publication of their clinical characteristics presented in Table 3. The study protocol was approved by the Erasmus Medical Centre Medical Ethics Committee (MEC-2012–583). CD4+ T cell isolation was performed using negative selection with the EasySep Human CD4+ T-cell Enrichment kit (StemCells Technologies) according to the manufacturer's instructions. After isolation, CD4+ T cells were allowed to rest for at least 4 h, maintained in RPMI-1640 medium (Sigma-Aldrich) supplemented with 10% FBS, 100 µg/ml penicillin-streptomycin and Raltegravir (3 µM) at 37 °C, in a humidified, 5% CO2 atmosphere. Cells were treated with DDX3 inhibitors or with PMA-Ionomycin as a positive control for viral reactivation (100 ng/ml PMA and 1 µg/ml Ionomycin). Eighteen hours post-treatment, cells were either lysed in TRIzol for RNA extraction and RT-qPCR or analysed by FISH-Flow. To measure the depletion in the size of the inducible viral reservoir, cells were cultured for 5 days in 2 µM RK-33 and 1 µM FH-1321 with a change in media and retreatment after 48 h. Five days post-treatment, media was changed, and cells were treated with PMA-Ionomycin for 12 h and collected for TILDA, or after 18 h for RT-qPCR and FISH-Flow.

Table 3: Characteristics of PLWHIV donors used in this study

Colour code	Sex	Age	Time from HIV-1 diagnosis to leukapheresis	Time on ART at leukapheresis	Time with continuous HIV-1 RNA <50 copies/mL
Donor 1 = Red	Male	66	52 months	52 months	48 months
Donor 2 = Dark Green	Male	75	108 months	81 months	75 months
Donor 3 = Blue	Male	47	85 months	72 months	64 months
Donor 4 = Black	Male	67	86 months	86 months	12 months
Donor 5 = Purple	Female	42	55 months	55 months	52 months
Donor 6 = Orange	Male	50	124 months	49 months	48 months
Donor 7 = Grey	Male	35	19 months	19 months	17 months
Donor 8 = Dark pink	Male	42	77 months	77 months	71 months
Donor 9 = Light pink	Male	57	18 months	17 months	2 months
Donor 10 = Khaki green	Male	50	100 months	42 months	37 months

Cell-associated vRNA measurement by nested RT-qPCR

Cell-associated vRNA[84] was measured by performing a first round of the PCR using the primers Gag1(5' TCAGCCCAGAAGTAATACCCATGT 3') and SK431 (5' TGCTATGTCAGTTCCCCTTGGTTCTCT 3') that amplifies a region within the HIV-1 gag gene in 25 µL of PCR mix containing 4 µL of cDNA, 2.5 µL 10X Platinum Taq buffer, 2 mM MgCl2, 0.4 mM concentrations of deoxynucleoside triphosphates, 0.2 µL Platinum Taq and 0.3 µM each of both primers. The PCR settings were as follows: 95 °C for 5 min, followed by 15 cycles of 95 °C for 30 s, 55 °C for 30 s and 72 °C for 1 min. The product of the first PCR was subsequently used as a template in the second, semi-nested, real-time, PCR amplification. A total of 2 µL of the first PCR product was added to a PCR mix with a final volume of 25 µL containing 2.5 µL 10X Platinum Taq buffer, 2mM MgCl2, 0.4mM concentrations of deoxynucleoside triphosphates, 0.2 µL Platinum Taq and 0.2 µM of the primers Gag1 (5' TCAGCCCAGAAGTAATACCCATGT 3') and Gag2 (5' CACTGTGTTTAGCATGGTGTTT 3') and 0.075 µM TaqMan dual-labelled fluorescent probe Gag3 (5' [6FAM]ATTATCAGAAGGAGCCACCCCACAAGA [BHQ1] 3'). Real time PCR settings were as follows: 95 °C for 5 min, followed by 45 cycles of 95 °C for 30s and 60 °C for 1 min. The amplicon sizes were 221 bp for the first PCR and 83 bp for the second (real-time) PCR. Serial dilutions of plasmid DNA standards were used to generate a standard curve to calculate the copies of vRNA and then normalised to the amount of input RNA.

Tat/rev-induced limiting dilution assay (TILDA)

TILDA was performed using a modified method as described in[85]. Briefly, total CD4+ T cells were isolated from PBMCs by negative magnetic separation using EasySep Human CD4+ T-cell isolation kit (StemCell Technology). Following treatment for 5 days (Fig. 6a), 2 x 10^6 cells/mL were stimulated for 12 h with 100 ng/mL phorbol 12-myristate 13-acetate (PMA) and 1 µg /mL ionomycin (both from Sigma-Aldrich). After stimulation, CD4+ T cells were washed and resuspended in RPMI-1640 at serial dilutions; 1.8 x 10^6 cells/mL, 9 x 10^5 cells/mL, 3 x 10^5 cells/mL and 1 x 10^5 cells/mL. In total, 10 µL of the cell suspension from each dilution was dispensed into 24 wells of a 96-well plate containing 2 µL One-step RT-PCR enzyme (Qiagen), 10 µL 5x One-step RT-PCR buffer (Qiagen), 10 µL Triton X-100 (0.3%), 0.25 µl RNAsin (40 U/µL), 2 µL dNTPs (10mM each), 1 µL of tat 1.4 forward primer (20 µM) and rev reverse primer (20 µM) (as published in[86]), and nuclease-free water to a final reaction volume of 50 µL. The one-step RT-PCR was run using the following thermocycling conditions: 50 °C for 30 min, 95 °C for 15 min, 25 cycles of 95 °C for 1 min, 55 °C for 1 min and 72 °C for 2 min, and a final extension at 72 °C for 5 min. Afterwards, 2 µL of the 1st PCR products were used as input for real-time PCR to detect *tat/rev* msRNA. The 20 µL reaction volume consisted of 5 µL Taqman Fast Advanced Master mix 4x (Thermo Fisher Scientific), 0.4 µL of tat 2.0 forward primer and rev reverse primer (each at 20 µM) and tat/rev probe (5 µM)[86]. The real-time PCR was performed in a LightCycler 480 Instrument II (Roche) using the following programme: 50 °C for 5 min, 95 °C for 20 s, 45 cycles of 95 °C for 3 s and 60 °C for 30 s. Positive wells at each dilution were recorded and used to determine the frequency of cells expressing *tat/rev* msRNA by maximum likelihood method using ELDA software[87].

Statistical analysis

All data are means ± SD of three or more independent biological replicates, as indicated in the figure legends. Statistical significance was calculated using a two-tailed t-test or as indicated in the figure legends. Analyses were performed using Prism version 8.3.0 (GraphPad software).

DATA AVAILABILITY

All data needed to evaluate the conclusions in the paper are present in the paper and/or the Supplementary materials. All RNA-seq data have been deposited to the Gene Expression Omnibus (GEO) database with accession code GSE167553. Additional data related to this paper may be requested from the authors. Source data are provided with this paper.

ACKNOWLEDGEMENTS

This work is dedicated to the memory of C.A.B.B. We would like to thank Jan-Willem Bakker, Alessia Tarditi and Matteo Andreini from First Health Pharmaceuticals Amsterdam for the generous provision of the DDX3 inhibitor FH-1321; and Tsung Wai Kan for technical help. The research leading to these results has received funding from the Dutch Aidsfonds (grants P-53302 and P-53601), Health Holland (grants LSHM19100-SGF and EMCLSH19023), ZonMW (grant 40-44600-98-333), the Federation of Medical Specialists (grant 59825822) and the EHVA T01 consortium, which is supported by the European Union's Horizon 2020 Research and Innovation Programme (grant 681032).

AUTHOR CONTRIBUTIONS

S.R. and T.M. designed the studies; S.R., C.L., R.C., T.H.S. and A.G. conducted experiments and performed data analysis; S.R., R.J.P. and W.V.I. participated in gene expression analysis; H.A.B.P., C.R. and A.V. recruited patients for the study; Y.M.M., P.D.K., J.J.A.V.K., C.A.B.B., R.A.G. and T.M. provided expertise and supervision; S.R. and T.M. wrote the manuscript with input from all authors. All authors read and approved the final manuscript.

SUPPLEMENTARY DATA

Rao S., Lungu C., et al., Nat Commun. 2021 Apr 30;12(1):2475. doi: 10.1038/s41467-021-22608-z

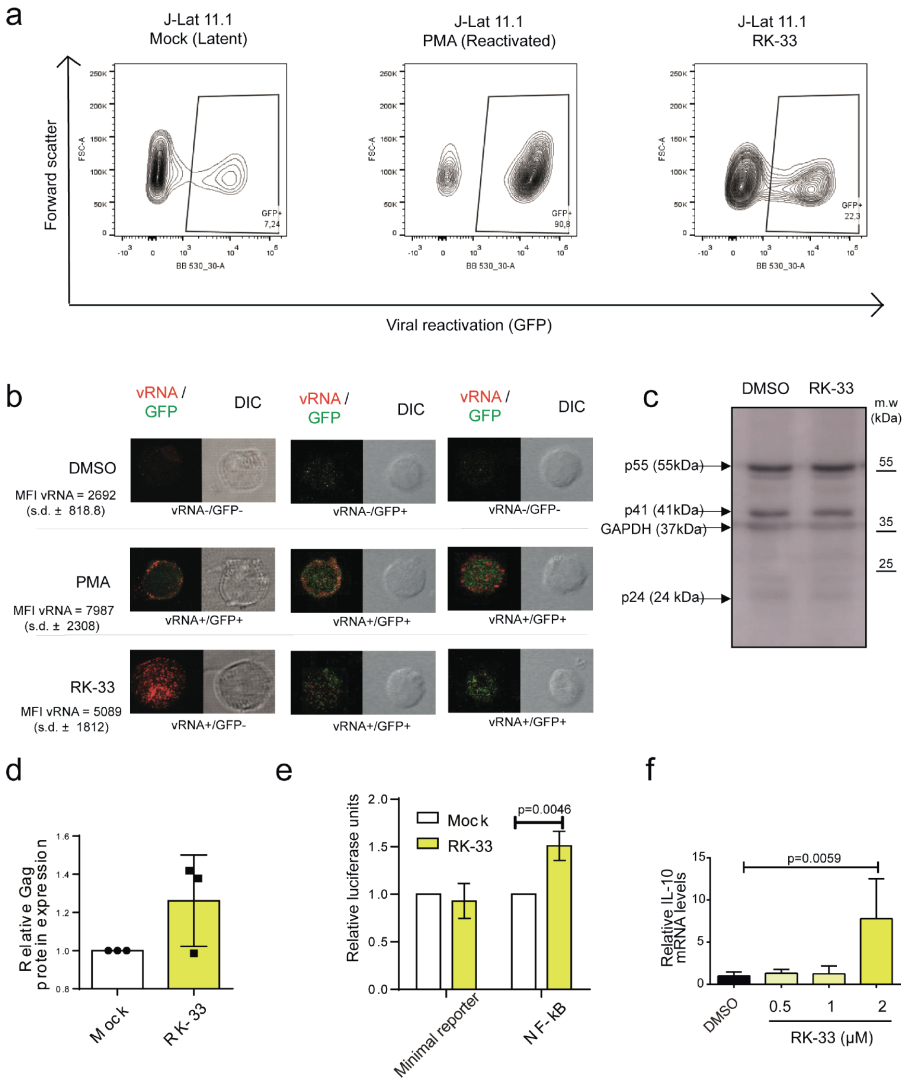

Fig. S1. Effects of RK-33 on J-Lat 11.1 cells. **a** Gating strategy, contour plots depicting % GFP expression of Mock, PMA and 2μM RK-33 treated J-Lat 11.1 cells. This gating strategy is used for graphs depicted in Fig. 1a, 1e and 2c. **b** Three representative images from each condition of J-Lat cells as treated in **a**, seeded as unsorted whole populations onto a coverslip and observed by confocal microscopy. vRNA is depicted in red, GFP in green and the differential interference contrast (DIC) in grey. Mean Fluorescence intensity (MFI) of the vRNA channel from three independent experiments are also quantitated and shown. Scale bars represent 5μM. **c** Representative Western blots depicting viral proteins Gag (p55), p41 and p24, and GAPDH in Mock and RK-33-treated J- Lat 11.1 cells. **d** Quantification of the densitometric analysis of Gag protein expression normalised to loading control GAPDH. Error bars represent mean ± SD from three independent experiments (Unpaired, two-tailed t-test). **e** Relative luciferase expression from cells transfected with a minimal reporter plasmid or

those containing NF-κB target sites normalised to Mock-treated condition. Error bars represent mean ± SD from three independent experiments (Unpaired, two-tailed t-test). **f** The relative mRNA expression levels of IL-10 in J-Lat 11.1 cells treated with increasing concentrations of RK-33 was quantified by RT-qPCR. Error bars represent mean ± SD from three independent experiments (Unpaired, two-tailed t-test).

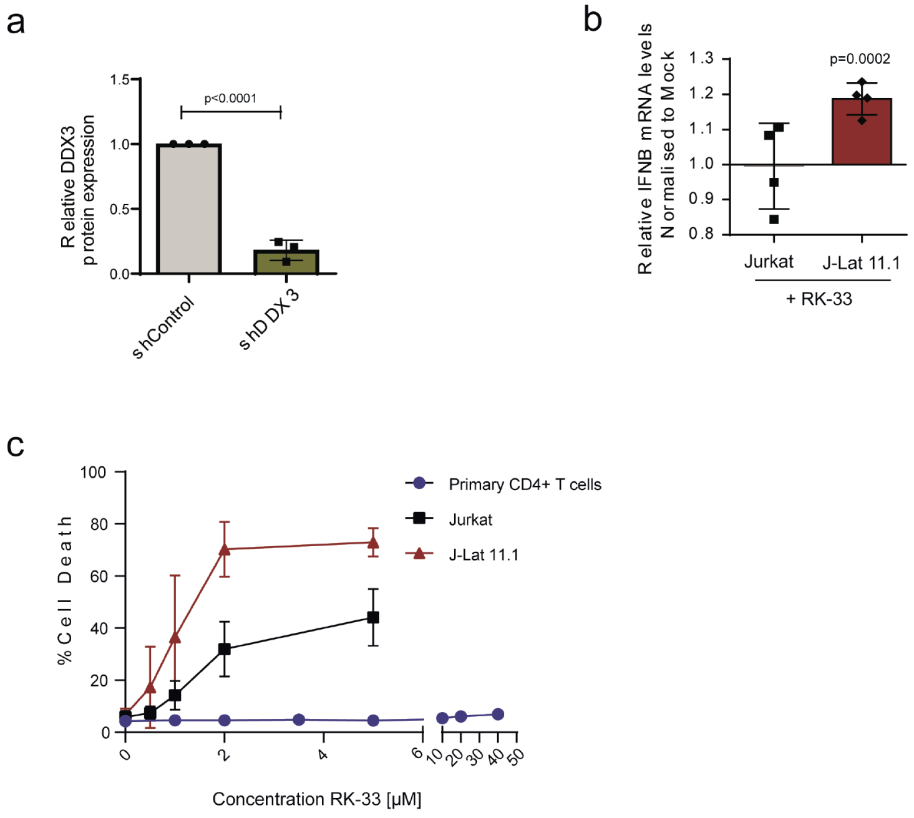

Fig.S2. Effects of DDX3 inhibition and vRNA expression in J-Lat 11.1 cells a Quantification of the densitometric analysis of DDX3 expression from Fig. 2b. normalised to loading control GAPDH. Error bars represent mean ± SD from three independent experiments (Unpaired, two-tailed t-test). **b** Jurkat and J-Lat 11.1 cells were treated with 2uM RK-33 and relative IFNβ mRNA expression levels were quantified by RT-qPCR and normalised to the mock-treated cells. Error bars represent mean ± SD from three independent experiments (Unpaired, two-tailed t-test). **c** % Cell death was measured in Jurkat, J-Lat and primary CD4+ T cells treated with increasing concentrations of RK-33 by flow cytometry. Error bars represent mean ± SD from three independent experiments for cell lines and from 3 independent donors for primary cells.

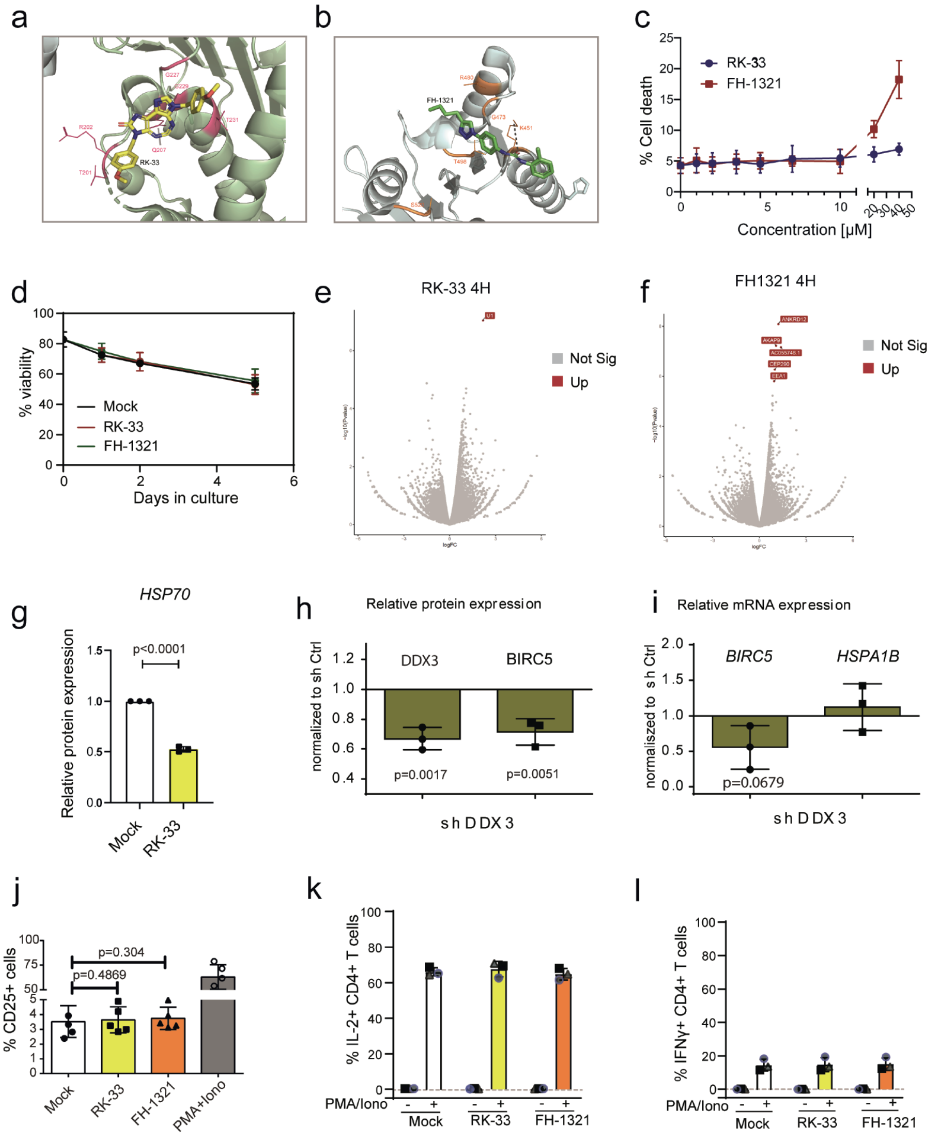

Fig. S3. Effects of DDX3 inhibitors on primary CD4+ T cells a Close up of ATP-binding pocket on the surface of DDX3 with bound RK-33 as predicted by AutoDock Vina. DDX3 domain 1 is shown as pale green cartoon, domain 2 is shown as pale blue cartoon and surface color code is pink for ATP-binding residues and orange for RNA-binding residues. Color code for RK33 is yellow for carbon, red for oxygen, dark blue for nitrogen. **b** Close up of RNA-binding pocket on the surface of DDX3 with bound FH- 1321. Color code for FH-1321 is green for carbon, red for oxygen, dark blue for nitrogen. The predicted hydrogen bond between FH-1321 and Lysine 541 from DDX3 RNA-binding pocket is indicated with a dashed line. **c** % Cell death of CD4+ T cells treated with increasing concentrations of either RK-33 or FH-1321. Error bars represent mean ± SD from freshly isolated CD4+ T cells from

three healthy donors. **d** % live cells (cell viability) of CD4+ T cells treated with 2 μM RK-33 or 1 μM FH-1321 for up to 5 days. Error bars represent mean ± SD from CD4+ T cells isolated from freeze-thawed PBMCs from three healthy donors. Volcano plot of differentially expressed genes from CD4+ T cells 4 hours post-treatment with **e** RK-33 and **f** FH-1321. **g** Quantification of the densitometric analysis of HSP70 protein expression from cells as treated in Fig 2h. Error bars represent mean ± SD from three donors. (Unpaired, two-tailed t-test; p-value <0.00001). **h** Quantification of the densitometric analysis of DDX3 and BIRC5 protein expression normalised to loading control GAPDH relative to shControl-treated cells. Error bars represent mean ± SD from three donors (Unpaired, two-tailed t-test). **i** Relative mRNA expression of BIRC5 and HSPA1B of shDDX3-treated cells normalised to shControl. Error bars represent mean ± SD from three donors (Unpaired, two-tailed t-test). **j** CD4+ T cells from healthy donors were treated with DMSO (Mock), RK-33, FH1321 or PMA-Ionomycin and the % of cells expressing the T-cell activation marker CD25 by flow cytometry. Error bars represent mean ± SD from independent experiments from 5 different donors (Paired, two-tailed t-test). Percentage of IL- 2 **k** and IFNγ **l** producing cells in unstimulated and stimulated primary CD4+ lymphocytes after treatment with RK-33 and FH-1321. Error bars represent mean ± SD from three donors.

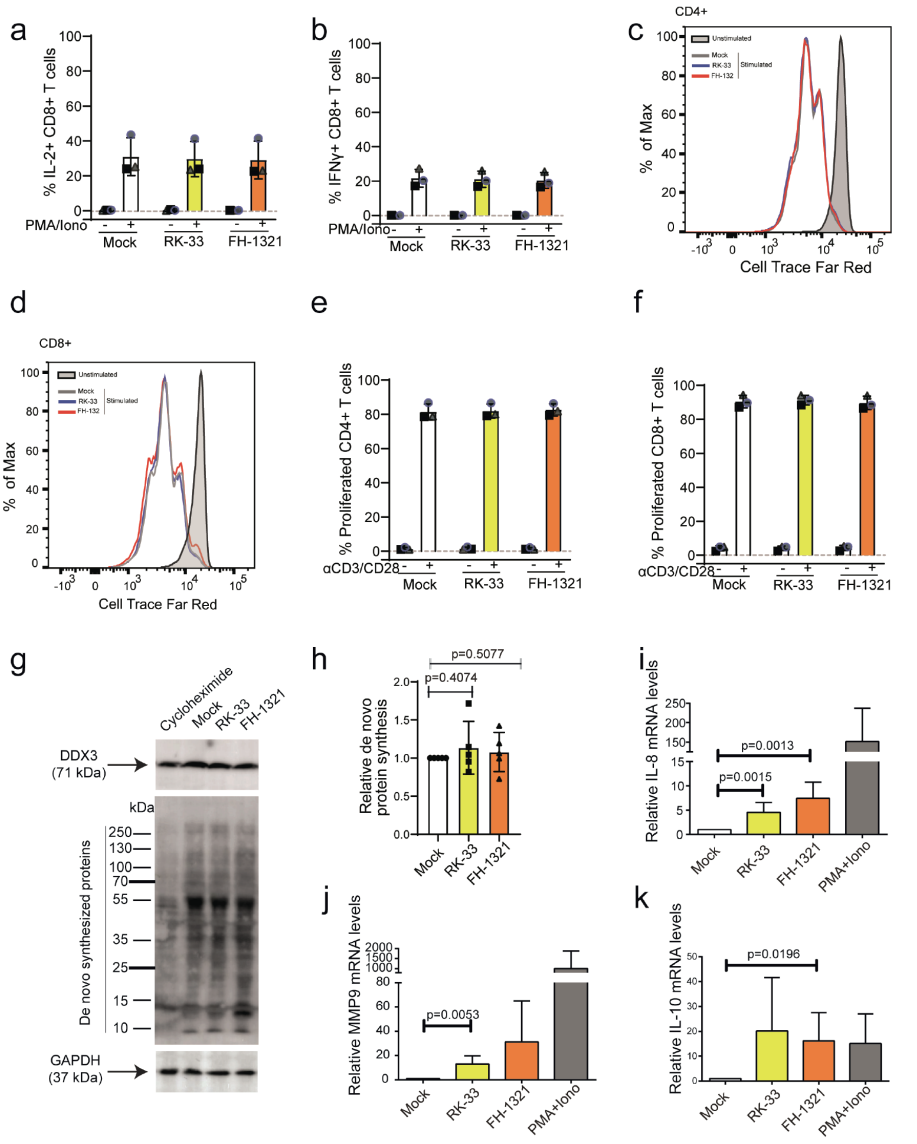

Fig. S4. DDX3 inhibition has negligible effects on uninfected CD4+ T cells Percentage of IL-2 **a** and IFNγ **b** producing CD8+ T cells after treatment with RK-33 and FH- 1321. Error bars represent mean ± SD from three donors. Representative histogram overlay of proliferative capacity of unstimulated or aCD3/CD28 stimulated **c** CD4+ T cells or **d** CD8+ T cells in the presence or absence DDX3 inhibitors. Percentage of proliferated **e** CD4+ T cells and **f** CD8+ T cells from 3 healthy donors as described in A. Error bars represent mean ± SD from freshly isolated CD4+ T cells from three donors. **g** Representative Western blots depicting DDX3, GAPDH and de novo synthesized proteins in mock, RK-33, FH-1321 and cycloheximide-treated conditions. **h** Quantification of the densitometric analysis of de novo synthesized proteins normalised to loading control GAPDH. Error bars represent mean ± SD from three donors (Unpaired, two-tailed t-test). Relative mRNA expression levels of **i** IL-8, **j** MMP9 and **k** IL-10 from cells treated as in (a) were quantified by RT-qPCR. Error bars represent mean ± SD from independent experiments from at 5 different donors (Unpaired, two- tailed t-test).

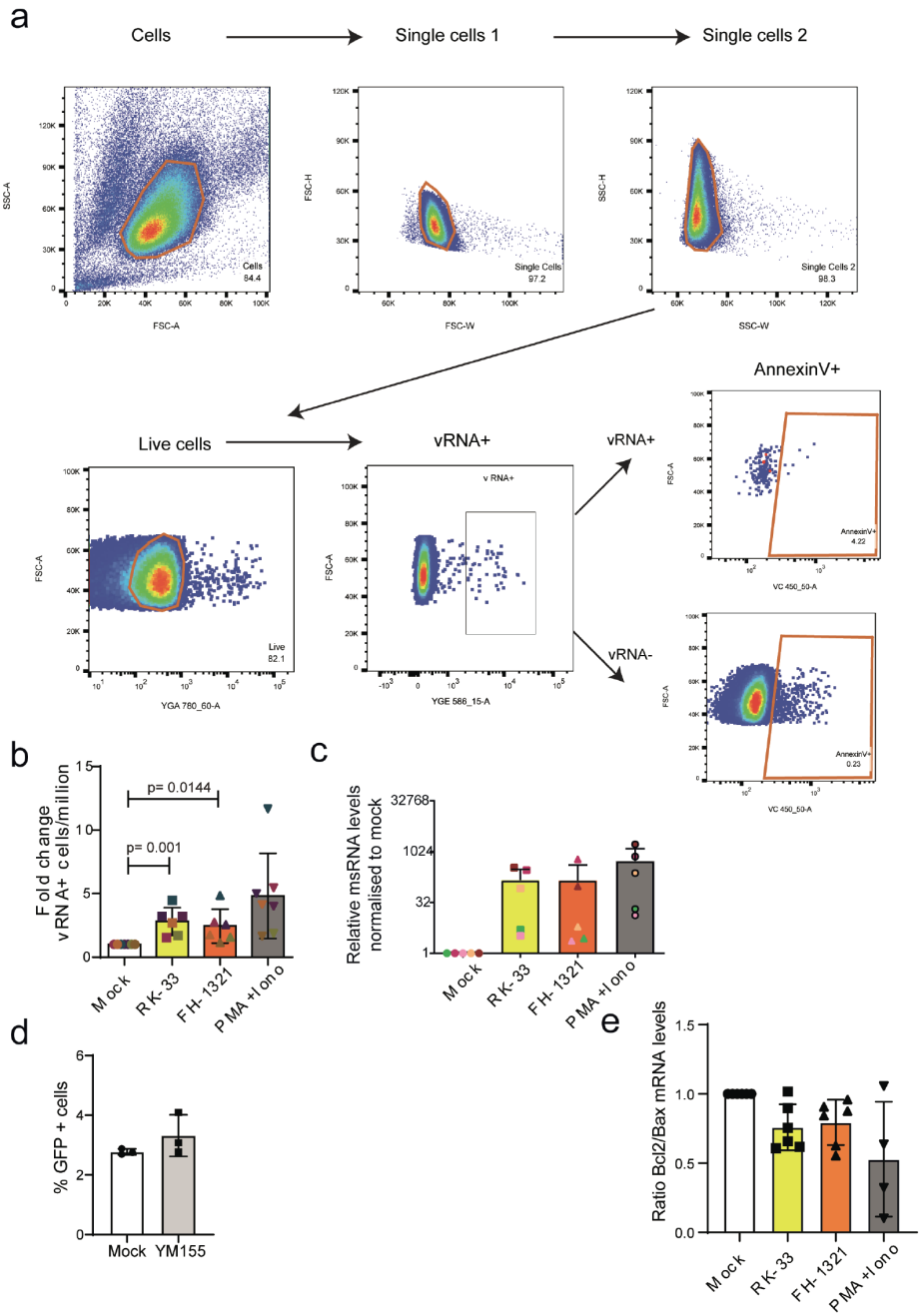

Fig. S5. DDX3 inhibitors in an in vitro model of HIV-1 latency a Gating strategy of FISH-Flow analysis from in vitro-infected CD4+ T cells. Each gate is labelled with a name and % of parent gate. This gating strategy is used for graphs depicted in Fig. 4c, 4f, 4g, 5c, 5d and 6c. **b** The fold change of

number of vRNA-expressing cells per million normalised to the Mock-treated condition as depicted in Fig 4c were quantified. Error bars represent mean ± SD from independent experiments from six - seven different donors, with a minimum of 100,000 events acquired for each condition (Unpaired, two-tailed t-test). **c** CD4+ T cells from healthy donors were infected in vitro and treated with DMSO (Mock), RK- 33, FH1321 or PMA-Ionomycin. The relative expression of multiply-spliced viral RNA (msRNA) was quantified by RT-qPCR. Error bars represent mean ± SD from independent experiments from 5 different donors. **d** Treatment of J-Lat 11.1 cells with YM155 does not induce latency reversal as measured by % GFP + cells by flow cytometry from 3 independent experiments. **e** CD4+ T cells from healthy donors were infected in vitro and treated with DMSO (Mock), RK-33, FH1321 or PMA-Ionomycin. The relative expression of ratios of Bcl2 and Bax mRNA expression were quantified by RT-qPCR. Error bars represent mean ± SD from independent experiments from 5 different donors.

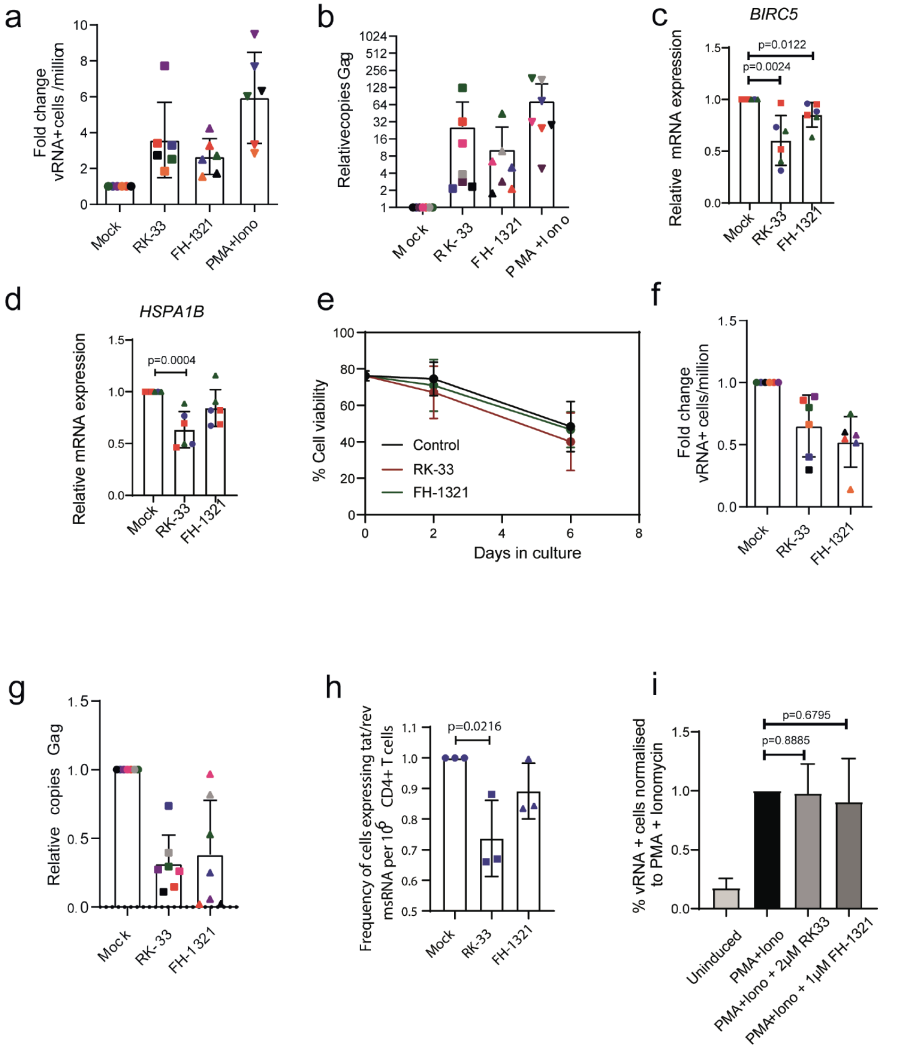

Fig. S6. DDX3 inhibitors in CD4+ T cells from PLWHIV a CD4+ T cells isolated from HIV-1-infected donors were treated with DMSO (Unstimulated), PMA/Ionomycin, and the DDX3 inhibitors RK-33 and FH1321. For all graphs, different donors are represented by an individual colour consistently. The fold change of number of vRNA- expressing cells per million normalised to the Mock-treated

condition as depicted in Fig 5c were quantified. Error bars represent mean ± SD from independent experiments from 6 different donors in duplicate, with a minimum of 100,000 events acquired for each condition. **b** Copies vRNA/µg total RNA 18 hours post treatments for each condition was quantified by RT-qPCR and normalised to Mock-treated condition. Error bars represent mean ± SD from independent experiments from 7 different donors. Relative mRNA expressions of **c** BIRC5 and **d** HSPA1B was quantified by RT-qPCR. Error bars represent mean ± SD from independent experiments from three donors in duplicate (Unpaired, two-tailed t-test). **e** % live cells (cell viability) of CD4+ T cells treated with 2 µM RK-33 or 1 µM FH-1321 for up to 5 days. Error bars represent mean ± SD from CD4+ T cells isolated from freeze-thawed PBMCs from three PLWHIV donors. **f** The fold change of number of vRNA-expressing cells per million normalised to the mock-treated condition as depicted in Fig 6c were quantified. Error bars represent mean ± SD from independent experiments from 6 different donors in duplicate, with a minimum of 100,000 events acquired for each condition (Unpaired, two-tailed t-test). **g** Copies vRNA/µg total RNA 6 days post treatment post treatments for each condition was quantified by RT-qPCR and normalised to mock-treated condition. Error bars represent mean ± SD from independent experiments from 7 different donors. **h** Fold change of the frequency of MS RNA+ cells as measured by TILDA upon treatment with RK-33 and FH-1321 ,normalised to the Mock-treated cells. Error bars represent mean ± SD of three independent experiments from one donor (Unpaired, two-tailed t-test). **i** In vitro HIV-1-infected CD4+ T cells were left uninduced or reactivated with PMA/Ionomycin with or without RK-33 and FH- 1321. % vRNA expression normalised to PMA-Ionomycin condition are depicted. Error bars represent mean ± SD from independent experiments from 3 different donors (Unpaired, two- tailed t-test).

Table S1. List of primers used in this study

Target gene:	Forward:	Reverse:
GFP	5′-GAAGCAGCACGACTTCTTCAA-3′	5′-GCTTGTCGGCCATGATATAGA-3′
vRNA	5′-GGTTTATTACAGGGACAGCAGAGA-3′	5′-ACCTGCCATCTGTTTTCCATA-3′
MMP9	5′-TGGTCCTGGTGCTCCTGGTG-3′	5′-GCTGCCTGTCGGTGAGATTGG-3′
BCL2	5′-GGTGGGGTCATGTGTGTGG -3′	5′-CGGTTCAGGTACTCAGTCATCC-3′
Bax	5′-CCCGAGAGGTCTTTTTCCGAG -3′	5′-CCAGCCCATGATGGTTCTGAT -3′
IL10	5′-CATCGATTTCTTCCCTGTGAA-3′	5′-TCTTGGAGCTTATTAAAGGCATTC-3′
GAPDH	5′-CAAGAAGGTGGTGAAGCAG-3′	5′-GCCAAATTCGTTGTCATACC-3′
RIG-I	5′-CCAAGCCAAAGCAGTTTTCAAG -3′	5′-CATGGATTCCCCAGTCATGG-3′
MAVS	5′-TGATTTCCTCGCAATCAGACG -3′	5′-GAAGCCGATTTCCAGCTGTATG-3′
BIRC5	5′-CAAGGACCACCGCATCTCTAC-3′	5′-AGTCTGGCTCGTTCTCAGTGG-3′
HSPA1B	5′-ACCTTCGACGTGTCCATCCTGA -3′	5′-TCCTCCACGAAGTGGTTCACCA -3′
IL8	5′-CTCTCTTGGCAGCCTTCC -3′	5′-TCCACTCTCAATCACTCTCAG-3′
Cyclophilin A	5′-TCATCTGCACTGCCAAGACTG-3′	5′-CATGCCTTCTTTCACTTTGCC-3′
DDX3X	5′-GGAGGAAGTACAGCCAGCAAAG-3′	5′-CTGCCAATGCCATCGTAATCACTC-3′
MS RNA	5′-GACTCATCAAGTTTCTCTATC AAA-3′	5′-AGTCTCTCAAGCGGTGGT-3′

CHAPTER 4

Analytical treatment interruption: detection of an increase in the latent, inducible HIV-1 reservoir more than a decade after viral resuppression

C. Lungu*, T. Hossain, H. A. B. Prins, K. S. Hensely, R. Crespo, C. Rokx, S. Rao, J. J.A. van Kampen, D. A.M.C. van de Vijver, T. Mesplède, P. D. Katsikis, Y. M. Mueller, R. A. Gruters, T. Mahmoudi*

* Corresponding author

Submitted

medRxiv 2023.11.14.23298452; doi: *https://doi.org/10.1101/2023.11.14.23298452*

ABSTRACT

Analytical treatment interruption (ATI) studies are increasingly being performed to evaluate the efficacy of putative strategies towards HIV-1 reservoir elimination or antiretroviral therapy (ART)-free viral control. A limited number of studies have evaluated the impact of ATI on the HIV-1 reservoir in individuals on suppressive ART. Available data suggests that ATIs have transient impact on the HIV-1 reservoir, mostly measured by levels of total or integrated HIV-1 DNA, in peripheral blood cells prior to ATI and shortly after ART-mediated viral re-suppression. The long-term impact of intervention ATI studies on the latent, inducible HIV-1 reservoir remains uncertain. We report the first clinical study demonstrating an increase in the latent, inducible HIV-1 reservoir, measured by expression of tat/rev multiply spliced RNA, in nine individuals, despite more than a decade of re-suppressive ART, after undergoing an immune intervention ATI conducted in 2006-2009. Our findings challenge the status quo on ATI risk of viral reservoir reseeding and the long-term outcomes thereof.

INTRODUCTION

A reservoir of immune cells harboring replication-competent HIV-1, established early during infection (within 3 to 6 days) [1], persists in the body despite suppressive antiretroviral therapy (ART) and presents a major hurdle to developing a cure for HIV-1 infection. Although raising several debatable ethical concerns [2-4], analytical treatment interruption (ATI) studies are increasingly being used to assess the efficacy of novel therapeutic strategies designed to target the viral reservoir and/or control HIV-1 in absence of ART [5-7]. Findings from past and recent studies indicate that HIV-1 viremia during ATI may be associated with long-term adverse clinical events, clearly warranting vigilant follow-up of ATI study participants [8-10]. One particular area of concern is the heightened risk of HIV-1 reservoir reseeding during ATI. Recent studies have reported viral reservoir diversity and dynamics shortly after ATI upon intervention, during ATI, but not after viral re-suppression [11-15]. A few studies have assessed the impact of ATI on the viral reservoir, mostly at the level of total or integrated HIV-1 DNA, and after only a limited time following ART-mediated re-suppression (ranging from 3 months to two years) [16-20], which provide insufficient insight with regards to the long-term outcomes of ATI on the stable, persistent viral reservoir. Here we examined the long-term impact of an intervention ATI by assessing different molecular compartments of the HIV-1 reservoir using peripheral blood samples, collected 15 years apart, from nine individuals who participated in an autologous dendritic cell (DC)-based immunotherapy ATI trial followed by more than 10 years of ART resuppression.

RESULTS

Cohort description

Between April 8, 2021 and June 6, 2021, we recruited nine chronically treated individuals with HIV-1 subtype B who interrupted ART during a non-randomized, phase I/IIa autologous DC-based immunotherapy trial conducted in 2006 (International Clinical Trial Registry Platform: Netherlands trial registry No. NTR2198) [21] (Fig. 1a**,** Extended Data Table 1). All participants were stably suppressed with undetectable plasma HIV RNA (<50 HIV-1 RNA copies/mL) for a median of 4.8 (IQR: 4.6-5) years, with CD4+ T cell counts >500 prior to enrollment into the trial. Although the DC vaccine was shown to be safe and well-tolerated [21], the elicited immune responses were not sufficient to control viral replication off ART as all participants experienced viral rebound (>1000 HIV-1 RNA copies/mL) within two to eight weeks after ATI [21].

The participants included in this study remained off ART for a median duration of 50 weeks (interquartile range (IQR): 28.5 - 96), with prolonged viremia, until

resuming ART (Fig. 1b), which was in accordance with protocol-defined criteria based on CD4+ T-cell count or necessity of re-treatment according to earlier guidelines [21]. From a retrospective analysis of routine clinical data, we observed that all participants achieved viral re-suppression (plasma HIV-RNA <50 copies/mL) within 18 months after resuming ART. Plasma antiretroviral drug levels measured one month after resuming ART were within therapeutic range. Approximately two years after resuming ART, while CD4+ T cell counts had increased to levels that were comparable to baseline, the CD4/CD8 ratio was significantly lower relative to baseline (pre vaccination, T0) (Extended Data Fig. 1). However, at enrollment into the current study, the participants had been virally suppressed for >10 years and the mean CD4+ T cell counts and CD4/CD8 ratio were comparable to baseline levels before vaccination and ATI (T0) (Extended Data Fig. 1). Viral blips (50-400 HIV-1 RNA copies/mL) after viral re-suppression were detected in three participants with no clear clinical explanation (see note, Extended Data Table 1). There was no indication of ART failure, non-adherence, or potential reservoir-targeting medication administered over the years post ATI.

Transient changes in HIV-1 DNA during ATI

We assessed HIV-1 persistence at different molecular levels using peripheral blood samples collected at various time points during the DC-TRN trial phase; Baseline (T0, prior to DC vaccination); Pre ATI (T1, one week after the 2nd DC vaccination; and T2, one week after the 4th DC vaccination); Early ATI (T3, four weeks after ATI start); Late ATI (T4, >24 weeks after ATI start, the last time point before restart ART); and recently collected samples Post ATI (T6, >10 years on stable ART) (Fig. 1a). Firstly, we used the intact proviral DNA assay (IPDA) [22], to analyze the dynamics of intact and defective proviral DNA in response to vaccination and ATI. The DC vaccination did not lead to significant changes in the levels of total proviral DNA per 1 x 10^6 CD4+ T cells (T2 relative to T0) (Fig. 1c). Before ATI (T0 to T2), the proportions of intact proviral DNA increased in two participants, and decreased in four participants (Extended Data Fig. 2). Given this apparent variation at T2 we assessed the relationship between intact proviral DNA and time to viral rebound (TVR) to >1000 c/mL. The levels and proportion of intact proviral DNA at T0 trended negatively with TVR, although not significant, given the small numbers and low frequency of intact HIV DNA. Total HIV DNA strongly associated with TVR (r =-0.94, P=0.017) (Extended Data Fig. 3a-c). In contrast, one week after the last vaccination (T2), the proportion of intact proviral DNA trended significantly with TVR (r =-0.8264, P=0.0158) (Extended Data Fig. 3d-f).

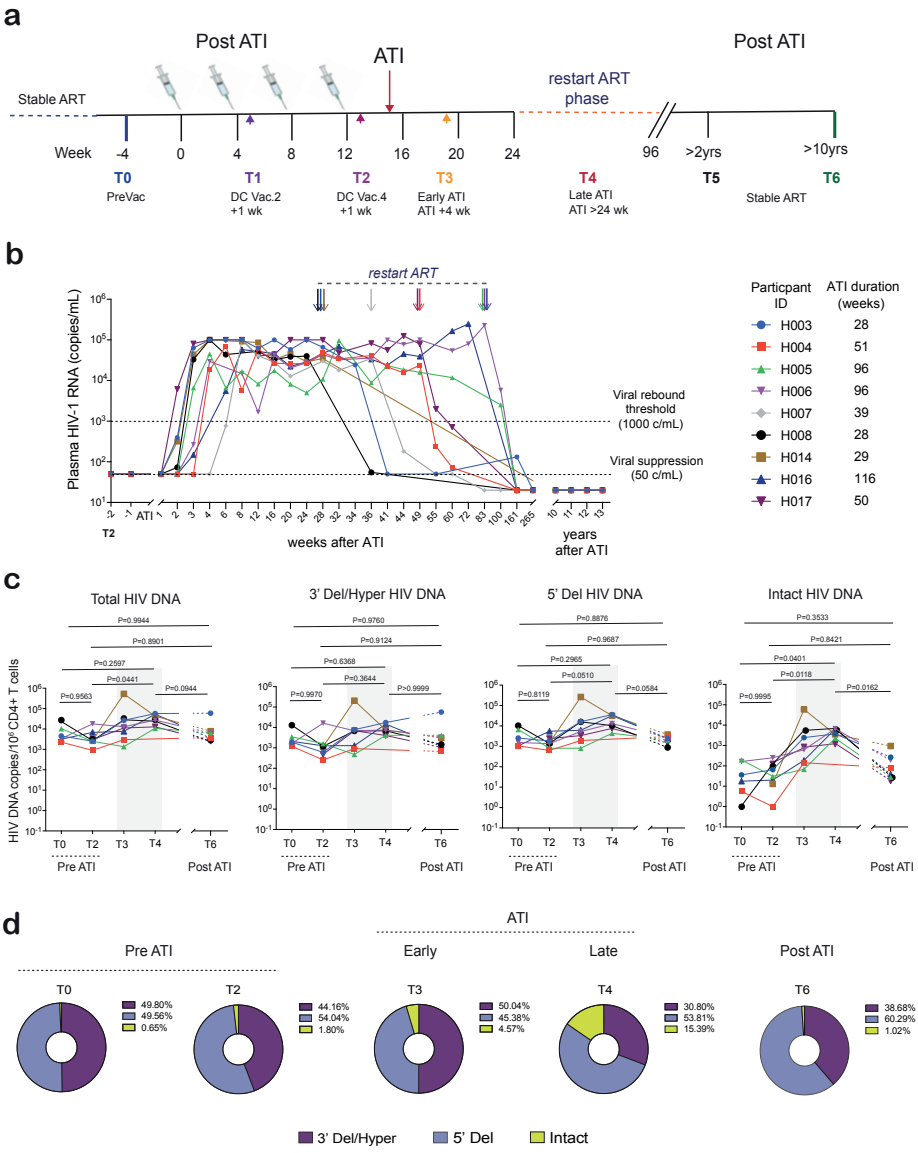

Fig. 1. Longitudinal Plasma HIV-1 RNA and proviral reservoir dynamics. **a**) Schematic overview of the longitudinal study phase during the DCTRN vaccination trial, ATI (pre-Vac to 96 weeks) and after 13 years on suppressive ART. The study timepoints (T0-T4) are indicated using colored upward arrows. Analytical ART interruption (ATI) is shown with a red downward arrow. The period during participants restarted ART is indicated using a dotted horizontal line. After the DCTRN trial, participants were not followed up. T5 is during a routine care visit, and no samples were available for reservoir analyses. T6 is 13 years after resuming ART, participants were included in a follow-up study for a single leukaphereses procedure. **b)** Longitudinal plasma HIV-1 RNA kinetics after ATI. The downward colored arrows mark the time of restart ART. **c)** Changes in levels of total, intact and defective proviral DNA in peripheral CD4+ T cells in response to DC vaccination, ATI and ART

(resuppression) (the shaded bars depict the ATI phase). Mixed effects model analyses and Tukey's multiple comparison test were used to compare viral reservoir frequencies across timepoints (Adjusted P values are shown). **d**) Change in proportions of intact to defective HIV-1 DNA.

During ATI, as expected, the levels of intact proviral DNA increased (T3 and T4), concomitant with rebounding plasma viremia (Fig.1c and d, Extended Data Fig. 2). At T6, after >10 years of suppressive ART, the levels of total, defective (3' Del/ Hypermutated or 5' Del), and intact proviral DNA were overall comparable to pre-ATI (T0, pre vaccination) and/or T2 (post vaccination) (Fig. 1c and d). Although, comparing T2 and T6, there was a clear upward trend in the levels and proportion of intact proviral DNA in four participants (Fig. 1c and Extended Data Fig. 2).

The frequency of gagpol viral RNA+ cells after a decade of re-suppressive ART is comparable to Pre-ATI

Intact proviral DNA assessment by IPDA does not indicate the capacity of proviruses to transcribe HIV-1 RNA. Therefore, we used a single cell approach, fluorescent in-situ hybridization coupled with flow cytometry (FISH-flow) [23], to determine the frequency of CD4+ T cells expressing unspliced HIV-1 *gagpol* viral RNA (vRNA) after *ex vivo* treatment with PMA/ionomycin. Due to the limited availability of clinical samples at T0, we were unable to assess the transcription-competent viral reservoir before vaccination. However, the frequency of *gagpol* vRNA+ cells per 1 x 10^6 CD4+ T cells did not differ significantly between the timepoints T1 (median 17.85, IQR: 12.84 - 62.60) and T2 (median 24.11, IQR: 12.05 - 51.34). In fact, the stability of this viral reservoir compartment was remarkable, with the frequency of *gagpol* vRNA+ cells before ATI comparable to T6, >10 years post ATI, on stable ART (median 17.6, IQR 12.32 – 43.62) (Fig. 2a). As viral translation inhibition has also been implicated to contribute to viral persistence [24,25], we assessed the frequency of cells simultaneously expressing *gagpol* vRNA and Gag p24+ protein (herein referred to as the translation-competent viral reservoir). Across all time points, the frequency of translation-competent reservoir cells was low to below detection limit, consistent with values reported in literature [23,25]. Despite this, the trends in the dynamics of the Gag protein translation-competent reservoir were similar to that of the *gagpol* transcription-competent reservoir (Fig. 2b).

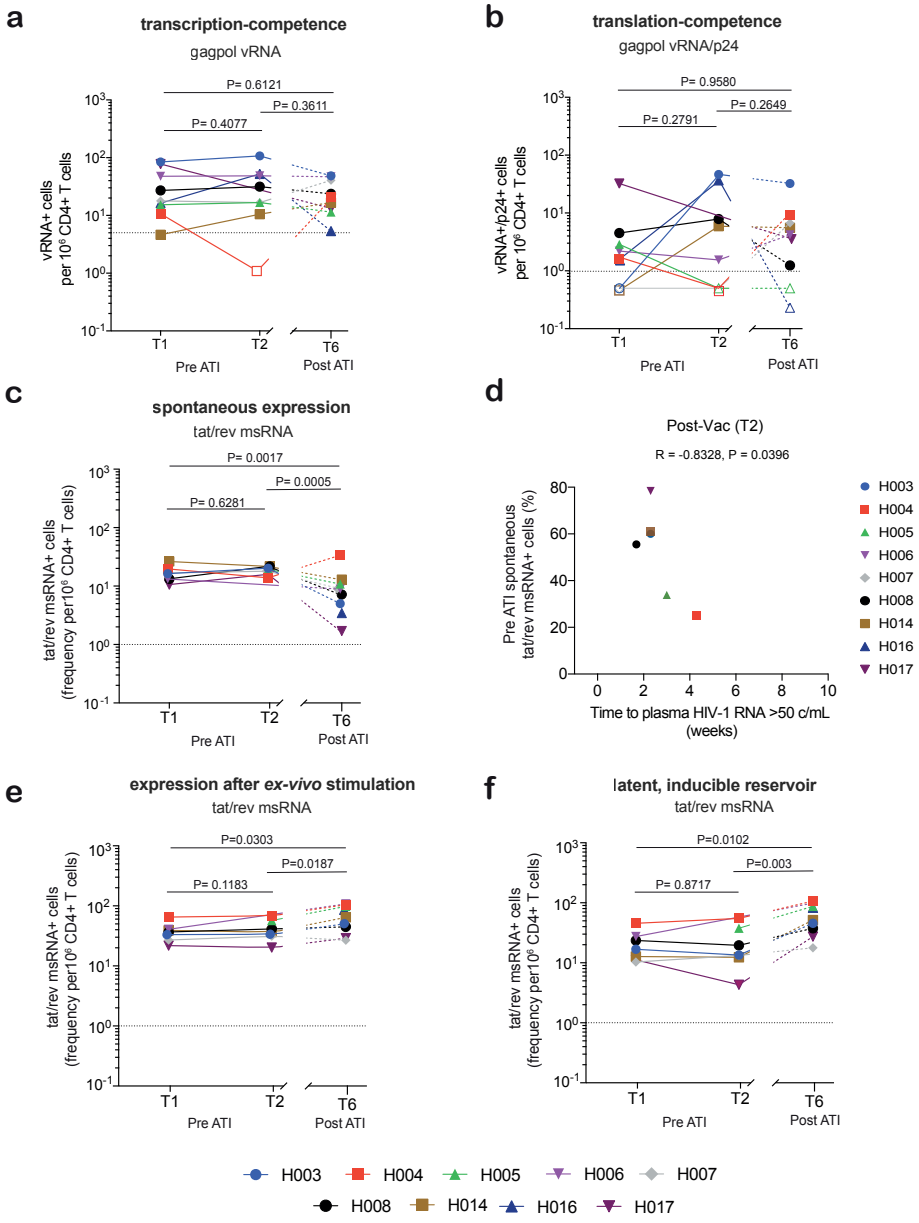

Fig. 2. Inducible viral reservoir dynamics after ATI and long-term ART. **a**) Change in reservoir cells expressing unspliced gagpol viral RNA after ex vivo treatment with PMA/ionomycin for 18 hours. **b**) Change in translation-competent reservoir (co-expressing gagpol vRNA and Gag p24 protein). Open symbols depict frequencies below the assay limit of detection (dotted line). **c**) Change in reservoir cells spontaneously expressing tat/rev msRNA (in vivo response). **d**) Pearson correlation between cells spontaneously expressing tat/rev msRNA before ATI and time to detectible plasma HIV-1 RNA

to >50 copies/mL. **e**) Change in reservoir cells expressing tat/rev msRNA after ex vivo treatment with PMA/ionomycin for 12 hours. **f)** Change in reservoir cells inducibly expressing tat/rev msRNA after ex vivo treatment with PMA/ionomycin for 12 hours (i.e., Difference between cells with spontaneous tat/rev msRNA expression and after stimulation). Mixed effects model analyses and Tukey's multiple comparison test were used to compare viral reservoir frequencies across timepoints. Adjusted P values are shown.

Sustained increase in the frequency of cells expressing multiply spliced RNA

Our group has recently developed a viral reservoir assay termed SQuHIVLa; Specific Quantification of inducible HIV-1 reservoir by LAMP, which leverages reverse transcription loop-mediated isothermal amplification (RT-LAMP) performed in a single reaction, to exclusively detect *tat/rev* multiply spliced (ms)RNA[26]. The frequency of CD4+ T cells expressing *tat/rev* msRNA, which in part reflects viral expression from intact viruses, is more likely to reflect virion production than unspliced *gagpol* vRNA and may therefore serve as a biomarker of the replication-competent viral reservoir [27]. Using SQuHIVLa we found that the median frequency of CD4+ T cells spontaneously expressing *tat/rev* msRNA at T1 (median 16.32, IQR: 13.23 -19.66) was comparable to T2 (median 19.31, IQR: 15.89 - 21.71. However, the significantly lower frequencies observed in 8/9 participants at T6, on stable ART (median 8.01, IQR: 3.84 -10.38) (Fig. 2c), suggests that more cells were spontaneously expressing *tat/rev* msRNA during the vaccination phase, possibly due to immune activation. The median frequency of CD4+ T cells spontaneously expressing *tat/rev* msRNA after DC vaccination trended negatively with time to detectable plasma HIV-1 RNA >50 copies/mL (Fig. 2d) and TVR to >1000 copies/mL (Extended Data Fig. 4a), the latter not statistically significant given the small sample size and limited variation in TVR to >1000 copies/mL, which was based on weekly plasma HIV-1 RNA measurements. After *ex vivo* treatment with PMA/ionomycin, we observed an increase in the total frequency of CD4+ T cells expressing tat/rev msRNA between the Pre ATI (T1 and T2) and Post ATI (T6) timepoints (Fig. 2e). Similar results were obtained using a 1-step *tat/rev* induced limiting dilution assay (1-step TILDA), as an alternative method to quantify cells expressing *tat/rev* msRNA, and the two assays positively correlate (Extended Data Fig. 4 b, c). Next, we assessed the frequency of cells that could be induced to express *tat/rev* msRNA after PMA/ionomycin treatment (i.e., the difference between the frequency of cells expressing *tat/rev* msRNA spontaneously and after *ex-vivo* stimulation, hereafter referred to as the latent, inducible viral reservoir). Markedly, this viral reservoir compartment was significantly higher at T6 relative to T1 and T2 (P=0.0102 and P=0.0030, respectively) (Fig. 2f), indicating an expansion of this viral reservoir compartment.

DISCUSSION

This study provides clear insights, which invite pause and further consideration for future combination ATI trials towards HIV-1 cure; which measures of persistent HIV-1 reservoirs are clinically meaningful and what virologic assays are most appropriate to guide and assess ATI risk? It is plausible that the DC vaccination induced latency reversal *in vivo*, determined by levels of spontaneous *tat/rev* msRNA expression, which significantly trended with time to viral rebound. This finding further confirms *tat/rev* msRNA expression as an attractive biomarker to incorporate into HIV-1 cure-focused trials. Earlier studies by Fischer et al. similarly demonstrated *tat/rev* msRNA expression concomitantly occurring with the re-emergence of PBMC-associated HIV-1 particles (cellular viral rebound) after two weeks of structured ART interruption, which was predicted by during-therapy levels of *nef* msRNA transcripts in PBMCs [28]. More recently, De Scheerder et al., showed an increase in *tat/rev* RNA transcripts, amongst elevated expression of restriction factors (SLFN11 and APOBEC3G), after ATI prior to viral rebound, indicating the use of these restriction factors and *tat/rev* RNA as potential biomarkers for imminent viral rebound [16]. Importantly, despite the fact that the participants in this study underwent unconventionally long ATI with less stringent monitoring and ART restart criteria, we report no significant impact on the HIV-1 reservoir at the level of proviral DNA and *gagpol* viral RNA expression, consistent with reports from several recent, well monitored, short-term ATI interventions [16-19,29-32]. After more than a decade of suppressive ART post ATI, defective and intact proviral DNA were overall comparable to baseline prior to ATI, although, a clear upward trend in the levels and proportion of intact proviral DNA was observed in four/nine participants. Cell associated HIV-1 *gagpol* vRNA expression at single cell level was remarkably stable across time points pre and post ATI, whereas the translation-competent viral reservoir, defined by *gagpol* viral RNA and Gag p24 protein co-expression, was more dynamic. Collectively, the available data, including ours, suggest that viral reservoir expansion during ATI is transient and supports the notion that sustained viral reservoir increase after ATI is not a concern, at least at the level of proviral DNA and cellular reservoirs expressing *gagpol* viral RNA. However, we also demonstrate a significant increase in the frequency of cells inducibly expressing *tat/rev* msRNA in all nine study participants, which challenges the status quo and demands further attention.

To explain our findings, we consider several factors. Indeed, the DC vaccination induced enhanced immune responses, which sustained throughout the ATI phase [33], although not sufficient to control viral replication. Consequently, persistent immune activation during ATI would increase the number of target cells and drive clonal expansion. Moreover, while establishment of the latent reservoir occurs

very early during primary infection[1], the prolonged duration of ATI in this trial, in an ART era where substantial levels of prolonged viremia and CD4 T-cell declines were more acceptable in routine care, could have likely contributed to continuous latent viral reservoir reseeding during untreated HIV-1 infection [34-36]. In addition, the discrepant outcomes on viral expression may be attributed to an altered proviral landscape and/or shifts in the replication-competent viral reservoir. In fact, transcription-competence determined by *gagpol* vRNA expression is shown to be a less proximate surrogate marker for replication-competence compared to *tat/rev* msRNA-expression [27,37] and the two viral markers poorly correlated with each other (Extended Data Fig. 4d and e). Moreover, recent work has demonstrated that defective proviruses can produce defective vRNA and proteins, which do not yield competent virions, but may drive changes in the proviral landscape [38-40]. Notably, the levels of intact HIV DNA at T6 associated more with the frequency of *tat/rev* msRNA+ cells and not with *gagpol* vRNA+ cells (Extended Data Fig. 4f-h). An important limitation of our study is the absence of a control group in the DC-TRN trial. Thus, we cannot definitively exclude increases in the latent, inducible reservoir following a normal clinical course or consequent to aging on suppressive ART. However, studies in individuals on long-term suppressive ART have revealed essentially stable defective proviral levels whereas intact proviral DNA gradually declines in majority of individuals [41,42], although the frequency of cells with inducible *tat/rev* msRNA were not investigated in these studies. We postulate that the inability of cytotoxic T lymphocyte (CTL) clearance together with the existence of intact but transcriptionally silent proviruses and clonal expansion is a plausible explanation for increases in latent, inducible viral reservoir compartment [41], triggered by the intervention ATI that these participants underwent. The clinical significance of this altered viral reservoir compartment and potential implications for future curative strategies warrants further research

To conclude, the discordant findings accentuate the complexity of assessing persistent viral reservoir dynamics in response to novel therapeutic interventions. Future intervention ATI trials should aim to include a comprehensive assessment of viral and immunological compartments before and during ATI, prior to viral rebound, to identify the most relevant biomarkers and gene signatures that are predictive of viral rebound. In this study, the frequency of intact proviral DNA and cells spontaneously expressing *tat/rev* msRNA trended negatively with time to viral rebound. It is important to further assess these parameters in combination with immunological and host gene expression profiles in prospective trials to ultimately guide decisions regarding the safety and risk of future intervention ATI trials. Indeed, the noticeable differences in the outcomes of the latent, inducible viral reservoir compartment warrant the need for vigilant monitoring for possible long-

term reservoir reseeding consequent to an (immune) intervention, viral rebound post ATI, and after ART-mediated viral re-suppression (short and long-term).

MATERIALS AND METHODS

Ethics statement

Participants of the DCTRN trial provided written informed consent prior to inclusion in accordance with the regulations of the institutional Medical Ethics Committee at Erasmus Medical Center, Rotterdam (MEC-2005-227 and MEC-2012-583). The remaining material from the DCTRN trial was stored in a registered biobank, which was approved by the Erasmus Medical Center Medical Ethics Committee (MEC-2022-0060). The HIV biobank is described at https://eheg.nl/en/Our-Projects/HIV-Biobank.

Plasma HIV-1 RNA monitoring

Quantification of plasma HIV-1 RNA was performed on three different platforms available at various longitudinal timepoints during DC-immunotherapy, at treatment interruption and on ART. Between 2002 and 2008, quantification was performed using the Roche Amplicor HIV-1 RNA monitor test (version 1.5) (LOQ 50 copies/mL). After 2009 plasma HIV-1 RNA was quantified using the COBAS TaqMan Assay (Roche); LOQ 20 copies/mL. As of 2021, plasma HIV-1 RNA was quantified using the Aptima HIV-1 Quant Dx assay; LOQ 30 copies/mL.

Clinical sample collection and cell isolations

Cryopreserved PBMCs obtained from large blood draws or leukapheresis material collected from the study participants during the trial phase and post intervention were used for this study. Upon thawing PBMCs, CD4+ T cells were isolated by negative magnetic selection using the EasySep Human CD4+ T cell Enrichment kit (StemCell Technologies) according to the manufacturer's instructions. The isolated CD4+ T cells were either directly used to quantitate HIV-1 DNA/RNA levels or treated with 100 ng/mL phorbol 12-myristate 13-acetate (PMA) and 1 µg/mL ionomycin to enhance viral reactivation.

Intact Proviral DNA Assay (IPDA)

The levels of intact proviral DNA were assessed using lysed extracts of CD4+ T cells. Nucleic acid was isolated from at least 2 x 10^6 CD4+ T cells using the PCI extraction method. Duplex digital PCR (dPCR) was performed on an Absolute Q digital

PCR platform (Thermo Fisher Scientific) using primer and probe sets targeting the packaging signal (Ψ) and Envelope gene (Env), following the manufacturer's instructions and adapted intact proviral DNA assay protocol [22,43,44]. Duplex HIV-1 dPCR reaction mix consisted of 1.8 µL Absolute Q DNA Digital PCR Master Mix 5X (Thermo Fisher Scientific), 1 µL packaging signal (Ψ) target FAM-probe (10x), 1 µL *env* target HEX-probe (10x), 700 ng gDNA, diluted in nuclease-free H_2O to a final reaction volume of 9 µL. The dark competition probe for APOBEC3G hypermutations in the *env* region was omitted in this reaction setup. Measurements of the cellular gene ribonuclease P/MRP subunit p30 (*RPP30*) in a replicate well were used to calculate the frequency of CD4+ T cells. The duplex *RPP30* dPCR was set up similarly using RPP30 primer and probe sets and 7 ng gDNA input. The primer and probe sequences used are provided below.

IPDA primers and probes

	Region	Sequence	Assay
PSI Forward primer	PSI	CAGGACTCGGCTTGCTGAAG	IPDA[22]
PSI Reverse primer	PSI	GCACCCATCTCTCTCCTTCTAGC	IPDA[22]
Psi Probe	PSI	/56-FAM/TTTTGGCGT/ZEN/ACTCACCAGT/3IABkFQ/	IPDA[44]
Env Forward Primer	Env	AGTGGTGCAGAGAGAAAAAAGAGC	IPDA[22]
Env Reverse Primer	Env	GTCTGGCCTGTACCGTCGC	IPDA[22]
Env Probe	Env	/5HEX/CCTTGGGTT/ZEN/CTTGGGA/3IABkFQ/	IPDA[44]

FISH-flow

The frequency of cells expressing *gagpol* viral RNA (vRNA) and p24 protein were assessed using the Primeflow RNA Assay (Thermo Fisher Scientific) following the manufacturer's instructions and as described previously [23,45]. Briefly, CD4+ T cells were isolated from PWHIV donor PBMCs by negative magnetic selection using the EasySep Human CD4+ T cell Enrichment kit (StemCell Technologies) according to the manufacturer's instructions. A minimum of 20 x 10^6 CD4+ T, was resuspended at 1.5 x 10^6 cells/mL in RPMI-1640 medium supplemented with 10% FBS, 100 µg/mL penicillin-streptomycin and Raltegravir (3 µM) and rested for at least 4 hours in a humidified incubator at 37°C and 5 % CO_2. Cells were then treated with 100 ng/mL PMA and 1 µg/mL ionomycin to enhance viral reactivation. Eighteen hours post stimulation, cells were washed, pellets resuspended in PBS, and counted using an automated cell counter (Countess II, Thermo Fisher Scientific). At least 10 x 10^6 cells, with >55% viability, were subjected to the FISH-flow assay. CD4+ T cells were first stained in Fixable Viability dye 780 (Thermo Fisher Scientific) for 20 min at room temperature (1:1000 dPBS) and then fixed and permeablized using regeants from the Primeflow RNA assay kit according to manufacturer's instructions. After

permeabilization, the cells were stained with two p24 antibodies; anti-p24 KC57-FITC (Beckman Coulter, 6604667) and anti-p24 28B7-APC (MediMabs, MM-0289-APC), incubated in the dark for 30 min at room temperature, and an additional 30 minutes at 4 °C. Cells were then washed and resuspended in RNA wash buffer with RNAsin. mRNA was labelled with a set of 40 probe pairs against the GagPol region of vRNA (catalogue number GagPol HIV-1VF10-10884, Thermo Fisher Scientific) diluted 1:5 in the probe diluent provided in the kit. Target mRNA hybridization was carried out for 2 hours at 40°C. Samples were washed to remove excess probes and stored overnight, at 4 °C, in the presence of RNAsin. Signal amplification was then performed by sequential 1.5-hour, 40 °C incubations with the pre-amplification and amplification mix. Amplified mRNA was labelled with fluorescently tagged probes for 1 hour at 40°C. Samples were washed, resuspended in 200-300 µL storage buffer and up to $5x10^6$ cells were acquired on a BD LSR Fortessa Analyser. Gates were set using stimulated, uninfected CD4+ t cells. Data were analyzed using the FlowJo V10 Software (Treestar).

Specific Quantitation of Inducible HIV-1 reservoir by LAMP (SQuHIVLa)

The frequency of cells spontaneously and inducibly expressing *tat/rev* multiply (MS) spliced HIV-1 RNA was assessed using a SQuHIVLa assay according to the protocol described elsewhere [26]. Briefly, 2 - 5 x 10^6 total CD4+T cells were resuspended (1.5 x 10^6 cells/mL) in culture RPMI-1640 medium supplemented with 10% FBS and 100 µg/mL penicillin-streptomycin, and rested for 6 hours in a humidified incubator at 37 °C and 5 % CO_2. After incubation, some cells were left untreated and directly used to determine basal viral RNA expression or treated with 100 ng/mL PMA and 1 µg/mL ionomycin for 12 hours to induce viral reactivation. Cells from either condition were washed twice in RPMI 1640 media with 3% FBS, then resuspended in PBS and counted using an automated cell counter (Countess II, Thermo Fisher Scientific). A minimum of 0.5 x 10^6 CD4+ T cells, with > 50 % viability, after PMA/ionomycin treatment were analyzed per SQuHIVLa assay performed on a CFX96 Touch Real-Time PCR Detection System thermocycler (BioRad) as described elsewhere [26].

One-step Tat/rev Induced Limiting Dilution Assay (TILDA)

The frequency of cells expressing *tat/rev* multiply spliced (ms) HIV-1 RNA was also assessed using a modified TILDA protocol [46] i.e., by direct amplification of *tat/rev* msRNA using a one-step RT-qPCR approach. Briefly, 2 - 5 x 10^6 CD4+ T cells isolated from PWHIV donor PBMCs were rested and treated with PMA/ionomycin as described for the other inducible reservoir assays. A minimum of 0.5 x 10^6 CD4+ T cells, with >50 % viability, after treatment with PMA/ionomycin were analyzed per

assay. CD4+ T cells were added in limiting dilution, ranging from 3 x 10^4 cells - 3 x 10^3 cells (22-24 replicates), to a white 96-well qPCR plate (Biorad) containing 20 µL One-step RT-qPCR reagent mix; 5 µL Luna Probe One-Step RT-qPCR 4X Mix with UDG (No ROX) (New England BioLabs), 0.1 µL *tat* 1.4 forward primer and 0.1 µL rev reverse primer (both at 100 µM), 0.8 µL HIV tat/rev probe (5 µM), and 14 µL nuclease free water to a final reaction volume of 25 µL. The primer and probe sequences used, as published [46]. The qPCR plates were sealed, briefly centrifuged at 600 x g for 1 min, and a CFX96 Touch Real-time PCR instrument (Biorad) was used to run the following thermocycling program; Carry over prevention step at 25°C for 30 seconds, reverse transcription at 55°C for 10 minutes, initial denaturation at 95°C for 3 minutes followed by 50 cycles of denaturation at 95°C for 10 seconds and extension at 60 °C for 1 minute. The amplification curves in all positive wells at each dilution manually inspected after each run and the number of positive wells were used to determine the frequency of cells positive for *tat/rev* msRNA using the maximum likelihood method.

Statistics and reproducibility

Data are presented as median with Inter Quartile Range. Spearman rank correlation coefficients were calculated for non-normally distributed variables. Two-tailed P values were calculated. $P < 0.05$ was considered statistically significant. For the inducible viral reservoir quantification data below the limit of detection, the arbitrary value of 0.5 cells/million were used to plot the data but were not included in statistical analyses. Likely outlier data points were identified using ROUT(Q=10%) and excluded from statistical analyses. Mixed effects model analyses and Tukey's multiple comparison test were used to compare viral reservoir frequencies across timepoints. Adjusted P values were calculated. $P < 0.05$ was considered statistically significant. Biological replicates (that is, samples at longitudinal timepoints) were measured in most experiments except for inducible HIV reservoir quantification given the limited availability or quality of clinical material (particularly baseline samples). Technical replicates (that is, repeated measurements of the same sample) were as follows: for intact proviral DNA quantification by dPCR, at least two technical replicates; for FISH-flow, experiments were not technically replicated given the limited clinical material; for SQuHIVLa and 1-step TILDA, at least two independent experiments were performed where clinical material was sufficient. Prism 9 for Mac (GraphPad Software) was used to generate graphs and to perform all statistical tests.

Data availability

All data needed to evaluate the results and conclusions in this article are provided in the main text, Methods section and Extended data section.

ACKNOWLEDGEMENTS

We express our deepest gratitude to all the study participants for their valuable contribution to the DCTRN trial in 2006-2009 and to the current study, without whom this research would not have been possible. We also thank the internist-infectious disease specialists at Erasmus MC for their assistance in recruiting the study participants. Leukapheresis procedures and sample logistics were greatly supported by Erasmus MC HIV research nurses and clinical laboratory staff. C.L. received funding from the Dutch Aidsfonds (grants P-60602 and P-263); SR received funding from Dutch Aidsfonds (grant P-53302); C.R. received funding from Dutch Aidsfonds (grant P-53601); R.A.G. received funding from Dutch Aidsfonds (grant P-60804) and Horizon Europe (grant 681032);TMa received funding from Health Holland (grants LSHM19100-SGF and EMCLSH19023) and ZonMW (grant 40-44600-98-333) and a Building Synergistic Infrastructure for NL4Cure grant.

AUTHOR CONTRIBUTIONS

Conceptualization, C.L, and T.Ma; Methodology, C.L., T.H. and T.Ma; Investigation, C.L., T.H., H.A.B.P., K.S.H., and R.C; Data Curation and Formal Analysis, C.L. and T.Ma; Data Visualization, C.L. and T.Ma., Project Administration, C.L., H.A.B.P., K.S.H. and T.Ma. Supervision, T.Ma; Material and Funding Acquisition, C.L., S.R., C.R., R.A.G and T.Ma., Writing – Original draft, C.L.; Writing – Review and Editing, C.L., T.H., H.A.B.P., K.S.H., R.C., C.R., S.R., J.J.A.vK., D.A.M.C.V., T.M., P.D.K., Y.M.M., R.A.G., and T.Ma.

EXTENDED DATA

Table 1 Participant Clinical characteristics

	Median	IQR	Range
Gender	Male (100%)		
Age at DC Vaccination (T0)	45	41.5 - 53	37 - 56
Age on stable ART post intervention (T6)	60	56.5 - 68	52 - 71
Year of HIV Diagnosis	1997	1994 -1999	1988 -2000
Time between HIV diagnosis and ART initiation (weeks)	32	18.5 - 198.0	2 - 442
Time on ART before vaccination (years)	9.9	7.0 -10.85	3.7 - 11.9
Time undetectable on ART before DC vaccination (years)	4.8	4.6 - 5.0	2.8 - 5.3
Peak plasma HIV RNA pre-ART (log10 c/mL)	5.01	4.86 -5.12	4.73 - 5.31
Nadir CD4 count	230	155 - 5.12	70 - 290
CD4 count pre-ART initiation	370	325 - 435	300 - 650
CD8 count pre-ART initiation	1850	1360 - 2370	1120 - 2890
CD4/CD8 ratio pre-ART initiation	0.24	0.14 - 0.33	0.12 - 0.38
CD4 count before DC vaccination (T0)	650	575 - 715	510 - 940
CD8 count before DC vaccination (T0)	610	470 - 835	400 - 970
CD4/CD8 ratio baseline (T0)	1.21	0.73 - 1.39	0.53 - 1.48
Analytical ART interruption			
Time to viral rebound >50 c/mL (weeks)	3.0	2.3 - 3.65	2.0 - 6.3
Time to viral rebound >500 c/mL (weeks)	3.3	2.65 - 5.15	2.0 - 6.3
Time to viral rebound >1000 c/mL (weeks)	3.3	2.65 - 5.15	2.0 - 8.3
Time to viral rebound >50000 c/mL (weeks)	6.3	3.15 -20.15	2.0 - 40.0
Lowest CD4 count	250	175 - 285	150 - 290
Peak CD8 count	1370	1195 - 2040	1060 - 4400
last CD4 count before ART resumption (T4)	250	180 - 300	150 - 350
Last CD8 count before ART resumption (T4)	820	685 - 1090	580 - 1650
CD4/CD8 ratio before ART resumption (T4)	0.25	0.20 - 0.39	0.17 - 0.43
Weeks off ART	50	28.5 - 96.0	28 - 116
ART resumption			
Time to viral resupression <50 c/mL (months)	8.5	4.0 - 16.0	3.0 - 18.0
Time on ART post resumption, early (years); T5	2.3	2.2 - 3.2	2.0 - 3.2
CD4 count (T5)	620	525 - 663	490 - 710
CD8 count (T5)	975	617.5 - 1098	520 - 1510
CD4/CD8 ratio (T5)	0.65	0.62 - 0.92	0.38 - 1.0
Time on ART post resumption, late (years); T6	12.4	11.9 - 13.05	11. - 13.3
Time on ART undetectable (years); T6	10.5	7.8 - 11.5	6.2 - 12.9
CD4 count (T6)	590	490 - 780	430 - 800
CD8 count (T6)	650	520 - 770	460 - 2240
CD4/CD8 ratio (T6)	1.02	0.67 - 1.20	0.30 - 1.42

Note: Three participants with viral blips (50-400 c/mL) since viral re-suppression. **H003** – 255 c/mL (Oct 2009), 132 c/mL (April 2010), 59 c/mL (Jan 2014); **H006** (slow to suppress after restarting ART) – 57 c/mL and 228 c/mL (Nov 2013); **H008** (slow to suppress after restarting ART); **H017** – 71 c/mL (Jan 2016).

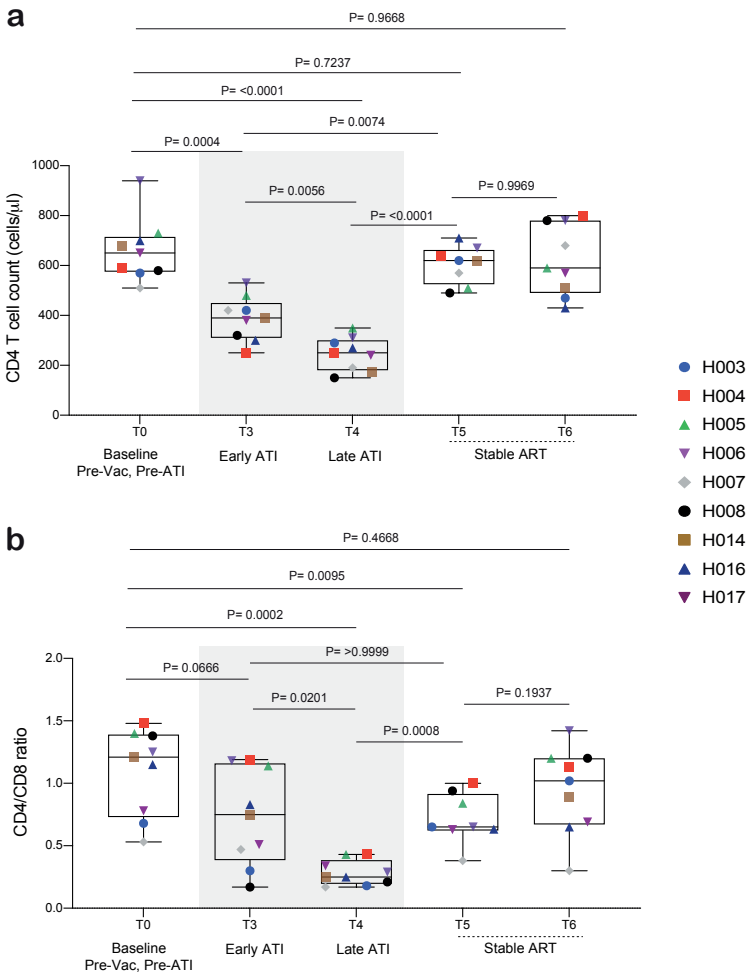

Extended Fig. 1. Longitudinal T cell counts before, during and after ATI. (**a**) CD4+ T cell counts measured at selected study timepoints (**b**) CD4/CD8 ratio dynamics. Box plots with mean and range are shown. The shaded bars depict the ART interruption phase). Statistics inferred using a mixed effect analysis with multiple comparisons of the means (Tukey-Kramer test). Adjusted P Values are shown above the graphs.

Extended Fig. 2. Longitudinal HIV-1 DNA dynamics. Pie charts of intact and defective HIV-1 DNA (5' Deleted [5'Del] and 3' Deleted/Hypermutated [3'Del/Hyper]) are shown. The proportions of intact and defective DNA are shown as percentages of total HIV DNA copies/million CD4+ T cells. Intact HIV DNA was distinguished from defective HIV DNA using the intact proviral DNA assay (IPDA). N/A = not available.

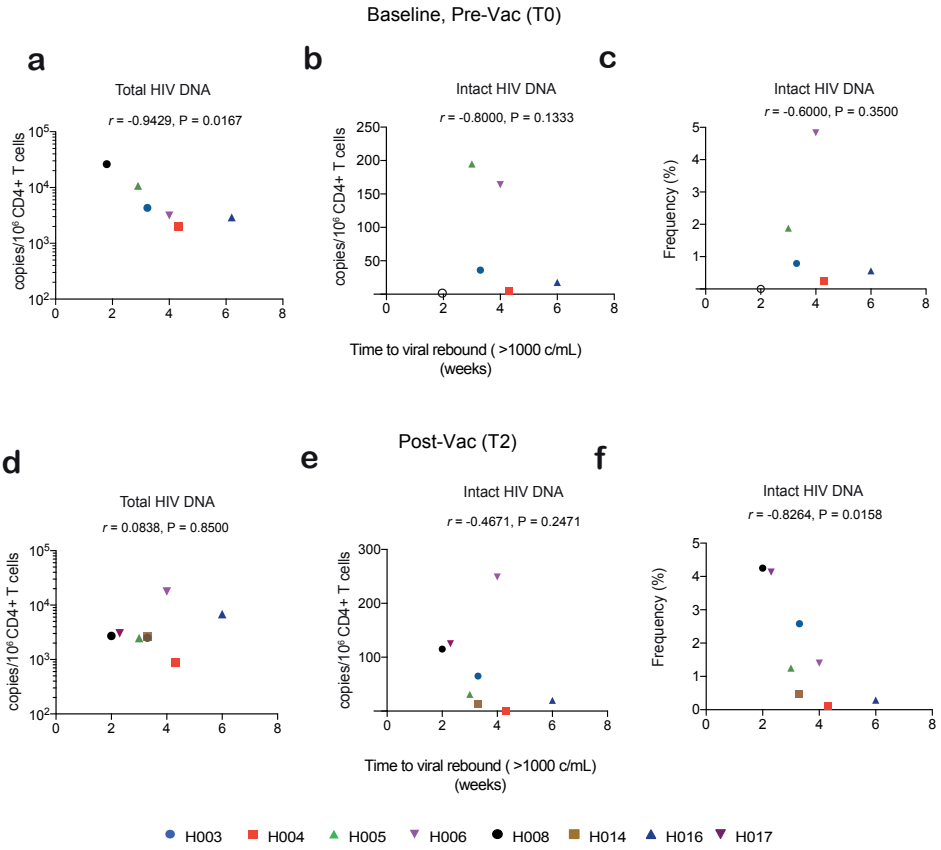

Extended Fig. 3. Relationship between proviral DNA and time to viral rebound. (**a-c**) Relationship with time to viral rebound assessed at timepoint T0, before vaccination. (**c**)The frequency (percentage), of intact cells represents the proportion of intact HIV DNA copies to total HIV DNA copies/million CD4+ T cells. Open symbol represent sample not detected and thus not included in the correlation analyses. (**d-f**) Relationship with time to viral rebound assessed at timepoint T2, one week after the last DC vaccination and ~two weeks prior to ATI. Spearman r correlations and two-tailed P values are shown.

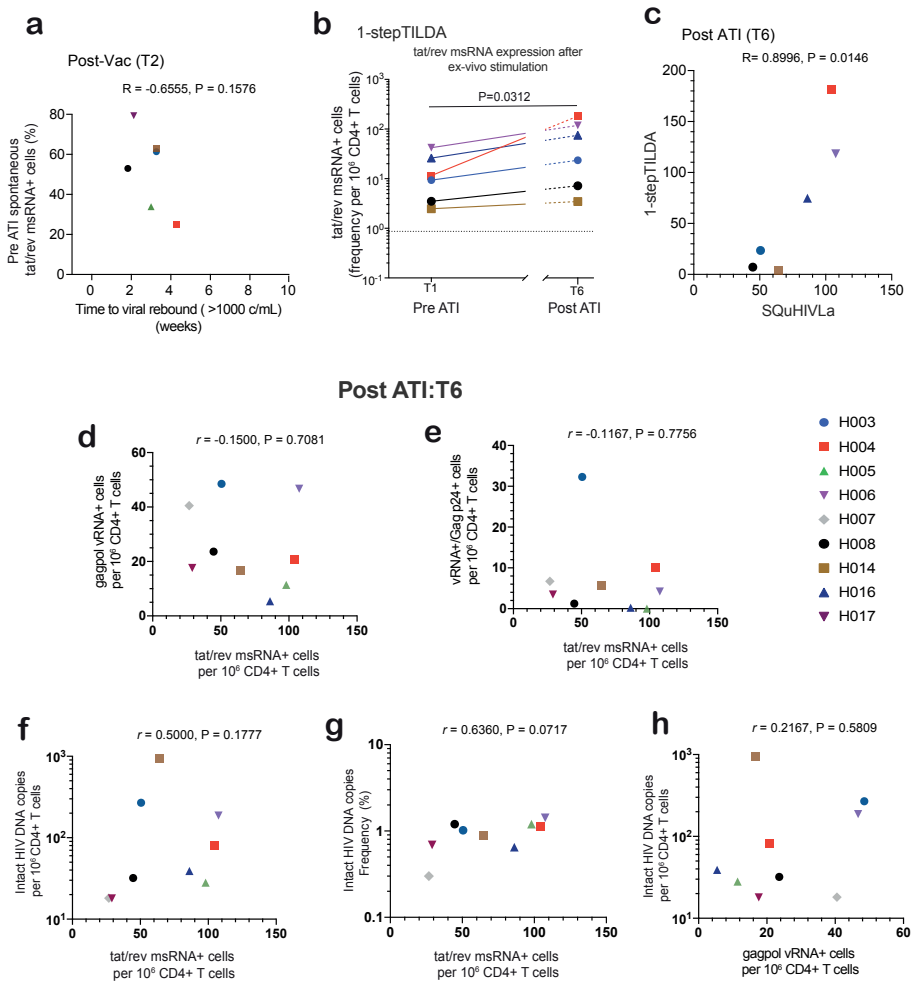

Extended Fig. 4. HIV-1 viral reservoir comparisons before ATI, and post ATI after >10 years of suppressive ART. a) Relationship between time to viral rebound and pre-ATI frequency of cells spontaneously expressing tat/rev msRNA at timepoint T2, one week after the last DC vaccination. The frequency shown is a ratio of cells with spontaneous expression of tat/rev msRNA to the number total number of cells expressing tat/rev msRNA after 12h ex vivo stimulation with PMA/ionomycin. Viral reservoir data were generated using a SQuHIVLa assay – 'Specific Quantification of inducible HIV by LAMP'. (**b**) Pre and post ATI comparison of the frequency of cells expressing tat/rev msRNA after 12h ex vivo stimulation with PMA/ionomycin. Viral reservoir data were generated using a 1-step TILDA approach. A Wilcoxon signed rank test was used to compare the means of the paired samples and a two-tailed P value is shown. (**c**) Pearson correlation of SQuHIVLa and 1-step TILDA using post ATI timepoint 6 viral reservoir data. Spearman correlations of the induced tat/rev msRNA+ reservoir and (**d**) the transcription-competent, gagpol viral RNA+ reservoir; (**e**) the translation-competent, gagpol vRNA+/Gag p24+, reservoir; (**f**) intact proviral reservoir (DNA copies/million CD4+ T cells) and (**g**) frequency of intact HIV DNA copies (ratio of intact to total HIV DNA). (**h**) Spearman correlation of the transcription-competent, gagpol viral RNA+ reservoir and the intact proviral reservoir (DNA copies/million CD4+ T cells).

CHAPTER 5

Summarizing Discussion

Approximately 40 million people live with HIV-1 (PLWH) globally (UNAIDS 2023). Modern, highly suppressive antiretroviral therapy (ART) effectively blocks viral replication to below detection limits, and has significantly curbed HIV-1 transmission and improved health outcomes for many people with access to ART (~75 % of global population of PLWH) (UNAIDS 2023). However, ART is not curative and must be taken lifelong, posing considerable socio-economic burdens, particularly in resource-limited, high HIV-burdened settings. Moreover, people with HIV-1 on long-term ART have increased risk for comorbidities consequent to persistence of HIV-1 in blood and tissues, chronic inflammation, accelerated aging and ART toxicity. Hence, multiple strategies are currently pursued in global scientific efforts to achieve ART-free control and thereby improve overall long-term health outcomes of PLWH [1]. These target distinct mechanisms of HIV-1 persistence and include either approaches to eliminate, reduce or inactivate the proviral latent reservoir, and/or to enhance viral clearance and control viremia in absence of ART[1]. Evaluating the safety and efficacy of such (combinatorial) strategies in clinical trials is complexed by major challenges including limited sample availability and accessibility to anatomical tissue sites; scarcity of the inducible, replication-competent HIV-1 reservoir in peripheral blood – hence requiring large volumes of blood to detect and accurately assess viral reservoirs; sub-optimal sensitivity of endpoint assays and the absence of robust, predictive biomarkers of cure or ART-free control. Therefore, analytical ART interruption (ATI), while risky and raising several ethical concerns, is used to definitively evaluate the efficacy of putative cure strategies [2,3]. The research described in this thesis focused on interrogating latent, inducible HIV-1 reservoirs, which lie at the intersection of innovative strategies towards HIV-1 cure. This chapter summarizes the findings of the research discussed under the following thematic areas; i) assessing HIV-1 proviral inducibility; ii) HIV-1 latency reversal *in vivo;* iii) inducing apoptosis of HIV-1 reservoir cells *ex vivo;* and iv) impact of immune-based approaches towards ART-free control.

ASSESSING HIV-1 PROVIRAL INDUCIBILITY

Precise assessment and interpretation of innovative strategies aimed at HIV clearance or control require semantic consistency, which is a challenge given the intricacies of HIV persistence. The proviral landscape is dominated by replication-defective HIV-1 genomes, which rapidly accumulate during primary acute HIV-1 infection and are remarkably stable over decades of suppressive ART [4-6]. While HIV-1 latency has traditionally been defined as 'transcriptionally silent', there has been a shift in this paradigm as emerging studies have demonstrated viral RNA and protein expression from defective proviruses [7-9], which, although unable to contribute to new infections, could contribute to various comorbidities and pathogenesis in PLWH on suppressive ART. In contrast, a small fraction of infected cells that harbor intact, but latent HIV-1 makes up 2-5% of the viral reservoir in peripheral blood mononuclear cells (PBMCs) and thus scarce in peripheral blood [10,11]. Indeed, virtually all measures of viral persistence determine the frequency of infected cells among the sampled cells, mostly from peripheral blood, leaving uncertain the total body burden of infected cells. Early studies established that the frequencies of latently infected cells in blood and lymph node are similar [12]. In addition, others have recently demonstrated through viral sequence analysis, that 98% of intact, or replication competent clonal sequences overlapped between blood and lymph node, which suggests that latently infected CD4+ T cells circulate between blood and lymphoid tissues in individuals on suppressive ART [13]. The intact latent reservoir that can be induced by T cell activation to express viral genes, leading to viral production, initiates viral rebound when ART is stopped, sub-optimal or failing. This latent, inducible replication-competent viral reservoir is therefore a crucial target in innovative strategies towards HIV-1 cure or ART-free control. The success of these strategies demands the ability to accurately and precisely assess the magnitude and reactivation kinetics of HIV-1 reservoirs before and after such interventions to guide ART interruption.

Numerous techniques, which evaluate different aspects of the provirus and its functionality, have been developed and used to assess proviral integrity and inducibility in latently infected cell lines and *ex vivo*-infected primary cell model systems. Several of these assays have been applied to quantitate and qualitatively characterize HIV-1 reservoirs in samples from PLWH on suppressive ART in cross-sectional, and longitudinal observational or interventional translational studies. The recently developed (droplet) digital PCR-based intact proviral DNA assay (IPDA) is thought to detect all genetically intact proviruses, albeit without sequence confirmation, providing a more sensitive and accurate upper limit of reservoir size than standard single-amplicon HIV-1 DNA PCR assays. However, misclassification of defective proviruses as intact is still possible with two-target IPDA (conserved

regions within the packaging signal and *env* region) [14]. A small frequency of proviruses may be intact at PCR probe locations, but defective in other parts of the genome [14,15]. Reeves et al., demonstrated defective provirus misclassification across measurements up to 5%, which was in agreement with sequence library-based predictions. In comparison to a near full length quantitative PCR approach targeting four regions (Q4PCR), IPDA revealed ~40-fold more intact proviruses [14]. Importantly, the misclassification can lead to underestimated efficacy of therapies that aim to reduce intact proviruses. With advancement in digital PCR platforms and the capacity to detect up to 5 targets, there have been several IPDA upgrades to introduce additional target regions across the HIV genome to improve IPDA accuracy[16,17]. However, (near)full length proviral sequencing assays are likely still necessary to document absolute and dynamic levels of intact HIV-1 proviruses. Moreover, proviral intactness alone is not a direct measurement of inducibility, which greatly depends on viral integration sites and therein the potential for viral expression. Indeed, current proviral DNA quantitative approaches cannot distinguish between intact non-inducible and inducible proviruses, which may lead to overestimation of the intact, inducible viral reservoir. Several studies have revealed the low inducibility of latent proviruses, which poses major challenges for HIV-1 latency reversal approaches and the end point assays needed to accurately assess inducible viral reservoirs and the efficacy of putative HIV-1 cure strategies (reviewed in [18]).

Viral gene expression is an important transcriptional feature that distinguishes HIV-1 infected cells from uninfected counterparts. As such, quantitating the levels of cell-associated (CA) HIV-1 RNA in Total RNA samples or at single cell level is an important primary readout in shock and kill approaches. Normally, unspliced CA HIV RNA transcripts are measured and normalized either to internal reference genes or by cell number. However, an intrinsic limitation of these assays is the fact that while unspliced CA HIV-1 RNA reflects transcriptionally competent provirus, it inclusively represents partial or full transcripts from defective genomes.

Indeed, it has been demonstrated that the levels of total DNA correlate with levels of most HIV-1 transcripts (initiated, proximally and distally elongated, unspliced and completed, but not multiply spliced), suggesting that a considerable proportion of HIV-1 transcripts likely originate from defective proviruses [19]. These findings highlight the need for advanced assays to assess the integrity and quality of CA HIV-1 RNA transcripts and their replication-competence potential. In this regard, recent work has established novel assays such as the intact viral RNA assay (IVRA) [20], which revealed that most transcribed HIV-1 RNA is 3' defective (94%) and only a very small percentage is intact (<1%). Though extremely rare, intact HIV RNA

serves as the genome of infectious virions that permit transmission and spread and contribute to viral rebound after stopping ART or upon ART failure. Others have established a multidimensional assay for HIV-1 reservoir cell profiling, designed to simultaneously capture the transcriptional activity, the sequence, and the chromosomal integration site of single HIV-1 proviruses (PRIP-SEQ), which revealed significantly lower transcriptional activity of HIV-1 proviruses integrated in intergenic regions of the human genome [21]. The vast majority (94%) of proviruses were transcriptionally silent, consistent with a state of "deep viral latency". Transcriptionally active HIV-1 proviruses are thus actively selected against during ART, which is consistent with earlier findings using a matched integration site and proviral sequencing approach (MIP-Seq) on primary samples from PLWH during long-term antiretroviral therapy. Collectively, albeit demonstrated in a very small number of individuals, these studies suggest that intact proviruses with features of deep viral latency are selected during prolonged antiretroviral therapy, and may possess limited abilities to drive viral rebound upon treatment interruptions [22,23]. More scalable and higher throughput approaches to assess strategies exclusively targeting this latent reservoir compartment are required to comprehensively evaluate putative cure interventions.

The detection of multiply spliced (ms) RNA, transcribed from *tat/rev/nef*-encoding genes, located in the highly diverse genomic region, which is prone to large internal deletions and hypermutation[11], significantly reduces but does not completely exclude the likelihood of detecting defective genomes. In principle, 5' defective proviral RNA transcripts (~5.6 % of total transcribed HIV-1 RNA), which are more abundant than intact viral RNA transcripts, could be detected in RNA-induction assays that use msRNA as a readout of proviral transcription [20]. Despite this limitation, early studies demonstrated a predictive value for msRNA and increase in intra-cellular viral RNA on suppressive ART (cellular viral rebound) and production of replication-competent virions, which correlated with the magnitude of plasma HIV-1 RNA following structured interruption of suppressive ART [24]. More recent studies demonstrated a strong correlation between msRNA and supernatant HIV-1 RNA compared to unspliced HIV-1 RNA following latency reversal treatment *ex vivo* and *in vivo* [25]. Overall, these studies suggest that msRNA is more likely to reflect an increase in virion production and thus a useful surrogate indicator for replication-competence [25]. For this reason, Inducible RNA assays such as the *tat/rev*-induced limiting dilution assay (TILDA) [26,27], have been widely used to assess intact proviral inducibility as well as estimate the size of the inducible viral reservoir (reviewed in [28] and Chapter 1.1 of this thesis [29]. Moreover, compared to quantitative viral outgrowth assays, inducible RNA assays provide more sensitivity and a greater dynamic range for monitoring the reduction of the viral reservoir by eradication

strategies and may serve as robust and useful tools to evaluate viral reservoirs in PLWH on suppressive ART [30].

However, the research findings described in this thesis and studies by others, highlight the need to strategically combine diverse HIV reservoir techniques to optimize the accuracy, reliability and comparability of findings across studies. Moreover, although well established, TILDA has several limitations, which hinder its application in large clinical settings as discussed in Chapter 1.1. Importantly, the assay may overestimate the size of the replication-competent viral reservoir as not all cells expressing *tat/rev* msRNA viral RNA may necessarily produce infectious virions. Furthermore, inherent technical limitations may lead to inclusive detection of proviral DNA leading to false positive detection. These important limitations underscore the need for continued development, optimization and validation of HIV-1 reservoir technologies to ensure accurate and precise evaluation of putative cure interventions. In light of this, we recently developed an assay, termed SQuHIVLa – Specific Quantification of Inducible HIV-1 by LAMP, which leverages isothermal reverse transcription-loop mediated amplification (RT-LAMP), performed in a single reaction, to detect *tat/rev* multiply spliced RNA with high sensitivity and specificity. This novel approach was applied and evaluated alongside other HIV-1 reservoir technologies in Chapter 4. The implications of this technological advancement are outlined later in this Chapter and in Chapter 6.

HIV-1 LATENCY REVERSAL *IN VIVO*

Most HIV-1 cure research efforts to date have explored the so called "Shock and Kill" approach, which assumes that potent reactivation of the latent reservoir by diverse pharmacological or biologic agents targeting distinct mechanisms of viral persistence, will trigger extrinsic or intrinsic destruction and clearance of reactivated reservoir cells [31]. HDAC inhibitors, which include valproic acid (VPA), vorinostat (SAHA), romidepsin, and panobinostat, have been investigated in a number of clinical trials. The focus on HDACi is due to their ability to unwind the compact chromatin structure at the latent proviral promoter [32,33]. While these may be interesting therapeutic targets, trials with HDACis administered as monotherapy have not yielded sufficient or sustained proviral transcription. These outcomes are hardly surprising given the highly complex nature of the latent proviral reservoir landscape and the multiple mechanisms that govern latent reservoir establishment, stability, proviral inducibility (extensively discussed in several reviews [32,34,35]). Moreover, where potent LRA activity has been demonstrated in *ex vivo* latency model systems, HIV-1 reactivation *in vivo* has proven harder to achieve, likely due to the low inducibility of proviruses owing to their site of integration and distinct

mechanisms repressing proviral reactivation and replication that exists in cells from PLWH on suppressive ART[18]. For this reason, a combination of LRAs, targeting distinct mechanisms of HIV-1 persistence, will likely be more effective in inducing or enhancing proviral transcription *in vivo*, which necessitates the identification of novel LRAs to incorporate into HIV-1 latency reversal approaches toward cure.

Earlier studies established that the BAF250/ARID1a–containing BAF chromatin remodeling complex was essential for HIV-1 repression and latency, and thus a therapeutic target for latency reversal [36]. In recent studies, small molecule inhibitors of BAF were identified and shown to reverse viral latency in various models of HIV-1 latency, including cells from PLWH. Interestingly, BAF complex inhibitors were shown to synergize with other LRAs-SAHA and prostratin in *ex vivo* primary cell models of latency [37]. One of the BAF inhibitors characterized, pyrimethamine, is an FDA-approved compound extensively used and characterized in the clinic in context of toxoplasmosis. Therefore, we repurposed this drug in order to examine its potential to induce proviral transcription *in vivo*, which was a pioneering proof-of-concept trial to advance BAF inhibitors as a new LRA class for inclusion in interventional efforts towards an HIV-1 cure (Chapter 2 of this thesis) [38].

Our data are supportive of the BAF inhibitor pyrimethamine, which has widespread use in the clinic, good safety profile, and favorable pharmacological features, including its efficient brain penetration and thus potential for penetration into HIV-1 reservoir sanctuary sites. Pyrimethamine is indeed an attractive candidate for inclusion in future pharmacological approaches toward an HIV-1 cure. Importantly, the trial demonstrated that pyrimethamine treatment alone induced significant reversal of HIV-1 latency *in vivo* marked by a twofold increase in unspliced HIV-1 cell-associated (CA) HIV-1 RNA after 6 hours post treatment with a lasting effect throughout the 14-day treatment phase [38]. Reflecting the observed induction of CA HIV-1 RNA, Pharmacokinetic/Pharmacodynamic studies indicated both the detection of pyrimethamine in plasma as well as the induction of BAF complex target genes as biomarkers of pyrimethamine activity from 6 hours post treatment through the 14-day treatment phase.

Interestingly, the impact on proviral transcription was only observed in the presence of measurable pyrimethamine plasma concentrations accompanied by selective induction of other BAF complex target genes, which were not observed in individuals not exposed to pyrimethamine. Indeed, identifying selective biomarkers of response is crucial to evaluating putative interventions targeting the latent, proviral reservoir. In contrast, high dose treatment with valproic acid, an HDACi, which we also evaluated as a monotherapy, did not result in latency reversal *in*

vivo. Furthermore, pyrimethamine and valproic acid administered as a combined treatment did not lead to synergistic reactivation.

This trial was one of the first randomized controlled clinical studies to evaluate combinations of LRAs and revealed several points for consideration in the design of future combinatorial LRA strategies. Notedly, the interventional treatment adjustments were more frequent in the combination arm, which highlights the need to monitor for drug tolerability and overall safety in future studies. Importantly, future studies will need to focus on optimizing dosing strategies using different LRA classes, which may potentiate latency reversal with sequential dosing during treatment or where latency reversal depends on a dichotomous (on/off) effect, such as was observed for pyrimethamine[38]. Moreover, this trial revealed that the combinational approach of pyrimethamine and a weak de-repressor HDACi, as a partner LRA, may be less likely to work synergistically compared to combining a de-repressing and an activating LRA. The latter points to the need to identify optimal partner drugs for different LRA classes to enhance latency reversal. Furthermore, there is need to identify the impact of LRAs in cellular and tissue reservoirs with distinct phenotypes and metabolic properties (reviewed in [39]). To date, most clinical studies with LRAs have measured reactivation mainly in peripheral CD4+ T cells. Furthermore, our findings from our very small population (n=28) of male, predominantly Caucasian participants diagnosed with HIV-1 subtype B, are not generalizable to all PLWH. Therefore, studies in different groups of participants are much needed to evaluate for instance sex-specific differences in response to LRA treatment (reviewed in [40]). Data thus far point towards more restricted viral reservoirs in women living with HIV-1 with a direct role for Estrogen in repressing HIV-1 promoter activity [41], which may influence efficacy of reservoir-targeting approaches and the choice of assays used to monitor spontaneous and inducible proviral expression.

In this work, pyrimethamine induced proviral transcription to modest levels (twofold increase in CA unspliced HIV-1 RNA) in men living with HIV-1. This level of reactivation is consistent with recent studies using other classes of LRAs (ranging from 1.5 – 2.6-fold inductions) [38]. However, given emerging evidence that most transcribed HIV-1 RNA is defective, future trial evaluations should aim to incorporate techniques that can assess HIV-1 RNA transcript integrity using novel assays such as IVRA [20]. Across all the different LRA studies, including our trial with pyrimethamine, the size of the latent, inducible viral reservoir has remained relatively stable despite the intended efforts to shock and "kill" HIV-1 latently infected cells [42-44]. There is very likely insufficient reactivation to trigger intrinsic apoptosis or extracellular killing of HIV-1 infected cells. However, whether the impact on the (inducible) viral

reservoir is truly absent, or merely beyond the detection limits/within technical variation of current viral reservoir assays, merits further investigation. The latter requires technologically advanced assays with improved specificity, sensitivity and scalability to detect fluctuations in reservoir size and reactivation kinetics over an extended timeframe with high precision.

INDUCING APOPTOSIS OF HIV-1 RESERVOIR CELLS *EX VIVO*

Viral gene expression is an important indication of infection, which can trigger cell-intrinsic viral cytopathic effects and extracellular immune responses. As such, proviral gene expression may likely influence the persistence, stability and fate of HIV-1-infected cells during suppressive ART. As outlined in the previous section, while latency reversal *in vivo* is achievable, the responses are modest and may not be sufficient to induce the "kill" aspect of the 'shock and kill' approach to eliminate cells harboring reactivated provirus (reviewed in [44]). Clinical trials with several LRAs have demonstrated limited to no reduction in the size of the viral reservoir. The success of this approach is however largely impeded by the dependency on the adaptive immune responses, which are markedly compromised in PLWH due to impaired CD4+ T cell help and exhausted immune cell compartments. Chapter 3 of this thesis focused on an alternative approach to eliminate the viral reservoir independently of the extracellular immune system.

Pharmacologically triggering innate pathways to intrinsically induce cell death in reactivated HIV-1 reservoir cells may be a viable therapeutic strategy towards a cure for HIV-1 infection. As a proof-of-concept, we conducted studies to evaluate the effect of inhibiting the host protein, Dead-box polypeptide 3, X-linked (DDX3), which is involved in HIV-1 RNA metabolism as well as in the regulation of apoptosis [45]. Interestingly, initial experiments unravelled a role for DDX3 inhibitors as LRAs and we established a plausible mechanism for induced cell death upon DDX3 inhibition. The treatment of latent HIV-1-infected cells with DDX3 inhibitors modestly reverses viral latency, possibly mediated by NF-κB, and impairs viral RNA export and translation, which leads to the accumulation of viral RNA. Transcribed HIV-1 RNA in turn activates innate antiviral signalling pathways, leading to IRF3 phosphorylation and production of IFN-β thereby rendering viral RNA-expressing cells pro-apoptotic. In addition, the DDX3-induced downregulation of anti-apoptotic proteins BIRC5 and HSPA1B, enhances the response leading to the selective induction of apoptosis in cells expressing HIV-1 viral RNA, sparing uninfected bystander cells not expressing pro-apoptotic IFN-β. Importantly, we demonstrated that DDX3 inhibition led to selective depletion of inducible viral reservoir following latency reversal, which may be a viable HIV-1 curative intervention. Indeed, the link between apoptosis

and latency reversal has been demonstrated in several other studies and is highly promising to further exploit in other reservoir compartments as well as in cells from women living with HIV-1, especially given the distinct differences in innate immune responses observed in women compared to men.

Extensive toxicology, biodistribution and pharmacokinetics of DDX3 inhibitors RK-33 and FH-1321, conducted in mice and rats respectively, have demonstrated a good toxicology profile in these pre-clinical studies, however future studies need to evaluate the impact of G1 cell cycle arrest caused by DDX3 inhibition in complex human tissue culture model systems. With the aim to enhance "killing", here *ex vivo* primary cell models are fundamentally important to evaluate compounds that induce selective apoptosis and their potential to reduce the size of the inducible viral reservoir. Such models will also enable studies to investigate the optimal concentrations and combinations of LRAs and cell apoptosis inducers that can be used to enhance latency reversal and induce selective apoptosis of cells expressing HIV-1 RNA upon reactivation. In our study, we established a primary CD4+ T cell model that enabled us to evaluate the impact of pharmacological inhibition of DDX3 on the latent proviral reservoir *in vitro*. We assessed proviral reservoir inducibility using three parallel methods of reservoir quantitation: unspliced HIV-1 RNA copies by RT-qPCR; *gagpol* viral RNA expression at single cell level by FISH-flow; multiply spliced *tat/rev* RNA by RT-qPCR in limiting dilution (Tat/rev induced limiting dilution assay). The size of the inducible viral reservoir, upon PMA/ionomycin stimulation, after 5 days of CD4+ T cell culture with DDX3 inhibitors significantly decreased by ~50% compared to Mock-treated cells.

Although DDX3 and several other compounds have been shown to induce selective apoptosis of HIV-1-infected cells, this approach remains conceptual – no studies yet have explored the impact of inducing cell apoptosis to reduce the size of the viral reservoir in PLWH. Given the diverse nature of the proviral reservoir landscape, low inducibility and the predominance of defective proviral genomes, it is unclear what compartment of proviruses are susceptible to reactivation by DDX3 inhibition and to subsequent selective depletion. Moreover, while DDX3 inhibition has demonstrated impact on HIV-1 RNA export and translation, it is highly unlikely that DDX3 treatment on its own is sufficient to control rebounding viremia in absence of ART. Here, CD4+ primary CD4+ T cell models, such as the one we have established to study selective depletion of the inducible viral reservoir, could be used to assess the impact of sustained DDX3 treatment on cellular viral rebound *ex vivo*, upon DDX3-mediated latency reversal and in absence of antiretroviral drugs. Furthermore, the inclusion of other immune cell compartments such as NK cells, biologics or broadly neutralizing antibodies to the *in vitro* model could

enable studies to assess possible enhancement of putative approaches towards mediating ART-free control.

IMPACT OF IMMUNE-BASED APPROACHES TOWARDS ART-FREE VIRAL CONTROL

Early studies demonstrated that the latent viral reservoir is established very early during Acute infection, likely during the eclipse phase[46,47]. The frequencies of infected cells reach maximal values in gut-associated lymphoid tissue and lymph nodes as early as Fiebig stage II, before seroconversion, exceeding the frequencies in blood until Fiebig stage III, after which infected cell frequencies are relatively equally distributed between blood and lymphoid tissue compartments [48]. ART administered during these early stages of acute infection profoundly restricts latent viral reservoir establishment although not sufficient enough to prevent viral rebound upon stopping ART [48,49].

As discussed, in relation to Chapters 1 to 3 of this thesis, the latent, inducible and replication-competent HIV-1 reservoir is a major obstacle to HIV-1 curative efforts. Putative strategies to reactivate, reduce or deplete this HIV-1 reservoir have limited efficacy thus far. Moreover, evaluating intervention efficacy is further complicated by numerous technical limitations of the assays currently applied to assess different aspects of the HIV-1 reservoir. Additionally, there is a crucial need to identify robust, predictive biomarkers of response to putative curative interventions. Consequently, analytical ART interruption (ATI), while risky and raising several ethical concerns, is used to definitively evaluate the efficacy of putative strategies towards ART-free viral control [2,50-52]. A valid concern is the heightened risk of latent HIV-1 reservoir reseeding during ART interruption. Indeed, studies have suggested that it is safe to say that periods of ART interruption up to 48 weeks do not lead to latent HIV-1 reservoir expansion or irreversible damage to the immune compartment [53-56] (reviewed in [57]). However, these insights are greatly influenced by the sub-optimal assays and imperfect surrogate markers of replication-competence used to evaluate HIV-1 reservoir dynamics. This latter aspect was the underlying rationale of the studies conducted In Chapter 4 of this thesis.

We assessed HIV-1 reservoir dynamics pre and post ATI, using a repository of paired samples obtained from nine participants during an autologous dendritic cell immunotherapy trial with ATI (conducted in 2006-2009), and samples recently collected more than a decade after ATI and ART-mediated viral re-suppression. We performed a comprehensive longitudinal analysis and comparison of the HIV-1 reservoir in distinct molecular compartments using different state of the

art technologies – including a novel assay, termed SQuHIVLa, that we recently developed to sensitively and specifically quantify inducible HIV-1 reservoirs expressing *tat/rev* multiply spliced (ms) RNA [58]. We found that after more than a decade of suppressive ART post intervention, defective and intact proviral DNA were overall comparable to baseline prior to ATI, although, a clear upward trend in the levels and proportion of intact proviral DNA was observed in four participants. The fraction of cells positive for HIV-1 *gagpol* viral RNA expression at single cell level was remarkably stable across time points pre and post ATI, whereas the translation-competent viral reservoir, defined by *gagpol* viral RNA and Gag p24 protein co-expression, was more dynamic. Intriguingly, the latent, viral reservoir inducibly expressing *tat/rev* msRNA was significantly higher post ATI relative to pre-ATI time points in all individuals, strongly indicating an expansion of this viral reservoir compartment.

This is the first application of the highly sensitive HIV-1 reservoir assay (SQuHIVLa) to evaluate viral reservoir activity (spontaneous *tat/rev* msRNA expression), and the dynamics of inducible HIV-1 reservoirs in context of an immunotherapy intervention with ATI and long-term follow-up. Indeed, the DCTRN trial was conducted during an ART era where substantial levels of prolonged viremia and CD4+ T cell declines were more acceptable in routine care, which could have likely contributed to sustained viral reservoir reseeding during exceptionally long ART interruption. One may indeed question how generalizable these findings may be to modern ATI trials but we could argue that this study reveals clear insights, which in the least, invite pause and further consideration towards evaluating (combinatorial) intervention ATI trials; which measures of persistent HIV-1 reservoirs are clinically meaningful and what virologic assays are most appropriate? We believe these insights are important to inform the evaluation of future (combinatorial) intervention ATI trials. In our study, pre-ATI levels of intact proviral DNA and the frequency of cells spontaneously expressing *tat/rev* msRNA, post DC vaccination, trended negatively with time to viral rebound. These virologic biomarkers will likely contribute to the identification of additional immunological and/or host gene biomarkers of imminent viral rebound for ART-free control to ultimately guide ATI risk assessment.

Most importantly, the noticeable (inter-patient) differences in the outcomes of the latent, inducible viral reservoir compartment post ATI warrant the need for vigilant monitoring for possible long-term viral reservoir reseeding; possibly consequent to immune-based interventions, viral rebound following ATI, and sustained clonal expansion after viral resuppression. It will be informative to monitor the dynamics of this viral reservoir compartment in modern ATIs with longer time to viral rebound (up to several months) due to viral control mediated by polyfunctional action of

bNAbs – currently promising components in future curative strategies [59] (reviewed in [60-62]).

The research described in this thesis has applied a broad spectrum of techniques to assess HIV-1 persistence in response to novel strategies targeting distinct mechanisms towards HIV-1 cure or ART-free viral control. Overall, the work has contributed important insights into HIV-1 persistence with a key focus on the latent inducible viral reservoir, identified by *tat/rev* msRNA expression, which serves as a surrogate marker for replication-competence. This reservoir compartment has been demonstrated to be a dynamic and relevant compartment to monitor responses in putative curative interventions. The proof-of-concept and pioneering use of small molecules that inhibit the BAF complex to activate proviral transcription *in vivo* may be important components in future combinatorial LRA strategies. Precision targeting of the latent HIV-1 reservoir, achieved through directed action on specific viral or cellular elements, minimizes off-target effects while optimizing therapeutic efficacy. This was demonstrated in the proof-of-concept and pioneering use of DDX3 inhibitors to pharmacologically trigger HIV-1 latency reversal and intrinsic cell apoptosis, leading to the selective depletion of cells expressing HIV-1 RNA while sparing uninfected bystander cells. This presents another promising strategy to circumvent the failure of adaptive immune responses in eliminating the latent HIV-1 reservoir – a significant challenge towards achieving a cure for HIV-1 infection.

Evidently, the findings from the research described in this thesis, relate to HIV-1 subtype B infection and viral persistence in peripheral blood CD4+ T cells. Moreover, the translational studies described in Chapter 2 and 4 were conducted in Male, predominantly Caucasian participants. Therefore, the research findings described in this work cannot be generalized to all people living with HIV-1. There are tremendous gaps in our understanding of HIV-1 persistence in diverse populations. Studies in high HIV-burdened, African settings, currently limited, are pivotal to inform the development of HIV-1 therapeutics that will be effective in African populations – More than 60% of the global population of PLWH reside in Sub-Saharan Africa.

CHAPTER 6

Perspective

HIV-1 PERSISTENCE RESEARCH IN LOW-RESOURCE SETTINGS: TECHNICAL CONSIDERATIONS

Evolving insights into HIV-1 persistence and underlying mechanisms iteratively shape scientific efforts towards achieving HIV-1 cure or ART-free viral control. Studies in genetically diverse people living with HIV (PLWH) in high HIV-burdened, African settings, currently limited, are pivotal to inform the development of HIV-1 therapeutics that will be effective in African populations – More than 60% of the global population of PLWH reside in Sub Saharan Africa.

Interestingly, a recent study in a cohort of Ugandan PLWH, a smaller, but more diverse, peripheral inducible HIV-1 reservoir was observed compared to a US cohort of PLWH, which might be associated with viral (e.g., higher cytopathicity of non-B HIV strains) and/or host factors (e.g., higher incidences of co-infections leading to less clonal expansion) [63]. A related study revealed a reduced frequency of viral outgrowth among women in Uganda, which may reflect low inducibility, less viral gene expression, or intrinsic elimination of reactivated cells, which warrants further elucidation [64]. In addition, an epidemiologic, host gene expression study has demonstrated a significant link between HIV-1 reservoir size and several well-known immunologic pathways (e.g., IL-1β, TLR7, TNF-α signaling pathways), as well as novel associations with potassium and gap junction channels (Kir2.1, connexin 26) [65]. Importantly, further studies are needed to validate these findings in female, African cohorts – women have a more robust type 1 interferon response during HIV-1 infection relative to men that contributes to lower initial plasma viremia [66]. Collectively, these findings raise important questions on potential responses to latency reversal and/or immune-based curative approaches in women with HIV.

To advance studies in a wider population of PLWH in diverse epidemiological settings, there is an urgent need to develop standardized and clinically validated assays to evaluate latent reservoirs and persistent proviral genomes in blood and tissue compartments to evaluate putative curative strategies. Importantly, efforts to ensure that HIV-1 persistence assays are cost-effective, scalable and amenable to resource-constrained settings in low-middle income countries (LMICs), where the burden of HIV-1 is significantly higher, should also be prioritized. In most instances, established PCR-based reservoir assays have been developed to optimally detect and quantitate viral reservoirs in individuals diagnosed with subtype B HIV-1 infection. Thus detection of non-B viral reservoirs will be sub-optimal (if at all). On the other hand, culture-based viral reservoir assays such as the quantitative viral outgrowth assay (QVOA), which assesses replication-competence of a reactivated provirus, are profoundly inapplicable given the requirement for large blood draws (250-500 mL) or leukapheresis sampling to provide sufficient number of cells to

run the assays. Moreover, QVOA and VOA-like assays are labor-intensive, time consuming (7-21 days of culture), and extremely costly (reagents, consumables and biosafety level-3 laboratory infrastructure requirements).

Alternative culture-based assays, herein referred to as inducible RNA assays, hold promise for broader application. These assays enable quantitative profiling or viral (unspliced, multiply spliced RNA, poly-A mature RNA transcripts) upon cell activation with latency reversal agents, activating biologics or other chemical stimuli. Quantitation of HIV-1 RNA transcripts are typically performed using single-round or semi-nested quantitative reverse transcription real time PCR (RT-qPCR) on bulk Total RNA or serially diluted RNA samples. However, recent technological advancements have led to the use of (droplet) digital PCR-based platforms to yield absolute measurements of viral RNA transcripts, which has enabled the development of novel assays such as the intact viral RNA assay (IVRA) used to assess genomic RNA integrity [20].

Inducible RNA assays such as the *tat/rev* induced limiting dilution assay (TILDA), as the name indicates, involves a two-step RT-qPCR detection of *tat/rev* multiply spliced RNA transcripts in limiting dilution format e.g., in 96 or 384 well plates, which significantly increases reagent and consumable costs. Moreover, the amplification procedure is instrument intensive with a long turnaround time, and increased risk of cross-contamination from manual handling of pre-amplified products [29]. These assay features are certain to limit assay application in large clinical trials, especially in low-resource settings. Thus, to address these technical limitations, we leveraged the high sensitivity and specificity of reverse transcription loop-mediated isothermal amplification (RT-LAMP) to develop a novel assay (SQuHIVLa) to detect and quantitate reservoirs spontaneously or inducibly expressing *tat/rev* multiply spliced RNA [58]. SQuHIVLa is an important technological advancement to enable sensitive and exclusive detection of multiply spliced RNA transcripts, which are less abundant. The limits of sensitivity in quantifying low viral reservoir sizes in samples from elite controllers or individuals that initiated ART during Acute HIV-1 infection (Fiebig I-III) merits further research. Moreover, future work will seek to advance the assay to a single cell approach, to exclude the current need for limiting dilution, further reducing assay costs and improving scalability. Meanwhile, SQuHIVLa is an attractive assay to exploit in ongoing HIV persistence studies in pre-clinical and clinical studies including in resource-constrained settings.

APPENDICES

References

REFERENCES

Chapter 1

1. Cohen, M.S., Shaw, G.M., McMichael, A.J. & Haynes, B.F. Acute HIV-1 Infection. *N Engl J Med* **364**, 1943-1954 (2011).
2. McMichael, A.J., Borrow, P., Tomaras, G.D., Goonetilleke, N. & Haynes, B.F. The immune response during acute HIV-1 infection: clues for vaccine development. *Nat Rev Immunol* **10**, 11-23 (2010).
3. Brenchley, J.M., *et al.* CD4+ T cell depletion during all stages of HIV disease occurs predominantly in the gastrointestinal tract. *J Exp Med* **200**, 749-759 (2004).
4. Doitsh, G., *et al.* Cell death by pyroptosis drives CD4 T-cell depletion in HIV-1 infection. *Nature* **505**, 509-514 (2014).
5. Monroe, K.M., *et al.* IFI16 DNA sensor is required for death of lymphoid CD4 T cells abortively infected with HIV. *Science* **343**, 428-432 (2014).
6. Douek, D.C., Roederer, M. & Koup, R.A. Emerging concepts in the immunopathogenesis of AIDS. *Annu Rev Med* **60**, 471-484 (2009).
7. Levy, J.A. HIV pathogenesis: 25 years of progress and persistent challenges. *AIDS* **23**, 147-160 (2009).
8. Centers for Disease, C. & Prevention. Revised surveillance case definition for HIV infection--United States, 2014. *MMWR Recomm Rep* **63**, 1-10 (2014).
9. Pantaleo, G. & Fauci, A.S. Immunopathogenesis of HIV infection. *Annu Rev Microbiol* **50**, 825-854 (1996).
10. Pantaleo, G. & Fauci, A.S. New concepts in the immunopathogenesis of HIV infection. *Annu Rev Immunol* **13**, 487-512 (1995).
11. Altfeld, M. & Gale, M., Jr. Innate immunity against HIV-1 infection. *Nat Immunol* **16**, 554-562 (2015).
12. Doyle, T., Goujon, C. & Malim, M.H. HIV-1 and interferons: who's interfering with whom? *Nat Rev Microbiol* **13**, 403-413 (2015).
13. Borrow, P. Innate immunity in acute HIV-1 infection. *Curr Opin HIV AIDS* **6**, 353-363 (2011).
14. Colby, D.J., *et al.* Rapid HIV RNA rebound after antiretroviral treatment interruption in persons durably suppressed in Fiebig I acute HIV infection. *Nat Med* **24**, 923-926 (2018).
15. Chun, T.W., *et al.* Rebound of plasma viremia following cessation of antiretroviral therapy despite profoundly low levels of HIV reservoir: implications for eradication. *AIDS* **24**, 2803-2808 (2010).
16. Farmer, A., *et al.* Factors associated with HIV viral load "blips" and the relationship between self-reported adherence and efavirenz blood levels on blip occurrence: a case-control study. *AIDS Res Ther* **13**, 16 (2016).
17. Maldarelli, F., *et al.* ART suppresses plasma HIV-1 RNA to a stable set point predicted by pretherapy viremia. *PLoS Pathog* **3**, e46 (2007).
18. Palmer, S., *et al.* Low-level viremia persists for at least 7 years in patients on suppressive antiretroviral therapy. *Proc Natl Acad Sci U S A* **105**, 3879-3884 (2008).

19. Sorstedt, E.*, et al.* Viral blips during suppressive antiretroviral treatment are associated with high baseline HIV-1 RNA levels. *BMC Infect Dis* **16**, 305 (2016).

20. Aldous, J.L. & Haubrich, R.H. Defining treatment failure in resource-rich settings. *Curr Opin HIV AIDS* **4**, 459-466 (2009).

21. Teira, R.*, et al.* Very low level viraemia and risk of virological failure in treated HIV-1-infected patients. *HIV Med* **18**, 196-203 (2017).

22. Vandenhende, M.A.*, et al.* Risk of virological failure in HIV-1-infected patients experiencing low-level viraemia under active antiretroviral therapy (ANRS C03 cohort study). *Antivir Ther* **20**, 655-660 (2015).

23. Hofstra, L.M.*, et al.* Residual viremia is preceding viral blips and persistent low-level viremia in treated HIV-1 patients. *PLoS One* **9**, e110749 (2014).

24. Kuller, L.H.*, et al.* Inflammatory and coagulation biomarkers and mortality in patients with HIV infection. *PLoS Med* **5**, e203 (2008).

25. Nabatanzi, R., Cose, S., Joloba, M., Jones, S.R. & Nakanjako, D. Effects of HIV infection and ART on phenotype and function of circulating monocytes, natural killer, and innate lymphoid cells. *AIDS Res Ther* **15**, 7 (2018).

26. Deeks, S.G., Tracy, R. & Douek, D.C. Systemic effects of inflammation on health during chronic HIV infection. *Immunity* **39**, 633-645 (2013).

27. Chun, T.W.*, et al.* Early establishment of a pool of latently infected, resting CD4(+) T cells during primary HIV-1 infection. *Proc Natl Acad Sci U S A* **95**, 8869-8873 (1998).

28. Finzi, D.*, et al.* Latent infection of CD4+ T cells provides a mechanism for lifelong persistence of HIV-1, even in patients on effective combination therapy. *Nat Med* **5**, 512-517 (1999).

29. Finzi, D.*, et al.* Identification of a reservoir for HIV-1 in patients on highly active antiretroviral therapy. *Science* **278**, 1295-1300 (1997).

30. Chun, T.W. & Fauci, A.S. Latent reservoirs of HIV: obstacles to the eradication of virus. *Proc Natl Acad Sci U S A* **96**, 10958-10961 (1999).

31. Deeks, S.G.*, et al.* Research priorities for an HIV cure: International AIDS Society Global Scientific Strategy 2021. *Nat Med* **27**, 2085-2098 (2021).

32. Cicilionyte, A., Berkhout, B. & Pasternak, A.O. Assessing proviral competence: current approaches to evaluate HIV-1 persistence. *Curr Opin HIV AIDS* **16**, 223-231 (2021).

33. Zerbato, J.M.*, et al.* Multiply spliced HIV RNA is a predictive measure of virus production ex vivo and in vivo following reversal of HIV latency. *EBioMedicine* **65**, 103241 (2021).

34. Bruner, K.M.*, et al.* Defective proviruses rapidly accumulate during acute HIV-1 infection. *Nat Med* **22**, 1043-1049 (2016).

35. Ananworanich, J. & Mellors, J.W. How Much HIV is Alive? The Challenge of Measuring Replication Competent HIV for HIV Cure Research. *EBioMedicine* **2**, 788-789 (2015).

36. Falcinelli, S.D.*, et al.* Longitudinal dynamics of intact HIV proviral DNA and outgrowth virus frequencies in a cohort of ART-treated individuals. *J Infect Dis* (2020).

37. Peluso, M.J.*, et al.* Differential decay of intact and defective proviral DNA in HIV-1-infected individuals on suppressive antiretroviral therapy. *JCI Insight* **5**(2020).

38. Imamichi, H.*, et al.* Defective HIV-1 proviruses produce viral proteins. *Proc Natl Acad Sci U S A* **117**, 3704-3710 (2020).

39. Imamichi, H.*, et al.* Defective HIV-1 proviruses produce novel protein-coding RNA species in HIV-infected patients on combination antiretroviral therapy. *Proc Natl Acad Sci U S A* **113**, 8783-8788 (2016).

40. Pollack, R.A.*, et al.* Defective HIV-1 Proviruses Are Expressed and Can Be Recognized by Cytotoxic T Lymphocytes, which Shape the Proviral Landscape. *Cell Host Microbe* **21**, 494-506 e494 (2017).

41. Kuniholm, J., Coote, C. & Henderson, A.J. Defective HIV-1 genomes and their potential impact on HIV pathogenesis. *Retrovirology* **19**, 13 (2022).

42. Chun, T.W., Engel, D., Mizell, S.B., Ehler, L.A. & Fauci, A.S. Induction of HIV-1 replication in latently infected CD4+ T cells using a combination of cytokines. *J Exp Med* **188**, 83-91 (1998).

43. Ho, Y.C.*, et al.* Replication-competent noninduced proviruses in the latent reservoir increase barrier to HIV-1 cure. *Cell* **155**, 540-551 (2013).

44. Brodin, J.*, et al.* Establishment and stability of the latent HIV-1 DNA reservoir. *Elife* **5**(2016).

45. Abrahams, M.R.*, et al.* The replication-competent HIV-1 latent reservoir is primarily established near the time of therapy initiation. *Sci Transl Med* **11**(2019).

46. Gandhi, R.T.*, et al.* Varied Patterns of Decay of Intact HIV-1 Proviruses Over two Decades of Art. *J Infect Dis* (2023).

47. Huang, A.S.*, et al.* Integration features of intact latent HIV-1 in CD4+ T cell clones contribute to viral persistence. *J Exp Med* **218**(2021).

48. Huang, S.H.*, et al.* Latent HIV reservoirs exhibit inherent resistance to elimination by CD8+ T cells. *J Clin Invest* **128**, 876-889 (2018).

49. Maldarelli, F.*, et al.* HIV latency. Specific HIV integration sites are linked to clonal expansion and persistence of infected cells. *Science* **345**, 179-183 (2014).

50. Symons, J., Cameron, P.U. & Lewin, S.R. HIV integration sites and implications for maintenance of the reservoir. *Curr Opin HIV AIDS* **13**, 152-159 (2018).

51. Siliciano, J.D. & Siliciano, R.F. Low Inducibility of Latent Human Immunodeficiency Virus Type 1 Proviruses as a Major Barrier to Cure. *J Infect Dis* **223**, 13-21 (2021).

52. Telwatte, S.*, et al.* Heterogeneity in HIV and cellular transcription profiles in cell line models of latent and productive infection: implications for HIV latency. *Retrovirology* **16**, 32 (2019).

53. Sherrill-Mix, S.*, et al.* HIV latency and integration site placement in five cell-based models. *Retrovirology* **10**, 90 (2013).

54. Spina, C.A.*, et al.* An in-depth comparison of latent HIV-1 reactivation in multiple cell model systems and resting CD4+ T cells from aviremic patients. *PLoS Pathog* **9**, e1003834 (2013).

55. Lassen, K.G., Hebbeler, A.M., Bhattacharyya, D., Lobritz, M.A. & Greene, W.C. A flexible model of HIV-1 latency permitting evaluation of many primary CD4 T-cell reservoirs. *PLoS One* **7**, e30176 (2012).

56. Olson, R.M.*, et al.* Innate immune regulation in HIV latency models. *Retrovirology* **19**, 15 (2022).

57. Bosque, A. & Planelles, V. Studies of HIV-1 latency in an ex vivo model that uses primary central memory T cells. *Methods* **53**, 54-61 (2011).

58. Sunshine, S.*, et al.* HIV Integration Site Analysis of Cellular Models of HIV Latency with a Probe-Enriched Next-Generation Sequencing Assay. *J Virol* **90**, 4511-4519 (2016).

59. Ait-Ammar, A.*, et al.* Current Status of Latency Reversing Agents Facing the Heterogeneity of HIV-1 Cellular and Tissue Reservoirs. *Front Microbiol* **10**, 3060 (2019).

60. Eshetu, A. & Ho, Y.C. A multidimensional HIV-1 persistence model for clonal expansion and viral rebound in vitro. *Cell Rep Methods* **1**, 100134 (2021).

61. Matsuda, K.*, et al.* A widely distributed HIV-1 provirus elimination assay to evaluate latency-reversing agents in vitro. *Cell Rep Methods* **1**, 100122 (2021).

62. Shukla, M.*, et al.* A Reliable Primary Cell Model for HIV Latency: The QUECEL (Quiescent Effector Cell Latency) Method. *Methods Mol Biol* **2407**, 57-68 (2022).

63. Macedo, A.B.*, et al.* Influence of Biological Sex, Age, and HIV Status in an In Vitro Primary Cell Model of HIV Latency Using a CXCR4 Tropic Virus. *AIDS Res Hum Retroviruses* **34**, 769-777 (2018).

64. Martins, L.J.*, et al.* Modeling HIV-1 Latency in Primary T Cells Using a Replication-Competent Virus. *AIDS Res Hum Retroviruses* **32**, 187-193 (2016).

65. Sarabia, I., Huang, S.H., Ward, A.R., Jones, R.B. & Bosque, A. The Intact Non-Inducible Latent HIV-1 Reservoir is Established In an In Vitro Primary T(CM) Cell Model of Latency. *J Virol* **95**(2021).

66. Rao, S.*, et al.* Selective cell death in HIV-1-infected cells by DDX3 inhibitors leads to depletion of the inducible reservoir. *Nat Commun* **12**, 2475 (2021).

67. Rainwater-Lovett, K.*, et al.* Paucity of Intact Non-Induced Provirus with Early, Long-Term Antiretroviral Therapy of Perinatal HIV Infection. *PLoS One* **12**, e0170548 (2017).

68. Leyre, L.*, et al.* Abundant HIV-infected cells in blood and tissues are rapidly cleared upon ART initiation during acute HIV infection. *Sci Transl Med* **12**(2020).

69. Ananworanich, J., Dube, K. & Chomont, N. How does the timing of antiretroviral therapy initiation in acute infection affect HIV reservoirs? *Curr Opin HIV AIDS* **10**, 18-28 (2015).

70. Henrich, T.J.*, et al.* HIV-1 persistence following extremely early initiation of antiretroviral therapy (ART) during acute HIV-1 infection: An observational study. *PLoS Med* **14**, e1002417 (2017).

71. Quivy, V., De Walque, S. & Van Lint, C. Chromatin-associated regulation of HIV-1 transcription: implications for the development of therapeutic strategies. *Subcell Biochem* **41**, 371-396 (2007).

72. Laspia, M.F., Rice, A.P. & Mathews, M.B. HIV-1 Tat protein increases transcriptional initiation and stabilizes elongation. *Cell* **59**, 283-292 (1989).

73. Rafati, H.*, et al.* Repressive LTR nucleosome positioning by the BAF complex is required for HIV latency. *PLoS Biol* **9**, e1001206 (2011).

74. Sadowski, I., Lourenco, P. & Malcolm, T. Factors controlling chromatin organization and nucleosome positioning for establishment and maintenance of HIV latency. *Curr HIV Res* **6**, 286-295 (2008).

75. Marsden, M.D. & Zack, J.A. Experimental Approaches for Eliminating Latent HIV. *For Immunopathol Dis Therap* **6**, 91-99 (2015).

76. Nixon, C.C., Mavigner, M., Silvestri, G. & Garcia, J.V. In Vivo Models of Human Immunodeficiency Virus Persistence and Cure Strategies. *J Infect Dis* **215**, S142-S151 (2017).

77. Debrabander, Q.*, et al.* The efficacy and tolerability of latency-reversing agents in reactivating the HIV-1 reservoir in clinical studies: a systematic review. *J Virus Erad* **9**, 100342 (2023).

78. Spivak, A.M. & Planelles, V. HIV-1 Eradication: Early Trials (and Tribulations). *Trends Mol Med* **22**, 10-27 (2016).

79. Subramanian, S., Bates, S.E., Wright, J.J., Espinoza-Delgado, I. & Piekarz, R.L. Clinical Toxicities of Histone Deacetylase Inhibitors. *Pharmaceuticals (Basel)* **3**, 2751-2767 (2010).

80. Suraweera, A., O'Byrne, K.J. & Richard, D.J. Combination Therapy With Histone Deacetylase Inhibitors (HDACi) for the Treatment of Cancer: Achieving the Full Therapeutic Potential of HDACi. *Front Oncol* **8**, 92 (2018).

81. Goey, A.K., Sissung, T.M., Peer, C.J. & Figg, W.D. Pharmacogenomics and histone deacetylase inhibitors. *Pharmacogenomics* **17**, 1807-1815 (2016).

82. Stoszko, M.*, et al.* Small Molecule Inhibitors of BAF; A Promising Family of Compounds in HIV-1 Latency Reversal. *EBioMedicine* **3**, 108-121 (2016).

83. Prins, H.A.B.*, et al.* The BAF complex inhibitor pyrimethamine reverses HIV-1 latency in people with HIV-1 on antiretroviral therapy. *Sci Adv* **9**, eade6675 (2023).

84. Kim, Y., Anderson, J.L. & Lewin, S.R. Getting the "Kill" into "Shock and Kill": Strategies to Eliminate Latent HIV. *Cell Host Microbe* **23**, 14-26 (2018).

85. Battivelli, E.*, et al.* Distinct chromatin functional states correlate with HIV latency reactivation in infected primary CD4(+) T cells. *Elife* **7**(2018).

86. Sadowski, I. & Hashemi, F.B. Strategies to eradicate HIV from infected patients: elimination of latent provirus reservoirs. *Cell Mol Life Sci* **76**, 3583-3600 (2019).

87. Olesen, R.*, et al.* Innate Immune Activity Correlates with CD4 T Cell-Associated HIV-1 DNA Decline during Latency-Reversing Treatment with Panobinostat. *J Virol* **89**, 10176-10189 (2015).

88. Palermo, E.*, et al.* Activation of Latent HIV-1 T Cell Reservoirs with a Combination of Innate Immune and Epigenetic Regulators. *J Virol* **93**(2019).

89. Hutter, G.*, et al.* Long-term control of HIV by CCR5 Delta32/Delta32 stem-cell transplantation. *N Engl J Med* **360**, 692-698 (2009).

90. Gupta, R.K.*, et al.* HIV-1 remission following CCR5Delta32/Delta32 haematopoietic stem-cell transplantation. *Nature* **568**, 244-248 (2019).

91. Hsu, J.*, et al.* HIV-1 remission and possible cure in a woman after haplo-cord blood transplant. *Cell* **186**, 1115-1126 e1118 (2023).

92. Jensen, B.O.*, et al.* In-depth virological and immunological characterization of HIV-1 cure after CCR5Delta32/Delta32 allogeneic hematopoietic stem cell transplantation. *Nat Med* **29**, 583-587 (2023).

93. Namazi, G.*, et al.* The Control of HIV After Antiretroviral Medication Pause (CHAMP) Study: Posttreatment Controllers Identified From 14 Clinical Studies. *J Infect Dis* **218**, 1954-1963 (2018).

94. Saez-Cirion, A.*, et al.* Post-treatment HIV-1 controllers with a long-term virological remission after the interruption of early initiated antiretroviral therapy ANRS VISCONTI Study. *PLoS Pathog* **9**, e1003211 (2013).

95. Turk, G.*, et al.* A Possible Sterilizing Cure of HIV-1 Infection Without Stem Cell Transplantation. *Ann Intern Med* **175**, 95-100 (2022).

96. Lian, X.*, et al.* Signatures of immune selection in intact and defective proviruses distinguish HIV-1 elite controllers. *Sci Transl Med* **13**, eabl4097 (2021).

97. Freen-van Heeren, J.J. Closing the Door with CRISPR: Genome Editing of CCR5 and CXCR4 as a Potential Curative Solution for HIV. *BioTech (Basel)* **11**(2022).

98. Khan, A., Paneerselvam, N. & Lawson, B.R. Antiretrovirals to CCR5 CRISPR/Cas9 gene editing - A paradigm shift chasing an HIV cure. *Clin Immunol*, 109741 (2023).

99. Mohamed, H.*, et al.* Targeting CCR5 as a Component of an HIV-1 Therapeutic Strategy. *Front Immunol* **12**, 816515 (2021).

100. Zerbato, J.M. & Lewin, S.R. A cure for HIV: how would we know? *Lancet HIV* **7**, e304-e306 (2020).

101. Magalhaes, M., Kuritzkes, D.R. & Eyal, N. The ethical case for placebo control in HIV-cure-related studies with ART interruption. *J Virus Erad* **8**, 100084 (2022).

102. Julg, B.*, et al.* Recommendations for analytical antiretroviral treatment interruptions in HIV research trials-report of a consensus meeting. *Lancet HIV* **6**, e259-e268 (2019).

103. Siliciano, J.D. & Siliciano, R.F. Assays to Measure Latency, Reservoirs, and Reactivation. *Curr Top Microbiol Immunol* **417**, 23-41 (2018).

104. Plantin, J., Massanella, M. & Chomont, N. Inducible HIV RNA transcription assays to measure HIV persistence: pros and cons of a compromise. *Retrovirology* **15**, 9 (2018).

105. Massanella, M.*, et al.* Improved assays to measure and characterize the inducible HIV reservoir. *EBioMedicine* **36**, 113-121 (2018).

106. Falcinelli, S.D., Ceriani, C., Margolis, D.M. & Archin, N.M. New Frontiers in Measuring and Characterizing the HIV Reservoir. *Front Microbiol* **10**, 2878 (2019).

107. Abdel-Mohsen, M.*, et al.* Recommendations for measuring HIV reservoir size in cure-directed clinical trials. *Nature Medicine* **26**, 1339-1350 (2020).

108. Bruner, K.M.*, et al.* A quantitative approach for measuring the reservoir of latent HIV-1 proviruses. *Nature* **566**, 120-125 (2019).

109. van Snippenberg, W.*, et al.* Triplex digital PCR assays for the quantification of intact proviral HIV-1 DNA. *Methods* **201**, 41-48 (2022).

110. Martin, H.A.*, et al.* New Assay Reveals Vast Excess of Defective over Intact HIV-1 Transcripts in Antiretroviral Therapy-Suppressed Individuals. *J Virol* **96**, e0160522 (2022).

111. Hiener, B.*, et al.* Identification of Genetically Intact HIV-1 Proviruses in Specific CD4(+) T Cells from Effectively Treated Participants. *Cell Rep* **21**, 813-822 (2017).

112. Einkauf, K.B.*, et al.* Intact HIV-1 proviruses accumulate at distinct chromosomal positions during prolonged antiretroviral therapy. *J Clin Invest* **129**, 988-998 (2019).

113. Wang, X.Q. & Palmer, S. Single-molecule techniques to quantify and genetically characterise persistent HIV. *Retrovirology* **15**, 3 (2018).

114. Yukl, S.A.*, et al.* HIV latency in isolated patient CD4(+) T cells may be due to blocks in HIV transcriptional elongation, completion, and splicing. *Sci Transl Med* **10**(2018).

115. Pasternak, A.O., Lukashov, V.V. & Berkhout, B. Cell-associated HIV RNA: a dynamic biomarker of viral persistence. *Retrovirology* **10**, 41 (2013).

116. Pasternak, A.O. & Berkhout, B. What do we measure when we measure cell-associated HIV RNA. *Retrovirology* **15**, 13 (2018).

117. Stuelke, E.L.*, et al.* Measuring the Inducible, Replication-Competent HIV Reservoir Using an Ultra-Sensitive p24 Readout, the Digital ELISA Viral Outgrowth Assay. *Front Immunol* **11**, 1971 (2020).

118. Prasad, V.R. & Kalpana, G.V. FISHing Out the Hidden Enemy: Advances in Detecting and Measuring Latent HIV-Infected Cells. *mBio* **8**(2017).

119. Baxter, A.E.*, et al.* Multiparametric characterization of rare HIV-infected cells using an RNA-flow FISH technique. *Nat Protoc* **12**, 2029-2049 (2017).

120. Grau-Exposito, J.*, et al.* A Novel Single-Cell FISH-Flow Assay Identifies Effector Memory CD4(+) T cells as a Major Niche for HIV-1 Transcription in HIV-Infected Patients. *mBio* **8**(2017).

121. Grau-Exposito, J.*, et al.* Latency reversal agents affect differently the latent reservoir present in distinct CD4+ T subpopulations. *PLoS Pathog* **15**, e1007991 (2019).

122. Hossain, T.*, et al.* SQuHIVLa: A novel assay for Specific Quantification of inducible HIV-1 reservoir by LAMP. *bioRxiv*, 2023.2007.2014.548928 (2023).

123. Procopio, F.A.*, et al.* A Novel Assay to Measure the Magnitude of the Inducible Viral Reservoir in HIV-infected Individuals. *EBioMedicine* **2**, 874-883 (2015).

124. Lungu, C. & Procopio, F.A. TILDA: Tat/Rev Induced Limiting Dilution Assay. *Methods Mol Biol* **2407**, 365-372 (2022).

125. Fisher, A.G.*, et al.* The trans-activator gene of HTLV-III is essential for virus replication. *Nature* **320**, 367-371 (1986).

126. Wodrich, H. & Krausslich, H.G. Nucleocytoplasmic RNA transport in retroviral replication. *Results Probl Cell Differ* **34**, 197-217 (2001).

127. Blissenbach, M., Grewe, B., Hoffmann, B., Brandt, S. & Uberla, K. Nuclear RNA export and packaging functions of HIV-1 Rev revisited. *J Virol* **84**, 6598-6604 (2010).

128. Lungu, C.*, et al.* Inter-Laboratory Reproducibility of Inducible HIV-1 Reservoir Quantification by TILDA. *Viruses* **12**(2020).

129. Lungu, C., Banga, R., Gruters, R.A. & Procopio, F.A. Inducible HIV-1 Reservoir Quantification: Clinical Relevance, Applications and Advancements of TILDA. *Front Microbiol* **12**, 686690 (2021).

130. Deeks, S.G. HIV: Shock and kill. *Nature* **487**, 439-440 (2012).

131. Almeida, M.J. & Matos, A. Designer Nucleases: Gene-Editing Therapies using CCR5 as an Emerging Target in HIV. *Curr HIV Res* **17**, 306-323 (2019).

132. Zhu, W.*, et al.* The CRISPR/Cas9 system inactivates latent HIV-1 proviral DNA. *Retrovirology* **12**, 22 (2015).

133. Wang, G., Zhao, N., Berkhout, B. & Das, A.T. CRISPR-Cas based antiviral strategies against HIV-1. *Virus Res* **244**, 321-332 (2018).

134. Qu, X.*, et al.* Zinc-finger-nucleases mediate specific and efficient excision of HIV-1 proviral DNA from infected and latently infected human T cells. *Nucleic Acids Res* **41**, 7771-7782 (2013).

135. Ahlenstiel, C.*, et al.* Novel RNA Duplex Locks HIV-1 in a Latent State via Chromatin-mediated Transcriptional Silencing. *Mol Ther Nucleic Acids* **4**, e261 (2015).

136. Mousseau, G.*, et al.* The Tat Inhibitor Didehydro-Cortistatin A Prevents HIV-1 Reactivation from Latency. *mBio* **6**, e00465 (2015).

137. Mendoza, P.*, et al.* Combination therapy with anti-HIV-1 antibodies maintains viral suppression. *Nature* **561**, 479-484 (2018).

138. Eriksson, S.*, et al.* Comparative analysis of measures of viral reservoirs in HIV-1 eradication studies. *PLoS Pathog* **9**, e1003174 (2013).

139. Laird, G.M., Rosenbloom, D.I., Lai, J., Siliciano, R.F. & Siliciano, J.D. Measuring the Frequency of Latent HIV-1 in Resting CD4(+) T Cells Using a Limiting Dilution Coculture Assay. *Methods Mol Biol* **1354**, 239-253 (2016).

140. Siliciano, J.D. & Siliciano, R.F. Enhanced culture assay for detection and quantitation of latently infected, resting CD4+ T-cells carrying replication-competent virus in HIV-1-infected individuals. *Methods Mol Biol* **304**, 3-15 (2005).

141. Rosenbloom, D.I.S.*, et al.* Assessing intra-lab precision and inter-lab repeatability of outgrowth assays of HIV-1 latent reservoir size. *PLoS Comput Biol* **15**, e1006849 (2019).

142. Stone, M.*, et al.* Assessing suitability of next-generation viral outgrowth assays as proxies for classic QVOA to measure HIV-1 latent reservoir size. *J Infect Dis* (2020).

143. Passaes, C.P.B.*, et al.* Ultrasensitive HIV-1 p24 Assay Detects Single Infected Cells and Differences in Reservoir Induction by Latency Reversal Agents. *J Virol* **91**(2017).

144. Zhang, Y.*, et al.* Improving HIV Outgrowth by Optimizing Cell-Culture Conditions and Supplementing With all-trans Retinoic Acid. *Front Microbiol* **11**, 902 (2020).

145. Alidjinou, E.K., Bocket, L. & Hober, D. Quantification of viral DNA during HIV-1 infection: A review of relevant clinical uses and laboratory methods. *Pathol Biol (Paris)* **63**, 53-59 (2015).

146. Avettand-Fenoel, V.*, et al.* Total HIV-1 DNA, a Marker of Viral Reservoir Dynamics with Clinical Implications. *Clin Microbiol Rev* **29**, 859-880 (2016).

147. Anderson, E.M. & Maldarelli, F. Quantification of HIV DNA Using Droplet Digital PCR Techniques. *Curr Protoc Microbiol* **51**, e62 (2018).

148. Vandergeeten, C.*, et al.* Cross-clade ultrasensitive PCR-based assays to measure HIV persistence in large-cohort studies. *J Virol* **88**, 12385-12396 (2014).

149. Gaebler, C.*, et al.* Combination of quadruplex qPCR and next-generation sequencing for qualitative and quantitative analysis of the HIV-1 latent reservoir. *J Exp Med* **216**, 2253-2264 (2019).

150. Simonetti, F.R.*, et al.* Intact proviral DNA assay analysis of large cohorts of people with HIV provides a benchmark for the frequency and composition of persistent proviral DNA. *Proc Natl Acad Sci U S A* **117**, 18692-18700 (2020).

151. Bullen, C.K., Laird, G.M., Durand, C.M., Siliciano, J.D. & Siliciano, R.F. New ex vivo approaches distinguish effective and ineffective single agents for reversing HIV-1 latency in vivo. *Nat Med* **20**, 425-429 (2014).

152. Cillo, A.R.*, et al.* Quantification of HIV-1 latency reversal in resting CD4+ T cells from patients on suppressive antiretroviral therapy. *Proc Natl Acad Sci U S A* **111**, 7078-7083 (2014).

153. Yucha, R.W.*, et al.* High-throughput Characterization of HIV-1 Reservoir Reactivation Using a Single-Cell-in-Droplet PCR Assay. *EBioMedicine* **20**, 217-229 (2017).

154. Papasavvas, E.*, et al.* Intact Human Immunodeficiency Virus (HIV) Reservoir Estimated by the Intact Proviral DNA Assay Correlates With Levels of Total and Integrated DNA in the Blood During Suppressive Antiretroviral Therapy. *Clin Infect Dis* **72**, 495-498 (2021).

155. Hong, F.*, et al.* Associations between HIV-1 DNA copy number, proviral transcriptional activity, and plasma viremia in individuals off or on suppressive antiretroviral therapy. *Virology* **521**, 51-57 (2018).

156. Hu, Y. & Smyth, G.K. ELDA: extreme limiting dilution analysis for comparing depleted and enriched populations in stem cell and other assays. *J Immunol Methods* **347**, 70-78 (2009).

157. Pardons, M.*, et al.* Single-cell characterization and quantification of translation-competent viral reservoirs in treated and untreated HIV infection. *PLoS Pathog* **15**, e1007619 (2019).

158. Buzon, M.J.*, et al.* HIV-1 persistence in CD4+ T cells with stem cell-like properties. *Nat Med* **20**, 139-142 (2014).

159. Bertoldi, A.*, et al.* Development of C-TILDA: A modified TILDA method for reservoir quantification in long term treated patients infected with subtype C HIV-1. *J Virol Methods* **276**, 113778 (2020).

160. Chun, T.W.*, et al.* Relationship between the size of the human immunodeficiency virus type 1 (HIV-1) reservoir in peripheral blood CD4+ T cells and CD4+:CD8+ T cell ratios in aviremic HIV-1-infected individuals receiving long-term highly active antiretroviral therapy. *J Infect Dis* **185**, 1672-1676 (2002).

161. Lu, W.*, et al.* CD4:CD8 ratio as a frontier marker for clinical outcome, immune dysfunction and viral reservoir size in virologically suppressed HIV-positive patients. *J Int AIDS Soc* **18**, 20052 (2015).

162. Stoszko, M., Ne, E., Abner, E. & Mahmoudi, T. A broad drug arsenal to attack a strenuous latent HIV reservoir. *Curr Opin Virol* **38**, 37-53 (2019).

163. Zerbato, J.M., Purves, H.V., Lewin, S.R. & Rasmussen, T.A. Between a shock and a hard place: challenges and developments in HIV latency reversal. *Curr Opin Virol* **38**, 1-9 (2019).

164. Sogaard, O.S.*, et al.* The Depsipeptide Romidepsin Reverses HIV-1 Latency In Vivo. *PLoS Pathog* **11**, e1005142 (2015).

165. Elliott, J.H.*, et al.* Activation of HIV transcription with short-course vorinostat in HIV-infected patients on suppressive antiretroviral therapy. *PLoS Pathog* **10**, e1004473 (2014).

166. Tietjen, I., *et al.* The Croton megalobotrys Mull Arg. traditional medicine in HIV/AIDS management: Documentation of patient use, in vitro activation of latent HIV-1 provirus, and isolation of active phorbol esters. *J Ethnopharmacol* **211**, 267-277 (2018).

167. Tietjen I., R.K., Williams D., Rivera-Ortiz J., Cai Y., Pagliuzza A., Chomont N., Andersen R., Montaner L., Andrae-Marobela K. Phorbol esters isolated from Croton megalobotrys reverse HIV latency ex vivo. *Journal of Virus Eradication* **5**(2019).

168. Fromentin, R., *et al.* CD4+ T Cells Expressing PD-1, TIGIT and LAG-3 Contribute to HIV Persistence during ART. *PLoS Pathog* **12**, e1005761 (2016).

169. Kulpa, D.A., *et al.* Differentiation into an Effector Memory Phenotype Potentiates HIV-1 Latency Reversal in CD4(+) T Cells. *J Virol* **93**(2019).

170. Wonderlich, E.R., *et al.* Effector memory differentiation increases detection of replication-competent HIV-l in resting CD4+ T cells from virally suppressed individuals. *PLoS Pathog* **15**, e1008074 (2019).

171. Rabezanahary, H., *et al.* Despite early antiretroviral therapy effector memory and follicular helper CD4 T cells are major reservoirs in visceral lymphoid tissues of SIV-infected macaques. *Mucosal Immunol* **13**, 149-160 (2020).

172. Kwon, K.J., *et al.* Different human resting memory CD4(+) T cell subsets show similar low inducibility of latent HIV-1 proviruses. *Sci Transl Med* **12**(2020).

173. Matsuda, K., *et al.* Benzolactam-related compounds promote apoptosis of HIV-infected human cells via protein kinase C-induced HIV latency reversal. *J Biol Chem* **294**, 116-129 (2019).

174. Zhang, G., *et al.* Selective cell death of latently HIV-infected CD4(+) T cells mediated by autosis inducing nanopeptides. *Cell Death Dis* **10**, 419 (2019).

175. Campbell, G.R., Bruckman, R.S., Chu, Y.L., Trout, R.N. & Spector, S.A. SMAC Mimetics Induce Autophagy-Dependent Apoptosis of HIV-1-Infected Resting Memory CD4+ T Cells. *Cell Host Microbe* **24**, 689-702 e687 (2018).

176. Chomont, N., *et al.* HIV reservoir size and persistence are driven by T cell survival and homeostatic proliferation. *Nat Med* **15**, 893-900 (2009).

177. Banga, R., *et al.* PD-1(+) and follicular helper T cells are responsible for persistent HIV-1 transcription in treated aviremic individuals. *Nat Med* **22**, 754-761 (2016).

178. Trautmann, L., *et al.* Upregulation of PD-1 expression on HIV-specific CD8+ T cells leads to reversible immune dysfunction. *Nat Med* **12**, 1198-1202 (2006).

179. Day, C.L., *et al.* PD-1 expression on HIV-specific T cells is associated with T-cell exhaustion and disease progression. *Nature* **443**, 350-354 (2006).

180. Petrovas, C., *et al.* PD-1 is a regulator of virus-specific CD8+ T cell survival in HIV infection. *J Exp Med* **203**, 2281-2292 (2006).

181. Aid, M., *et al.* Follicular CD4 T Helper Cells As a Major HIV Reservoir Compartment: A Molecular Perspective. *Front Immunol* **9**, 895 (2018).

182. Cicala, C., *et al.* The integrin alpha4beta7 forms a complex with cell-surface CD4 and defines a T-cell subset that is highly susceptible to infection by HIV-1. *Proc Natl Acad Sci U S A* **106**, 20877-20882 (2009).

183. Kader, M., *et al.* Alpha4(+)beta7(hi)CD4(+) memory T cells harbor most Th-17 cells and are preferentially infected during acute SIV infection. *Mucosal Immunol* **2**, 439-449 (2009).

184. Martinelli, E.*, et al.* The frequency of alpha(4)beta(7)(high) memory CD4(+) T cells correlates with susceptibility to rectal simian immunodeficiency virus infection. *J Acquir Immune Defic Syndr* **64**, 325-331 (2013).

185. Sivro, A.*, et al.* Integrin alpha4beta7 expression on peripheral blood CD4(+) T cells predicts HIV acquisition and disease progression outcomes. *Sci Transl Med* **10**(2018).

186. Uzzan, M.*, et al.* Anti-alpha4beta7 therapy targets lymphoid aggregates in the gastrointestinal tract of HIV-1-infected individuals. *Sci Transl Med* **10**(2018).

187. Hemelaar, J.*, et al.* Global and regional molecular epidemiology of HIV-1, 1990-2015: a systematic review, global survey, and trend analysis. *Lancet Infect Dis* **19**, 143-155 (2019).

188. Dhummakupt, A.*, et al.* Differences in inducibility of the latent HIV reservoir in perinatal and adult infection. *JCI Insight* **5**(2020).

189. Whitney, J.B.*, et al.* Rapid seeding of the viral reservoir prior to SIV viraemia in rhesus monkeys. *Nature* **512**, 74-77 (2014).

190. Frank, I.*, et al.* A Tat/Rev Induced Limiting Dilution Assay to Measure Viral Reservoirs in Non-Human Primate Models of HIV Infection. *Sci Rep* **9**, 12078 (2019).

191. Pezzi, H.M., Berry, S.M., Beebe, D.J. & Striker, R. RNA-mediated TILDA for improved cell capacity and enhanced detection of multiply-spliced HIV RNA. *Integr Biol (Camb)* **9**, 876-884 (2017).

192. Autran, B., Descours, B., Avettand-Fenoel, V. & Rouzioux, C. Elite controllers as a model of functional cure. *Curr Opin HIV AIDS* **6**, 181-187 (2011).

193. Siliciano, J.D.*, et al.* Long-term follow-up studies confirm the stability of the latent reservoir for HIV-1 in resting CD4+ T cells. *Nat Med* **9**, 727-728 (2003).

194. Galvez, C.*, et al.* Extremely low viral reservoir in treated chronically HIV-1-infected individuals. *EBioMedicine* **57**, 102830 (2020).

Chapter 2

1. Chun T. W., *et al.* Early establishment of a pool of latently infected, resting CD4+ T cells during primary HIV-1 infection. *Proc. Natl. Acad. Sci. U.S.A.* **95**, 8869-8873 (1998).

2. Chun T. W., *et al*. Relationship between pre-existing viral reservoirs and the re-emergence of plasma viremia after discontinuation of highly active anti-retroviral therapy. *Nat. Med.* **6**, 757 761 (2000).

3. Strategies for Management of Antiretroviral Therapy (SMART) Study Group, El-Sadr W. M., *et al*. CD4+ count guided interruption of antiretroviral treatment. *N. Engl. J. Med*. **355**, 2283-2296 (2006).

4. Deeks S. G. Shock and kill. *Nature* **487**, 439-440 (2012).

5. Deeks S. G., *et al*. The International AIDS Society (IAS) Global Scientific Strategy working group, Research priorities for an HIV cure: International AIDS Society Global Scientific Strategy 2021. *Nat. Med.* **27**, 2085 2098 (2021).

6. Margolis D. M., *et al*. Curing HIV: Seeking to target and clear persistent infection. *Cell* **181**, 189-206 (2020).

7. Stoszko M., Ne T., Abner E. & Mahmoudi T. A broad drug arsenal to attack a strenuous latent HIV reservoir. *Curr. Opin. Virol.* **38**, 37 53 (2019).

8. Ait-Ammar M., *et al*. Current status of latency reversing agents facing the heterogeneity of HIV-1 cellular and tissue reservoirs. *Front. Microbiol.* **10**, 3060 (2019).

9. Yukl S. A., et al., HIV latency in isolated patient CD4+ T cells may be due to blocks in HIV transcriptional elongation, completion, and splicing. *Sci. Transl. Med.* **10**, eaap9927 (2018).

10. Telwatte S. A., *et al*. Heterogeneity in HIV and cellular transcription profiles in cell line models of latent and productive infection: Implications for HIV latency. *Retrovirology* **16**, 32 (2019).

11. Rao S., et al., Selective cell death in HIV-1-infected cells by DDX3 inhibitors leads to depletion of the inducible reservoir. *Nat. Commun.* **12**, 2475 (2021).

12. Crespo S., Rao S. & Mahmoudi T. HibeRNAtion: HIV-1 RNA metabolism and viral latency. *Front. Cell. Infect. Microbiol.* **12**, 855092 (2022).

13. Kumar A., Darcis A., Van Lint C. & Herbein G. Epigenetic control of HIV-1 post integration latency: Implications for therapy. *Clin. Epigenetics* **7**, 103 (2015).

14. Van Lint C., Bouchat S., Marcello A., HIV-1 transcription and latency: An update. *Retrovirology* **10**, 67 (2013).

15. Ne A., Palstra R. J. & Mahmoudi T., Transcription: Insights from the HIV-1 promoter. *Int. Rev. Cell Mol. Biol.* **335**, 191 243 (2018).

16. Wightman F., Ellenberg P., Churchill M. & Lewin S. R., HDAC inhibitors in HIV. *Immunol. Cell Biol.* **90**, 47 54 (2012).

17. Lehrman G., *et al*. Depletion of latent HIV-1 infection in vivo: A proof-of-concept study. *Lancet* **366**, 549-555 (2005).

18. Siliciano J. D., *et al*. Stability of the latent reservoir for HIV-1 in patients receiving valproic acid. *J. Infect. Dis.* **195**, 833-836 (2007).

19. Archin N. M., *et al*. Valproic acid without intensified antiviral therapy has limited impact on persistent HIV infection of resting CD4+ T cells. *AIDS* **22**, 1131-1135 (2008).

20. Sagot-Lerolle N. M., et al. ANRS EP39 study, Prolonged valproic acid treatment does not reduce the size of latent HIV reservoir. *AIDS* **22**, 1125-1129 (2008).

21. Archin N. M., *et al*. Antiretroviral intensification and valproic acid lack sustained effect on residual HIV-1 viremia or resting CD4+ cell infection. *PLOS ONE* **5**, e9390 (2010).

22. Routy J. P., *et al*. Valproic acid in association with highly active antiretroviral therapy for reducing systemic HIV-1 reservoirs: Results from a multi-centre randomized clinical study. *HIV Med.* **13**, 291-296 (2012).

23. Archin N. M., *et al*. Expression of latent HIV induced by the potent HDAC inhibitor suberoylanilide hydroxamic acid. *AIDS Res. Hum. Retrovir.* **25**, 207-212 (2009).

24. Archin N. M., *et al*. Administration of vorinostat disrupts HIV-1 latency in patients on antiretroviral therapy. *Nature* **487**, 482-485 (2012).

25. Archin N. M., *et al*. HIV-1 expression within resting $CD4^+$ T cells after multiple doses of vorinostat. *J. Infect. Dis.* **210**, 728-735 (2014).

26. Elliott J. H., *et al*. Activation of HIV transcription with short-course vorinostat in HIV-infected patients on suppressive antiretroviral therapy. *PLOS Pathog.* **10**, e1004473 (2014).

27. Archin N. M., *et al*. Interval dosing with the HDAC inhibitor vorinostat effectively reverses HIV latency. *J. Clin. Invest.* **127**, 3126-3135 (2017).

28. Fidler S., *et al*. RIVER trial study group, Antiretroviral therapy alone versus antiretroviral therapy with a kick and kill approach, on measures of the HIV reservoir in participants with recent HIV infection (the RIVER trial): A phase 2, randomised trial. *Lancet* **395**, 888-898 (2020).

29. Ramos J. C., *et al*. Impact of Myc in HIV-associated non-Hodgkin lymphomas treated with EPOCH and outcomes with vorinostat (AMC-075 trial). *Blood* **136**, 1284-1297 (2020).

30. Kroon E., *et al*; SEARCH 019 and RV254 Study Teams, A randomized trial of vorinostat with treatment interruption after initiating antiretroviral therapy during acute HIV-1 infection. *J. Virus Erad.* **6**, 100004 (2020).

31. Gay C. L., *et al*. Stable latent HIV infection and low-level viremia despite treatment with the broadly neutralizing antibody VRC07-523LS and the latency reversal agent vorinostat. *J. Infect. Dis.* **225**, 856-861 (2022).

32. McMahon J. H., *et al*. Neurotoxicity with high-dose disulfiram and vorinostat used for HIV latency reversal. *AIDS* **36**, 75-82 (2022).

33. Scully E. P., *et al.*; A5366 study team, Impact of tamoxifen on vorinostat-induced human immunodeficiency virus expression in women on antiretroviral therapy: AIDS Clinical Trials Group A5366, the MOXIE trial. *Clin. Infect. Dis.* **75**, 1389-1396 (2022).

34. Rasmussen T. A., *et al*. Panobinostat, a histone deacetylase inhibitor, for latent-virus reactivation in HIV-infected patients on suppressive antiretroviral therapy: A phase 1/2, single group, clinical trial. *Lancet HIV* **1**, e13-e21 (2014).

35. Sogaard O. S., *et al*. The depsipeptide romidepsin reverses HIV-1 latency in vivo. *PLOS Pathog.* **11**, e1005142 (2015).

36. Leth S., *et al*. Combined effect of Vacc-4x, recombinant human granulocyte macrophage colony-stimulating factor vaccination, and romidepsin on the HIV-1 reservoir (REDUC): A single-arm, phase 1B/2A trial. *Lancet HIV* **3**, e463-e472 (2016).

37. Mothe B., *et al*. The BCN02 Study Investigators, HIVconsv vaccines and romidepsin in early-treated HIV-1-Infected individuals: Safety, immunogenicity and e ect on the viral reservoir (Study BCN02). *Front. Immunol.* **11**,823 (2020).

38. McMahon D. K., *et al*. A phase 1/2 randomized, placebo-controlled trial of romidespin in persons with HIV-1 on suppressive antiretroviral therapy. *J. Infect. Dis.* **224**, 648-656 (2021).

39. Gruell H., *et al*. Effect of 3BNC117 and romidepsin on the HIV-1 reservoir in people taking suppressive antiretroviral therapy (ROADMAP): A randomised, open-label, phase 2A trial. *Lancet Microbe* **3**, e203-e214 (2022).

40. Elliott J. H., *et al*. Short-term administration of disulfiram for reversal of latent HIV infection: A phase 2 dose-escalation study. *Lancet HIV* **2**, e520-e529 (2015). C. Gutierrez, S. Serrano-Villar,

41. Madrid-Elena N., *et al*. Bryostatin-1 for latent virus reactivation in HIV-infected patients on antiretroviral therapy. *AIDS* **30**, 1385-1392 (2016).

42. Vibholm L., *et al*. Short-course Toll-like receptor 9 agonist treatment impacts innate immunity and plasma viremia in individuals with human immunodeficiency virus infection. *Clin. Infect. Dis*. **64**, 1686-1695 (2017).

43. Uldrick T. S., *et al*. Pembrolizumab induces HIV latency reversal in people living with HIV and cancer on antiretroviral therapy. *Sci. Transl. Med.* **14**, eabl3836 (2022).

44. Stoszko M., *et al*. Small molecule inhibitors of BAF: A promising family of compounds in HIV-1 latency reversal. *EBioMedicine* **3**, 108-121 (2016).

45. Marian C. A., *et al*. Small molecule targeting of specific BAF (mSWI/SNF) complexes for HIV latency reversal. *Cell Chem. Biol.* **25**, 1443 1455.e14 (2018).

46. Ne E., *et al*. Catchet-MS identifies IKZF1-targeting thalidomide analogues as novel HIV-1 latency reversal agents. *Nucleic Acids Res.* **50**, 5577-5598 (2022).

47. Mahmoudi T., The BAF complex and HIV latency. *Transcription* **3**, 171-176 (2012).

48. Rafati H., *et al*. Repressive LTR nucleosome positioning by the BAF complex is required for HIV latency. *PLOS Biol.* **9**, e1001206 (2011).

49. Jacobson J. M., *et al*. Pyrimethamine pharmacokinetics in human immunodeficiency virus-positive patients seropositive for toxoplasma gondii. *Antimicrob. Agents Chemother.* **40**, 1360-1365 (1996).

50. Klinker H., Langmann P. & Richter E. Pyrimethamine alone as prophylaxis for cerebral toxoplasmosis in patients with advanced HIV infection. *Infection* **24**, 324-327 (1996).

51. Klinker H., Langmann P. & Richter E. Plasma pyrimethamine concentrations during long-term treatment for cerebral toxoplasmosis in patients with AIDS. *Antimicrob. Agents Che-mother.* **40**, 1623-1627 (1996).

52. Schmidt D. R., *et al*. Treatment of infants with congenital toxoplasmosis: Tolerability and plasma concentrations of sulfa-diazine and pyrimethamine. *Eur. J. Pediatr.* **165**, 19-25 (2006).

53. Kongsaengdao S., *et al*. Randomized controlled trial of pyrimethamine plus sulfadiazine versus trimethoprim plus sulfamethoxazole for treatment of toxoplasmic encephalitis in AIDS patients. *J. Int. Assoc. Physicians AIDS Care (Chic.)* **7**, 11-16 (2008).

54. Jacobson J. M., *et al*.; ACTG 156 Study Team, Dose-escalation, phase I/II study of azithromycin and pyrimethamine for the treatment of toxoplasmic encephalitis in AIDS. *AIDS* **15**, 583-589 (2001).

55. Unger H. W., *et al*. Sulpha-doxine-pyrimethamine plus azithromycin for the prevention of low birthweight in Papua New Guinea: A randomised controlled trial. *BMC Med.* **13**, 9 (2015).

56. Chirgwin K., *et al*.; AIDS Clinical Trials Group 237/ Agence Nationale de Recherche sur le SIDA Essai 039 Study Team, Randomized phase II trial of atovaquone with pyrimethamine or sulfadiazine for treatment of toxoplasmic encephalitis in patients with acquired immunodeficiency syndrome: ACTG 237/ANRS 039 Study. *Clin. Infect. Dis.* **34**, 1243 1250 (2002).

57. U.S. Food and Drug Administration, Pyrimethamine summary of product charachteristics; www.accessdata.fda.gov/drugsatfda_docs/label/2003/08578slr016_daraprim_lbl.pdf.

58. Ylisastigui L., *et al*. Coaxing HIV-1 from resting CD4 T cells: Histone deacetylase inhibition allows latent viral expression. *AIDS* **18**, 1101-1108 (2004).

59. Reuse S., *et al*. Synergistic activation of HIV-1 expression by deacetylase inhibitors and prostratin: Implications for treatment of latent infection. *PLOS ONE* **4**, e6093 (2009).

60. McLeod S., *et al*. Levels of pyrimethamine in sera and cerebrospinal and ventricular fluids from infants treated for congenital toxoplasmosis. Toxoplasmosis study group. *Antimicrob. Agents Chemother.* **36**, 1040-1048 (1992).

61. Bollen P. D. J., *et al*. The dolutegravir/valproic acid drug-drug interaction is primarily based on protein displacement. *J. Antimicrob. Chemother.* **76**, 1273 1276 (2021).

62. U.S. Food and Drug Administration, Valproic acid summary of product characteristics;www.accessdata.fda.gov/drugsatfda_docs/label/2009/018081s047,018082s032lbl.pdf.

63. Wurster A. L., *et al.* IL-10 transcription is negatively regulated by BAF180, a component of the SWI/SNF chromatin remodeling enzyme. *BMC Immunol.* **13**, 9 (2012).

64. Dykhuizen E. C., *et al*. Screening for inhibitors of an essential chromatin remodeler in mouse embryonic stem cells by monitoring transcriptional regulation. *J. Biomol. Screen.* **17**, 1221-1230 (2012).

65. Barker N., *et al*. The chromatin remodelling factor Brg-1 interacts with β-catenin to promote target gene activation. *EMBO J.* **20**, 4935 4943 (2001).

66. Ni Z. & Bremner R. Brahma-related gene 1-dependent STAT3 recruitment at IL-6-inducible genes. *J. Immunol.* **178**, 345 351 (2007).

67. Procopio F. A., *et al*. Chomont, A Novel Assay to Measure the Magnitude of the Inducible Viral Reservoir in HIV-infected Individuals. *EBioMedicine* **2**, 874 883 (2015).

68. Lungu C., *et al*. Inter-laboratory reproducibility of inducible HIV-1 reservoir quantification by TILDA. *Viruses* **12**, 973 (2020).

69. Kim S. Y., *et al*. Temporal aspects of DNA and RNA synthesis during human immunodeficiency virus infection: Evidence for di erential gene expres-sion. *J. Virol.* **63**, 3708 3713 (1989).

70. Mary C., *et al*. Quantitative and discriminative detection of individual HIV-1 mRNA subspecies by an RNAse mapping assay. *J. Virol. Methods* **49**, 9 23 (1994).

71. van Baalen C. A., *et al*. Impact of antigen expression kinetics on the effectiveness of HIV-specific cytotoxic T lymphocytes. *Eur. J. Immunol.* **32**, 2644-2652 (2002).

72. Pasternak A. O., *et al*. Highly sensitive methods based on seminested real-time reverse tran-scription-PCR for quantitation of human immunodeficiency virus type 1 unspliced and multiply spliced RNA and proviral DNA. *J. Clin. Microbiol.* **46**, 2206 2211 (2008).

73. Schmittgen T. D., & Livak K. J. Analyzing real-time PCR data by the comparative CT method. *Nat. Protoc.* **3**, 1101 1108 (2008).

Chapter 3

1. Finzi, D., *et al*. Identification of a reservoir for HIV-1 in patients on highly active antiretroviral therapy. *Science* **278**, 1295–1300 (1997).

2. Chun, T. W., Moir, S. & Fauci, A. S. HIV reservoirs as obstacles and opportunities for an HIV cure. *Nat. Immunol.* **16**, 584–589 (2015).

3. Deeks, S. G., HIV: shock and kill. *Nature* **487**, 439–440 (2012).

4. Delagrèverie, H. M., Delaugerre, C., Lewin, S. R., Deeks, S. G. & Li, J. Z. Ongoing clinical trials of human immunodeficiency virus latency-reversing and immunomodulatory agents. *Open Forum Infect. Dis.* **3**, ofw189 (2016).

5. Rasmussen, T. A., Lewin, S. R. Shocking HIV out of hiding: where are we with clinical trials of latency reversing agents? *Curr. Opin. HIV AIDS* **11**, 394–401 (2016).

6. Zerbato, J. M., Purves, H. V., Lewin, S. R. & Rasmussen, T. A. Between a shock and a hard place: challenges and developments in HIV latency reversal. *Curr. Opin. Virol.* **38**, 1–9 (2019).

7. Thorlund, K., Horwitz, M. S., Fife, B. T., Lester, R. & Cameron, D. W. Landscape review of current HIV 'kick and kill' cure research - some kicking, not enough killing. *BMC Infect. Dis.* **17**, 595–595 (2017).

8. Leth, S., *et al*. Combined effect of Vacc-4x, recombinant human granulocyte macrophage colony-stimulating factor vaccination, and romidepsin on the HIV-1 reservoir (REDUC): a single-arm, phase 1B/2A trial. *Lancet HIV* **3**, e463–e472 (2016).

9. Fidler, S., *et al*. Antiretroviral therapy alone versus antiretroviral therapy with a kick and kill approach, on measures of the HIV reservoir in participants with recent HIV infection (the RIVER trial): a phase 2, randomised trial. *Lancet* **395**, 888–898 (2020).

10. Gay, C. L., *et al*. Assessing the impact of AGS-004, a dendritic cell-based immunotherapy, and vorinostat on persistent HIV infection. *Sci. Rep.* **10**, 5134 (2020).

11. Margolis, D. M., *et al*. Curing HIV: seeking to target and clear persistent infection. *Cell* **181**, 189–206 (2020).

12. Cummins, N. W. & Badley, A. D., Mechanisms of HIV-associated lymphocyte apoptosis: 2010. *Cell Death Dis*. **1**, e99 (2010).

13. Kim, Y., Anderson, J. L. & Lewin, S. R. Getting the "Kill" into "Shock and Kill": strategies to eliminate latent HIV. *Cell Host Microbe* **23**, 14–26 (2018).

14. Cooney, J., Allison, C., Preston, S. & Pellegrini, M. Therapeutic manipulation of host cell death pathways to facilitate clearance of persistent viral infections. *J. Leukoc. Biol*. **103**, 287–293 (2018).

15. Baxter, A. E., *et al*. Single-cell characterization of viral translation-competent reservoirs in HIV-infected individuals. *Cell Host Microbe* **20**, 368–380 (2016).

16. Grau-Exposito, J., *et al*. A novel single-cell FISH-Flow assay identifies effector memory CD4(+) T cells as a major niche for HIV-1 transcription in HIV-infected patients. *mBio* **8**, e00876–17 (2017).

17. Berg, R. K., *et al*. Genomic HIV RNA induces innate immune responses through RIG-I-dependent sensing of secondary-structured RNA. *PLoS ONE* **7**, e29291 (2012).

18. Fong, L. E., Sulistijo, E. S., & Miller-Jensen, K. Systems analysis of latent HIV reversal reveals altered stress kinase signaling and increased cell death in infected T cells. *Sci. Rep*. **7**, 16179 (2017).

19. Baxter, A. E., O'Doherty, U. & Kaufmann, D. E. Beyond the replication-competent HIV reservoir: transcription and translation-competent reservoirs. *Retrovirology* **15**, 18 (2018).

20. Baxter, A. E., *et al*. Multiparametric characterization of rare HIV-infected cells using an RNA-flow FISH technique. *Nat. Protoc*. **12**, 2029–2049 (2017).

21. Rao, S., Amorim, R., Niu, M., Temzi, A. & Mouland, A. J. The RNA surveillance proteins UPF1, UPF2 and SMG6 affect HIV-1 reactivation at a post-transcriptional level. *Retrovirology* **15**, 42 (2018).

22. Grau-Expósito, J., *et al*. Latency reversal agents affect differently the latent reservoir present in distinct CD4+ T subpopulations. *PLoS Pathog*. **15**, e1007991 (2019).

23. Linder, P. & Jankowsky, E. From unwinding to clamping—the DEAD box RNA helicase family. *Nat. Rev. Mol. Cell Biol*. **12**, 505–516 (2011).

24. Zhao, L., *et al*. Multifunctional DDX3: dual roles in various cancer development and its related signaling pathways. *Am. J. Cancer Res*. **6**, 387–402 (2016).

25. Soto-Rifo, R. & Ohlmann, T. The role of the DEAD-box RNA helicase DDX3 in mRNA metabolism. *Wiley Interdiscip. Rev. RNA* **4**, 369–385 (2013).

26. Lin, T. C. DDX3X multifunctionally modulates tumor progression and serves as a prognostic indicator to predict cancer outcomes. *Int. J. Mol. Sci*. **21**, 281 (2019).

27. Bol, G. M., Xie, M. & Raman, V. DDX3, a potential target for cancer treatment. *Mol. Cancer* **14**, 188 (2015).

28. Heerma van Voss, M. R., van Diest, P. J. & Raman, V. Targeting RNA helicases in cancer: the translation trap. *Biochim. Biophys. Acta Rev.* Cancer **1868**, 510–520 (2017).

29. He, Y., *et al*. A double-edged function of DDX3, as an oncogene or tumor suppressor, in cancer progression (Review). *Oncol. Rep*. **39**, 883–892 (2018).

30. Kukhanova, M. K., Karpenko, I. L. & Ivanov, A. V. DEAD-box RNA helicase DDX3: functional properties and development of DDX3 inhibitors as antiviral and anticancer drugs. *Molecules* **25**, 1015 (2020).

31. Valiente-Echeverria, F., Hermoso, M. A. & Soto-Rifo, R. RNA helicase DDX3: at the crossroad of viral replication and antiviral immunity. *Rev. Med. Virol*. **25**, 286–299 (2015).

32. Yedavalli, V. S., Neuveut, C., Chi, Y. H., Kleiman, L. & Jeang, K. T. Requirement of DDX3 DEAD box RNA helicase for HIV-1 Rev-RRE export function. *Cell* **119**, 381–392 (2004).

33. Mahboobi, S. H., Javanpour, A. A. & Mofrad, M. R. The interaction of RNA helicase DDX3 with HIV-1 Rev-CRM1-RanGTP complex during the HIV replication cycle. *PLoS ONE* **10**, e0112969 (2015).

34. Soto-Rifo, R., *et al*. DEAD-box protein DDX3 associates with eIF4F to promote translation of selected mRNAs. *Embo J.* **31**, 3745–3756 (2012).

35. Frohlich, A., *et al*. DEAD-box RNA helicase DDX3 connects CRM1-dependent nuclear export and translation of the HIV-1 unspliced mRNA through its N-terminal domain. *Biochim. Biophys. Acta* **1859**, 719–730 (2016).

36. Soto-Rifo, R., Rubilar, P. S. & Ohlmann, T. The DEAD-box helicase DDX3 substitutes for the cap-binding protein eIF4E to promote compartmentalized translation initiation of the HIV-1 genomic RNA. *Nucleic Acids Res.* **41**, 6286–6299 (2013).

37. Gringhuis, S. I., *et al*. Erratum: HIV-1 blocks the signaling adaptor MAVS to evade antiviral host defense after sensing of abortive HIV-1 RNA by the host helicase DDX3. *Nat. Immunol.* **18**, 474 (2017).

38. Brai, A., *et al*. Human DDX3 protein is a valuable target to develop broad spectrum antiviral agents. *Proc. Natl Acad. Sci. USA* **113**, 5388–5393 (2016).

39. Jordan, A., Bisgrove, D. & Verdin, E. HIV reproducibly establishes a latent infection after acute infection of T cells in vitro. *Embo J*. **22**, 1868–1877 (2003).

40. Bol, G. M., *et al*. Targeting DDX3 with a small molecule inhibitor for lung cancer therapy. *EMBO Mol. Med*. **7**, 648–669 (2015).

41. Kondaskar, A., *et al*. Novel, broad spectrum anti-cancer agents containing the tricyclic 5:7:5-fused diimidazodiazepine ring system. *ACS Med Chem. Lett*. **2**, 252–256 (2010).

42. Heerma van Voss, M. R. et al. Identification of the DEAD box RNA helicase DDX3 as a therapeutic target in colorectal cancer. *Oncotarget* **6**, 28312–28326 (2015).

43. Xie, M., *et al*. RK-33 radiosensitizes prostate cancer cells by blocking the RNA helicase DDX3. *Cancer Res*. **76**, 6340–6350 (2016).

44. Heerma van Voss, M. R., *et al*. Targeting mitochondrial translation by inhibiting DDX3: a novel radiosensitization strategy for cancer treatment. *Oncogene* **37**, 63–74 (2018).

45. Wang, X., *et al*. (DEAD)-box RNA helicase 3 modulates NF-kappaB signal pathway by controlling the phosphorylation of PP2A-C subunit. *Oncotarget* **8**, 33197–33213 (2017).

46. Xiang, N., *et al*. The DEAD-Box RNA Helicase DDX3 interacts with NF-κB subunit p65 and suppresses p65-mediated transcription. *PLoS ONE* **11**, e0164471 (2016).

47. Akira, S., Uematsu, S. & Takeuchi, O. Pathogen recognition and innate immunity. *Cell* **124**, 783–801 (2006).

48. Yoneyama, M. & Fujita, T. RNA recognition and signal transduction by RIGI-like receptors. *Immunol. Rev*. **227**, 54–65 (2009).

49. Hiscott, J. Convergence of the NF-kappaB and IRF pathways in the regulation of the innate antiviral response. *Cytokine Growth Factor Rev*. **18**, 483–490 (2007).

50. Balachandran, S., *et al*. Alpha/beta interferons potentiate virus-induced apoptosis through activation of the FADD/Caspase-8 death signaling pathway *J. Virol*. **74**, 1513–1523 (2000).

51. Chawla-Sarkar, M., *et al*. Apoptosis and interferons: role of interferon-stimulated genes as mediators of apoptosis. *Apoptosis* **8**, 237–249 (2003).

52. Juang, S. H., *et al*. IFN-beta induces caspase-mediated apoptosis by disrupting mitochondria in human advanced stage colon cancer cell lines. *J. Interferon Cytokine Res*. **24**, 231–243 (2004).

53. Radi, M., *et al*. Discovery of the first small molecule inhibitor of human DDX3 specifically designed to target the RNA binding site: towards the next generation HIV-1 inhibitors. *Bioorg. Med Chem. Lett*. **22**, 2094–2098 (2012).

54. Kuo, H. H., *et al*. Anti-apoptotic protein BIRC5 maintains survival of HIV-1-Infected CD4(+) T cells. *Immunity* **48**, 1183–1194 (2018).

55. Iordanskiy, S., *et al*. Heat shock protein 70 protects cells from cell cycle arrest and apoptosis induced by human immunodeficiency virus type 1 viral protein R. *J. Virol*. **78**, 9697–9704 (2004).

56. Kumar, M., *et al*. Reciprocal regulation of human immunodeficiency virus-1 gene expression and replication by heat shock proteins 40 and 70. *J. Mol. Biol*. **410**, 944–958 (2011).

57. Chaudhary, P., *et al*. HSP70 binding protein 1 (HspBP1) suppresses HIV-1 replication by inhibiting NF-κB mediated activation of viral gene expression. *Nucleic Acids Res*. **44**, 1613–1629 (2016).

58. Lassen, K. G., Hebbeler, A. M., Bhattacharyya, D., Lobritz, M. A. & Greene,W. C. A flexible model of HIV-1 latency permitting evaluation of many primary CD4 T-cell reservoirs. *PLoS ONE* **7**, e30176 (2012).

59. Stoszko, M., *et al*. Small molecule inhibitors of BAF; a promising family of compounds in HIV-1 latency reversal. *EBioMedicine* **3**, 108–121 (2015).

60. Marian, C. A., *et al*. Small molecule targeting of specific BAF (mSWI/SNF) complexes for HIV latency reversal. *Cell Chem. Biol*. **25**, 1443–1455 (2018).

61. Nakahara, T., *et al*. YM155, a novel small-molecule survivin suppressant, induces regression of established human hormone-refractory prostate tumor xenografts. *Cancer Res*. **67**, 8014–8021 (2007).

62. Akiyama, H., *et al*. HIV-1 intron-containing RNA expression induces innate immune activation and T cell dysfunction. *Nat. Commun*. **9**, 3450 (2018).

63. McCauley, S. M., *et al*. Intron-containing RNA from the HIV-1 provirus activates type I interferon and inflammatory cytokines. *Nat. Commun*. **9**, 5305 (2018).

64. Pache, L., *et al*. BIRC2/cIAP1 is a negative regulator of HIV-1 transcription and can be targeted by SMAC mimetics to promote reversal of viral latency. *Cell Host Microbe* **18**, 345–353 (2015).

65. Nixon, C. C., *et al*. Systemic HIV and SIV latency reversal via non-canonical NF-kappaB signalling in vivo. *Nature* **578**, 160–165 (2020).

66. Bobardt, M., *et al*. The inhibitor apoptosis protein antagonist Debio 1143 is an attractive HIV-1 latency reversal candidate. *PLoS ONE* **14**, e0211746 (2019).

67. Matsuda, K., *et al*. Benzolactam-related compounds promote apoptosis of HIV-infected human cells via protein kinase C-induced HIV latency reversal. *J. Biol. Chem*. **294**, 116–129 (2019).

68. Hattori, S. I., *et al*. Combination of a latency-reversing agent with a SMAC mimetic minimizes secondary HIV-1 infection in vitro. *Front. Microbiol*. **9**, 2022 (2018).

69. Rosás-Umbert, M., *et al*. In vivo effects of romidepsin on T-cell activation, apoptosis and function in the BCN02 HIV-1 Kick&Kill clinical trial. *Front. Immunol*. **11**, (2020).

70. Brai, A., *et al*. DDX3X inhibitors, an effective way to overcome HIV-1 resistance targeting host proteins. *Eur. J. Med. Chem*. **200**, 112319 (2020).

71. Cummins, N. W., *et al*. Maintenance of the HIV reservoir is antagonized by selective BCL2 inhibition. *J. Virol*. **91,** e00012–e00017 (2017).

72. Chandrasekar, A. P., Cummins, N. W. & Badley, A. D. The role of the BCL-2 family of proteins in HIV-1 pathogenesis and persistence. *Clin. Microbiol. Rev*. **33**, e00107–19 (2019).

73. Campbell, G. R., Bruckman, R. S., Chu, Y. L., Trout, R. N. & Spector, S. A. SMAC mimetics induce autophagy-dependent apoptosis of HIV-1-infected resting memory CD4+ T cells. *Cell Host Microbe* **24**, 689–702 (2018).

74. Zhang, G., *et al*. Selective cell death of latently HIV-infected CD4(+) T cells mediated by autosis inducing nanopeptides. *Cell Death Dis*. **10**, 419 (2019).

75. Lucas, A., *et al*. Targeting the PI3K/Akt cell survival pathway to induce cell death of HIV-1 infected macrophages with alkylphospholipid compounds. *PLoS ONE* **5**, e13121 (2010).

76. Tateishi, H., *et al*. A clue to unprecedented strategy to HIV eradication: "Lockin and apoptosis". *Sci. Rep*. **7**, 8957 (2017).

77. Stoszko, M., *et al*. Gliotoxin, identified from a screen of fungal metabolites, disrupts 7SK snRNP, releases P-TEFb and reverses HIV-1 latency. *Sci Adv*. **6** (33): eaba6617, (2020)

78. Stoszko, M., Ne, E., Abner, E. & Mahmoudi, T. A broad drug arsenal to attack a strenuous latent HIV reservoir. *Curr. Opin. Virol*. **38**, 37–53 (2019).

79. Schmittgen, T. D. & Livak, K. J. Analyzing real-time PCR data by the comparative C(T) method. Nat. Protoc. 3, 1101–1108 (2008).

80. Naldini, L., Blömer, U., Gage, F. H., Trono, D. & Verma, I. M. Efficient transfer, integration, and sustained long-term expression of the transgene in adult rat brains injected with a lentiviral vector. *Proc. Natl Acad. Sci. USA* **93,** 11382–11388 (1996).

81. Pettersen, E. F., *et al*. UCSF Chimera-a visualization system for exploratory research and analysis. *J. Comput. Chem*. **25**, 1605–1612 (2004).

82. Trott, O. & Olson, A. J. AutoDock Vina: improving the speed and accuracy of docking with a new scoring function, efficient optimization, and multithreading. *J. Comput. Chem*. **31**, 455–461 (2010).

83. Schmidt, E. K., Clavarino, G., Ceppi, M. & Pierre, P. SUnSET, a nonradioactive method to monitor protein synthesis. *Nat. Methods* **6**, 275–277 (2009).

84. Pasternak, A. O., *et al*. Highly sensitive methods based on semi-nested real-time reverse transcription-PCR for quantitation of human immunodeficiency virus type 1 unspliced and multiply spliced RNA and proviral DNA. *J. Clin. Microbiol*. **46**, 2206–2211 (2008).

85. Lungu, C., *et al*. Inter-laboratory reproducibility of inducible HIV-1 reservoir quantification by TILDA. *Viruses* **12**, 973 (2020).

86. Procopio, F. A., *et al*. A novel assay to measure the magnitude of the inducible viral reservoir in HIV-infected individuals. *EBioMedicine* **2**, 874–883 (2015).

87. Hu, Y. & Smyth, G. K. ELDA: extreme limiting dilution analysis for comparing depleted and enriched populations in stem cell and other assays. *J. Immunol. Methods* **347**, 70–78 (2009).

88. Robinson, M. D., McCarthy, D. J. & Smyth, G. K. edgeR: a Bioconductor package for differential expression analysis of digital gene expression data. *Bioinformatics* **26**, 139–140 (2010).

Chapter 4

1. Chun, T. W., *et al.* Early establishment of a pool of latently infected, resting CD4(+) T cells during primary HIV-1 infection. *Proc Natl Acad Sci U S A* **95**, 8869-8873 (1998).

2. Abdel-Mohsen, M., *et al.* Recommendations for measuring HIV reservoir size in cure-directed clinical trials. *Nature Medicine* **26**, 1339-1350 (2020).

3. Garner, S. A., *et al.* Interrupting antiretroviral treatment in HIV cure research: scientific and ethical considerations. *J Virus Erad* **3**, 82-84 (2017).

4. Magalhaes, M., Kuritzkes, D. R. & Eyal N. The ethical case for placebo control in HIV-cure-related studies with ART interruption. *J Virus Erad* **8**, 100084 (2022).

5. Julg, B., *et al.*, Recommendations for analytical antiretroviral treatment interruptions in HIV research trials-report of a consensus meeting. *Lancet HIV* **6**, e259-e268 (2019).

6. Kutzler, M. A. & J. M. Jacobson, Treatment interruption as a tool to measure changes in immunologic response to HIV-1. *Curr Opin HIV AIDS* **3**, 131-135 (2008).

7. Lau, J. S. Y., Smith M. Z., Lewin S. R., McMahon J. H. Clinical trials of antiretroviral treatment interruption in HIV-infected individuals. *AIDS* **33**, 773-791 (2019).

8. Richart, V., *et al.* High rate of long-term clinical events after antiretroviral therapy resumption in HIV-positive patients exposed to antiretroviral therapy interruption. *AIDS* **35**, 2463-2468 (2021).

9. Strategies for Management of Antiretroviral Therapy (SMART) Study Group; El Sadr W.M., *et al.*, CD4+ count-guided interruption of antiretroviral treatment. *N Engl J Med* **355**, 2283-2296 (2006).

10. Imaz, A., *et al.* Short-term and long-term clinical and immunological consequences of stopping antiretroviral therapy in HIV-infected patients with preserved immune function. *Antivir Ther* **18**, 125-130 (2013).

11. Gunst, J. D, *et al.* Impact of a TLR9 agonist and broadly neutralizing antibodies on HIV-1 persistence: the randomized phase 2a TITAN trial. *Nat Med* 10.1038/s41591-023-02547-6 (2023).

12. Gaebler, C., *et al.* Prolonged viral suppression with anti-HIV-1 antibody therapy. *Nature* **606**, 368-374 (2022).

13. Gruell H., *et al.* Effect of 3BNC117 and romidepsin on the HIV-1 reservoir in people taking suppressive antiretroviral therapy (ROADMAP): a randomised, open-label, phase 2A trial. *Lancet Microbe* **3**, e203-e214 (2022).

14. Cole B., *et al.* Extensive characterization of HIV-1 reservoirs reveals links to plasma viremia before and during analytical treatment interruption. *Cell Rep* **39**, 110739 (2022).

15. Wedrychowski A., *et al.* Transcriptomic Signatures of Human Immunodeficiency Virus Post-Treatment Control. *J Virol* **97**, e0125422 (2023).

16. De Scheerder M. A., *et al.* Evaluating predictive markers for viral rebound and safety assessment in blood and lumbar fluid during HIV-1 treatment interruption. *J Antimicrob Chemother* **75**, 1311-1320 (2020).

17. Papasavvas E., *et al.* Analytical antiretroviral therapy interruption does not irreversibly change preinterruption levels of cellular HIV. *AIDS* **32**, 1763-1772 (2018).

18. Scutari R, *et al.* Impact of Analytical Treatment Interruption on Burden and Diversification of HIV Peripheral Reservoir: A Pilot Study. *Viruses* **13** (2021).

19. Strongin Z., *et al.* Effect of Short-Term Antiretroviral Therapy Interruption on Levels of Integrated HIV DNA. *J Virol* **92** (2018).

20. Montserrat, M., *et al.* Impact of long-term antiretroviral therapy interruption and resumption on viral reservoir in HIV-1 infected patients. *AIDS* **31**, 1895-1897 (2017).

21. Allard S.D., *et al.* A phase I/IIa immunotherapy trial of HIV-1-infected patients with Tat, Rev and Nef expressing dendritic cells followed by treatment interruption. *Clin Immunol* **142**, 252-268 (2012).

22. Bruner, K. M., *et al.* A quantitative approach for measuring the reservoir of latent HIV-1 proviruses. *Nature* **566**, 120-125 (2019).

23. Baxter, A. E., *et al.* Multiparametric characterization of rare HIV-infected cells using an RNA-flow FISH technique. *Nat Protoc* **12**, 2029-2049 (2017).

24. Sannier G., *et al.* Combined single-cell transcriptional, translational, and genomic profiling reveals HIV-1 reservoir diversity. *Cell Rep* **36**, 109643 (2021).

25. Grau-Exposito, J., *et al.* Latency reversal agents affect differently the latent reservoir present in distinct CD4+ T subpopulations. *PLoS Pathog* **15**, e1007991 (2019).

26. Hossain T., *et al.*, SQuHIVLa: A novel assay for Specific Quantification of inducible HIV-1 reservoir by LAMP. *bioRxiv* 10.1101/2023.07.14.548928, 2023.2007.2014.548928 (2023).

27. Zerbato, J. M., *et al.* Multiply spliced HIV RNA is a predictive measure of virus production ex vivo and in vivo following reversal of HIV latency. *EBioMedicine* **65**, 103241 (2021).

28. Fischer, M., *et al.* Cellular viral rebound after cessation of potent antiretroviral therapy predicted by levels of multiply spliced HIV-1 RNA encoding nef. *J Infect Dis* **190**, 1979-1988 (2004).

29. Clarridge, K. E., *et al.*, Effect of analytical treatment interruption and reinitiation of antiretroviral therapy on HIV reservoirs and immunologic parameters in infected individuals. *PLoS Pathog* **14**, e1006792 (2018).

30. Salantes, D. B., *et al.* HIV-1 latent reservoir size and diversity are stable following brief treatment interruption. *J Clin Invest* **128**, 3102-3115 (2018).

31. Huiting, E. D., *et al.* Impact of Treatment Interruption on HIV Reservoirs and Lymphocyte Subsets in Individuals Who Initiated Antiretroviral Therapy During the Early Phase of Infection. *J Infect Dis* **220**, 270-274 (2019).

32. Pannus, P., *et al.* Rapid viral rebound after analytical treatment interruption in patients with very small HIV reservoir and minimal on-going viral transcription. *J Int AIDS Soc* **23**, e25453 (2020).

33. de Goede, A. L., *et al.*, DC immunotherapy in HIV-1 infection induces a major blood transcriptome shift. *Vaccine* **33**, 2922-2929 (2015).

34. Abrahams, M. R., *et al.* The replication-competent HIV-1 latent reservoir is primarily established near the time of therapy initiation. *Sci Transl Med* **11** (2019).

35. Brodin, J., *et al.* Establishment and stability of the latent HIV-1 DNA reservoir. *Elife* **5** (2016).

36. Jones B. R. & Joy J. B. Inferring Human Immunodeficiency Virus 1 Proviral Integration Dates With Bayesian Inference. *Mol Biol Evol* **40** (2023).

37. Baxter A. E., O'Doherty, U. & Kaufmann, D. E. Beyond the replication-competent HIV reservoir: transcription and translation-competent reservoirs. *Retrovirology* **15**, 18 (2018).

38. Pollack, R. A., *et al.* Defective HIV-1 Proviruses Are Expressed and Can Be Recognized by Cytotoxic T Lymphocytes, which Shape the Proviral Landscape. *Cell Host Microbe* **21**, 494-506 e494 (2017).

39. Imamichi, H. *et al.* Defective HIV-1 proviruses produce viral proteins. *Proc Natl Acad Sci U S A* **117**, 3704-3710 (2020).

40. Imamichi, H. *et al.* Defective HIV-1 proviruses produce novel protein-coding RNA species in HIV-infected patients on combination antiretroviral therapy. *Proc Natl Acad Sci U S A* **113**, 8783-8788 (2016).

41. Gandhi, R. T., *et al.* Varied Patterns of Decay of Intact HIV-1 Proviruses Over two Decades of Art. *J Infect Dis* 10.1093/infdis/jiad039 (2023).

42. Peluso, M. J., *et al.* Differential decay of intact and defective proviral DNA in HIV-1-infected individuals on suppressive antiretroviral therapy. *JCI Insight* **5** (2020).

43. van Snippenberg, W., *et al.* Triplex digital PCR assays for the quantification of intact proviral HIV-1 DNA. *Methods* **201**, 41-48 (2022).

44. Sarabia I., Huang, S. H., Ward A. R., Jones R. B. & Bosque A. The Intact Non-Inducible Latent HIV-1 Reservoir is Established In an In Vitro Primary T(CM) Cell Model of Latency. *J Virol* **95** (2021).

45. Rao, S. *et al.* Selective cell death in HIV-1-infected cells by DDX3 inhibitors leads to depletion of the inducible reservoir. *Nat Commun* **12**, 2475 (2021).

46. C. Lungu & F. A. Procopio, TILDA: Tat/Rev Induced Limiting Dilution Assay. *Methods Mol Biol* **2407**, 365-372 (2022).

Chapter 5 – 6

1. Deeks, S.G., *et al.* Research priorities for an HIV cure: International AIDS Society Global Scientific Strategy 2021. *Nat Med* **27**, 2085-2098 (2021).

2. Garner, S.A., *et al.* Interrupting antiretroviral treatment in HIV cure research: scientific and ethical considerations. *J Virus Erad* **3**, 82-84 (2017).

3. Magalhaes, M., Kuritzkes, D.R. & Eyal, N. The ethical case for placebo control in HIV-cure-related studies with ART interruption. *J Virus Erad* **8**, 100084 (2022).

4. Gandhi, R.T., *et al.* Varied Patterns of Decay of Intact HIV-1 Proviruses Over two Decades of Art. *J Infect Dis* (2023).

5. Brodin, J., *et al.* Establishment and stability of the latent HIV-1 DNA reservoir. *Elife* **5**(2016).

6. Peluso, M.J., *et al.* Differential decay of intact and defective proviral DNA in HIV-1-infected individuals on suppressive antiretroviral therapy. *JCI Insight* **5**(2020).

7. Imamichi, H., *et al.* Defective HIV-1 proviruses produce viral proteins. *Proc Natl Acad Sci U S A* **117**, 3704-3710 (2020).

8. Imamichi, H., *et al.* Defective HIV-1 proviruses produce novel protein-coding RNA species in HIV-infected patients on combination antiretroviral therapy. *Proc Natl Acad Sci U S A* **113**, 8783-8788 (2016).

9. Pollack, R.A., *et al.* Defective HIV-1 Proviruses Are Expressed and Can Be Recognized by Cytotoxic T Lymphocytes, which Shape the Proviral Landscape. *Cell Host Microbe* **21**, 494-506 e494 (2017).

10. Chun, T.W., Engel, D., Mizell, S.B., Ehler, L.A. & Fauci, A.S. Induction of HIV-1 replication in latently infected CD4+ T cells using a combination of cytokines. *J Exp Med* **188**, 83-91 (1998).

11. Ho, Y.C.*, et al.* Replication-competent noninduced proviruses in the latent reservoir increase barrier to HIV-1 cure. *Cell* **155**, 540-551 (2013).

12. Chun, T.W.*, et al.* Quantification of latent tissue reservoirs and total body viral load in HIV-1 infection. *Nature* **387**, 183-188 (1997).

13. Vibholm, L.K.*, et al.* Characterization of Intact Proviruses in Blood and Lymph Node from HIV-Infected Individuals Undergoing Analytical Treatment Interruption. *J Virol* **93**(2019).

14. Reeves, D.B.*, et al.* Impact of misclassified defective proviruses on HIV reservoir measurements. *Nat Commun* **14**, 4186 (2023).

15. Gaebler, C.*, et al.* Sequence Evaluation and Comparative Analysis of Novel Assays for Intact Proviral HIV-1 DNA. *J Virol* **95**(2021).

16. Cassidy, N.A.J.*, et al.* HIV reservoir quantification using cross-subtype multiplex ddPCR. *iScience* **25**, 103615 (2022).

17. Levy, C.N.*, et al.* A highly multiplexed droplet digital PCR assay to measure the intact HIV-1 proviral reservoir. *Cell Rep Med* **2**, 100243 (2021).

18. Siliciano, J.D. & Siliciano, R.F. Low Inducibility of Latent Human Immunodeficiency Virus Type 1 Proviruses as a Major Barrier to Cure. *J Infect Dis* **223**, 13-21 (2021).

19. Tumpach, C.*, et al.* Adaptation of Droplet Digital PCR-Based HIV Transcription Profiling to Digital PCR and Association of HIV Transcription and Total or Intact HIV DNA. *Viruses* **15**(2023).

20. Martin, H.A.*, et al.* New Assay Reveals Vast Excess of Defective over Intact HIV-1 Transcripts in Antiretroviral Therapy-Suppressed Individuals. *J Virol* **96**, e0160522 (2022).

21. Einkauf, K.B.*, et al.* Parallel analysis of transcription, integration, and sequence of single HIV-1 proviruses. *Cell* **185**, 266-282 e215 (2022).

22. Einkauf, K.B.*, et al.* Intact HIV-1 proviruses accumulate at distinct chromosomal positions during prolonged antiretroviral therapy. *J Clin Invest* **129**, 988-998 (2019).

23. Lian, X.*, et al.* Progressive transformation of the HIV-1 reservoir cell profile over two decades of antiviral therapy. *Cell Host Microbe* **31**, 83-96 e85 (2023).

24. Fischer, M.*, et al.* Cellular viral rebound after cessation of potent antiretroviral therapy predicted by levels of multiply spliced HIV-1 RNA encoding nef. *J Infect Dis* **190**, 1979-1988 (2004).

25. Zerbato, J.M.*, et al.* Multiply spliced HIV RNA is a predictive measure of virus production ex vivo and in vivo following reversal of HIV latency. *EBioMedicine* **65**, 103241 (2021).

26. Lungu, C. & Procopio, F.A. TILDA: Tat/Rev Induced Limiting Dilution Assay. *Methods Mol Biol* **2407**, 365-372 (2022).

27. Procopio, F.A.*, et al.* A Novel Assay to Measure the Magnitude of the Inducible Viral Reservoir in HIV-infected Individuals. *EBioMedicine* **2**, 874-883 (2015).

28. Plantin, J., Massanella, M. & Chomont, N. Inducible HIV RNA transcription assays to measure HIV persistence: pros and cons of a compromise. *Retrovirology* **15**, 9 (2018).

29. Lungu, C., Banga, R., Gruters, R.A. & Procopio, F.A. Inducible HIV-1 Reservoir Quantification: Clinical Relevance, Applications and Advancements of TILDA. *Front Microbiol* **12**, 686690 (2021).

30. Massanella, M.*, et al.* Improved assays to measure and characterize the inducible HIV reservoir. *EBioMedicine* **36**, 113-121 (2018).

31. Deeks, S.G. HIV: Shock and kill. *Nature* **487**, 439-440 (2012).

32. Quivy, V., De Walque, S. & Van Lint, C. Chromatin-associated regulation of HIV-1 transcription: implications for the development of therapeutic strategies. *Subcell Biochem* **41**, 371-396 (2007).

33. Wu, G.*, et al.* HDAC inhibition induces HIV-1 protein and enables immune-based clearance following latency reversal. *JCI Insight* **2**(2017).

34. Mahmoudi, T. The BAF complex and HIV latency. *Transcription* **3**, 171-176 (2012).

35. Kulpa, D.A. & Chomont, N. HIV persistence in the setting of antiretroviral therapy: when, where and how does HIV hide? *J Virus Erad* **1**, 59-66 (2015).

36. Rafati, H.*, et al.* Repressive LTR nucleosome positioning by the BAF complex is required for HIV latency. *PLoS Biol* **9**, e1001206 (2011).

37. Stoszko, M., Ne, E., Abner, E. & Mahmoudi, T. A broad drug arsenal to attack a strenuous latent HIV reservoir. *Curr Opin Virol* **38**, 37-53 (2019).

38. Prins, H.A.B.*, et al.* The BAF complex inhibitor pyrimethamine reverses HIV-1 latency in people with HIV-1 on antiretroviral therapy. *Sci Adv* **9**, eade6675 (2023).

39. Ait-Ammar, A.*, et al.* Current Status of Latency Reversing Agents Facing the Heterogeneity of HIV-1 Cellular and Tissue Reservoirs. *Front Microbiol* **10**, 3060 (2019).

40. Rao, S. Sex differences in HIV-1 persistence and the implications for a cure. *Front Glob Womens Health* **3**, 942345 (2022).

41. Scully, E.P.*, et al.* Sex-Based Differences in Human Immunodeficiency Virus Type 1 Reservoir Activity and Residual Immune Activation. *J Infect Dis* **219**, 1084-1094 (2019).

42. Kim, Y., Anderson, J.L. & Lewin, S.R. Getting the "Kill" into "Shock and Kill": Strategies to Eliminate Latent HIV. *Cell Host Microbe* **23**, 14-26 (2018).

43. Spivak, A.M. & Planelles, V. HIV-1 Eradication: Early Trials (and Tribulations). *Trends Mol Med* **22**, 10-27 (2016).

44. Thorlund, K., Horwitz, M.S., Fife, B.T., Lester, R. & Cameron, D.W. Landscape review of current HIV 'kick and kill' cure research - some kicking, not enough killing. *BMC Infect Dis* **17**, 595 (2017).

45. Rao, S.*, et al.* Selective cell death in HIV-1-infected cells by DDX3 inhibitors leads to depletion of the inducible reservoir. *Nat Commun* **12**, 2475 (2021).

46. Chun, T.W.*, et al.* Early establishment of a pool of latently infected, resting CD4(+) T cells during primary HIV-1 infection. *Proc Natl Acad Sci U S A* **95**, 8869-8873 (1998).

47. Cohen, M.S., Shaw, G.M., McMichael, A.J. & Haynes, B.F. Acute HIV-1 Infection. *N Engl J Med* **364**, 1943-1954 (2011).

48. Leyre, L.*, et al.* Abundant HIV-infected cells in blood and tissues are rapidly cleared upon ART initiation during acute HIV infection. *Sci Transl Med* **12**(2020).

49. Colby, D.J.*, et al.* Rapid HIV RNA rebound after antiretroviral treatment interruption in persons durably suppressed in Fiebig I acute HIV infection. *Nat Med* **24**, 923-926 (2018).

50. Julg, B.*, et al.* Recommendations for analytical antiretroviral treatment interruptions in HIV research trials-report of a consensus meeting. *Lancet HIV* **6**, e259-e268 (2019).

51. Stecher, M.*, et al.* Systematic Review and Meta-analysis of Treatment Interruptions in Human Immunodeficiency Virus (HIV) Type 1-infected Patients Receiving Antiretroviral Therapy: Implications for Future HIV Cure Trials. *Clin Infect Dis* **70**, 1406-1417 (2020).

52. Kutzler, M.A. & Jacobson, J.M. Treatment interruption as a tool to measure changes in immunologic response to HIV-1. *Curr Opin HIV AIDS* **3**, 131-135 (2008).

53. Huiting, E.D.*, et al.* Impact of Treatment Interruption on HIV Reservoirs and Lymphocyte Subsets in Individuals Who Initiated Antiretroviral Therapy During the Early Phase of Infection. *J Infect Dis* **220**, 270-274 (2019).

54. De Scheerder, M.A.*, et al.* Evaluating predictive markers for viral rebound and safety assessment in blood and lumbar fluid during HIV-1 treatment interruption. *J Antimicrob Chemother* **75**, 1311-1320 (2020).

55. Clarridge, K.E.*, et al.* Effect of analytical treatment interruption and reinitiation of antiretroviral therapy on HIV reservoirs and immunologic parameters in infected individuals. *PLoS Pathog* **14**, e1006792 (2018).

56. Salantes, D.B.*, et al.* HIV-1 latent reservoir size and diversity are stable following brief treatment interruption. *J Clin Invest* **128**, 3102-3115 (2018).

57. Leal, L., Feher, C., Richart, V., Torres, B. & Garcia, F. Antiretroviral Therapy Interruption (ATI) in HIV-1 Infected Patients Participating in Therapeutic Vaccine Trials: Surrogate Markers of Virological Response. *Vaccines (Basel)* **8**(2020).

58. Hossain, T.*, et al.* SQuHIVLa: A novel assay for Specific Quantification of inducible HIV-1 reservoir by LAMP. *bioRxiv*, 2023.2007.2014.548928 (2023).

59. Gunst, J.D.*, et al.* Impact of a TLR9 agonist and broadly neutralizing antibodies on HIV-1 persistence: the randomized phase 2a TITAN trial. *Nat Med* (2023).

60. Frattari, G.S., Caskey, M. & Sogaard, O.S. Broadly neutralizing antibodies for HIV treatment and cure approaches. *Curr Opin HIV AIDS* **18**, 157-163 (2023).

61. Vrignaud, L.L., Schwartz, O. & Bruel, T. Polyfunctionality of broadly neutralizing HIV-1 antibodies. *Curr Opin HIV AIDS* **18**, 178-183 (2023).

62. Gunst, J.D., Hojen, J.F. & Sogaard, O.S. Broadly neutralizing antibodies combined with latency-reversing agents or immune modulators as strategy for HIV-1 remission. *Curr Opin HIV AIDS* **15**, 309-315 (2020).

63. Joussef-Pina, S.*, et al.* Reduced and highly diverse peripheral HIV-1 reservoir in virally suppressed patients infected with non-B HIV-1 strains in Uganda. *Retrovirology* **19**, 1 (2022).

64. Prodger, J.L.*, et al.* Reduced HIV-1 latent reservoir outgrowth and distinct immune correlates among women in Rakai, Uganda. *JCI Insight* **5**(2020).

65. Dwivedi, A.K.*, et al.* Differences in expression of tumor suppressor, innate immune, inflammasome, and potassium/gap junction channel host genes significantly predict viral reservoir size during treated HIV infection. *bioRxiv* (2023).

66. Guery, J.C. Sex Differences in Primary HIV Infection: Revisiting the Role of TLR7-Driven Type 1 IFN Production by Plasmacytoid Dendritic Cells in Women. *Front Immunol* **12**, 729233 (2021).

APPENDICES

Nederlandse Samenvatting

NEDERLANDSE SAMENVATTING

Wereldwijd leven ongeveer 40 miljoen mensen met hiv-1 (PLWH) (UNAIDS 2023). Moderne, sterk onderdrukkende antiretrovirale therapie (ART) blokkeert virale replicatie effectief tot onder de detectie grenzen en beperkt de overdracht van hiv-1 aanzienlijk waardoor de gezondheid verbetert voor mensen die toegang hebben tot ART (~75% van de wereldwijde populatie van mensen met hiv-1) (UNAIDS 2023). ART is echter niet genezend (curatief) en moet levenslang worden ingenomen. Dit brengt aanzienlijke sociaaleconomische lasten met zich mee, vooral op plaatsen met beperkte toegang tot antivirale middelen en een hoge hiv-prevalentie. Bovendien hebben mensen met hiv-1 die langdurig ART gebruiken een verhoogd risico op co-morbiditeit. Dit is waarschijnlijk te wijten aan de persistentie van hiv-1 in bloed en weefsels, chronische ontsteking, versnelde veroudering en ART-toxiciteit. Daarom worden momenteel in diverse wereldwijde wetenschappelijke inspanningen strategieën onderzocht om ART-vrije controle van hiv-1 infectie te bereiken en zo de algehele gezondheid van mensen met hiv-1 te verbeteren voor lange termijn. Deze strategieën zijn gericht op verschillende mechanismen van HIV-1 persistentie en omvatten manieren om het provirale latente reservoir te elimineren, verminderen of inactiveren en/of om opruiming van het virus te verbeteren en viremie onder controle te houden in afwezigheid van ART. Het evalueren van de veiligheid en doeltreffendheid van dergelijke (combinatie) strategieën in klinische studies wordt bemoeilijkt door grote uitdagingen, waaronder beperkte beschikbaarheid van monsters en moeilijke toegankelijkheid van anatomische weefsels. Vanwege de kleine omvang van het induceerbare, replicatiecompetente HIV-1-reservoir, grote hoeveelheden bloed nodig zijn om het hiv-1 reservoir te detecteren en nauwkeurig te onderzoeken. Bovendien hebben de eindpunttesten een suboptimale gevoeligheid en zijn er geen robuuste, voorspellende biomarkers voor genezing of ART-vrije controle. Daarom wordt analytische ART-interruptie (ATI), hoewel riskant en ethisch discutabel, gebruikt om de werkzaamheid van potentiële genezingsstrategieën te evalueren. Het onderzoek beschreven in dit proefschrift richt zich op het in kaart brengen van latente, induceerbare hiv-1 reservoirs, die op het kruispunt liggen van verschillende innovatieve strategieën voor HIV-behandeling.

Het virale reservoir in perifere mononucleaire cellen in het bloed (PBMC's) is klein en bevat slechts fractie (2-5%) geïnfecteerde cellen die latent, maar intact hiv-1 herbergen. Het latente hiv-1 reservoir kan door T cel activatie geïnduceerd worden om virale genen tot expressie te brengen (=induceerbaar), wat leidt tot de productie van infectieus virus (=replicatiecompetent). Deze cellen zijn hierdoor in staat om virale een rebound te initiëren wanneer ART gestopt wordt of faalt. Dit latente, induceerbare, replicatiecompetente virale reservoir is daarom een cruciaal doelwit

in innovatieve strategieën voor hiv-1 genezing of ART-vrije controle. Het succes van deze strategieën vereist de mogelijkheid om nauwkeurig en precies de omvang van hiv-1 reservoirs vòòr, en de re-activatie kinetiek na, dergelijke interventies te bepalen om de onderbreking van ART te begeleiden. Gevestigde en nieuwe hiv-1 reservoir tests vereisen een rigoureuze evaluatie van de prestatiekenmerken (gevoeligheid, specificiteit, reproduceerbaarheid, toepasbaarheid) en hun relatie tot de resultaten van preklinische en klinische hiv-1 genezingsstudies. Deze studies zijn noodzakelijk om essentiële vragen te beantwoorden, voor de evaluatie van therapeutische interventies voor hiv-1 genezing. Gezien de veelzijdige aard van HIV-1 persistentie is de vraag, welke moleculaire compartimenten van het latente hiv-1 reservoir moeten prioriteit krijgen (DNA, RNA, eiwit, virus?) en welke methodes moeten worden gebruikt om veranderingen in deze moleculaire compartimenten te volgen?

Meervoudig gespliced (ms) RNA, wordt getranscribeerd van tat/rev/nef-coderende exonen, gelegen op verschillende hoog variabele plaatsen in het hiv-genoom. De detectie hiervan is gevoelig voor grote interne deleties en hypermutatie, van de aanzienlijke hoeveelheid defecte genomen, al kan de detectie van defectieve genomen niet worden uitgesloten. Vroege en meer recente studies hebben een voorspellende waarde voor msRNA en toename van intracellulair viraal RNA bij suppressieve ART en productie van replicatiecompetente virionen aangetoond, die correleert met de grootte van plasma hiv-1 RNA load na onderbreking van suppressieve ART. Detectie van msRNA door de tat/rev geïnduceerde limiting dilution assay (TILDA) een van de weinige gevestigde technieken die op grote schaal toepasbaar is. TILDA kan de fractie van latent geïnfecteerde cellen bepalen die in staat zijn tat/rev msRNA tot expressie te brengen, wat een veelbelovende surrogaatindicator is voor hiv-1-replicatiecompetentie (besproken in hoofdstuk 1 en 1.1).

In hoofdstuk 2 hebben we de bevindingen van een veelbelovende ex vivo, preklinische studie gemeld. De in vivo werkzaamheid van een nieuw middel om de latentie om te keren (LRA) gericht op het BAF-complex werd geëvalueerd. Het betreft een chromatine remodeler, waarvan eerder is aangetoond dat het een sleutelrol speelt bij de totstandkoming en instandhouding van HIV-latentie. Bij 28 deelnemers met ART onderdrukte hiv-1 infectie voerden we een (van de eerste) gerandomiseerde gecontroleerde klinische onderzoek uit. Doel was om een combinatie strategie voor het omkeren van latentie te evalueren. Cel-geassocieerd hiv-1 RNA metingen werden gebruikt om veranderingen in hiv-1 provirale transcriptie te monitoren in reactie op twee enkelvoudige of in combinatie geteste interventiemedicijnen - pyrimethamine en valproïnezuur. Deze medicijnen

zijn al goedgekeurd voor de behandeling van andere klinische aandoeningen. De tat/rev induced limiting dilution assay (TILDA) werd toegepast om de potentiële impact van de LRA-interventie op de grootte van het latente, induceerbare hiv-1-reservoir te beoordelen. We bewijzen de conceptuele benadering om de omkering van de hiv-1 latentie te induceren, via remming van het BAF-complex, bij personen met ART-onderdrukte hiv-infectie.

In hoofdstuk 3 onderzochten we een alternatieve farmacologische benadering om de depletie van het induceerbare hiv-1 reservoir te bevorderen na omkering van de latentie. We evalueerden de rol van DDX3-inhibitie in het induceren van selectieve cel apoptose ex vivo. Provirale induceerbaarheid werd gemeten door expressie van niet-gespliced en meervoudig gespliced viraal RNA met behulp van parallelle hiv-1 reservoirtechnieken; respectievelijk "single cell fluorescente in situ hybridisatie" (Fish-flow) en TILDA. We tonen een nieuwe rol aan voor DDX3 in de omkering van HIV-1 latentie en een potentieel mechanisme dat ten grondslag ligt aan de selectieve depletie van het induceerbare HIV-1 reservoir bewerkstelligd door aangeboren immuunresponsen.

In hoofdstuk 4 brachten we de dynamiek van het hiv-1 reservoir met verschillende moleculaire technieken in CD4+ T-cellen uit perifeer bloed in kaart. Deze klinische studie werd gedaan in vrijwilligers die hun ART onderbraken na een vaccinatie autologe dendritische cellen. De vaccinatie gericht was op het induceren van verbeterde cellulaire immuniteit tegen hiv-1 en mogelijk ART-vrije virale controle. Meer dan tien jaar na onderbreking van ART, met als gevolg virale rebound en daaropvolgende ART-gemedieerde virale resuppressie deden deelnemers mee aan een vervolgstudie op. Provirale intactheid werd beoordeeld met de intacte proviraal DNA-test (IPDA) en provirale induceerbaarheid werd beoordeeld met een virale RNA- en/of eiwitinductie-tests (FISH-flow, one-step TILDA en SQuHIVLa). We observeerden discordante uitkomsten met de verschillende moleculaire technieken van het latente hiv-1 reservoir met mogelijke implicaties voor het monitoren van hiv-1 reservoir dynamiek in toekomstige immuun gebaseerde, combinatie ATI-trials.

In het algemeen heeft het werk belangrijke nieuwe inzichten verschaft in hiv-1 persistentie met een focus op het latente induceerbare virale reservoir, geïdentificeerd door tat/rev msRNA expressie, dat dient als een surrogaatmarker voor replicatiecompetentie. Het is aangetoond dat dit reservoir een dynamisch en relevant compartiment is om de respons op potentieel curatieve interventies te monitoren. De proof-of-concept en het baanbrekende gebruik van kleine moleculen die het BAF-complex remmen om provirale transcriptie in vivo te activeren, kunnen belangrijke componenten zijn in toekomstige combinatie LRA-strategieën. Een gerichte impact op het latente hiv-1 reservoir, kan worden bereikt

door gerichte actie op specifieke virale of cellulaire elementen. Dit minimaliseert off-target effecten terwijl de therapeutische werkzaamheid wordt geoptimaliseerd. Dit werd aangetoond in de proof-of-concept en het baanbrekende gebruik van DDX3-remmers om farmacologisch de omkering van hiv-1 latentie en intrinsieke cel apoptose teweeg te brengen, wat leidt tot de selectieve depletie van cellen die hiv-1 RNA tot expressie brengen, terwijl niet-geïnfecteerde omstandercellen gespaard blijven. Dit is een veelbelovende strategie om het falen van adaptieve immuunreacties in het elimineren van het latente hiv-1 reservoir te omzeilen - een belangrijke uitdaging in het bereiken van genezing voor hiv-1 infectie.

De bevindingen van het onderzoek beschreven in dit proefschrift hebben vooralsnog betrekking op hiv-1 subtype B-infectie en virale persistentie in CD4+ T-cellen in perifeer bloed. Bovendien werden de translationele onderzoeken beschreven in hoofdstuk 2 en 4 uitgevoerd bij mannelijke, voornamelijk blanke deelnemers. Daarom kunnen de onderzoeksresultaten beschreven in dit werk niet gegeneraliseerd worden naar alle mensen die leven met hiv-1. Er zijn enorme hiaten in ons begrip van hiv-1 persistentie in verschillende populaties. Studies in genetisch diverse populaties en met een hoge hiv-prevalentie zoals bij mensen die leven in Afrika, zijn momenteel beperkt. Deze studies zijn van cruciaal belang om de ontwikkeling van hiv-1 therapeutica die effectief zullen zijn in Afrikaanse populaties, te ondersteunen. Meer dan 60% van de wereldwijde populatie van mensen met hiv-1 leeft in Sub-Sahara Afrika.

APPENDICES

About the author

Cynthia Lungu, was on born on 2nd September, 1988 in Lusaka, Zambia. She lived in Gaborone, Botswana from 1992-2003 before returning to Zambia for Higher & Tertiary education. She obtained a BSc degree in Biological Sciences; Microbiology from the University of Zambia in 2012. She worked as a freelance research assistant evaluating various implementation programmes for Malaria and HIV prevention in Zambia until 2014 when she traveled to the Netherlands to pursue graduate studies. She completed a Research MSc degree in Infection and Immunity from Erasmus University Rotterdam in 2016 and commenced doctoral studies at Erasmus University Medical Center where she led the development, validation, and implementation of several quantitative and qualitative technologies to study HIV persistence in putative strategies towards HIV cure or ART-free viral control. In 2022 she received independent funding and is currently affiliated to Erasmus Medical Center and the Centre for Infectious Disease Research in Zambia where she leads translational HIV studies in a high-burden, resource-limited setting, to generate locally relevant evidence to inform future research, development and implementation of novel therapeutics for diverse populations living with HIV.

CURRICULUM VITAE

EDUCATION

PhD Candidate | Erasmus University Rotterdam, Erasmus Medical Center, The Netherlands, *2016-2021*

MSc. Infection and Immunity | Erasmus University Rotterdam, Erasmus Medical Center, The Netherlands, *2014-2016*

BSc. Biological Sciences, Major Microbiology | University of Zambia, *2007-2012*

EMPLOYMENT

Current

Visiting Research Fellow – Infrastructure Building, Implementation Studies, Biomarker Research

Center for Infectious Disease Research in Zambia (CIDRZ), Zambia – ***February 2023 - Present***

- Primary Investigator of a project to establish an HIV-1 persistence research programme in clinical research centers in Zambia – ***Independent research grant***
- Viral persistence and immunological studies in young people with HIV in Zambia

Post-doctoral researcher – HIV-1 Persistence and Immunological Profiling Studies

Department of Biochemistry, Erasmus MC, Rotterdam, The Netherlands – ***November 2021 - Present***

- Developing scalable and cost-effective HIV-1 viral reservoir quantification techniques for implementation in clinical trial and resource-constrained settings – ***Independent research grant***
- Utilizing molecular and immune-based assays to investigate the impact of antiretroviral treatment interruption or treatment failure on the inducible viral reservoir, and on immune cell phenotypes and function – ***Independent research grant***

Past

Doctoral researcher – Interrogating latent viral reservoirs in treated HIV infection

Departments of Viroscience & Biochemistry, Erasmus MC, Rotterdam, The Netherlands – ***November 2016 -October 2021***

- Utilized viral reservoir quantification techniques to investigate the impact of long-term antiretroviral treatment interruption on the HIV-1 viral reservoir

- Contributed to clinical endpoint analyses; HIV-1 viral reservoir techniques to investigate the efficacy of pyrimethamine and valproic acid as latency reversing agents in a proof-of-concept, randomized controlled trial (Clinicaltrials.go: NCT03525730)
- Utilized viral reservoir quantification techniques to study the efficacy of cell death-inducing compounds to selectively target the HIV-1 viral reservoir
- Optimized and validated several molecular and culture-based HIV-1 viral reservoir quantification techniques
- Performed Sanger sequence analysis to identify HIV-1 drug resistance mutations in clinical samples of participants failing on dolutegravir maintenance monotherapy

Master of Science Research Intern - Investigating viral and host factors driving HIV-2 elite control
Department of Viroscience, Erasmus MC, Rotterdam, The Netherlands – ***October 2015 -October 2016***

- Utilized Sanger sequencing to generate full-length sequences of HIV-2 biological clones obtained from individuals with progressive or elite control of HIV-2 infection to identify viral factors associated with biological and clinical phenotype.

PERSONAL RESEARCH GRANTS

- SANTHE Collaborative Grant (2023-2024) **US$ 50 000**
- Aidsfonds Research Award (Amsterdam Diner Foundation & Xandi Buys Foundation) (2023-2025). **€150 000**
- Aidsfonds HIV Cure Small Research Subsidy (2020). **€10 000**
- Erasmus MC Vriendenfonds Research Subsidy (2016). **€ 5000**

SCHOLARSHIP AWARDS

- Research Master Infection & Immunity Scholarship Award (2014-2016). **€18 000**
- Medical Education Partnership Initiative (MEPI) Scholarship Award (2014-2016). **€16 000**

PUBLICATIONS

Lungu C., Overmars R.J., Grundeken E., Boers P.H.M., van der Ende M.E., Mesplède T. and Gruters R.A. *Genotypic and Phenotypic Characterization of Replication-Competent HIV-2 Isolated from Controllers and Progressors*. **Viruses** (**2023**), 15,2236. https://doi.org/10.3390/v15112236

Laeremans, T., den Roover, S., **Lungu, C**. D'haese S., Gruters, R.A., Allard, S.D., Aerts, L. J. *Autologous dendritic cell vaccination against HIV-1 induces changes in natural killer cell phenotype and functionality*. ***npj Vaccines* 8**, 29 **(2023)**. https://doi.org/10.1038/s41541-023-00631-z

Prins, H.A.B*., Crespo, R*., **Lungu, C***., Rao, S., Li L., Overmars R.J., Papageorgiou G., Mueller Y.M., Hossain T., Kan T.W., Rijnders B.J.A., Bax H.I., Gorp E.C.M., Nouwen J.L., de Vries-Sluijs T.E.M.S., Schurink C.A.M., de Mendonça Melo M., van Nood E., Colbers A., Burger D., Palstra R-J., van Kampen J.J.A., van de Vijver D.A.M.C., Mesplède T., Katsikis P.D., Gruters R.A., Koch B.C.P., Verbon A., Mahmoudi T. and Rokx C. *The BAF complex inhibitor pyrimethamine reverses HIV-1 latency in ART suppressed people with HIV-1 on antiretroviral therapy*. **Sci Adv. (2023)** Mar 17;9(11):eade6675. doi: 10.1126/sciadv.ade6675
**Co-First Authorship*

van Kampen J.J.A., Pham H.T., Yoo S., Overmars R.J., **Lungu C.**, Mahmud R., Schurink C.A.M., van Boheemen S., Gruters R.A., Fraaij P.L.A., Burger D.M., Voermans J.J.C., Rokx C., van de Vijver D.A.M.C., Mesplède T. *HIV-1 resistance against dolutegravir fluctuates rapidly alongside erratic treatment adherence: a case report*. **J Glob Antimicrob Resist. (2022)** Dec;31:323-327. doi:10.1016/j.jgar.2022.11.001.

Lungu C., Procopio F.A. TILDA: Tat/Rev Induced Limiting Dilution Assay. ***Methods Mol Biol. (2022)***;2407:365-372. doi: 10.1007/978-1-0716-1871-4_24

Rao, S., **Lungu, C.**, Crespo, R., Steijaert, T.H., Górska, A., Palstra, R.J., Prins, H. A. B., van Ijcken, W., Mueller, Y. M. , van Kampen, J. J. A., Verbon, A., Katsikis, P. D., Boucher, C. A. B., Rokx, C., Gruters R. A, and Mahmoudi, T. *Selective cell death in HIV-1-infected cells by DDX3 inhibitors leads to depletion of the inducible reservoir.* ***Nature Communications (2021)***; 12, 2475, doi.org/10.1038/s41467-021-22608-z

Lungu C., Banga R., Gruters R.A, Procopio F.A. *Inducible HIV-1 Reservoir Quantification: Clinical Relevance, Applications and Advancements of TILDA*. ***Front Microbiol. (2021)*** Jun 15;12:686690. doi: 10.3389/fmicb.2021.686690.

Lungu C*., Procopio F.A., Overmars R.J, Beerkens R.J.J, Voermans J.J.C, Rao S., Prins H.A.B, Rokx C, Pantaleo G, Vijver DAMCV, Mahmoudi T, Boucher C.A.B, Gruters

R.A., Kampen J.J.AV. *Inter-Laboratory Reproducibility of Inducible HIV-1 Reservoir Quantification by TILDA*. ***Viruses. (2020)*** Sep 2;12(9):973. doi: 10.3390/v12090973. **Corresponding author*

Wijting I.E.A., **Lungu C.**, Rijnders B.J.A., van der Ende M.E., Pham H.T., Mesplède T., Pas S.D., Voermans J.J.C., Schuurman R., van de Vijver D.A.M.C., Boers P.H.M., Gruters R.A., Boucher C.A.B., van Kampen J.J.A. *Reply to Darcis and Berkhout*. ***J Infect Dis. (2018)*** Nov 5;218(12):2020-2021. doi: 10.1093/infdis/jiy475.

Pham H.T., Labrie L., Wijting I.E.A., Hassounah S., Lok K.Y., Portna I, Goring M.E., Han Y., **Lungu C.**, van der Ende ME, Brenner B.G., Boucher C.A., Rijnders B.J.A., van Kampen J.J.A., Mesplède T., Wainberg M.A. *The S230R Integrase Substitution Associated With Virus Load Rebound During Dolutegravir Monotherapy Confers Low-Level Resistance to Integrase Strand-Transfer Inhibitors*. ***J Infect Dis. (2018)*** Jul 24;218(5):698-706. doi: 10.1093/infdis/jiy175.

Wijting I.E.A., **Lungu C.**, Rijnders B.J.A., van der Ende M.E., Pham H.T., Mesplède T., Pas S.D., Voermans J.J.C., Schuurman R., van de Vijver D.A.M.C., Boers P.H.M., Gruters R.A., Boucher C.A.B., van Kampen J.J.A. *HIV-1 Resistance Dynamics in Patients with Virologic Failure to Dolutegravir Maintenance Monotherapy*. ***J Infect Dis. (2018)*** Jul 24;218(5):688-697. doi: 10.1093/infdis/jiy176.

Stoszko M., De Crignis E., Rokx C., Khalid M.M., **Lungu C**., Palstra RJ. Kan TW, Boucher C., Verbon A., Dykhuizen E.C. and Mahmoudi T. *Small Molecule Inhibitors of BAF; A Promising Family of Compounds in HIV-1 Latency Reversal* ***Ebiomedicine (2016)*** volume 3, 108-121

MANUSCRIPTS SUBMITTED/UNDER REVIEW

Lungu C., Hossain T., Prins, H. A. B., Hensley K. S., Crespo R., Rokx C., Rao S., van Kampen J.J.A., van de Vijver D.A.M.C., Mesplède T., Katsikis, P. D., Mueller, Y. M., Gruters R.A., Mahmoudi T. *Analytical treatment interruption: detection of an increase in the latent, inducible HIV-1 reservoir more than a decade after viral resuppression.*. (Under review, 1st Nov 2023)

Hossain, T.*, **Lungu C.***, Schrijver S. d., Kuali M., Rao S., Ngubane A., Kan T. W., Palstra R.-J., Madlala P., Ndung'u T., Mahmoudi T. (2023). "*SQuHIVLa: A novel assay for Specific Quantification of inducible HIV-1 reservoir by LAMP*." *Co-First Authorship

SELECTED SCIENTIFIC COMMUNICATIONS

- Analytical treatment interruption after autologous dendritic cell vaccination reshapes the HIV-1 functional reservoir. Sub-Saharan African Network for TB/HIV Research Excellence (SANTHE) Annual Consortium Meeting (2023). ***Oral Presentation***
- Evaluating the impact of prolonged cART interruption on the inducible HIV-1 reservoir. Immuno-Zambia Meeting (2022). ***Oral and Poster presentations***
- Adaptation and performance evaluation of TILDA for use in clinical settings. European HIV Vaccine Alliance (EHVA) Consortium Meeting (2019). ***Poster presentation***
- Changes outside integrase in a patient failing on Dolutegravir maintenance monotherapy points to a new resistance mechanism. The 2nd Global HIV Clinical Forum: Integrase inhibitors (2017). ***Poster presentation***
- Changes outside integrase in a patient failing on Dolutegravir maintenance monotherapy points to a new resistance mechanism. European HIV Clinical forum (2017). ***Oral presentation***

PRESS, DISSEMINATION AND COMMUNITY OUTREACH

- Interview for Amazing Erasmus MC Newsletter (March 2023) **|** Anti-parasite drug awakens dormant virus in people with HIV - Amazing Erasmus MC
- Interview for Aidsfonds Newsletter (June 2022) **|** Onderzoek naar het hiv-reservoir bij jongeren in Zambia | Aidsfonds (in Dutch)
- Interview for News Article (June 2022)**|** Met haar Afrikaanse roots strijdt wetenschapper Cynthia tegen hiv (32) - LINDA.nl (in Dutch)

COLLABORATIVE RESEARCH PROJECTS

- **Principal Investigator**: SANTHE Collaborative Grant (Dec 2023- Dec 2024), Integrated profiling of sex-specific differences in HIV-1 persistence and immune responses in a Zambian cohort of individuals on suppressive antiretroviral therapy. Collaborative grant with the Ndhlovu Lab at Africa Health Research Institute (AHRI)
- **Investigator**: SPIRAL consortium, **Work package co-lead**, Viral reservoir dynamics in diverse HIV infection contexts. An interdisciplinary collaborative project to investigate integrated interventions to control HIV-1 infection. International collaborating Scientists from Netherlands, South Africa, Uganda and Zambia. KIC NWO-Aidsfonds grant (starts December 2023, 5-year project)

- **Principal investigator**: Mapping viral reservoir landscapes in young people with HIV in Zambia
- Aidsfonds – HIV Cure Research Grant (2022-2025). Collaboration with Center for Infectious Disease Research in Zambia (CIDRZ) and Center for Family Health Research Zambia (CFHRZ)
- **Principal investigator**: HIV-1 Reservoir dynamics in relation to cART interruption and resumption (HIVRESATI) – a longitudinal cohort study. Aidsfonds Subsidy 2020 – HIV-1 Cure Small Grants. Collaboration with Erasmus HIV Eradication Group
- **Investigator**: LRAs united as a novel anti-HIV strategy **(**LUNA) Randomized Controlled Trial Phase 1/2 (2016 -2022)
- **Investigator**: Ex-vivo HIV-1 cohort pre-clinical studies (Acute HIV, chronic HIV, Elite controllers) (2016 - present)

ADDITIONAL RESEARCH AND TRAINING EXPERIENCE

- ICH Good Clinical Practice E6 (R2)- The Global Health Network e-learning course (June 2023)
- Knowledge and Innovation Covenant (KIC) Aidsfonds-NWO – Sandpit workshop "HIV cure for everyone" (9th-13th January 2023)
- Immunology workshop: Immuno-Zambia (5th-9th December 2022)
- Research training: High-dimensional flow cytometry using a 5 laser Aurora spectral flow cytometer (June 2022-present)
- Research Integrity: Department Medical Ethics and Philosophy of Medicine, Erasmus Medical Center Rotterdam, The Netherlands (July 2020)
- Workshop: HIV Reservoir Characterization Workshop. Ghent, Belgium. (18-20th September 2019)
- Workshop: 1st Max Plank Society Workshop on HIV Reservoirs and Evolution. St Lucia, KwaZulu-Natal, South Africa. (20th-23rd January 2019)
- Workshop: 22nd International Bioinformatics Workshop on Virus Evolution and Molecular Epidemiology (VEME 2017), Lisbon, Portugal (August 27th -September 1st 2017)
- Research Intern: Screened compounds for their potential to reactivate latent HIV-1. Department of Biochemistry, Erasmus MC, Rotterdam, The Netherlands (January-October 2015)
- Research Assistant: Zambia-Led Prevention Initiative (ZPI) End-of-Project Performance Evaluation. USAID/Zambia, (July -August 2014). Participated in

methods and toolkit development for focus group discussions and stakeholder interviews.

- Laboratory intern: Introduction to HIV-1 drug resistance monitoring. Center for infectious Disease Research (CIDRZ), Lusaka, Zambia (April-July 2014)

RESEARCH NETWORKS AND AFFILIATIONS

- Sub-Saharan African Network for TB/HIV Research Excellence (SANTHE):Research Fellow and HIV Cure research **Work Group Chair**. January 2023 - present.
- SPIRAL Consortium – an international, interdisciplinary collaboration of Scientists to investigate integrated interventions towards control of HIV infection: **Work package co-lead**, Investigator. January 2023 – present.
- HIV Cure Africa Acceleration Partnership (HCAAP). January 2023 – present.
- NL4Cure Consortium – a collaboration of Dutch stakeholders involved in cure research: Investigator. 2018 – present.

PHD PORTFOLIO

Cynthia Lungu
Erasmus University Medical Center
Departments of Viroscience and Biochemistry
PhD period: October 2016 - October 2021
Promoters: Prof. Charles A. Boucher (1958-2021) & Prof. Tokameh Mahmoudi
Co-Promoter: Dr. Rob. A. Gruters

Courses

Annual Course in Virology – Rotterdam, Netherlands. 2016
22nd International Bioinformatics Workshop on Virus Evolution and Molecular Epidemiology(VEME) – Lisbon, Portugal. 2017
1st Max Planck Society- AHRI Workshop on HIV Reservoirs and Evolution – St. Lucia, KZN, South Africa. 2018
Annual HIV Reservoir Characterization Workshop – Ghent, Belgium. 2019
BD Flow Cytometry course – Rotterdam, Netherlands. 2019
Scientific Integrity – Erasmus MC Graduate School, Rotterdam, Netherlands. 2020
Gene expression data analysis using R: How to make sense of your RNA-Seq/microarray data – Rotterdam, Netherlands. 2021
IUS-FAIS-SANTHE-ISZ Immuno-Zambia Course. 2022

Research Meetings

Viroscience department and workgroup weekly meetings. 2016 - 2020
Biochemistry department weekly workgroup meetings. 2019 - 2022
Erasmus HIV Eradication group bi-weekly meetings. 2016 - 2022

Seminars and Conferences

2nd Global HIV Clinical Forum: Integrase inhibitors, Paris, France – poster and oral presentation. 2017
9th International AIDS Society (IAS), Paris, France – poster presentation. 2017
European HIV Clinical Forum: Integrase inhibitors, Milan, Italy – poster presentation. 2017
European HIV Vaccine Alliance (EHVA) Consortium Meeting, Madrid Spain – poster presentation. 2019

Teaching activities

Supervision

Jochem Weekers, BSc. thesis project, 2021 – Investigating the inducible viral reservoir in people living with HIV-1

Esmée Grundeken, MSc. thesis project, 2021 – Investigating LTR-Tat interactions to gain insight into HIV-2 latency

Andreas Kyrou, MSc. thesis project, 2020 – Investigating LTR-Tat interactions to gain insight into HIV-2 phenotype

Teaching assistant: Population dynamics course, Infection and Immunity Research Master Programme, Erasmus MC - October 2017; 2018; 2019

Other activities*:*

Article Peer Review (2021): Reviewed the article by Mehta et al., An Improved Tat/Rev Induced Limiting Dilution Assay with Enhanced Sensitivity and Breadth of Detection. Front. Immunol., Sec. Viral Immunology, Volume **12** - 2021 | https://doi.org/10.3389/fimmu.2021.715644

Grants

Aidsfonds HIV Cure Small Research Subsidy (2020). €10 000

Erasmus MC Vriendenfonds Research Subsidy (2016). € 5000

APPENDICES

Acknowledgements

ACKNOWLEDGEMENTS

Moving to the Netherlands to further my studies was a real turning point for my life and career. This PhD thesis serves to remind me of the enduring resilience it has required to get here. It has been such a challenging and transformative experience building up from very little and with the support of so many that I cannot acknowledge everyone by name. Thank you all!

Prof. dr. C. A. B., dear Charles, I am deeply grateful for the opportunity to pursue my doctoral studies in your Research group. I appreciate every time that you reminded me to think about the bigger picture and to trust the process. You laid a strong foundation for me to build on. You invited me along to multi-national consortia meetings to network, practice my scientific communication skills and foster collaborations from the first year of my PhD studies – Paris, Milan, Madrid, Barcelona! You truly inspired and shaped the direction of my career. I'm deeply sad that you are not here to read this note or to witness my accomplishments. I have so much to tell you, so much to show you! Thank you so much Charles – you are dearly missed. May your soul rest in perfect peace.

Prof. dr T. Mahmoudi**,** dear Tokameh, we have known each other for nearly 10 years now! It's an unforgettable experience with a lot of twists and turns. My first MSc research internship was in your laboratory, early 2015, where I started to work on my technical skills, while contributing to a critical project at the time; *the pre-clinical validation of BAF complex inhibition in reversing HIV-1 latency* - prelude to the clinical trial several years later and Chapter 2 of my PhD thesis! I could never have imagined that you would play such a big role in my personal and career development. I have a lot to say to you but I especially want to thank you for throwing me a lifeline at very critical moments over the past years. At some point, I felt that my research was not going anywhere, sitting in a lot of uncertainties and my confidence was at its lowest point. That first conversation with you, after we met in the Ee. Building elevator one day, eventually turned into weekly consultations, each one bringing me more clarity and renewed hope. So, thank you so much for re-opening the doors to your laboratory and for accommodating every phase of my life throughout this academic journey. Thank you for the unique opportunities to contribute to impactful science and, most of all, for giving me the creative freedom and space to discover my passions and potential!

Dr. R. Gruters**,** dear Rob, thank you for your long-standing commitment to HIV research – not even retirement is stopping you it seems! Hopefully this PhD thesis will serve to remind you of all the support, training and supervision you have given me over the years. Patrick, our key HIV research technician, left the group shortly before I started my PhD studies, which meant that I had to step up and manage

my research very early on. Thank you for trusting me with your laboratory at the time and for the unique opportunity to work on my personal leadership skills!

Department of Viroscience – HIV Research Group.
Patrick H. M. Boers, dear Patrick, I learnt invaluable skills from you that set me up for my PhD research – Thank you so much! Ronald Overmars, dear Ronald, thank you for all the technical support and words of encouragement over the years. Dr David van de Vijver, always available to help with statistics - Thank you! Dr Thibault Mesplède, thank you for your support and career advice.

Dr. Jeroen van Kampen, dear Jeroen, many thanks for pulling all the strings to ensure that I could successfully carry out my experiments in the Clinical Virology Diagnostics unit. It was a very supportive and enabling environment. Thank you, as well, for your guidance and invaluable input on various diagnostic protocols and manuscripts.

Guido van der Net, dear Guido, thank you for training me in the BSL3 laboratory and for supporting me with my experiments until I could independently work at BSL3.

Jolanda Voermans, dear Jolanda, I really appreciate all the time you took to guide and advise me during assay optimizations for a clinical diagnostic laboratory setting. Thank you for constantly encouraging me to press on even when I felt frustrated. I learnt so much from our interactions. Rob Beerkens, dear Rob, thank you for all your hard work and support in setting up the HIV-1 reservoir assays.

Rachel Scheuer and Georgina Aron, I could always count on you – thank you for your tremendous support. Georgina, I had the best times at your Laboratory section! Thank you for accommodating me and my experiments and for the cheerful atmosphere. Rachel, I especially want to thank you for all the light moments and pep talks whenever we bumped into each other in the hall ways of the Viroscience Department!

Dr. Miruna Rosu, dear Miruna, Thank you for all the fun lunch and dinner dates! Always so much drama! We have come such a long way – thank you for always encouraging me to never give up even when I could not see the end!

Raissa Davis, dear Raissa, I am so grateful to have connected with you during your MSc internship at the Viroscience department all those years ago! I have very fond memories of extremely fun and relaxing weekend afternoons with you. I also want to thank you for your support and advice through some of the difficult moments. Thank you for inspiring me!

Thank you Widagdo, Gadissa Hundie, Brigitta Laksono and Nisreen Okba, for being a solid support system when I started out at the department of Viroscience. I received some of the best advice in life from you, Widagdo!

Carola van der Meer, dear Carola, we were always the first to arrive in the office at 7:00-7:30 am in the morning! I really enjoyed the conversations before I went off to my experiments. I deeply appreciate your kindness and incredible support over the years. Thank you, Carola!

Dear Colleagues from the 10th, 16th and 17th floor; Thank you for every form of help and support you have provided me during my time at the Viroscience department. I am grateful for the unique opportunity to interact with you during my PhD trajectory.

Dr. Wesley de Jong, dear Wesley, you were always ready to assist me with my clinical databases. Thank you for your kindness and support. Dr Stephanie Popping, dear Stephanie, thank you for helping me to navigate through some of the most difficult phases of my PhD trajectory.

Erasmus MC HIV Eradication Group (EHEG) – The translational research that this thesis is built on would not be possible without your unwavering commitment to HIV (cure) research. Thank you for all the collaborations, co-authored publications and continued scientific support.

Dr. Henrieke Prins, dear Henrieke, you have been a very unique source of support for me, since the start. Thank you for showing me the clinical side of HIV research - I learnt a lot from you whilst establishing and working on the HIV biomarker, LUNA trial and HIVRESATI cohorts. It was such an enriching experience and I now get to apply a lot of those insights in the next phase of my career.

Dr. Katie Hensley, dear Katie, thank you for your help with the HIVRESATI cohort and for your valuable clinical and scientific input.

Dr. Yvonne Muller, dear Yvonne, I am grateful for all your support and encouragement. Thank you for introducing me to multi-parameter flow cytometry – I am looking forward to learning more from you!

Harm de Wit, dear Harm, I really enjoyed working with you at the immunology lab! Thank you for all the help.

Dr. Francesco Procopio, dear Francesco, I shipped PBMC samples from the Netherlands to Switzerland so we could perform an inter-laboratory validation of "TILDA", an HIV-1 reservoir assay that you developed, and a focal assay used in my

research. We then conceptualized and published a perspective article together. Thank you for the rare opportunity to work with you and for your invaluable contribution to this thesis!

Department of Biochemistry – Mahmoudi Laboratory, you have been a continuous source of inspiration. I especially want to thank;

Dr. Shringar Rao, dear Shringar, I am deeply grateful for the unwavering support you have shown me over the years. You are a brilliant scientist – it was such an enriching experience to work with you on the DDX3 project. Mentally exhausting but fun at the same time! Thank you for taking time to train me in new laboratory techniques and for helping me improve my scientific writing skills. Thank you for your invaluable contribution to this thesis!

Drs Raquel Crespo, dear Raquel… Here is to all the unexpected strings we have pulled over the last years! I will forever cherish the unique opportunity we got to co-lead the evaluation of the LUNA trial! It has been a one-of-a-kind experience working with you – you're exceptionally talented with an amazing drive and passion for science!

Drs Tanvir Hossain, dear Tonmoy, we continued to stare at the computer screen from the moment we clicked on "run", anxiously waiting for a real-time LAMP fluorescent signal to turn up on display – the very first experiment, leading up to a new HIV-1 reservoir assay "SQuHIVLa". It has been such a great learning experience working with you. I hope we can collaborate on more projects in the future. Thank you for your invaluable contribution to this thesis and for being a great friend through it all!

Tsung Wai and Dr. R-J Palstra, thank you for helping me settle in when I joined the lab, twice! Tsung Wai, thank you for all the technical support!

Shalla, thank you for the heart-to-heart conversations and all the fun moments we shared together in and outside of the lab.

Over the years, I am privileged to have connected with so many people from all walks of life. I cherish all the interactions that have left a lasting impact. Many of these connections have contributed to my personal and career development.

My Family –
Eunice, dearest mom, you have sacrificed a lot for me and I cannot thank you enough! It's been very hard being away from you all this time. Thank you for your emotional and spiritual support. Thank you for all your daily prayers. Mom, I am deeply grateful for every day that I have you in my life. I love you so much!

Kelvin, David & Rhoda, dearest brothers and sister, living so far away from you, on another continent, for the past 9+ years has made it very difficult for us to keep in constant touch. I have missed out on some important events in each of your lives but I am grateful for the love and closeness we share and the support we continue to give one another. Thank you!

My love, you have seen it all – the chaos and the calm, the gloom and the hopes, the failures and wins, the health and mental breakdowns, and the tremendous come-backs, all of that, and so much more! This is "our" PhD! You have done so much behind the scenes to keep me grounded and on course and we have had to put so much on hold in support of my career endeavours. Thank you for your patience, understanding and for your confidence in me. Thank you for all the love and joy you bring to my life. I am deeply grateful that I have had you by my side all these years. *Dziękuję kochanie, bardzo cię kocham.*